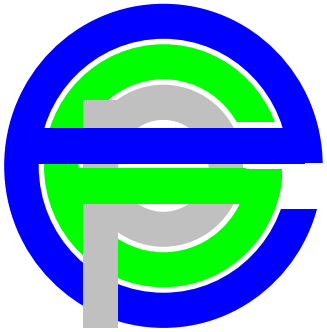

Konstantin K. Likharev

Essential Graduate Physics

Lecture Notes and Problems

Beta version

Open online access at
https://sites.google.com/site/likharevegp/
and
http://commons.library.stonybrook.edu/egp/

Part CM:
Classical Mechanics

Table of Contents

Chapter 1. Review of Fundamentals (14 pp.)
- 1.1. Mechanics and dynamics
- 1.2. Kinematics: Basic notions
- 1.3. Dynamics: Newton laws
- 1.4. Conservation laws
- 1.5. Potential energy and equilibrium
- 1.6. OK, can we go home now?
- 1.7. Self-test problems (12)

Chapter 2. Lagrangian Formalism (14 pp.)
- 2.1. Lagrange equation
- 2.2. Examples
- 2.3. Hamiltonian
- 2.4. Other conservation laws
- 2.5. Exercise problems (10)

Chapter 3. A Few Simple Problems (20 pp.)
- 3.1. One-dimensional and 1D-reducible systems
- 3.2. Equilibrium and stability
- 3.3. Hamiltonian 1D systems
- 3.4. Planetary problems
- 3.5. 2nd Kepler law
- 3.6. 1st and 3rd Kepler laws
- 3.7. Elastic scattering
- 3.8. Exercise problems (16)

Chapter 4. Oscillations (34 pp.)
- 4.1. Free and forced oscillations
- 4.2. Weakly nonlinear oscillations
- 4.3. RWA equations
- 4.4. Self-oscillations and phase locking
- 4.5. Parametric excitation
- 4.6. Fixed point classification
- 4.7. Numerical approach
- 4.8. Harmonic and subharmonic oscillations
- 4.9. Exercise problems (14)

Chapter 5. From Oscillations to Waves (22 pp.)
- 5.1. Two coupled oscillators
- 5.2. *N* coupled oscillators
- 5.3. 1D Waves in periodic systems
- 5.4. Interfaces and boundaries
- 5.5. Dissipative, parametric, and nonlinear phenomena
- 5.6. Exercise problems (15)

Chapter 6. Rigid Body Motion (30 pp.)
- 6.1. Angular velocity vector
- 6.2. Inertia tensor
- 6.3. Fixed-axis rotation
- 6.4. Free rotation
- 6.5. Torque-induced precession
- 6.6. Non-inertial reference frames
- 6.7. Exercise problems (22)

Chapter 7. Deformations and Elasticity (38 pp.)
- 7.1. Strain
- 7.2. Stress
- 7.3. Hooke's law
- 7.4. Equilibrium
- 7.5. Rod bending
- 7.6. Rod torsion
- 7.7. 3D acoustic waves
- 7.8. Elastic waves in restricted geometries
- 7.9. Exercise problems (15)

Chapter 8. Fluid Mechanics (26 pp.)
- 8.1. Hydrostatics
- 8.2. Surface tension effects
- 8.3. Kinematics
- 8.4. Dynamics: Ideal fluids
- 8.5. Dynamics: Viscous fluids
- 8.6. Turbulence
- 8.7. Exercise problems (19)

Chapter 9. Deterministic Chaos (14 pp.)
- 9.1. Chaos in maps
- 9.2. Chaos in dynamic systems
- 9.3. Chaos in Hamiltonian systems
- 9.4. Chaos and turbulence
- 9.5. Exercise problems (4)

Chapter 10. A Bit More of Analytical Mechanics (14 pp.)
- 10.1. Hamiltonian equations
- 10.2. Adiabatic invariance
- 10.3. The Hamilton principle
- 10.4. The Hamilton-Jacobi equation
- 10.5. Exercise problems (9)

* * *

Additional file (available upon request):

Exercise and Test Problems with Model Solutions (136 + 40 = 176 problems; 227 pp.)

This page is intentionally left blank

Chapter 1. Review of Fundamentals

After elaborating a bit on the title and contents of the course, this short introductory chapter lists the basic notions and facts of the classical mechanics, that are supposed to be known to the reader from undergraduate studies.[1] *Due to this reason, the explanations are very brief.*

1.1. Mechanics and dynamics

A more fair title of this course would be *Classical Mechanics and Dynamics*, because the notions of mechanics and dynamics, though much intertwined, are still somewhat different. Term m*echanics*, in its narrow sense, means deriving the equations of motion of point-like particles and their systems (including solids and fluids), solution of these equations, and interpretation of the results. *Dynamics* is a more ambiguous term; it may mean, in particular:

(i) the part of mechanics that deals with motion (in contrast to *statics*);

(ii) the part of mechanics that deals with reasons for motion (in contrast to *kinematics*);

(iii) the part of mechanics that focuses on its two last tasks, i.e. the solution of the equations of motion and discussion of the results.

The last definition invites a question. It may look that mechanics and dynamics are just two sequential steps of a single process; why should they be considered separate disciplines? The main reason is that the many differential equations of motion, obtained in classical mechanics, also describe processes in different systems, so that their analysis may reveal important features of these systems as well. For example, the famous ordinary differential equation

$$\ddot{x} + \omega_0^2 x = 0 \tag{1.1}$$

describes sinusoidal 1D oscillations not only of a mass on a spring, but also of an electric or magnetic field in a resonator, and many other systems. Similarly, the well-known partial differential equation

$$\left(\frac{1}{v^2} \frac{\partial^2}{\partial t^2} - \nabla^2 \right) f(\mathbf{r}, t) = 0 , \tag{1.2}$$

where v is a constant and ∇^2 is the Laplace operator,[2] describes not only acoustic waves in an elastic mechanical continuum (solid or fluid), but also electromagnetic waves in a non-dispersive media, certain chemical reactions, etc. Thus the results of analysis of the dynamics described by these equations may be reused for applications well beyond mechanics.

---

[1] The reader is advised to perform a self-check by solving a few problems of the dozen listed in Sec. 1.7. If the results are not satisfactory, it may make sense to start from some remedial reading. For that, I could recommend, for example (in the alphabetical order): G. R. Fowles and G. L. Cassiday, *Analytical Mechanics*, 7th ed., Brooks Cole, 2004; K. R. Symon, *Mechanics*, 3rd ed., Addison-Wesley, 1971; or J. B. Marion and S. T. Thornton, *Classical Dynamics of Particles and Systems,* 4th ed., Saunders, 1995.

[2] This series assumes reader's familiarity with the basic calculus and vector algebra. The formulas most important for this series are listed in the *Selected Mathematical Formulas* appendix, referred below as MA. In particular, a reminder of the definition and the basic properties of the Laplace operator may be found in MA Sec. 9.

To summarize, term "dynamics" is so ambiguous[3] that, after some hesitation, I have opted to using for this course the traditional name *Classical Mechanics*, implying its broader meaning, which includes (similarly to *Quantum Mechanics* and *Statistical Mechanics*) studies of dynamics of some non-mechanical systems.

1.2. Kinematics: Basic notions

The basic notions of kinematics may be defined in various ways, and some mathematicians pay a lot of attention to analyzing such systems of axioms and relations between them. In physics, we typically stick to less rigorous ways (in order to proceed faster to particular problems), and end debating a definition as soon as everybody in the room agrees that we are all speaking about the same thing. Let me hope that the following notions used in classical mechanics do satisfy this criterion:

(i) All the *Euclidean geometry* notions, including the *geometric point* (the mathematical abstraction for the position of a very small object), straight line, etc.

(ii) The *orthogonal, linear* ("Cartesian") *coordinates*[4] r_j of a geometric point in a particular *reference frame* – see Fig. 1.[5]

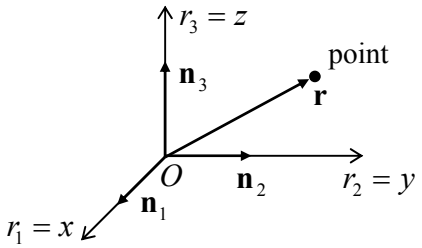

Fig. 1.1. Cartesian coordinates and radius-vector of a point/particle.

The coordinates may be used to define the point's *radius-vector*[6]

[3] Another important issue is: Definition (iii) of dynamics is suspiciously close to the part of mathematics devoted to the differential equation analysis; what is the difference? To answer, we have to dip, for just a second, into the philosophy of physics. Physics may be described as an art (and a bit of science :-) of description of Mother Nature by mathematical means; hence in many cases the approaches of a mathematician and a physicist to a problem are very similar. The main difference is that physicists try to express the results of their analysis in terms of *system's motion* rather than *function properties*, and as a result develop some sort of intuition ("gut feeling") about how other, apparently similar, systems may behave, even if their exact equations of motion are somewhat different - or not known at all. The intuition so developed has an enormous heuristic power, and most discoveries in physics have been made through gut-feeling-based insights rather than by plugging one formula into another one.

[4] In these notes the Cartesian coordinates are denoted either as either $\{r_1, r_2, r_3\}$ or $\{x, y, z\}$, depending on convenience in the particular case. Note that axis numbering is important for operations like the vector ("cross") product; the "correct" (meaning generally accepted) numbering order is such that rotation $\mathbf{n}_1 \to \mathbf{n}_2 \to \mathbf{n}_3 \to \mathbf{n}_1 \ldots$ looks counterclockwise if watched from a point with all $r_i > 0$ – see Fig. 1.

[5] In references to figures, formulas, problems and sections within the same chapter of these notes, the chapter number is dropped for brevity.

[6] From the point of view of the tensor theory (in which the physical vectors like $\mathbf{r}$ are considered the *rank-1 tensors*), it would be more natural to use superscripts in the components r_j and other "contravariant" vectors. However, the superscripts may be readily confused with the power signs, and I will postpone this notation (as well as the implied summation over the repeated indices) until the discussion of relativity in EM Chapter 9.

Radius-vector

$$\mathbf{r} = \sum_{j=1}^{3} \mathbf{n}_j r_j \,, \tag{1.3}$$

where $\mathbf{n}_1, \mathbf{n}_2, \mathbf{n}_3$ are the unit vectors along coordinate axis directions, with the *Euclidean metric*:

Euclidean metric

$$r^2 = \sum_{j=1}^{3} r_j^2 \,. \tag{1.4}$$

which is independent, in particular, of the distribution of matter in space.

(iii) The *time* – as described by a continuous scalar variable (say, t), typically considered an independent argument of various physical observables, in particular the point's radius-vector $\mathbf{r}(t)$. By accepting Eq. (4), and an implicit assumption that time t runs similarly in all reference frames, we subscribe to the notion of the *absolute* ("Newtonian") *space/time*, and hence abstain from a discussion of relativistic effects.[7]

(iv) The (instant) *velocity* of the point,

Velocity

$$\mathbf{v}(t) \equiv \frac{d\mathbf{r}}{dt} \equiv \dot{\mathbf{r}} \,, \tag{1.5}$$

and its *acceleration*:

Acceleration

$$\mathbf{a}(t) \equiv \frac{d\mathbf{v}}{dt} \equiv \dot{\mathbf{v}} = \ddot{\mathbf{r}} \,. \tag{1.6}$$

Since the above definitions of vectors $\mathbf{r}$, $\mathbf{v}$, and $\mathbf{a}$ depend on the chosen reference frame (are "reference-frame-specific"), there is a need to relate those vectors as observed in different frames. Within the Euclidean geometry, for two reference frames with the corresponding axes parallel in the moment of interest (Fig. 2), the relation between the radius-vectors is very simple:

Radius-vector's transformation

$$\mathbf{r}\big|_{\text{in } O'} = \mathbf{r}\big|_{\text{in } O} + \mathbf{r}_O\big|_{\text{in } O'} \,. \tag{1.7}$$

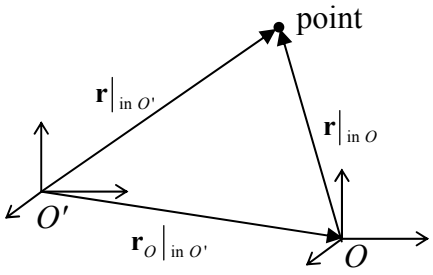

Fig. 1.2. Coordinate transfer between two reference frames.

[7] Following tradition, an introduction to special relativity is included into the *Classical Electrodynamics* ("EM") part of these notes. The relativistic effects are small if all particles velocities are much lower than the speed of light, $c \approx 3.00\times10^8$ m/s, and all distances are much larger then the system's *Schwarzschild radius* $r_s \equiv 2Gm/c^2$, where $G \approx 6.67\times10^{-11}$ SI units ($m^3/kg\cdot s$) is the Newtonian gravity constant, and m is system's mass. (More exact values of c, G, and some other physical constants may be found in appendix *CA: Selected Physical Constants*.)

If the frames move versus each other by *translation* only (no mutual rotation!), similar relations are valid for velocity and acceleration as well:

$$\mathbf{v}\big|_{\text{in } O'} = \mathbf{v}\big|_{\text{in } O} + \mathbf{v}_O\big|_{\text{in } O'}, \tag{1.8}$$

$$\mathbf{a}\big|_{\text{in } O'} = \mathbf{a}\big|_{\text{in } O} + \mathbf{a}_O\big|_{\text{in } O'}. \tag{1.9}$$

In the case of mutual rotation of the reference frames, notions like $\mathbf{v}_O\big|_{\text{in } O'}$ are not well defined. (Indeed, different points of a rigid body connected to frame *O* may have different velocities in frame *O'*.) As a result, the transfer laws for velocities and accelerations are more complex than those given by Eqs. (8) and (9). It will be more natural for me to discuss them in the end of Chapter 5 that is devoted to rigid body motion.

(v) The *particle*: a localized physical object whose size is negligible, and shape unimportant *for the given problem*. Note that the last qualification is extremely important. For example, the size and shape of a Space Shuttle are not too important for the discussion of its orbital motion, but are paramount when its landing procedures are being developed. Since classical mechanics neglects the quantum mechanical uncertainties,[8] particle's position, at any particular instant *t*, may be identified with a single geometric point, i.e. one radius-vector $\mathbf{r}(t)$. Finding the *laws of motion* $\mathbf{r}(t)$ of all particles participating in the given problem is frequently considered the final goal of classical mechanics.

1.3. Dynamics: Newton laws

Generally, the classical dynamics is fully described (in addition to the kinematic relations given above) by three *Newton laws*.[9] In contrast to the impression some textbooks on theoretical physics try to create, these laws are experimental in nature, and cannot be derived from *purely* theoretical arguments.[10]

I am confident that the reader of these notes is already familiar with the Newton laws, in one or another formulation. Let me note only that in some formulations the *1st Newton law* looks just as a particular case of the 2nd law - for the case of zero net force acting on a particle. In order to avoid this duplication, the 1st law may be formulated as the following postulate:

1st Newton law

- There exists at least one reference frame, called *inertial*, in which any *free particle* (i.e. a particle isolated from the rest of the Universe) moves with $\mathbf{v} = \text{const}$, i.e. with $\mathbf{a} = 0$.

According to Eq. (9), this postulate immediately means that there is also an infinite number of inertial frames, because all frames *O'* moving without rotation or acceleration relative to the postulated inertial frame *O* (i.e. having $\mathbf{a}_O\big|_{\text{in } O'} = 0$) are also inertial.

[8] This approximation is legitimate, crudely, when the product of the coordinate and momentum scales of the particle motion is much larger than the Planck's constant $\hbar \approx 1.054\times10^{-34}$ J·s. A more exact formulation may be found, e.g., in the *Quantum Mechanics* ("QM") part of these note series.

[9] Due to the genius of Sir Isaac Newton, these laws were formulated as early as in 1687, far ahead of the science of that time.

[10] Some laws of Nature (including the Newton laws) may be derived from certain more general postulates, such as the *Hamilton* (or "least action") *principle* - see Sec. 10.2 below. Note, however, that such derivations are only acceptable because all known corollaries of the postulates comply with all known experimental results.

On the other hand, the 2nd and 3rd Newton laws may be postulated *together* in the following elegant way. Each particle, say number k, may be characterized by a scalar constant (called *mass* m_k), such that at any interaction of N particles (isolated from the rest of the Universe), in any inertial system,

Total momentum and its conservation

$$\mathbf{P} \equiv \sum_{k=1}^{N} m_k \mathbf{v}_k = \text{const}. \tag{1.10}$$

(Each component of this sum,

Particle's momentum

$$\mathbf{p}_k \equiv m_k \mathbf{v}_k, \tag{1.11}$$

is called the *mechanical momentum* of the corresponding particle, and the whole sum $\mathbf{P}$, the *total momentum* of the system.)

Let us apply this postulate to just two interacting particles. Differentiating Eq. (10), written for this case, over time, we get

$$\dot{\mathbf{p}}_1 = -\dot{\mathbf{p}}_2. \tag{1.12}$$

Let us give the derivative $\dot{\mathbf{p}}_1$ (i.e., a vector) the name of *force* $\mathbf{F}_1$ excerted on particle 1. In our current case, when the only possible source of force is particle 2, the force may be denoted as $\mathbf{F}_{12}$. Similarly, $\mathbf{F}_{21} \equiv \dot{\mathbf{p}}_2$, so that we get the *3rd Newton law*

3rd Newton law

$$\mathbf{F}_{12} = -\mathbf{F}_{21}. \tag{1.13}$$

Now, returning to the general case of several interacting particles, we see that an additional (but very natural) assumption that all partial forces $\mathbf{F}_{kk'}$ acting on particle k add up as vectors, leads to the general form of the *2nd Newton law*[11]

2nd Newton law

$$m_k \mathbf{a}_k \equiv \dot{\mathbf{p}}_k = \sum_{k' \neq k} \mathbf{F}_{kk'} \equiv \mathbf{F}_k, \tag{1.14}$$

that allows a clear interpretation of the mass as a measure of particle's *inertia*.

As a matter of principle, if the dependence of all pair forces $\mathbf{F}_{kk'}$ of particle positions (and generally maybe of time as well) is known, Eq. (14) augmented with kinematic relations (4) and (5), allows the calculation of the laws of motion $\mathbf{r}_k(t)$ of all particles of the system. For example, for one particle the 2nd law (14) gives the ordinary differential equation of the second order,

$$m\ddot{\mathbf{r}} = \mathbf{F}(\mathbf{r}, t), \tag{1.15}$$

that may be integrated – either analytically or numerically.

For certain cases, this is very simple. As an elementary example, the Newton's gravity field

Newton's gravity law

$$\mathbf{F} = -G\frac{mm'}{R^3}\mathbf{R} \tag{1.16a}$$

(where $\mathbf{R} \equiv \mathbf{r} - \mathbf{r}'$ is the distance between particles of masses m and m')[12], is virtually uniform and may be approximated as

[11] Of course, for composite bodies of varying mass (e.g., rockets emitting jets, see Problem 1), momentum's derivative may differ from $m\mathbf{a}$.

$$\boxed{\mathbf{F} = m\mathbf{g},} \qquad (1.16b)$$

Uniform gravity field

with the vector $\mathbf{g} \equiv (Gm'/r'^3)\mathbf{r}'$ being constant, for local, relatively small-scale motions, with $r << r'$.[13] As a result, m in Eq. (15) cancels, it is reduced to just $\ddot{\mathbf{r}} = \mathbf{g}$, and may be easily integrated twice:

$$\dot{\mathbf{r}}(t) \equiv \mathbf{v}(t) = \int_0^t \mathbf{g}\, dt' + \mathbf{v}(0) = \mathbf{g}t + \mathbf{v}(0), \qquad (1.17)$$

$$\mathbf{r}(t) = \int_0^t \mathbf{v}(t')dt' + \mathbf{r}(0) = \mathbf{g}\frac{t^2}{2} + \mathbf{v}(0)t + \mathbf{r}(0)\,, \qquad (1.18)$$

thus giving the full solution of all those undergraduate problems on the projectile motion, which should be so familiar to the reader.

All this looks (and indeed is) very simple, but in most other cases leads to more complex calculations. As an example, let us consider another simple problem: a bead of mass m sliding, without friction, along a round ring of radius R in a gravity field obeying Eq. (16b) – see Fig. 3.

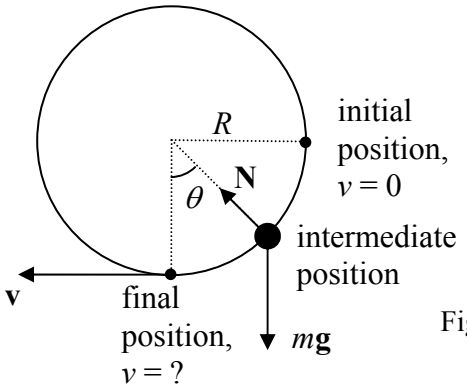

Fig. 1.3. Bead moving on a vertical ring.

Suppose we are only interested in bead's velocity v in the lowest point, after it has been dropped from the rest at the rightmost position. If we want to solve this problem using only the Newton laws, we have to do the following steps:

(i) consider the bead in an arbitrary intermediate position on a ring, described, for example by the angle θ shown in Fig. 3;

(ii) draw all the forces acting on the particle - in our current case, the gravity force $m\mathbf{g}$ and the reaction force $\mathbf{N}$ exerted by the ring;

---

[12] Note that the fact that the masses participating in Eqs. (14) and (16) are equal, the so-called *weak equivalence principle*, is highly nontrivial, but has been verified experimentally to the relative accuracy of at least 10^{-13}. Due to its conceptual significance of the principle, new space experiments, such as MISCROSCOPE (http://smsc.cnes.fr/MICROSCOPE/), are being planned for a substantial, nearly 100-fold accuracy improvement.

[13] Of course, the most important particular case of Eq. (1.16b) is the motion of objects near Earth's surface. In this case, using the fact that (1.16a) remains valid for the gravity field created by a heavy sphere, we get $g = GM_E/R_E^2$, where M_E and R_E are the Earth mass and radius. Plugging in their values, $M_E \approx 5.92\times10^{24}$ kg, $R_E \approx 6.37\times10^6$ m, we get $g \approx 9.74$ m/s^2. The effective value of g varies from 9.78 to 9.83 m/s^2 at various locations on Earth's surface (due to the deviations of Earth's shape from a sphere, and the location-dependent effect of the centrifugal "inertial force" – see Sec. 6.5 below), with an average value of $g \approx 9.807$ m/s^2 .

(iii) write the 2nd Newton law for two nonvanishing components of the bead acceleration, say for its vertical and horizontal components a_x and a_y;

(iv) recognize that in the absence of friction, the force **N** should be normal to the ring, so that we can use two additional equations, $N_x = -N\sin\theta$ and $N_y = N\cos\theta$;

(v) eliminate unknown variables N, N_x, and N_y from the resulting system of four equations, thus getting a single second-order differential equation for one variable, for example θ;

(vi) integrate this equation once to get the expression relating the velocity $\dot{\theta}$ and the angle θ; and, finally,

(vii) using our specific initial condition ($\dot{\theta} = 0$ at $\theta = \pi/2$), find the final velocity as $v = R\dot{\theta}$ at $\theta = 0$.

All this is very much doable, but please agree that the procedure it too cumbersome for such a simple problem. Moreover, in many other cases even writing equations of motion along relevant coordinates is very complex, and any help the general theory may provide is highly valuable. In many cases, such help is given by *conservation laws*; let us review the most general of them.

1.4. Conservation laws

(i) *Energy* conservation is arguably the most general law of physics, but in mechanics it takes a more humble form of *mechanical energy conservation* that has limited applicability. To derive it, we first have to define the *kinetic energy* of a particle as

Kinetic energy

$$T \equiv \frac{m}{2}v^2, \tag{1.19}$$

and then recast its differential as[14]

$$dT = d\left(\frac{m}{2}v^2\right) = d\left(\frac{m}{2}\mathbf{v}\cdot\mathbf{v}\right) = m\mathbf{v}\cdot d\mathbf{v} = m\frac{d\mathbf{v}\cdot d\mathbf{r}}{dt} = \frac{d\mathbf{p}}{dt}\cdot d\mathbf{r}. \tag{1.20}$$

Now plugging in the momentum's derivative from the 2nd Newton law, $d\mathbf{p}/dt = \mathbf{F}$, where **F** is the full force acting on the particle, we get relation $dT = \mathbf{F}\cdot d\mathbf{r}$. Its integration along particle's trajectory between some points A and B gives the relation that is sometimes called the *work-energy principle*:

Energy-work principle

$$\Delta T \equiv T(\mathbf{r}_B) - T(\mathbf{r}_A) = \int_A^B \mathbf{F}\cdot d\mathbf{r}, \tag{1.21}$$

where the integral in the right-hand part is called the *work* of the force **F** on the path from A to B.

The further step may be made only for *potential* (also called "conservative") forces that may be presented as (minus) gradients of some scalar function $U(\mathbf{r})$, called the *potential energy*.[15] The vector operator ∇ (called either *del* or *nabla*) of spatial differentiation[16] allows a very compact expression of this fact:

[14] Symbol $\mathbf{a}\cdot\mathbf{b}$ denotes the scalar (or "dot-") product of vectors **a** and **b** - see, e.g., MA Eq. (7.1).

[15] Note that because of its definition via the gradient, the potential energy is only defined to an arbitrary additive constant.

[16] Its basic properties are listed in MA Sec. 8.

$$\mathbf{F} = -\nabla U\,. \tag{1.22}$$

Potential energy

For example, for the uniform gravity field (16b),

$$U = mgh + \text{const}, \tag{1.23}$$

where h is the vertical coordinate directed "up" - opposite to the direction of the vector $\mathbf{g}$.

Integrating the tangential component F_τ of the vector $\mathbf{F}$, given by Eq. (22), along an arbitrary path connecting points A and B, we get

$$\int_A^B F_\tau dr \equiv \int_A^B \mathbf{F}\cdot d\mathbf{r} = U(\mathbf{r}_A) - U(\mathbf{r}_B)\,, \tag{1.24}$$

i.e. work of potential forces may be presented as the difference of values of function $U(\mathbf{r})$ in the initial and final point of the path. (Note that according to Eq. (24), work of a potential force on any closed trajectory, with $\mathbf{r}_A = \mathbf{r}_B$, is zero.)

Now returning to Eq. (21) and comparing it with Eq. (24), we see that

$$T(\mathbf{r}_B) - T(\mathbf{r}_A) = U(\mathbf{r}_A) - U(\mathbf{r}_B)\,, \tag{1.25}$$

so that the *total mechanical energy* E, defined as

$$E \equiv T + U\,, \tag{1.26}$$

Total mechanical energy

is indeed conserved:

$$E(\mathbf{r}_A) \equiv E(\mathbf{r}_B)\,, \tag{1.27}$$

Mechanical energy conservation

but for conservative forces only. (Non-conservative forces, e.g., friction, typically transfer energy from the mechanical form into some other form, e.g., heat.)

The mechanical energy conservation allows us to return for a second to the problem shown in Fig. 3 and solve it in one shot by writing Eq. (27) for the initial and final points:[17]

$$0 + mgR = \frac{m}{2}v^2 + 0. \tag{1.28}$$

Solving Eq. (28) for v immediately gives us the desired answer. Let me hope that the reader agrees that this way of problem solution is much simpler, and I have got his or her attention to discuss other conservation laws – which may be equally effective.

(ii) *Momentum*. Actually, the conservation of the full momentum of any system of particles isolated from the rest of the world, has already been discussed and may serve as the basic postulate of classical dynamics – see Eq. (10). In the case of one free particle the law is reduced to a trivial result $\mathbf{p}$ = const, i.e. $\mathbf{v}$ = const. If the system of N particles *is* affected by external forces $\mathbf{F}^{(\text{ext})}$, we may write

$$\mathbf{F}_k = \mathbf{F}_k^{(\text{ext})} + \sum_{k=1}^{N} \mathbf{F}_{kk'}\,. \tag{1.29}$$

[17] Here the arbitrary constant in Eq. (32) is chosen so that the potential energy is zero in the finite point.

If we sum up the resulting Eqs. (14) for all particles of the system then, due to the 3rd Newton law (13), the contributions of all internal forces to this double sum in the right-hand part cancel, and we get the equation

System's momentum evolution

$$\dot{\mathbf{P}} = \mathbf{F}^{(\text{ext})}, \quad \text{where } \mathbf{F}^{(ext)} \equiv \sum_{k=1}^{N} \mathbf{F}_k^{(\text{ext})}, \tag{1.30}$$

which tells us that the translational motion of the system as the whole is similar to that of a single particle, under the effect of the *net external force* $\mathbf{F}^{(\text{ext})}$. As a simple sanity check, if the external forces have a zero sum, we return to postulate (10). Just one reminder: Eq. (30), just as its precursor Eq. (14), is only valid in an inertial reference frame.

(iii) *Angular momentum* of a particle[18] is defined as the following vector:

Angular momentum: definition

$$\mathbf{L} \equiv \mathbf{r} \times \mathbf{p}, \tag{1.31}$$

where $\mathbf{a}\times\mathbf{b}$ means the vector (or "cross-") product of the vector operands.[19] Now, differentiating Eq. (31) over time, we get

$$\dot{\mathbf{L}} = \dot{\mathbf{r}} \times \mathbf{p} + \mathbf{r} \times \dot{\mathbf{p}}. \tag{1.32}$$

In the first product, $\dot{\mathbf{r}}$ is just the velocity vector $\mathbf{v}$ which is parallel to the particle momentum $\mathbf{p} = m\mathbf{v}$, so that this product vanishes, since the vector product of any two parallel vectors is zero. In the second product, $\dot{\mathbf{p}}$ equals the full force $\mathbf{F}$ acting on the particle, so that Eq. (32) is reduced to

Angular momentum: evolution

$$\dot{\mathbf{L}} = \boldsymbol{\tau}, \tag{1.33}$$

where vector

Torque

$$\boldsymbol{\tau} \equiv \mathbf{r} \times \mathbf{F}, \tag{1.34}$$

is called the *torque* of force $\mathbf{F}$. (Note that the torque is evidently reference-frame specific - and again, the frame has to be inertial for Eq. (33) to be valid.) For an important particular case of a *central* force $\mathbf{F}$ that is parallel to the radius vector $\mathbf{r}$ of a particle (as measured from the force source point), the torque vanishes, so that (in that particular reference frame only!) the angular momentum is conserved:

Angular momentum: conservation

$$\mathbf{L} = \text{const}. \tag{1.35}$$

For a system of N particles, the total angular momentum is naturally defined as

$$\mathbf{L} \equiv \sum_{k=1}^{N} \mathbf{L}_k. \tag{1.36}$$

Differentiating this equation over time, using Eq. (33) for each $\dot{\mathbf{L}}_k$, and again partitioning each force in a accordance with Eq. (29), we get

[18] Here we imply that the internal motions of the particle, including its rotation about its own axis, are negligible. (Otherwise it could not be represented by a geometrical point, as was postulated in Sec. 1.) For a body with substantial rotation (see Chapter 6 below), vector $\mathbf{L}$ retains its definition (32), but is only a part of the total angular momentum and is called the *orbital momentum* – even if the particle does not move along a closed orbit.

[19] See, e.g., MA Eq. (7.3).

$$\dot{\mathbf{L}} = \sum_{\substack{k,k'=1 \\ k'\neq k}}^{N} \mathbf{r}_k \times \mathbf{F}_{kk'} + \boldsymbol{\tau}^{(ext)}, \quad \text{where } \boldsymbol{\tau}^{(ext)} \equiv \sum_{k=1}^{N} \mathbf{r}_k \times \mathbf{F}_k^{(ext)}. \tag{1.37}$$

The first (double) sum may be always divided into pairs of the type ($\mathbf{r}_k \times \mathbf{F}_{kk'} + \mathbf{r}_{k'} \times \mathbf{F}_{k'k}$). With a natural assumption of the central forces ($\mathbf{F}_{kk'} \parallel \mathbf{r}_k - \mathbf{r}_{k'}$), each of these pairs equals zero. Indeed, in this case both components of the pair are vectors perpendicular to the plane passed through positions of both particles and the reference frame origin, i.e. to the plane of drawing of Fig. 4. Also, due to the 3rd Newton law (13) the two forces are equal and opposite, and the magnitude of each term in the sum may be presented as $|F_{kk'}| h_{kk'}$, with equal "lever arms" $h_{kk'} = h_{k'k}$. As a result, each sum ($\mathbf{r}_k \times \mathbf{F}_{kk'} + \mathbf{r}_{k'} \times \mathbf{F}_{k'k}$), and hence the whole double sum in Eq. (37) vanish, and it is reduced to a very simple result,

System' s angular momentum evolution

$$\boxed{\dot{\mathbf{L}} = \boldsymbol{\tau}^{(ext)}}, \tag{1.38}$$

that is similar to Eq. (33) for a single particle, and is the angular analog of Eq. (30). In particular, Eq. (38) shows that if the full external torque $\boldsymbol{\tau}^{(ext)}$ vanishes by some reason (e.g., if the system of particles is isolated from the rest of the Universe), the conservation law (35) is valid for the full angular momentum $\mathbf{L}$, even if its individual components $\mathbf{L}_k$ are not conserved due to inter-particle interactions.

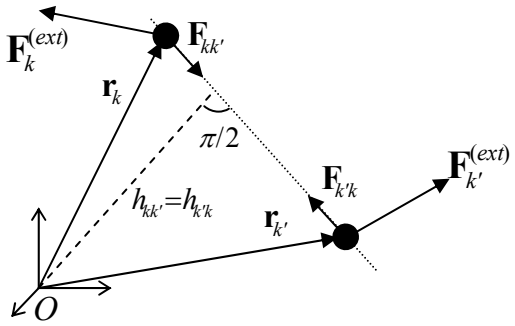

Fig. 1.4. Internal and external forces, and the internal torque cancellation in a system of two particles.

From the mathematical point of view, most conservation laws present *the first integrals of motion* which sometimes liberate us from the necessity to integrate the second-order differential equations of motion, following from the Newton laws, twice.

1.5. Potential energy and equilibrium

Another important role of the potential energy U, especially for dissipative systems whose total mechanical energy E is *not* conserved because it may be drained to the environment, is finding the positions of equilibrium (sometimes called the *fixed points* of the system under analysis) and analyzing their stability with respect to small perturbations. For a single particle, this is very simple: force (22) vanishes at each extremum (minimum or maximum) of the potential energy.[20] Of those fixed points, only the minimums of $U(\mathbf{r})$ are stable – see Sec. 3.2 below for a discussion of this point.

[20] Assuming that the additional, non-conservative forces (such as viscosity) responsible for the mechanical energy drain, vanish at equilibrium – as they typically do. (Static friction is one counter-example.)

A slightly more subtle case is a particle with potential energy $U(\mathbf{r})$, subjected to an *additional* external force $\mathbf{F}^{(\text{ext})}(\mathbf{r})$. In this case, the stable equilibrium is reached at the minimum of not function $U(\mathbf{r})$, but of what is sometimes called the *Gibbs potential energy*

Gibbs' potential energy

$$U_{\text{G}}(\mathbf{r}) \equiv U(\mathbf{r}) - \int^{\mathbf{r}} \mathbf{F}^{(\text{ext})}(\mathbf{r}') \cdot d\mathbf{r}', \tag{1.39}$$

which is defined, just as $U(\mathbf{r})$ is, to an arbitrary constant. The proof of Eq. (39) is very simple: in an extremum of this function, the total force acting on the particle,

$$\mathbf{F}^{(\text{tot})} = \mathbf{F} + \mathbf{F}^{(\text{ext})} \equiv -\nabla U + \nabla \int^{\mathbf{r}} \mathbf{F}^{(\text{ext})}(\mathbf{r}') \cdot d\mathbf{r}' = -\nabla U_{\text{G}}, \tag{1.40}$$

vanishes, as it should.[21] For the simplest (and very frequent) case of the applied force independent on particle's position, the Gibbs potential energy is just

$$U_{\text{G}}(\mathbf{r}) \equiv U(\mathbf{r}) - \mathbf{F}^{(\text{ext})} \cdot \mathbf{r} + \text{const}. \tag{1.41}$$

This is all very straightforward, but since the notion of U_{G} is not well known to some students,[22] let me offer a very simple example. Consider a 1D deformation of the usual elastic spring providing the returning force $(-\kappa x)$, where x is the deviation from spring's equilibrium. In order for the force to comply with Eq. (22), its potential energy should equal to $U = \kappa x^2/2 + \text{const}$, so that its minimum corresponds to $x = 0$. This works fine until the spring comes under effect of a nonvanishing external force F, say independent of x. Then the equilibrium deformation of the spring, $x_0 = F/\kappa$, evidently corresponds not to the minimum of U but rather to that of the Gibbs potential energy (41): $U_{\text{G}} = U - Fx = \kappa x^2/2 - Fx + \text{const}$.

1.6. OK, we've got it - can we go home now?

Not yet. In many cases the conservation laws discussed above provide little help, even in systems without dissipation. Consider for example a generalization of the bead-on-the-ring problem shown in Fig. 3, in which the ring is rotated by external forces, with a constant angular velocity ω, about its vertical diameter (Fig. 5).[23] In this problem (to which I will repeatedly return below, using it as

[21] Physically, the difference $U_{\text{G}} - U$ specified by Eq. (39) may be considered the $\mathbf{r}$-dependent part of the potential energy $U^{(\text{ext})}$ of the external system responsible for the force $\mathbf{F}^{(\text{ext})}$, so that U_{G} is just the total potential energy $U + U^{(\text{ext})}$, besides the part of $U^{(\text{ext})}$ which does not depend on $\mathbf{r}$ and hence is irrelevant for the fixed point analysis. According to the 3rd Newton law, the force exerted by the particle on the external system equals $(-\mathbf{F}^{(\text{ext})})$, so that its work (and hence the change of $U^{(\text{ext})}$ due to the change of $\mathbf{r}$) is given by the second term in the right-hand part of Eq. (39). Thus the condition of equilibrium, $-\nabla U_{\text{G}} = 0$, is just the condition of an extremum of the total potential energy, $U + U^{(ext)}$, of the two interacting systems.

[22] Unfortunately, in most physics teaching plans the introduction of U_{G} is postponed until a course of statistical mechanics and/or thermodynamics - where it is a part of the *Gibbs free energy*, in contrast to U, which is a part of the *Helmholtz free energy* - see, e.g., Sec. 1.4 of the *Statistical Mechanics* ("SM") part of my notes. However, the reader should agree that the difference between U_{G} and U, and hence that between the Gibbs and Helmholtz free energies, has nothing to do with statistics or thermal motion, and belongs to the basic mechanics.

[23] This is essentially a simplified model of the famous mechanical control device called the *centrifugal* (or "flyball, or "centrifugal flyball") *governor* – see, e.g., http://en.wikipedia.org/wiki/Centrifugal_governor.

an analytical mechanics "testbed"), none of the three conservation laws listed in the last section, holds. In particular, bead's energy,

$$E = \frac{m}{2}v^2 + mgh, \tag{1.42}$$

is *not* constant, because the external forces rotating the ring may change it. Of course, we still can solve the problem using the Newton laws, but this is even more complex than for the above case of the ring at rest, in particular because the force **N** exerted on the bead by the ring now may have three rather than two Cartesian components, which are not simply related. One can readily see that if we could exclude the so-called *reaction forces* such as **N**, that ensure *external constraints* of the particle motion, in advance, that would help a lot. Such an exclusion may be provided by analytical mechanics, in particular its Lagrangian formulation, which will be discussed in the next chapter.

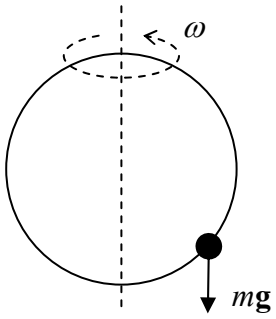

Fig. 1.5. Bead sliding along a rotating ring.

An even more important motivation for analytical mechanics is given by dynamics of "non-mechanical" systems, for example, of the electromagnetic field – possibly interacting with charged particles, conducting bodies, etc. In many such systems, the easiest (and sometimes the only practicable) way to find the equations of motion is to derive then from the Lagrangian or Hamiltonian function of the system. In particular, the Hamiltonian formulation of the analytical mechanics (to be discussed in Chapter 10) offers a direct pathway to deriving Hamiltonian operators of systems, which is the standard entry point for analysis of their quantum-mechanical properties.

1.7. Self-test problems

1.1. A bicycle, ridden with velocity v on a wet pavement, has no mudguards on its wheels. How far behind should the following biker ride to avoid being splashed over? Neglect the air resistance effects.

1.2. Two round disks of radius R are firmly connected with a coaxial cylinder of a smaller radius r, and a thread is wound on the resulting spool. The spool is placed on a horizontal surface, and thread's end is being pooled out at angle φ - see Fig. on the right. Assuming that the spool does not slip on the surface, what direction would it roll?

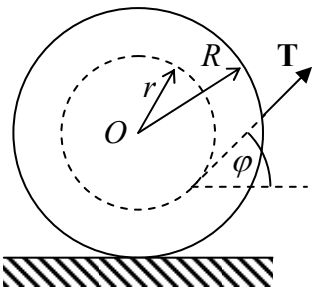

(Sometimes the device is called the "Watt's governor", after the famous engineer J. Watts who used it in 1788 in one of his first steam engines, though it had been used in European windmills at least since the 1600s.)

1.3. Calculate the equilibrium shape of a flexible, heavy rope of length l, with a constant mass μ per unit length, if it is hung in a uniform gravity field between two points separated by a horizontal distance d – see Fig. on the right.

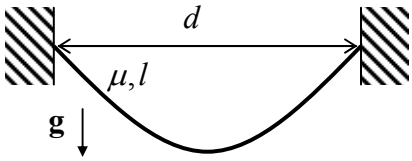

1.4. A uniform, long, thin bar is placed horizontally on two similar round cylinders rotating toward each other with the same angular velocity ω and displaced by distance d – see Fig. on the right. Calculate the laws of relatively slow horizontal motions of the bar within the plane of drawing for both possible directions of cylinder rotation, assuming that the friction force between the slipping surfaces of the bar and each cylinder obeys the usual simple law $|F| = \mu N$, where N is the normal pressure force between them, and μ is a constant (velocity-independent) coefficient. Formulate the condition of validity of your result.

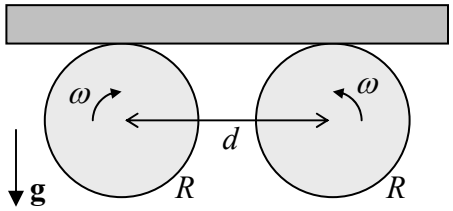

1.5. A small block slides, without friction, down a smooth slide that ends with a round loop of radius R – see Fig. on the right. What smallest initial height h allows the block to make its way around the loop without dropping from the slide, if it is launched with negligible initial velocity?

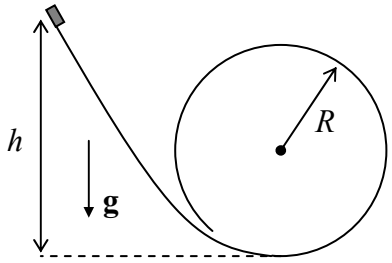

1.6. A satellite of mass m is being launched from height H over the surface of a spherical planet with radius R and mass $M >> m$ - see Fig. on the right. Find the range of initial velocities $\mathbf{v}_0$ (normal to the radius) providing closed orbits above the planet's surface.

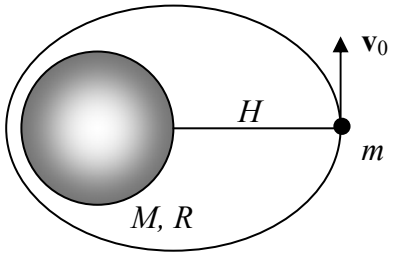

1.7. Prove that the thin-uniform-disk model of a galaxy describes small harmonic oscillations of stars inside it along the direction normal to the disk, and calculate the frequency of these oscillations in terms of the Newton's gravitational constant G and the average density ρ of the star/dust matter of the galaxy.

1.8. Derive the differential equations of motion for small oscillations of two similar pendula coupled with a spring (see Fig. on the right), within the vertical plane. Assume that at the vertical position of both pendula, the spring is not stretched ($\Delta L = 0$).

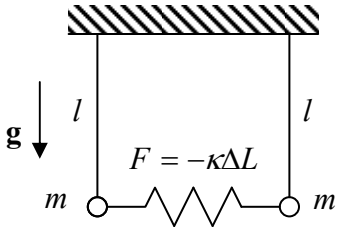

1.9. One of popular futuristic concepts of travel is digging a straight railway tunnel through the Earth and letting a train go through it, without initial velocity - driven only by gravity. Calculate train's travel time through such a tunnel, assuming that the Earth's density ρ is constant, and neglecting the friction and planet rotation effects.

1.10. A small bead of mass m may slide, without friction, along a light horizontal string, stretched with a force $\mathcal{T} >> mg$ between two points separated by a horizontal distance $2d$ – see Fig. on the right. Find the frequency of small oscillations of the bead about its equilibrium position.

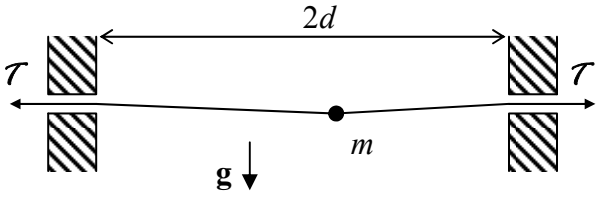

1.11. Find the acceleration of a rocket due to the working jet motor, and explore the resulting equation of rocket's motion.

Hint: For the sake of simplicity, you may consider a 1D motion.

1.12. Prove the following *virial theorem*:[24] for a set of N particles performing a periodic motion,

$$\overline{T} = -\frac{1}{2}\sum_{k=1}^{N}\overline{\mathbf{F}_k \cdot \mathbf{r}_k},$$

where (as everywhere in these notes), the top bar means time averaging – in this case over the motion period. What does the virial theorem say about:

(i) the 1D motion of a particle in a confining potential $U(x) = ax^{2s}$, with $a > 0$ and $s > 0$, and
(ii) the orbital motion of a particle moving in a central potential $U(r) = -C/r$?

Hint: Explore the time derivative of the following scalar function of time: $G(t) \equiv \sum_{k=1}^{N}\mathbf{p}_k \cdot \mathbf{r}_k$.

[24] It was first stated by R. Clausius in 1870.

Chapter 2. Lagrangian Formalism

The goal of this chapter is to describe the Lagrangian formulation of analytical mechanics, which is extremely useful for obtaining the differential equations of motion (*and sometimes their first integrals*) *not only for mechanical systems with holonomic constraints, but also other dynamic systems.*

2.1. Lagrange equations

In many cases, the constraints imposed on 3D motion of a system of N particles may be described by N vector (i.e. $3N$ scalar) algebraic equations

$$\mathbf{r}_k = \mathbf{r}_k(q_1, q_2, ..., q_j, ..., q_J, t), \quad 1 \le k \le N, \tag{2.1}$$

where q_j are certain *generalized coordinates* which (together with constraints) completely define the system position, and $J \le 3N$ is the number of the actual *degrees of freedom*. The constraints that allow such description are called *holonomic*. [1]

For example, for our testbed, bead-on-rotating-ring problem (see Fig. 1.5 and Fig. 1 below) $J = 1$, because taking into account the constraints imposed by the ring, bead's position may be uniquely determined by just one generalized coordinate – for example, its polar angle θ. Indeed, selecting the reference frame as shown in Fig. 1 and using the well-known formulas for the spherical coordinates,[2] we see that in this case Eq. (1) in Cartesian coordinates has the form

$$\mathbf{r} \equiv \{x, y, z\} = \{R\sin\theta\cos\varphi, R\sin\theta\sin\varphi, R\cos\theta\}, \quad \text{where } \varphi = \omega t + \text{const}, \tag{2.2}$$

where the constant depends on the exact selection of axes x and y and the time origin. Since $\varphi(t)$ is a fixed function of time, and R is a fixed constant, the position of particle in space at any instant t is indeed completely determined by the value of its only generalized coordinate θ. Note that the dimensionality of the generalized coordinate may be different from that of Cartesian coordinates (meters)!

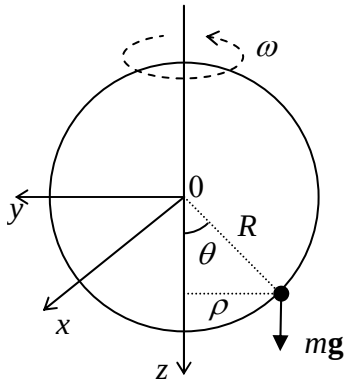

Fig. 2.1. Bead on a rotating ring as a example of the system with just one degree of freedom: $J = 1$.

[1] Possibly, the simplest example of a *non-holonomic* constraint is a set of inequalities describing the hard walls confining the motion of particles in a closed volume. Non-holonomic constraints are better dealt with other methods, e.g., by imposing proper boundary conditions on the (otherwise unconstrained) motion.

[2] See, e.g., MA Eq. (10.7).

Now returning to the general case of J degrees of freedom, let us consider a set of small *variations* (alternatively called "virtual displacements") δq_j allowed by the constraints. Virtual displacements differ from the actual small displacements (described by *differentials* dq_j proportional to time variation dt) in that δq_j describes not the system's motion as such, but rather its possible variation – see Fig. 1.

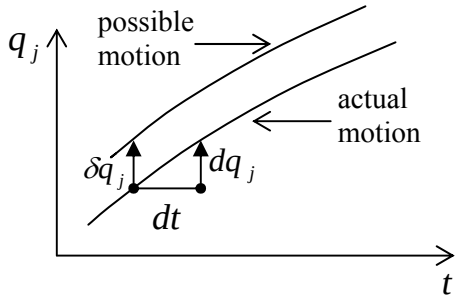

Fig. 2.2. Actual displacement dq_j vs. the virtual one (i.e. variation) δq_j.

Generally, operations with variations are the subject of a special field of mathematics, the calculus of variations.[3] However, the only math background necessary for our current purposes is the understanding that operations with variations are similar to those with the usual differentials, though we need to watch carefully what each variable is a function of. For example, if we consider the variation of the radius-vectors (1), at a fixed time t, as a function of independent variations δq_j, we may use the usual formula for the differentiation of a function of several arguments:[4]

$$\delta \mathbf{r}_k = \sum_j \frac{\partial \mathbf{r}_k}{\partial q_j} \delta q_j . \tag{2.3}$$

Now let us break the force acting upon the k-th particle into two parts: the frictionless, constraining part $\mathbf{N}_k$ of the reaction force and the remaining part $\mathbf{F}_k$ – including the force components from other sources and possibly the friction part of the reaction force. Then the 2nd Newton law for k-th particle of the system may be presented as

$$m_k \dot{\mathbf{v}}_k - \mathbf{F}_k = \mathbf{N}_k . \tag{2.4}$$

Since any variation of the motion has to be allowed by the constraints, its $3N$-dimensional vector with N 3D-vector components $\delta \mathbf{r}_k$ has to be perpendicular to the $3N$-dimensional vector of the constraining forces, also with N 3D-vector components $\mathbf{N}_k$. (For example, for the problem shown in Fig. 2.1, the virtual displacement vector $\delta \mathbf{r}_k$ may be directed only along the ring, while the constraining force **N,** exerted by the ring, has to be perpendicular to that direction.) This condition may be expressed as

$$\sum_k \mathbf{N}_k \cdot \delta \mathbf{r}_k = 0 , \tag{2.5}$$

[3] For a concise introduction to the field see, e.g., I. Gelfand and S. Fomin, *Calculus of Variations*, Dover, 2000 or L. Elsgolc, *Calculus of Variations*, Dover, 2007. An even shorter review may be found in Chapter 17 of Arfken and Weber - see MA Sec. 16. For a more detailed discussion, using many examples from physics, see R. Weinstock , *Calculus of Variations*, Dover, 2007.

[4] See, e.g., MA Eq. (4.2). In all formulas of this section, all summations over index j are from 1 to J, while those over the particle number k are from 1 to N.

where the scalar product of 3*N*-dimensional vectors is defined exactly as that of 3D vectors, i.e. as the sum of the products of the corresponding components of the operands. The substitution of Eq. (4) into Eq. (5) results in the so-called *D'Alembert principle*:[5]

D'Alembert principle

$$\sum_k (m_k \dot{\mathbf{v}}_k - \mathbf{F}_k) \cdot \delta \mathbf{r}_k = 0 . \tag{2.6}$$

Now we may plug Eq. (3) into Eq. (6) to get

$$\sum_j \left\{ \sum_k m_k \dot{\mathbf{v}}_k \cdot \frac{\partial \mathbf{r}_k}{\partial q_j} - \mathcal{F}_j \right\} \delta q_j = 0 \tag{2.7}$$

where scalars $\mathcal{F}_j$, called *generalized forces*, are defined as follows:[6]

$$\mathcal{F}_j \equiv \sum_k \mathbf{F}_k \cdot \frac{\partial \mathbf{r}_k}{\partial q_j} . \tag{2.8}$$

Now we may use the standard argument of the calculus of variations: in order for the left-hand part of Eq. (7) to be zero for an arbitrary selection of independent variations δq_j, the expressions in the curly brackets, for every j, should equal zero. This gives us a set of J equations

$$\sum_k m_k \dot{\mathbf{v}}_k \cdot \frac{\partial \mathbf{r}_k}{\partial q_j} - \mathcal{F}_j = 0 ; \tag{2.9}$$

let us present them in a more convenient form. First, using the differentiation by parts to calculate the following time derivative:

$$\frac{d}{dt}\left(\mathbf{v}_k \cdot \frac{\partial \mathbf{r}_k}{\partial q_j} \right) = \dot{\mathbf{v}}_k \cdot \frac{\partial \mathbf{r}_k}{\partial q_j} + \mathbf{v}_k \frac{d}{dt}\left(\frac{\partial \mathbf{r}_k}{\partial q_j} \right), \tag{2.10}$$

we may notice that the first term in the right-hand part is exactly the scalar product in the first term of Eq. (9).

Second, let us use another key fact of the calculus of variations (which is, essentially, evident from Fig. 3): the differentiation of a variable over time and over the generalized coordinate variation (at fixed time) are interchangeable operations.

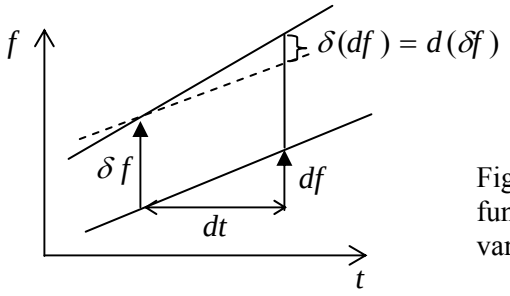

Fig. 2.3. Variation of the differential (of any function *f*) equals the differential of its variation.

[5] It had been spelled out in a 1743 work by J.-B. le Rond d'Alembert, though the core of this result has been traced to an earlier work by J. Bernoulli (1667 – 1748).

[6] Note that since the dimensionality of generalized coordinates may be arbitrary, that of generalized forces may also differ from the newton.

As a result, in the second term on the right-hand part of Eq. (10) we may write

$$\frac{d}{dt}\left(\frac{\partial \mathbf{r}_k}{\partial q_j}\right) = \frac{\partial}{\partial q_j}\left(\frac{d\mathbf{r}_k}{dt}\right) \equiv \frac{\partial \mathbf{v}_k}{\partial q_j}. \tag{2.11}$$

Finally, let us differentiate of Eq. (1) over time:

$$\mathbf{v}_k \equiv \frac{d\mathbf{r}_k}{dt} = \sum_j \frac{\partial \mathbf{r}_k}{\partial q_j}\dot{q}_j + \frac{\partial \mathbf{r}_k}{\partial t}. \tag{2.12}$$

This equation shows that particle velocities $\mathbf{v}_k$ may be considered as linear functions of the generalized velocities $\dot{q}_j$ *considered as independent variables*, with proportionality coefficients

$$\frac{\partial \mathbf{v}_k}{\partial \dot{q}_j} = \frac{\partial \mathbf{r}_k}{\partial q_j}. \tag{2.13}$$

With the account of Eqs. (10), (11), and (13), Eq. (9) turns into

$$\frac{d}{dt}\sum_k m_k \mathbf{v}_k \cdot \frac{\partial \mathbf{v}_k}{\partial \dot{q}_j} - \sum_k m_k \mathbf{v}_k \frac{\partial \mathbf{v}_k}{\partial q_j} - \mathcal{F}_j = 0 \tag{2.14}$$

This result may be further simplified by making, for the total kinetic energy of the system,

$$T \equiv \sum_k \frac{m_k}{2} v_k^2 = \frac{1}{2}\sum_k m_k \mathbf{v}_k \cdot \mathbf{v}_k, \tag{2.15}$$

the same commitment as for $\mathbf{v}_k$, i.e. considering T a function of not only the generalized coordinates q_j and time t, but also of the generalized velocities $\dot{q}_i$ - as variables independent of q_j and t. Then we may calculate the partial derivatives of T as

$$\frac{\partial T}{\partial q_j} = \sum_k m_k \mathbf{v}_k \cdot \frac{\partial \mathbf{v}_k}{\partial q_j}, \qquad \frac{\partial T}{\partial \dot{q}_j} = \sum_k m_k \mathbf{v}_k \cdot \frac{\partial \mathbf{v}_k}{\partial \dot{q}_j}, \tag{2.16}$$

and notice that they are exactly the two sums participating in Eq. (13). As a result, we get a system of J *Lagrange equations*,[7]

$$\boxed{\frac{d}{dt}\frac{\partial T}{\partial \dot{q}_j} - \frac{\partial T}{\partial q_j} - \mathcal{F}_j = 0, \quad \text{for } j = 1, 2, \ldots, J.} \tag{2.17}$$

General Lagrange equations

Their big advantage over the initial Newton law equations (4) is that the Lagrange equations do not include the constraining forces $\mathbf{N}_k$.

This is as far as we can go for arbitrary forces. However, if all the forces may be expressed in the form similar but somewhat more general than Eq. (1.31), $\mathbf{F}_k = -\nabla_k U(\mathbf{r}_1, \mathbf{r}_2, \ldots, \mathbf{r}_N, t)$, where U is the

[7] They were derived in 1788 by J.-L. Lagrange who pioneered the whole field of analytical mechanics - not to mention his key contributions to number theory and celestial mechanics.

effective potential energy of the system,[8] and sign ∇_k denotes differentiation over coordinates of k-th particle, we may recast Eq. (8) into a simpler form:

$$\mathcal{T}_j \equiv \sum_k \mathbf{F}_k \cdot \frac{\partial \mathbf{r}_k}{\partial q_j} = -\sum_k \left(\frac{\partial U}{\partial x_k} \cdot \frac{\partial x_k}{\partial q_j} + \frac{\partial U}{\partial y_k} \cdot \frac{\partial y_k}{\partial q_j} + \frac{\partial U}{\partial z_i} \cdot \frac{\partial z_i}{\partial q_j} \right) \equiv -\frac{\partial U}{\partial q_j}. \tag{2.18}$$

Since we assume that U depends only on particle coordinates (and possibly time), but not velocities, $\partial U / \partial \dot{q}_j = 0$, with the substitution of Eq. (18), the Lagrange equation (17) may be presented in its *canonical form*

Canonical Lagrange equations

$$\boxed{\frac{d}{dt}\frac{\partial L}{\partial \dot{q}_j} - \frac{\partial L}{\partial q_j} = 0, \quad \text{where } L \equiv T - U.} \tag{2.19a}$$

where L is called the *Lagrangian function* (or just the "Lagrangian"), defined as

Lagrangian function

$$\boxed{L \equiv T - U\ .} \tag{2.19b}$$

It is crucial to distinguish this function from the mechanical energy (1.26), $E = T + U$.

Using the Lagrangian formalism in practice, the reader should always remember that:

(i) Each system has only *one* Lagrange function L, but is described by $J \geq 1$ Lagrange equations of motion (for $j = 1, 2, \ldots, J$).

(ii) Differentiating T, we have to consider the generalized velocities $\dot{q}_j$ as independent variables, ignoring the fact they are actually the time derivatives of q_j.

2.2. Examples

As the first, simplest example, consider a particle constrained to move along one axis (say, x):

$$T = \frac{m}{2}\dot{x}^2, \quad U = U(x,t). \tag{2.20}$$

In this case, it is natural to consider x as the (only) generalized coordinate, and $\dot{x}$ as the generalized velocity, so that

$$L \equiv T - U = \frac{m}{2}\dot{x}^2 - U(x,t). \tag{2.21}$$

Considering $\dot{x}$ an independent variable, we get $\partial L / \partial \dot{x} = m\dot{x}$, and $\partial L / \partial x = -\partial U / \partial x$, so that the Lagrange equation of motion (only one equation in this case of the single degree of freedom!) yields

$$\frac{d}{dt}(m\dot{x}) - \left(-\frac{\partial U}{\partial x} \right) = 0, \tag{2.22}$$

[8] Note that due to the possible time dependence of U, Eq. (17) does not mean that forces $\mathbf{F}_k$ have to be conservative – see the next section for more discussion. With this understanding, I will still use for function U the convenient name of "potential energy".

evidently the same result as the *x*-component of the 2nd Newton law with $F_x = -\partial U/\partial x$. This is a good sanity check, but we see that the Lagrange formalism does not provide too much advantage in this particular case.

This advantage is, however, evident for our testbed problem – see Fig. 1. Indeed, taking the polar angle θ for the (only) generalized coordinate, we see that in this case the kinetic energy depends not only on the generalized velocity, but also on the generalized coordinate:[9]

$$T = \frac{m}{2}R^2\left(\dot{\theta}^2 + \omega^2 \sin^2\theta\right), \qquad U = -mgz + \text{const} = -mgR\cos\theta + \text{const},$$
$$L \equiv T - U = \frac{m}{2}R^2\left(\dot{\theta}^2 + \omega^2 \sin^2\theta\right) + mgR\cos\theta + \text{const}. \tag{2.23}$$

Here it is especially important to remember that at substantiating the Lagrange equation, θ and $\dot{\theta}$ have to be treated as independent arguments of *L*, so that

$$\frac{\partial L}{\partial \dot{\theta}} = mR^2\dot{\theta}, \quad \frac{\partial L}{\partial \theta} = mR^2\omega^2 \sin\theta\cos\theta - mgR\sin\theta, \tag{2.24}$$

giving us the following equation of motion:

$$\frac{d}{dt}\left(mR^2\dot{\theta}\right) - \left(mR^2\omega^2 \sin\theta\cos\theta - mgR\sin\theta\right) = 0. \tag{2.25}$$

As a sanity check, at $\omega = 0$, Eq. (25) is reduced to the correct equation of the usual pendulum:

$$\ddot{\theta} + \Omega^2 \sin\theta = 0, \quad \text{where } \Omega \equiv \left(\frac{g}{R}\right)^{1/2}. \tag{2.26}$$

We will explore the full dynamic equation (25) in more detail later, but please note how simple its derivation was - in comparison with writing the Newton laws and then excluding the reaction force.

Next, though the Lagrangian formalism was derived from the Newton law for mechanical systems, the resulting equations (19) are applicable to other dynamic systems, especially those for which the kinetic and potential energies may be readily expressed via some generalized coordinates. As the simplest example, consider the well-known connection (Fig. 4) of a capacitor with capacitance *C* to an inductive coil with self-inductance *L*.[10] (Electrical engineers frequently call it the *LC tank circuit*.)

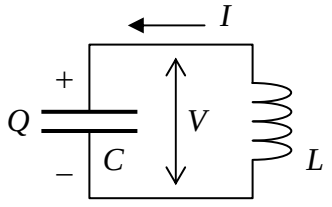

Fig. 2.4. *LC* tank circuit.

[9] This expression for $T \equiv (m/2)(\dot{x}^2 + \dot{y}^2 + \dot{z}^2)$ may be readily obtained either by the formal differentiation of Eq. (2) over time, or just by noticing that the velocity vector has two perpendicular components: one along the ring (with magnitude $R\dot{\theta}$) and another one normal to the ring plane (with magnitude $\omega\rho = \omega R\sin\theta$ - see Fig. 1).

[10] Let me hope that this traditional notation would not lead to the confusion between the inductance and the Lagrange function.

As the reader certainly knows, at relatively low frequencies we may use the so-called lumped-circuit approximation, in which the total energy of the system as the sum of two components, the electric energy E_C localized inside the capacitor, and the magnetic energy E_L localized inside the inductance coil

$$E_C = \frac{Q^2}{2C}, \quad E_L = \frac{LI^2}{2}. \tag{2.27}$$

Since the electric current I through the coil and the electric charge Q on the capacitor are connected by the charge continuity equation $dQ/dt = I$ (evident from Fig. 4), it is natural to declare the charge a generalized coordinate, and the current, the generalized velocity. With this choice, the electrostatic energy E_C (Q) should may be treated as the potential energy U of the system, and the magnetic energy $E_L(I)$, as its kinetic energy T. With this attribution, we get

$$\frac{\partial T}{\partial \dot{q}} \equiv \frac{\partial E_L}{\partial I} = LI \equiv L\dot{Q}, \qquad \frac{\partial T}{\partial q} \equiv \frac{\partial E_L}{\partial Q} = 0, \qquad \frac{\partial U}{\partial q} \equiv \frac{\partial E_C}{\partial Q} = \frac{Q}{C}, \tag{2.28}$$

so that the Lagrange equation of motion is

$$\frac{d}{dt}\left(L\dot{Q}\right) - \left(-\frac{Q}{C}\right) = 0. \tag{2.29}$$

Note, however, that the above choice of the generalized coordinate and velocity is not unique. Instead, one can use as the generalized coordinate the magnetic flux Φ through the inductive coil, related to the common voltage V across the circuit (Fig. 4) by Faraday's induction law $V = -d\Phi/dt$. With this choice, $(-V)$ becomes the generalized velocity, $E_L = \Phi^2/2L$ should be understood as the *potential* energy, and $E_C = CV^2/2$ treated as the *kinetic* energy. It is straightforward to verify that for this choice, the resulting Lagrange equation of motion is equivalent to Eq. (29). If both parameters of the circuit, L and C, are constant in time, Eq. (29) is just the harmonic oscillator equation similar to Eq. (1.1), and describes sinusoidal oscillations with frequency

$$\omega_0 = \frac{1}{(LC)^{1/2}}. \tag{2.30}$$

This is of course a very well known result that may be derived in the more standard way by equating the voltage drops across the capacitor ($V = Q/C$) and the inductor ($V = -LdI/dt = -Ld^2Q/dt^2$). However, the Lagrangian approach is much more convenient for more complex systems, for example, for the description of electromagnetic field and its interaction with charged relativistic particles.[11]

2.3. Hamiltonian function and energy

The canonical form (19) of the Lagrange equation has been derived using Eq. (18), which is formally similar to Eq. (1.22) for a potential force. Does this mean that the system described by Eq. (19) always conserves energy? Not necessarily, because the "potential energy" U, that participates in Eq. (18), may depend not only on the generalized coordinates, but on time as well. Let us start the analysis of this issue with the introduction of two new (and very important!) notions: the *generalized momenta* corresponding to each generalized coordinate q_j,

[11] See, e.g., EM Sec. 9.8.

$$p_j \equiv \frac{\partial L}{\partial \dot{q}_j}, \tag{2.31}$$

Generalized momentum

and the *Hamiltonian function*[12]

$$H \equiv \sum_j \frac{\partial L}{\partial \dot{q}_j}\dot{q}_j - L \equiv \sum_j p_j \dot{q}_j - L\,. \tag{2.32}$$

Hamiltonian function

In order to see whether the Hamiltonian function is conserved, let us differentiate its definition (32) over time:

$$\frac{dH}{dt} = \sum_j \left[\frac{d}{dt}\left(\frac{\partial L}{\partial \dot{q}_j} \right)\dot{q}_j + \frac{\partial L}{\partial \dot{q}_j}\ddot{q}_j \right] - \frac{dL}{dt}. \tag{2.33}$$

If we want to make use of the Lagrange equation (19), the last derivative has to be calculated considering L as a function of independent arguments q_j, $\dot{q}_j$, and t:

$$\frac{dL}{dt} = \sum_j \left(\frac{\partial L}{\partial q_j}\dot{q}_j + \frac{\partial L}{\partial \dot{q}_j}\ddot{q}_j \right) + \frac{\partial L}{\partial t}, \tag{2.34}$$

where the last term is the derivative of L as an *explicit* function of time. We see that the last term in the square brackets of Eq. (33) immediately cancels with the last term in the parentheses of Eq. (34). Moreover, using the Lagrange equation (19) for the first term in the square brackets of Eq. (33), we see that it cancels with the first term in the parentheses of Eq. (34). Thus we arrive at a very simple and important result:

$$\frac{dH}{dt} = -\frac{\partial L}{\partial t}. \tag{2.35}$$

Hamiltonian function's evolution

The most important corollary of this formula is that if the Lagrangian function does not depend on time *explicitly* ($\partial L / \partial t = 0$), the Hamiltonian function is an integral of motion:

$$H = \text{const}. \tag{2.36}$$

Let us see how it works, using the first two examples discussed in the previous section. For a 1D particle, definition (31) of the generalized momentum yields

$$p_x \equiv \frac{\partial L}{\partial v} = mv, \tag{2.37}$$

so that it coincides with the usual momentum - or rather with its x-component. According to Eq. (32), the Hamiltonian function for this case (with just one degree of freedom) is

$$H \equiv p\dot{x} - L = m\dot{x}^2 - \left(\frac{m}{2}\dot{x}^2 - U \right) = \frac{m}{2}\dot{x}^2 + U\,, \tag{2.38}$$

[12] It is sometimes called just the "Hamiltonian", but it is advisable to use the full term "Hamiltonian function" in classical mechanics, in order to distinguish it from the *Hamiltonian operator* used in quantum mechanics. (Their relation will be discussed in Sec. 10.1.)

and coincides with particle's mechanical energy $E = T + U$. Since the Lagrangian does not depend on time explicitly, both H and E are conserved.

However, it is not always that simple! Indeed, let us return again to our testbed problem (Fig. 1). In this case, the generalized momentum corresponding to the generalized coordinate θ is

$$p_\theta \equiv \frac{\partial L}{\partial \dot{\theta}} = mR^2\dot{\theta}, \tag{2.39}$$

and Eq. (32) yields:

$$\begin{aligned} H \equiv p_\theta\dot{\theta} - L &= mR^2\dot{\theta}^2 - \left[\frac{m}{2}R^2\left(\dot{\theta}^2 + \omega^2\sin^2\theta\right) + mgR\cos\theta\right] + \text{const} \\ &= \frac{m}{2}R^2\left(\dot{\theta}^2 - \omega^2\sin^2\theta\right) - mgR\cos\theta + \text{const}. \end{aligned} \tag{2.40}$$

This means that (as soon as $\omega \neq 0$), the Hamiltonian function *differs* from the mechanical energy

$$E \equiv T + U = \frac{m}{2}R^2\left(\dot{\theta}^2 + \omega^2\sin^2\theta\right) - mgR\cos\theta + \text{const}. \tag{2.41}$$

The difference, $E - H = mR^2\omega^2\sin^2\theta$ (besides an inconsequential constant), may change at bead's motion along the ring, so that although H *is* an integral of motion (since $\partial L/\partial t = 0$), energy E is *not* conserved.

Let us find out when do these two functions, E and H, coincide. In mathematics, there is a notion of a *homogeneous function* $f(x_1, x_2, ...)$ *of degree* λ, defined in the following way: for an arbitrary constant a,

$$f(ax_1, ax_2, ...) = a^\lambda f(x_1, x_2, ...). \tag{2.42}$$

Such functions obey the following *Euler theorem*:[13]

$$\sum_j \frac{\partial f}{\partial x_j}x_j = \lambda f, \tag{2.43}$$

that may be readily proven by differentiating both parts of Eq. (42) over a and then setting this parameter to the particular value $a = 1$. Now, consider the case when the kinetic energy is a quadratic form of all generalized velocities $\dot{q}_j$:

$$T = \sum_{j,j'} t_{jj'}(q_1, q_2, ..., t)\dot{q}_j\dot{q}_{j'}, \tag{2.44}$$

with no other terms. It is evident that such T satisfies the definition of a homogeneous function of the velocities with $\lambda = 2$,[14] so that the Euler theorem (43) gives

$$\sum_j \frac{\partial T}{\partial \dot{q}_j}\dot{q}_j = 2T. \tag{2.45}$$

[13] This is just one of many theorems bearing the name of the mathematics genius L. Euler (1707-1783).
[14] Such functions are called *quadratic-homogeneous*.

But since U is independent of the generalized velocities, $\partial L/\partial \dot{q}_j = \partial T/\partial \dot{q}_j$, and the left-hand part of Eq. (45) is exactly the first term in the definition (32) of the Hamiltonian function, so that in this case

$$H = 2T - L = 2T - (T - U) = T + U = E. \tag{2.46}$$

So, for the kinetic energy of the type (44), for example a free particle with the kinetic energy considered as a function of its Cartesian velocities,

$$T = \frac{m}{2}\left(v_x^2 + v_y^2 + v_z^2\right), \tag{2.47}$$

the notions of the Hamiltonian function and mechanical energy are identical. (Indeed, some textbooks, very regretfully, do not distinguish these notions at all!) However, as we have seen from our bead-on-the-rotating-ring example, this is not always true. For that problem, the kinetic energy, in addition to the term proportional to $\dot{\theta}^2$, has another, velocity-independent term – see the first of Eqs. (23) - and hence is *not* a quadratic-homogeneous function of the angular velocity.

Thus, Eq. (36) expresses a new conservation law, generally different from that of the mechanical energy conservation.

2.4. Other conservation laws

Looking at the Lagrange equation (19), we immediately see that if $L \equiv T - U$ as a whole is independent of some generalized coordinate q_j, $\partial L/\partial q_j = 0$,[15] then the corresponding generalized momentum is an integral of motion:[16]

$$p_j \equiv \frac{\partial L}{\partial \dot{q}_j} = \text{const}. \tag{2.48}$$

For example, for a 1D particle with Lagrangian (21), momentum p_x is conserved if the potential energy is constant (the x-component of force is zero) – of course. As a less obvious example, let us consider a 2D motion of a particle in the field of central forces. If we use polar coordinates r and φ in the role of the generalized coordinates, the Lagrangian function,[17]

$$L \equiv T - U = \frac{m}{2}\left(\dot{r}^2 + r^2\dot{\varphi}^2\right) - U(r), \tag{2.49}$$

is independent of φ and hence the corresponding generalized momentum,

$$p_\varphi \equiv \frac{\partial L}{\partial \dot{\varphi}} = mr^2\dot{\varphi}, \tag{2.50}$$

[15] Such coordinates are frequently called *cyclic*, because in some cases (like in the second example considered below) they represent periodic coordinates such as angles. However, this terminology is misleading, because some "cyclic" coordinates (e.g., x in our first example) have nothing to do with rotation.

[16] This fact may be considered a particular case of a more general mathematical statement called the *Noether theorem* (named after its author, A. E. Nöther, sometimes called the "greatest woman mathematician ever lived"). For its discussion see, e.g., Sec. 13.7 in H. Goldstein *et al.*, *Classical Mechanics*, 3rd ed. Addison Wesley, 2002.

[17] Note that here $\dot{r}^2$ is just the square of the scalar derivative $\dot{r}$, rather than the square of vector $\dot{\mathbf{r}} = \mathbf{v}$.

is conserved. This is just a particular (2D) case of the angular momentum conservation – see Eq. (1.24). Indeed, for the 2D motion within the [*x, y*] plane, the angular momentum vector,

$$\mathbf{L} \equiv \mathbf{r} \times \mathbf{p} = \begin{vmatrix} \mathbf{n}_x & \mathbf{n}_y & \mathbf{n}_z \\ x & y & z \\ m\dot{x} & m\dot{y} & m\dot{z} \end{vmatrix}, \tag{2.51}$$

has only one nonvanishing component, perpendicular to the motion plane:

$$L_z = x(m\dot{y}) - y(m\dot{x}). \tag{2.52}$$

Differentiating the well-known relations between the polar and Cartesian coordinates,

$$x = r\cos\varphi, \quad y = r\sin\varphi, \tag{2.53}$$

over time, and plugging the result into Eq. (52), we see that $L_z = mr^2\dot{\varphi} = p_\varphi$.

Thus the Lagrangian formalism provides a powerful way of searching for non-evident integrals of motion. On the other hand, if such conserved quantity is evident or known *a priori*, it is helpful for the selection of the most appropriate generalized coordinates, giving the simplest Lagrange equations. For example, in the last problem, if we have known in advance that p_φ had to be conserved, this could provide a motivation for using angle φ as one of generalized coordinates.

2.5. Exercise problems

In each of Problems 2.1-2.10:

(i) introduce a set of convenient generalized coordinate(s) q_j of the system,
(ii) write down Lagrangian L as a function of $q_j, \dot{q}_j$, and (if appropriate) time,
(iii) write down the Lagrangian equation(s) of motion,
(iv) calculate the Hamiltonian function H; find out whether it is conserved,
(v) calculate energy E; is $E = H$?; is energy conserved?
(vi) any other evident integrals of motion?

2.1. Double pendulum – see Fig. on the right. Consider only the motion confined to a vertical plane containing the suspension point.

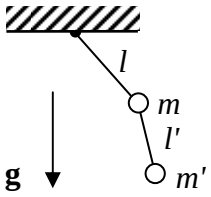

2.2. Stretchable pendulum (i.e. a mass hung on an elastic cord that exerts force $F = -\kappa(l - l_0)$, where κ and l_0 are positive constants), confined to a vertical plane:

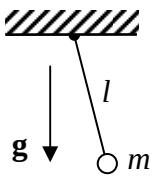

2.3. Fixed-length pendulum hanging from a horizontal support whose motion law $x_0(t)$ is fixed. (No vertical plane constraint here.)

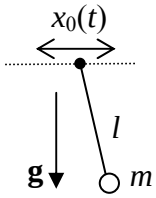

2.4. A pendulum of mass m hung on another point mass m' that may slide, without friction, along a straight horizontal rail (see Fig. on the right). Its motion is confined to the vertical plane that contains the rail.

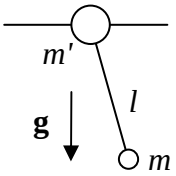

2.5. A bead of mass m, sliding without friction along a light string stretched by fixed force $\mathcal{T}$ between two horizontally displaced points – see Fig. on the right. Here, in contrast to the similar Problem 1.10, string tension $\mathcal{T}$ may be comparable with bead's weight mg, and the motion is not restricted to the vertical plane.

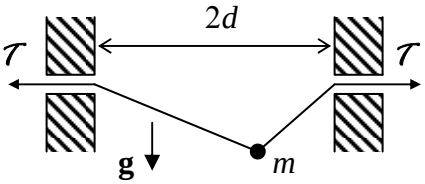

2.6. A bead of mass m, sliding without friction along a light string of fixed length $2l$, which is hung between two points, horizontally displaced by distance $2d < 2l$ – see Fig. on the right. As in the previous problem, the motion is not restricted to the vertical plane.

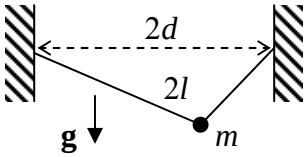

2.7. A block of mass m that can slide, without friction, along the inclined plane surface of a heavy wedge with mass m'. The wedge is free to move, also without friction, along a horizontal surface – see Fig. on the right. (Both motions are within the vertical plane containing the steepest slope line.)

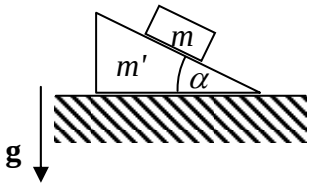

2.8. The two-pendula system that was the subject of Problem 1.8 – see Fig. on the right.

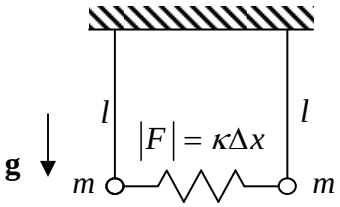

2.9. A system of two similar, inductively-coupled LC circuits – see Fig. on the right.

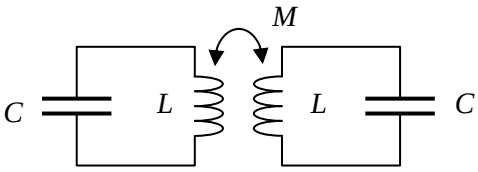

2.10.* A small Josephson junction, i.e. a system of two superconductors coupled by Cooper-pair tunneling through a thin insulating layer that separates them (see Fig. on the right).

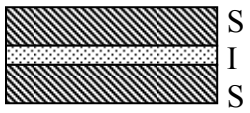

Hints:

(i) At not very high frequencies (whose quantum $\hbar\omega$ is lower than the binding energy 2Δ of the Cooper pairs), the Josephson effect may be described by coupling energy

$$U(\varphi) = -E_J \cos\varphi + \text{const},$$

where constant E_J describes the coupling strength, and variable φ (called the *Josephson phase difference*) is related to voltage V across the junction via the famous frequency-to-voltage relation

$$\frac{d\varphi}{dt} = \frac{2e}{\hbar}V,$$

where $e \approx 1.6\times10^{-19}$ C is the fundamental electric charge and $\hbar \approx 1.054\times10^{-34}$ J·s is the Plank constant.[18]

(ii) The junction (as any system of two close conductors) has a substantial electric capacitance C.

[18] More discussion of the Josephson effect and the physical sense of the variable φ may be found, for example, in EM Sec. 6.4 and QM Secs. 2.3 and 2.8 of this lecture note series.

This page is intentionally left blank

Chapter 3. A Few Simple Problems

In this chapter, I will review the solutions of a few simple but very important problems of particle motion, that may be reduced to one dimension, including the famous "planetary" problem of two particles interacting via a spherically-symmetric potential. In the process, we will discuss several methods that will be useful for the analysis of more complex systems.

3.1. One-dimensional and 1D-reducible systems

If a particle is confined to motion along a straight line (say, axis x), its position, of course, is completely defined by this coordinate. In this case, as we already know, particle's Lagrangian is given by Eq. (2.21):

$$L = T(\dot{x}) - U(x,t), \quad T(\dot{x}) = \frac{m}{2}\dot{x}^2, \tag{3.1}$$

so that the Lagrange equation of motion (2.22)

$$m\ddot{x} = -\frac{\partial U(x,t)}{\partial x} \tag{3.2}$$

is just the x-component of the 2nd Newton law.

It is convenient to discuss the dynamics of such *really 1D* systems in the same breath with that of *effectively 1D systems* whose position, due to holonomic constraints and/or conservation laws, is also fully determined by one generalized coordinate q, and whose Lagrangians may be presented in a form similar to Eq. (1):

Effectively-1D system

$$L = T_{\text{ef}}(\dot{q}) - U_{\text{ef}}(q,t), \quad T_{\text{ef}} = \frac{m_{\text{ef}}}{2}\dot{q}^2, \tag{3.3}$$

where m_{ef} is some constant which may be considered as the *effective mass* of the system, and the function U_{ef} its *effective potential energy*. In this case the Lagrange equation (2.19) describing the system dynamics has a form similar to Eq. (2):

$$m_{\text{ef}}\ddot{q} = -\frac{\partial U_{\text{ef}}(q,t)}{\partial q}. \tag{3.4}$$

As an example, let us return again to our testbed system shown in Fig. 1.5. We have already seen that for that system, having one degree of freedom, the genuine kinetic energy T, expressed by the first of Eqs. (2.23), is *not* a quadratically-homogeneous function of the generalized velocity. However, the system's Lagrangian (2.23) still may be presented in form (3),

$$L = \frac{m}{2}R^2\dot{\theta}^2 + \frac{m}{2}R^2\omega^2\sin^2\theta + mgR\cos\theta + \text{const} = T_{\text{ef}} - U_{\text{ef}}, \tag{3.5}$$

if we take

$$T_{\text{ef}} \equiv \frac{m}{2}R^2\dot{\theta}^2, \quad U_{\text{ef}} \equiv -\frac{m}{2}R^2\omega^2\sin^2\theta - mgR\cos\theta + \text{const}. \tag{3.6}$$

In this new partitioning of function L, which is legitimate because U_{ef} depends only on the generalized coordinate θ, but not on the corresponding generalized velocity, T_{ef} includes only a part of the full kinetic energy T of the bead, while U_{ef} includes not only the real potential energy U of the bead in the gravity field, but also an additional term related to ring rotation. (As we will see in Sec. 6.6, this term may be interpreted as the effective potential energy due to the inertial centrifugal "force".)

Returning to the general case of effectively 1D systems with Lagrangian (3), let us calculate their Hamiltonian function, using its definition (2.32):

$$H = \frac{\partial L}{\partial \dot{q}}\dot{q} - L = m_{ef}\dot{q}^2 - (T_{ef} - U_{ef}) = T_{ef} + U_{ef}. \tag{3.7}$$

So, H is expressed via T_{ef} and U_{ef} exactly as the mechanical energy E is expressed via genuine T and U.

3.2. Equilibrium and stability

Autonomous systems are defined as the dynamic systems whose equations of motion do not depend on time. For 1D (and effectively 1D) systems obeying Eq. (4), this means that their function U_{ef}, and hence the Lagrangian function (5) should not depend on time explicitly. According to Eqs. (2.35), in such systems the Hamiltonian function (7), i.e. the sum $T_{ef} + U_{ef}$, is an integral of motion. However, be careful! This may not be true for system's mechanical energy E; for example, as we already know from Sec. 2.2, for our testbed problem, with the generalized coordinate $q = \theta$ (Fig. 2.1), $H \neq E$.

According to Eq. (4), an autonomous system, at appropriate initial conditions, may stay in equilibrium at one or several *stationary* (alternatively called *fixed*) *points* q_n, corresponding to either the minimum or a maximum of the effective potential energy (see Fig. 1):

$$\frac{dU_{ef}}{dq}(q_n) = 0. \tag{3.8}$$

Fixed-point condition

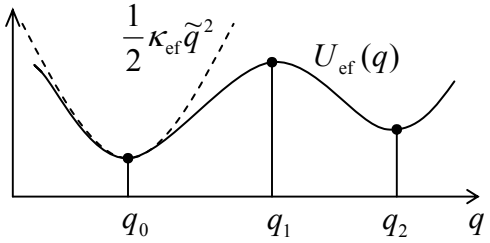

Fig. 3.1. Effective potential energy profile near stable (q_0, q_2) and unstable (q_1) fixed points, and its quadratic approximation (10) near point q_0 – schematically.

In order to explore the *stability* of such fixed points, let us analyze the dynamics of small deviations

$$\tilde{q}(t) \equiv q(t) - q_n \tag{3.9}$$

from the equilibrium. For that, let us expand function $U_{ef}(q)$ in the Taylor series at a fixed point,

$$U_{ef}(q) = U_{ef}(q_n) + \frac{dU_{ef}}{dq}(q_n)\tilde{q} + \frac{1}{2}\frac{d^2U_{ef}}{dq^2}(q_n)\tilde{q}^2 + \ldots. \tag{3.10}$$

The first term in the right-hand part, $U_{ef}(q_n)$, is arbitrary and does not affect motion. The next term, linear in deviation $\tilde{q}$, is equal zero – see the fixed point definition (8). Hence the fixed point stability is determined by the next term, quadratic in $\tilde{q}$, more exactly by its coefficient,

$$\kappa_{ef} \equiv \frac{d^2 U_{ef}}{dq^2}(q_n) \tag{3.11}$$

which plays the role of the effective spring constant. Indeed, neglecting the higher terms of the Taylor expansion (10),[1] we see that Eq. (4) takes the familiar form - cf. Eq. (1.1):

$$m_{ef}\ddot{\tilde{q}} + \kappa_{ef}\tilde{q} = 0. \tag{3.12}$$

I am confident that the reader of these notes knows everything about this equation, but since we will soon run into similar but more complex equations, let us review the formal procedure of its solution. From the mathematical standpoint, Eq. (12) is an ordinary, linear differential equation of the second order, with constant coefficients. The theory of such equations tells us that its general solution (for any initial conditions) may be presented as

$$\tilde{q}(t) = c_+ e^{\lambda_+ t} + c_- e^{\lambda_- t}, \tag{3.13}$$

where constants $c_\pm$ are determined by initial conditions, while the so-called *characteristic exponents* $\lambda_\pm$ are completely defined by the equation itself. In order to find the exponents, it is sufficient to plug just one partial solution, $\exp\{\lambda t\}$, into the equation. In our simple case (12), this yields the following *characteristic equation*:

$$m_{ef}\lambda^2 + \kappa_{ef} = 0. \tag{3.14}$$

If the ratio k_{ef}/m_{ef} is positive,[2] i.e. the fixed point corresponds to the minimum of potential energy (e.g., points q_0 and q_2 in Fig. 1), the characteristic equation yields

$$\lambda_\pm = \pm i\omega_0, \quad \omega_0 \equiv \left(\frac{\kappa_{ef}}{m_{ef}}\right)^{1/2}, \tag{3.15}$$

(where i is the imaginary unity, $i^2 = -1$), so that Eq. (13) describes sinusoidal oscillations of the system,

$$\tilde{q}(t) = c_+ e^{+i\omega_0 t} + c_- e^{-i\omega_0 t} = c_c \cos\omega_0 t + c_s \sin\omega_0 t, \tag{3.16}$$

with *eigenfrequency* (or "own frequency") ω_0, about the fixed point which is thereby *stable*. On the other hand, at the potential energy maximum ($k_{ef} < 0$, e.g., at point q_1 in Fig. 1), we get

$$\lambda_\pm = \pm\lambda, \quad \lambda \equiv \left(\frac{|\kappa_{ef}|}{m_{ef}}\right)^{1/2}, \quad \tilde{q}(t) = c_+ e^{+\lambda t} + c_- e^{-\lambda t}. \tag{3.17}$$

Since the solution has an exponentially growing part,[3] the fixed point is *unstable*.

[1] Those terms may be important only in the very special case then κ_{ef} is exactly zero, i.e. when a fixed point is an *inflection point* of function $U_{ef}(q)$.

[2] In what follows, I will assume that the effective mass m_{ef} is positive, which is true in most (but not all!) dynamic systems. The changes necessary if it is negative are obvious.

Note that the *quadratic* expansion of function $U_{ef}(q)$, given by Eq. (10), is equivalent to a *linear* expansion of the effective force:

$$F_{ef} \equiv -\frac{dU_{ef}}{dq}\Big|_{q=q_n} \approx -\kappa_{ef}\tilde{q}, \tag{3.18}$$

immediately resulting in the linear equation (12). Hence, in order to analyze the stability of a fixed point q_n, it is sufficient to *linearize* the equation of motion in small deviations from that point, and study possible solutions of the resulting linear equation.

As an example, let us return to our testbed problem (Fig. 2.1) whose function U_{ef} we already know – see the second of Eqs. (6). With it, the equation of motion (4) becomes

$$mR^2\ddot{\theta} = -\frac{dU_{ef}}{d\theta} = mR^2\left[\omega^2\cos\theta - \Omega^2\right]\sin\theta, \quad \text{i.e. } \ddot{\theta} = \left[\omega^2\cos\theta - \Omega^2\right]\sin\theta, \tag{3.19}$$

where $\Omega \equiv (g/R)^{1/2}$ is the frequency of small oscillations of the system at $\omega = 0$ - see Eq. (2.26).[4] From requirement (8), we see that on any 2π-long segment of angle θ,[5] the system may have four fixed points:

$$\theta_0 = 0, \qquad \theta_1 = \pi, \qquad \theta_{2,3} = \pm\arccos\frac{\Omega^2}{\omega^2}, \tag{3.20}$$

The last two fixed points, corresponding to the bead rotating on either side of the ring, exist only if the angular velocity ω of ring rotation exceeds Ω. (In the limit of very fast rotation, $\omega >> \Omega$, Eq. (20) yields $\theta_{2,3} \to \pm\pi/2$, i.e. the stationary positions approach the horizontal diameter of the ring - in accordance with physical intuition.)

In order to analyze the fixed point stability, similarly to Eq. (9), we plug $\theta = \theta_n + \tilde{\theta}$ into Eq. (19) and Taylor-expand the trigonometric functions of θ up to the first term in $\tilde{\theta}$:

$$\ddot{\tilde{\theta}} = \left[\omega^2\left(\cos\theta_n - \sin\theta_n\,\tilde{\theta}\right) - \Omega^2\right]\left(\sin\theta_n + \cos\theta_n\,\tilde{\theta}\right). \tag{3.21}$$

Generally, this equation may be linearized further by purging its right-hand part of the term proportional to $\tilde{\theta}^2$; however in this simple case, Eq. (21) is already convenient for analysis. In particular, for the fixed point $\theta_0 = 0$ (corresponding to the bead position at the bottom of the ring), we have $\cos\theta_0 = 1$ and $\sin\theta_0 = 0$, so that Eq. (21) is reduced to a linear differential equation

$$\ddot{\tilde{\theta}} = \left(\omega^2 - \Omega^2\right)\tilde{\theta}\ , \tag{3.22}$$

whose characteristic equation is similar to Eq. (14) and yields

$$\lambda^2 = \omega^2 - \Omega^2, \quad \text{for } \theta \approx \theta_0\,. \tag{3.23a}$$

---

[3] Mathematically, the growing part vanishes at some special (exact) initial conditions which give $c_+ = 0$. However, the futility of this argument for real physical systems should be obvious for anybody who had ever tried to balance a pencil on its sharp point.

[4] Note that Eq. (19) coincides with Eq. (2.25). This is a good sanity check illustrating that the procedure (5)-(6) of moving of a term from the potential to kinetic energy within the Lagrangian function is indeed legitimate.

[5] For this particular problem, the values of θ that differ by a multiple of 2π, are physically equivalent.

This result shows that if $\omega < \Omega$, when both roots λ are imaginary, this fixed point is stable. However, the roots become real, $\lambda_{\pm} = (\omega^2 - \Omega^2)^{1/2}$, with one of them positive, so that the fixed point becomes unstable beyond this threshold, i.e. as soon as fixed points $\theta_{2,3}$ exist. An absolutely similar calculations for other fixed points yield

$$\lambda^2 = \Omega^2 + \omega^2 > 0, \quad \text{for } \theta \approx \theta_1, \tag{3.23b}$$

$$\lambda^2 = \Omega^2 - \omega^2, \quad \text{for } \theta \approx \theta_{2,3}. \tag{3.23c}$$

These results show that fixed point θ_1 (bead on the top of the ring) is always unstable – just as we could foresee, while the side fixed points $\theta_{2,3}$ are stable as soon as they exist (at $\omega > \Omega$).

Thus, our fixed-point analysis may be summarized in a simple way: an increase of the ring rotation speed ω beyond a certain threshold value, equal to Ω (2.26), causes the bead to move on one of the ring sides, oscillating about one of the fixed points $\theta_{2,3}$. Together with the rotation about the vertical axis, this motion yields quite a complex spatial trajectory as observed from a lab frame, so it is fascinating that we could analyze it qualitatively in such a simple way.

Later in this course we will repeatedly use the linearization of the equations of motion for the analysis of stability of more complex systems, including those with energy dissipation.

3.3. Hamiltonian 1D systems

The autonomous systems that are described by time-independent Lagrangians, are frequently called *Hamiltonian,* because their Hamiltonian function H (again, not necessarily equal to the genuine mechanical energy E!) is conserved. In our current 1D case, described by Eq. (3),

$$H = \frac{m_{\text{ef}}}{2}\dot{q}^2 + U_{\text{ef}}(q) = \text{const}. \tag{3.24}$$

This is the first integral motion. Solving Eq. (24) for $\dot{q}$, we get the first-order differential equation,

$$\frac{dq}{dt} = \pm\left\{\frac{2}{m_{\text{ef}}}\left[H - U_{\text{ef}}(q)\right]\right\}^{1/2}, \tag{3.25}$$

which may be readily integrated:

$$\pm\left(\frac{m_{\text{ef}}}{2}\right)^{1/2} \int_{q(t_0)}^{q(t)} \frac{dq'}{\left[H - U_{\text{ef}}(q')\right]^{1/2}} = t - t_0. \tag{3.26}$$

Since constant H (as well as the proper sign before the integral – see below) is fixed by initial conditions, Eq. (26) gives the reciprocal form, $t = t(q)$, of the desired law of system motion, $q(t)$. Of course, for any particular problem the integral in Eq. (26) still has to be worked out, either analytically or numerically, but even the latter procedure is typically much easier than the numerical integration of the initial, second-order differential equation of motion, because at addition of many values (to which the numerical integration is reduced[6]) the rounding errors are effectively averaged out.

[6] See, e.g., MA Eqs. (5.2) and (5.3).

Moreover, Eqs. (24)-(25) also allow a general classification of 1D system motion. Indeed:

(i) If $H > U_{ef}(q)$ in the whole range of interest, the effective kinetic energy T_{ef} (3) is always positive. Hence derivative dq/dt cannot change sign, so that the effective velocity retains the sign it had initially. This is the unbound motion in one direction (Fig. 2a).

(ii) Now let the particle approach a *classical turning point A* where $H = U_{ef}(x)$ - see Fig. 2b.[7] According to Eqs. (25), (26), at that point the particle velocity vanishes, while its acceleration, according to Eq. (4), is still finite. Evidently, this corresponds to the particle reflection from the "potential wall", with the change of velocity sign.

(iii) If, after the reflection from point *A*, the particle runs into another classical turning point *B* (Fig. 2c), the reflection process is repeated again and again, so that the particle is bound to a periodic motion between two turning points.

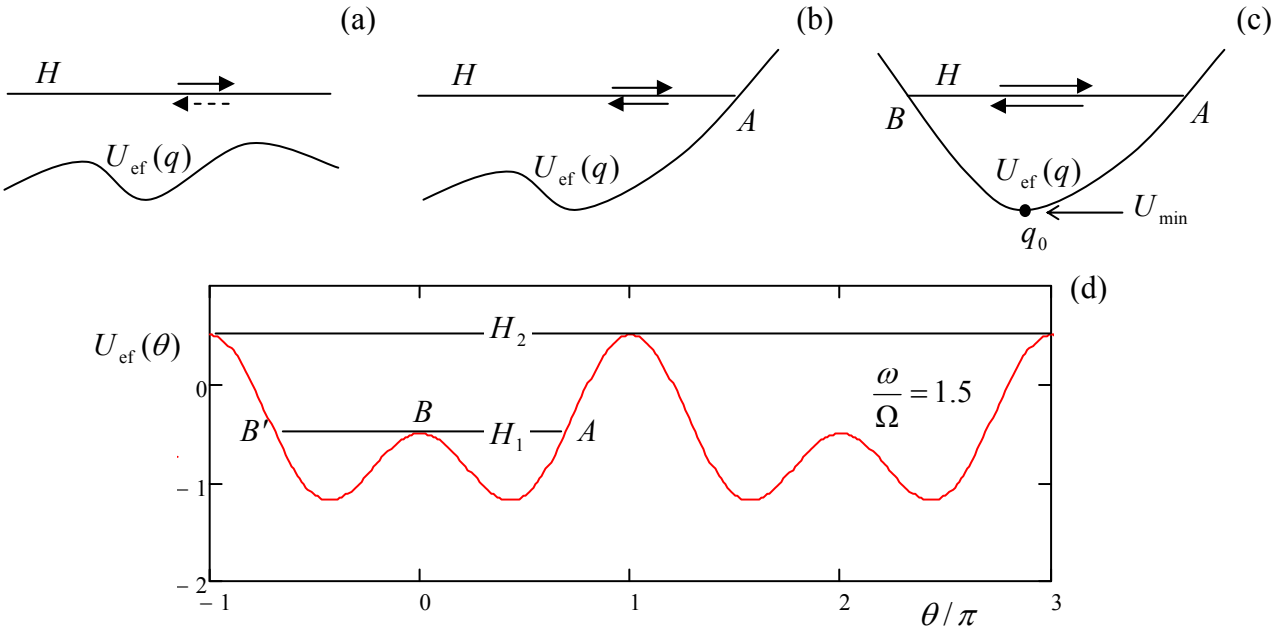

Fig. 3.2. Graphical representation of Eq. (25) for three different cases: (a) unbound motion, with the velocity sign conserved, (b) reflection from the "classical turning point", accompanied with the velocity sign change, and (c) bound, periodic motion between two turning points – schematically. (d) Effective potential energy (6) of the bead on the rotating ring (Fig. 1.5) for $\omega > \Omega$, in units of $2mgR$.

The last case of *periodic oscillations* presents large practical interest, and the whole next chapter will be devoted to a detailed analysis of this phenomenon and numerous associated effects. Here I will only note that Eq. (26) immediately enables us to calculate the oscillation period:

$$\mathcal{T} = 2\left(\frac{m_{ef}}{2}\right)^{1/2} \int_B^A \frac{dq}{[H - U_{ef}(q)]^{1/2}}, \qquad (3.27)$$

Oscillation period

[7] This terminology comes from quantum mechanics which shows that actually a particle (or rather its wavefunction) can, to a certain extent, penetrate the "classically forbidden range" where $H < U_{ef}(x)$.

where the additional upfront factor 2 accounts for two time intervals: for the motion from *B* to A and back (Fig. 2c). Indeed, according to Eq. (25), in each classically allowed point *q* the velocity magnitude is the same, so that these time intervals are equal to each other.[8]

Now let us link Eq. (27) to the fixed point analysis carried out in the previous section. As Fig. 2c shows, if *H* is reduced to approach $U_{\min}$, the oscillations described by Eq. (27) take place at the very bottom of "potential well", about a stable fixed point q_0. Hence, if the potential energy profile is smooth enough, we may limit the Taylor expansion (10) by the quadratic term. Plugging it into Eq. (27), and using the mirror symmetry of this particular problem about the fixed point q_0, we get

$$\mathcal{T} = 4\left(\frac{m_{\text{ef}}}{2}\right)^{1/2}\int_0^A \frac{d\tilde{q}}{\left[H-\left(U_{\min}+\kappa_{\text{ef}}\tilde{q}^2/2\right)\right]^{1/2}} = \frac{4}{\omega_0}I, \quad \text{with } I \equiv \int_0^1 \frac{d\xi}{\left(1-\xi^2\right)^{1/2}}, \tag{3.28}$$

where $\xi \equiv \tilde{q}/A$, with $A \equiv (2/\kappa_{\text{ef}})^{1/2}[H - U_{\min}]^{1/2}$ being the classical turning point, i.e. the oscillation amplitude, and ω_0 is the eigenfrequency given by Eq. (15). Taking into account that the elementary integral *I* in that equation equals $\pi/2$,[9] we finally get

$$\mathcal{T} = \frac{2\pi}{\omega_0}, \tag{3.29}$$

as it should be for harmonic oscillations (16). Note that the oscillation period does not depend on the oscillation amplitude *A*, i.e. on the difference (H - $U_{\min}$) - while it is small.

3.4. Planetary problems

Leaving a more detailed study of oscillations for the next chapter, let us now discuss the so-called *planetary systems*[10] whose description, somewhat surprisingly, may be also reduced to an effectively 1D problem. Consider two particles that interact via a conservative, central force $\mathbf{F}_{21} = -\mathbf{F}_{12} = \mathbf{n}_r F(r)$, where r and $\mathbf{n}_r$ are, respectively, the magnitude and direction of the *distance vector* $\mathbf{r} \equiv \mathbf{r}_1 - \mathbf{r}_2$ connecting the two particles (Fig. 3).

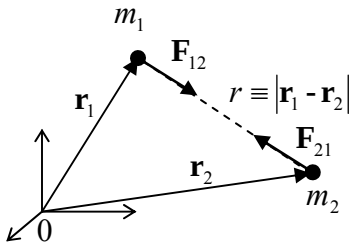

Fig. 3.3. Vectors in the "planetary" problem.

[8] Note that the dependence of points *A* and *B* on the "energy" *H* is not necessarily continuous. For example, for our testbed problem, whose effective potential energy is plotted in Fig. 2d (for a particular value of $\omega > \Omega$), a gradual increase of *H* leads to a sudden jump, at $H = H_1$, of point *B* to position *B'*, corresponding to a sudden switch from oscillations about one fixed point $\theta_{2,3}$ to oscillations about two adjacent fixed points (before the beginning of a persistent rotation along the ring at $H > H_2$).

[9] Introducing a new variable ζ by relation $\xi \equiv \sin\zeta$, we get $d\xi = \cos\zeta\, d\zeta = (1 - \xi^2)^{1/2}\, d\zeta$, so that the function under the integral is just $d\zeta$.

[10] This name is very conditional, because this group of problems includes, for example, charged particle scattering (see Sec. 3.7 below).

Generally, two particles moving without constrains in 3D space, have 3 + 3 = 6 degrees of freedom that may described, e.g., by their Cartesian coordinates $\{x_1, y_1, z_1, x_2, y_2, z_2\}$ However, for this particular form of interaction, the following series of tricks allows the number of essential degrees of freedom to be reduced to just one.

First, the central, conservative force of particle interaction may be described by time-independent potential energy $U(r)$. Hence the Lagrangian of the system is

$$L \equiv T - U(r) = \frac{m_1}{2}\dot{\mathbf{r}}_1^2 + \frac{m_2}{2}\dot{\mathbf{r}}_2^2 - U(r). \tag{3.30}$$

Let us perform the transfer from the initial six scalar coordinates of the particles to six generalized coordinates: three Cartesian components of the distance vector

$$\mathbf{r} \equiv \mathbf{r}_1 - \mathbf{r}_2, \tag{3.31}$$

and three components of vector

$$\boxed{\mathbf{R} \equiv \frac{m_1\mathbf{r}_1 + m_2\mathbf{r}_2}{M}, \quad M \equiv m_1 + m_2,} \tag{3.32}$$

Center of mass

which defines the position of the *center of mass* of the system. Solving the system of two linear equations (31) and (32) for the $\mathbf{r}_1$ and $\mathbf{r}_2$, we get

$$\mathbf{r}_1 = \mathbf{R} + \frac{m_2}{M}\mathbf{r}, \quad \mathbf{r}_2 = \mathbf{R} - \frac{m_1}{M}\mathbf{r}. \tag{3.33}$$

Plugging these relations into Eq. (30), we may reduce it to

$$L = \frac{M}{2}\dot{\mathbf{R}}^2 + \frac{m}{2}\dot{\mathbf{r}}^2 - U(r), \tag{3.34}$$

where m is the so-called *reduced mass*:

$$\boxed{m \equiv \frac{m_1 m_2}{M}, \quad \text{so that} \quad \frac{1}{m} \equiv \frac{1}{m_1} + \frac{1}{m_2}.} \tag{3.35}$$

Reduced mass

Note that according to Eq. (35), the reduced mass is lower than that of the lightest component of the two-body system. If one of $m_{1,2}$ is much less that is counterpart (like it is in most star-planet or planet-satellite systems), then with a good precision $m \cong \min [m_1, m_2]$.

Since the Lagrangian function (34) depends only on $\dot{\mathbf{R}}$ rather than $\mathbf{R}$ itself, according to our discussion in Sec. 2.4, the Cartesian components of R are cyclic coordinates, and the corresponding generalized momenta are conserved:

$$P_j \equiv \frac{\partial L}{\partial \dot{R}_j} = M\dot{R}_j = \text{const}, \quad j = 1, 2, 3. \tag{3.36}$$

Physically, this is just the conservation law for the full momentum $\mathbf{P} \equiv M\mathbf{R}$ of our system, due to absence of external forces. Actually, in the axiomatics used in Sec. 1.3 this law is postulated – see Eq. (1.10) – but now we may attribute momentum $\mathbf{P}$ to a certain geometric point, the center of mass $\mathbf{R}$. In particular, since according to Eq. (36) the center moves with constant velocity in the inertial reference

frame used to write Eq. (30), we may create a new inertial frame with the origin at point **R**. In this new frame, **R** ≡ 0, so that vector **r** (and hence scalar *r*) remain the same as in the old frame (because the frame transfer vector adds equally to $\mathbf{r}_1$ and $\mathbf{r}_2$, and cancels in $\mathbf{r} = \mathbf{r}_1 - \mathbf{r}_2$), and the Lagrangian (34) is now reduced to

$$L = \frac{m}{2}\dot{\mathbf{r}}^2 - U(r). \tag{3.37}$$

Thus our initial problem has been reduced to just three degrees of freedom - three scalar components of vector **r**. Moreover, Eq. (37) shows that dynamics of vector **r** of our initial, two-particle system is identical to that of the radius-vector of a *single particle* with the effective mass *m*, moving in the central potential field $U(r)$.

3.5. 2nd Kepler law

Two more degrees of freedom may be excluded from the planetary problem by noticing that according to Eq. (1.35), the angular momentum $\mathbf{L} = \mathbf{r}\times\mathbf{p}$ of our effective particle is also conserved, both in magnitude and direction. Since the direction of **L** is, by its definition, perpendicular to both of **r** and $\mathbf{v} = \mathbf{p}/m$, this means that particle's motion is confined to a plane (whose orientation in space is determined by the initial directions of vectors **r** and **v**). Hence we can completely describe particle's position by just two coordinates in that plane, for example by distance *r* to the center, and the polar angle φ. In these coordinates, Eq. (37) takes the form identical to Eq. (2.49):

$$L = \frac{m}{2}\left(\dot{r}^2 + r^2\dot{\varphi}^2\right) - U(r). \tag{3.38}$$

Moreover, the latter coordinate, polar angle φ, may be also eliminated by using the conservation of angular momentum's magnitude, in the form of Eq. (2.50): [11]

$$L_z = mr^2\dot{\varphi} = \text{const}. \tag{3.39}$$

A direct corollary of this conservation is the so-called *2nd Kepler law*:[12] the radius-vector **r** sweeps equal areas *A* in equal times. Indeed, in the linear approximation in $dA << A$, the area differential *dA* equals to the area of a narrow right triangle with the base being the arc differential $rd\varphi$, and the height equal to *r* - see Fig. 4. As a result, according to Eq. (39), the time derivative of the area,

$$\frac{dA}{dt} = \frac{r(rd\varphi)/2}{dt} = \frac{1}{2}r^2\dot{\varphi} = \frac{L_z}{2m}, \tag{3.40}$$

remains constant. Integration of this equation over an arbitrary (not necessarily small!) time interval proves the 2nd Kepler law.

[11] Here index *z* stands for the coordinate perpendicular to the motion plane. Since other components of the angular momentum are equal zero, the index is not really necessary, but I will still use it, just to make a clear distinction between the angular momentum L_z and the Lagrangian function *L*.

[12] One of three laws deduced almost exactly 400 years ago by J. Kepler (1571 – 1630), from the extremely detailed astronomical data collected by T. Brahe (1546-1601). In turn, the set of three Kepler laws were the main basis for Isaac Newton's discovery of the gravity law (1.16). That's how physics marched on…

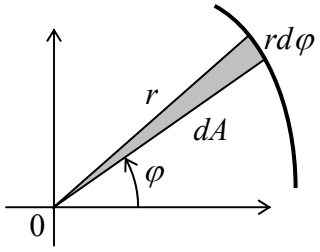

Fig. 3.4. Area differential in the polar coordinates.

Now note that since $\partial L/\partial t = 0$, the Hamiltonian function H is also conserved, and since, according to Eq. (38), the kinetic energy of the system is a quadratic-homogeneous function of the generalized velocities $\dot{r}$ and $\dot{\varphi}$, $H = E$, so that the system energy E,

$$E = \frac{m}{2}\dot{r}^2 + \frac{m}{2}r^2\dot{\varphi}^2 + U(r), \tag{3.41}$$

is also a first integral of motion.[13] But according to Eq. (39), the second term of Eq. (41) may be presented as

$$\frac{m}{2}r^2\dot{\varphi}^2 = \frac{L_z^2}{2mr^2}, \tag{3.42}$$

so that energy (41) may be expressed as that of a 1D particle moving along axis r,

$$E = \frac{m}{2}\dot{r}^2 + U_{\text{ef}}(r), \tag{3.43}$$

in the following effective potential:

$$U_{\text{ef}}(r) \equiv U(r) + \frac{L_z^2}{2mr^2}. \tag{3.44}$$

Effective potential energy

So the planetary motion problem has been reduced to the dynamics of an effectively 1D system.[14]

Now we may proceed just like we did in Sec. 3, with due respect for the very specific effective potential (44) which, in particular, diverges at $r \to 0$ - possibly besides the very special case of an exactly radial motion, $L_z = 0$. In particular, we may solve Eq. (43) for dr/dt to get

$$dt = \left(\frac{m}{2}\right)^{1/2} \frac{dr}{[E - U_{\text{ef}}(r)]^{1/2}}. \tag{3.45}$$

The integration of this relation allows us not only to get a direct relation between time t and distance r, similar to Eq. (26),

[13] One may claim that this fact should have been evident from the very beginning, because the effective particle of mass m moves in a potential field $U(r)$ which conserves energy.

[14] Note that this reduction has been done in a way different from that used for our testbed problem (shown in Fig. 2.1) in Sec. 2 above. (The reader is encouraged to analyze this difference.) In order to emphasize this fact, I will keep writing E instead of H here, though for the planetary problem we are discussing now these two notions coincide.

$$t = \pm\left(\frac{m}{2}\right)^{1/2}\int\frac{dr}{[E-U_{\text{ef}}(r)]^{1/2}} = \pm\left(\frac{m}{2}\right)^{1/2}\int\frac{dr}{[E-U(r)-L_z^2/2mr^2]^{1/2}}, \tag{3.46}$$

but also do a similar calculation of angle φ. Indeed, integrating Eq. (39),

$$\varphi \equiv \int\dot{\varphi}\,dt = \frac{L_z}{m}\int\frac{dt}{r^2}. \tag{3.47}$$

and plugging dt from Eq. (45), we get an explicit expression for particle's trajectory $\varphi(r)$:

$$\varphi = \pm\frac{L_z}{(2m)^{1/2}}\int\frac{dr}{r^2[E-U_{\text{ef}}(r)]^{1/2}} = \pm\frac{L_z}{(2m)^{1/2}}\int\frac{dr}{r^2[E-U(r)-L_z^2/2mr^2]^{1/2}}. \tag{3.48}$$

Note that according to Eq. (39), derivative $d\varphi/dt$ does *not* change sign at the reflection from any classical turning point $r \neq 0$, so that, in contrast to Eq. (46), the sign in the right-hand part of Eq. (48) is uniquely determined by the initial conditions and cannot change during the motion.

Let us use these results, valid for any interaction law $U(r)$, for the planetary motion's classification. The following cases should be distinguished. (Following a good tradition, in what follows I will select the arbitrary constant in the potential energy in the way to provide $U_{\text{ef}} \to 0$ at $r \to \infty$.)

If the particle interaction is *attractive*, and the divergence of the attractive potential at $r \to 0$ is faster than $1/r^2$, then $U_{\text{ef}}(r) \to -\infty$ at $r \to 0$, so that at appropriate initial conditions ($E < 0$) the particle may drop on the center even if $L_z \neq 0$ – the event called the *capture*. On the other hand, with $U(r)$ either converging or diverging slower than $1/r^2$ at $r \to 0$, the effective energy profile $U_{\text{ef}}(r)$ has the shape shown schematically in Fig. 5. This is true, in particular, for the very important case

Attractive Coulomb potential

$$U(r) = -\frac{\alpha}{r}, \quad \alpha > 0, \tag{3.49}$$

which describes, in particular, the *Coulomb* (electrostatic) *interaction* of two particles with electric charges of the opposite sign, and Newton's gravity law (1.16a). This particular case will be analyzed in the following section, but now let us return to the analysis of an arbitrary attractive potential $U(r) < 0$ leading to the effective potential shown in Fig. 5, when the angular-momentum term dominates at small distances r.

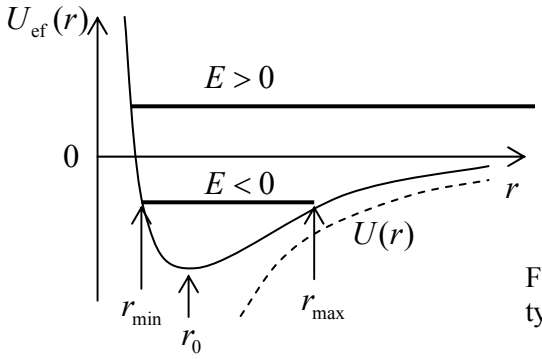

Fig. 3.5. Effective potential profile of, and two types of motion in an attractive central field.

According to the analysis of Sec. 3, such potential profile, with a minimum at some distance r_0, may sustain two types of motion, depending on the energy E (which is of course determined by the initial conditions):

(i) If $E > 0$, there is only one classical turning point where $E = U_{ef}$, so that distance r either grows with time from the very beginning, or (if the initial value of $\dot{r}$ was negative) first decreases and then, after the reflection from the increasing potential U_{ef}, starts to grow indefinitely. The latter case, of course, describes *scattering*.

(ii) On the opposite, if the energy is within the range

$$U_{ef}(r_0) \le E < 0, \tag{3.50}$$

the system moves periodically between two classical turning points r_{min} and r_{max}. These oscillations of distance r correspond to the bound orbital motion of our effective particle about the attracting center. [15]

Let us start with the discussion of the bound motion, with energy within the range (50). If energy has its minimal possible value,

$$E = U_{ef}(r_0) = \min[U_{ef}(r)], \tag{3.51}$$

the distance cannot change, $r = r_0 = \text{const}$, so that the orbit is circular, with the radius r_0 satisfying the condition $dU_{ef}/dr = 0$. Let us see whether this result allows for an elementary explanation. Using Eq. (44) we see that the condition for r_0 may be written as

$$\frac{L_z^2}{mr_0^3} = \frac{dU}{dr}\Big|_{r=r_0}. \tag{3.52}$$

Since in a circular motion, velocity **v** is perpendicular to the radius vector **r,** L_z is just mr_0v, the left-hand part of Eq. (52) equals mv^2/r_0, while its right-hand part is just the magnitude of the attractive force, so that this equation expresses the well-known 2nd Newton law for the circular motion. Plugging this result into Eq. (47), we get a linear law of angle change, $\varphi = \omega t + \text{const}$, with angular velocity

$$\omega = \frac{L_z}{mr_0^2} = \frac{v}{r_0}, \tag{3.53}$$

and hence the rotation period $\mathcal{T}_\varphi \equiv 2\pi/\omega$ obeys the elementary relation

$$\mathcal{T}_\varphi = \frac{2\pi r_0}{v}. \tag{3.54}$$

Now, let the energy be above its minimum value. Using Eq. (46) just as in Sec. 3, we see that distance r now oscillates with period

$$\mathcal{T}_r = (2m)^{1/2} \int_{r_{min}}^{r_{max}} \frac{dr}{[E - U(r) - L_z^2/2mr^2]^{1/2}}. \tag{3.55}$$

[15] In the opposite case when the interaction is *repulsive*, $U(r) > 0$, the addition of the positive angular energy term only increases the trend, and only the scattering scenario is possible.

This period is, in general, different from $\mathcal{T}_\varphi$. Indeed, the change of angle φ between two sequential points of the nearest approach, that follows from Eq. (48),

$$|\Delta\varphi| = 2\frac{L_z}{(2m)^{1/2}}\int_{r_{min}}^{r_{max}} \frac{dr}{r^2\left[E - U(r) - L_z^2/2mr^2\right]^{1/2}}, \tag{3.56}$$

is generally different from 2π. Hence, the general trajectory of the bound motion has a spiral shape – see, e.g., an illustration in Fig. 6.

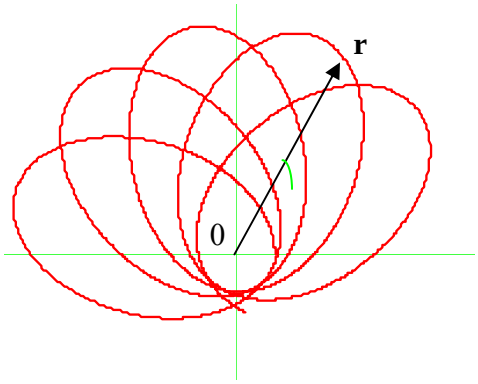

Fig. 3.6. Typical open orbit of a particle moving in a non-Coulomb central field.

3.6. 1st and 3rd Kepler laws

The situation is special, however, for a very important particular case, namely that of the *Coulomb potential* described by Eq. (49). Indeed, plugging this potential into Eq. (48), we get

$$\varphi = \pm\frac{L_z}{(2m)^{1/2}}\int \frac{dr}{r^2\left(E + \alpha/r - L_z^2/2mr^2\right)^{1/2}}. \tag{3.57}$$

This is a table integral,[16] equal to

$$\varphi = \pm\arccos\frac{L_z^2/m\alpha r - 1}{\left(1 + 2EL_z^2/m\alpha^2\right)^{1/2}} + \text{const}. \tag{3.58}$$

The reciprocal function, $r(\varphi)$, is 2π - periodic:

$$r = \frac{p}{1 + e\cos(\varphi + \text{const})}, \tag{3.59}$$

Elliptic orbit and its parameters

so that at $E < 0$, the orbit a closed line,[17] characterized with the following parameters:

$$p \equiv \frac{L_z^2}{m\alpha}, \qquad e \equiv \left[1 + \frac{2EL_z^2}{m\alpha^2}\right]^{1/2}. \tag{3.60}$$

[16] See, e.g., MA Eq. (6.3a).

[17] It may be proved that for the power-law interaction, $U \propto r^\nu$, the orbits are closed line only if $\nu = -1$ (i.e. our current case of the Coulomb potential) or $\nu = +2$ (the 3D harmonic oscillator) – the so-called *Bertrand theorem*.

The physical meaning of these parameters is very simple. Indeed, according to the general Eq. (52), in the Coulomb potential, for which $dU/dr = \alpha/r^2$, we see that p is just the circular orbit radius[18] for given L_z: $r_0 = L_z^2/m\alpha \equiv p$, and

$$\min\left[U_{\text{ef}}(r)\right] \equiv U_{\text{ef}}(r_0) = -\frac{\alpha^2 m}{2L_z^2}, \tag{3.61}$$

Using this equality, parameter e (called *eccentricity*) may be presented just as

$$e = \left\{1 - \frac{E}{\min[U_{\text{ef}}(r)]}\right\}^{1/2}. \tag{3.62}$$

Analytical geometry tells us that Eq. (59), with $e < 1$, is one of canonical forms for presentation of an *ellipse,* with one of its two focuses located at the origin. This fact is known as the *1st Kepler law*. Figure 7 shows the relation between the main dimensions of the ellipse and parameters p and e.[19]

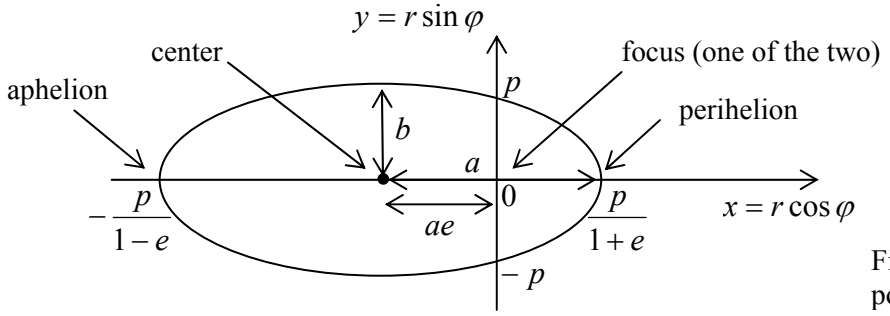

Fig. 3.7. Ellipse, and its special points and dimensions.

In particular, the major axis a and minor axis b are simply related to p and e and hence, via Eqs. (60), to the motion integrals E and L_z:

$$a = \frac{p}{1-e^2} = \frac{\alpha}{2|E|}, \qquad b = \frac{p}{\left(1-e^2\right)^{1/2}} = \frac{L_z}{\left(2m|E|\right)^{1/2}}. \tag{3.63}$$

As was mentioned above, at $E \to \min\,[U_{\text{ef}}(r)]$ the orbit is almost circular, with $r(\varphi) \cong r_0 = p$. On the contrary, as E is increased to approach zero (its maximum value for the closed orbit), then $e \to 1$, so that the aphelion point $r_{\max} = p/(1 - e)$ tends to infinity, i.e. the orbit becomes extremely extended. If the energy is exactly zero, Eq. (59) (with $e = 1$) is still valid for all values of φ (except for one special point $\varphi = \pi$ where r becomes infinite) and describes a *parabolic* (i.e. open) trajectory. At $E > 0$, Eq. (59) is still valid within a certain sector of angles φ (in that it yields positive results for r), and describes an open, *hyperbolic* trajectory - see the next section.

For $E < 0$, the above relations also allow a ready calculation of the rotation period $\mathcal{T} \equiv \mathcal{T}_r = \mathcal{T}_\varphi$. (In the case of a closed trajectory, $\mathcal{T}_r$ and $\mathcal{T}_\varphi$ have to coincide.) Indeed, it is well known that the ellipse area $A = \pi ab$. But according to the 2nd Kepler law (40), $dA/dt = L_z/2m = \text{const}$. Hence

[18] Mathematicians prefer a more solemn terminology: parameter $2p$ is called the *latus rectum* of the elliptic trajectory – see Fig. 7.

[19] In this figure, the constant participating in Eqs. (58)-(59) is assumed to be zero. It is evident that a different choice of the constant corresponds just to a constant turn of the ellipse about the origin.

$$\mathcal{T} = \frac{A}{dA/dt} = \frac{\pi ab}{L_z/2m}. \tag{3.64a}$$

Using Eqs. (60) and (63), this result may be presented in several other forms:

$$\mathcal{T} = \frac{\pi p^2}{(1-e^2)^{3/2}(L_z/2m)} = \pi\alpha\left(\frac{m}{2|E|^3}\right)^{1/2} = 2\pi a^{3/2}\left(\frac{m}{\alpha}\right)^{1/2}. \tag{3.64b}$$

Since for the Newtonian gravity (1.16a), $\alpha = Gm_1m_2 = GmM$, at $m_1 << m_2$ (i.e. $m << M$) this constant is proportional to m, and the last form of Eq. (64b) yields the *3rd Kepler law*: periods of motion of different planets in the same central field, say that of our Sun, scale as $T \propto a^{3/2}$. Note that in contrast to the 2nd Kepler law (that is valid for any central field), the 1st and 3rd Kepler laws are potential-specific.

3.7. Classical theory of elastic scattering

If $E > 0$, the motion is unbound for any interaction potential. In this case, the two most important parameters of the particle trajectory are the *scattering angle* θ and *impact parameter* b (Fig. 8), and the main task for theory is to find the relation between them in the given potential $U(r)$. For that, it is convenient to note that b is related to two conserved quantities, particle's energy[20] E and its angular momentum L_z, in a simple way:[21]

$$L_z = b(2mE)^{1/2}. \tag{3.65}$$

Hence the angular contribution to the effective potential (44) may be presented as

$$\frac{L_z^2}{2mr^2} = E\frac{b^2}{r^2}. \tag{3.66}$$

Second, according to Eq. (48), the trajectory sections from infinity to the nearest approach point ($r = r_{min}$), and from that point to infinity, have to be similar, and hence correspond to equal angle changes φ_0 - see Fig. 8.

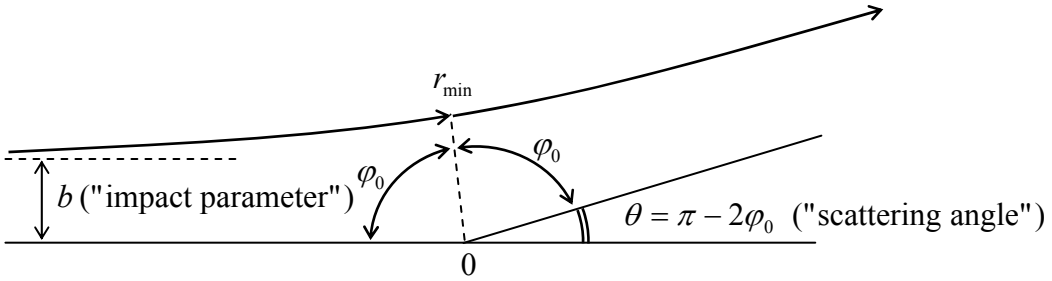

Fig. 3.8. Main geometric parameters of the scattering problem.

[20] The energy conservation law is frequently emphasized by calling this process *elastic scattering*.

[21] Indeed, at $r >> b$, the definition $\mathbf{L} = \mathbf{r}\times(m\mathbf{v})$ yields $L_z = bmv_\infty$, where $v_\infty = (2E/m)^{1/2}$ is the initial (and hence the final) velocity of the particle.

Hence we may apply the general Eq. (48) to just one of the sections, say $[r_{\min}, \infty]$, to find the scattering angle:

$$\theta = \pi - 2\varphi_0 = \pi - 2\frac{L_z}{(2m)^{1/2}}\int_{r_{\min}}^{\infty}\frac{dr}{r^2\left[E - U(r) - L_z^2/2mr^2\right]^{1/2}} = \pi - 2\int_{r_{\min}}^{\infty}\frac{bdr}{r^2\left[1 - U(r)/E - b^2/r^2\right]^{1/2}}. \quad (3.67)$$

In particular, for the Coulomb potential (49), now with an arbitrary sign of α, we can apply the same table integral as in the previous section to get[22]

$$\theta = \left|\pi - 2\arccos\frac{\alpha/2Eb}{\left[1 + (\alpha/2Eb)^2\right]^{1/2}}\right|. \quad (3.68a)$$

This result may be more conveniently rewritten as

$$\tan\frac{|\theta|}{2} = \frac{|\alpha|}{2Eb}. \quad (3.68b)$$

Very clearly, the scattering angle's magnitude increases with the potential strength α, and decreases as either the particle energy or the impact parameter (or both) are increased.

The general equation (67) and the Coulomb-specific relations (68) present a formally complete solution of the scattering problem. However, in a typical experiment on elementary particle scattering the impact parameter b of a single particle is random and unknown. In this case, our results may be used to obtain statistics of the scattering angle θ, in particular the so-called *differential cross-section*[23]

$$\boxed{\frac{d\sigma}{d\Omega} \equiv \frac{1}{n}\frac{dN}{d\Omega},} \quad (3.69)$$

Differential cross-section

where n is the average number of the incident particles per unit area, and dN is the average number of particles scattered into a small solid angle range $d\Omega$. For a spherically-symmetric scattering center, which provides an axially-symmetric scattering pattern, $d\sigma/d\Omega$ may be calculated by counting the number of incident particles within a small range db of the impact parameter:

$$dN = n\,2\pi\,bdb. \quad (3.70)$$

and hence scattered into the corresponding small solid angle range $d\Omega = 2\pi\sin\theta\,d\theta$. Plugging these relations into Eq. (69), we get the following general geometric relation:

$$\frac{d\sigma}{d\Omega} = \frac{b}{\sin\theta}\left|\frac{db}{d\theta}\right|. \quad (3.71)$$

In particular, for the Coulomb potential (49), a straightforward differentiation of Eq. (68) yields the so-called *Rutherford scattering formula*

[22] Alternatively, this result may be recovered directly from Eq. (59) whose parameters, at $E > 0$, may be expressed via the same dimensionless parameter $(2Eb/\alpha)$: $p = b(2Eb/\alpha)$, $e = [1 + (2Eb/\alpha)^2]^{1/2} > 1$.

[23] This terminology stems from the fact that an integral of $d\sigma/d\Omega$ over the full solid angle, called the *full cross-section* σ, has the dimension of area: $\sigma = N/n$, where N is the total number of scattered particles.

Rutherford scattering formula

$$\frac{d\sigma}{d\Omega} = \left(\frac{\alpha}{4E}\right)^2 \frac{1}{\sin^4(\theta/2)}. \tag{3.72}$$

This result, which shows very strong scattering to small angles (so strong that the integral that expresses the full cross-section σ is formally diverging at $\theta \to 0$),[24] and weak *backscattering* (scattering to angles $\theta \approx \pi$) was historically extremely significant: in the early 1910s its good agreement with α-particle scattering experiments carried out by E. Rutherford's group gave a strong justification for "planetary" models of atoms, with electrons moving about very small nuclei.

Note that elementary particle scattering is frequently accompanied with electromagnetic radiation and/or other processes leading to the loss of the initial mechanical energy of the system, leading to *inelastic scattering*, that may give significantly different results. (In particular, a capture of an incoming particle becomes possible even for a Coulomb attracting center.) Also, quantum-mechanical effects may be important at scattering, so that the above results should be used with caution.

3.8. Exercise problems

3.1. For the system considered in Problem 2.5 (a bead sliding along a string with fixed tension $\mathcal{T}$, see Fig. on the right), analyze small oscillations of the bead near the equilibrium.

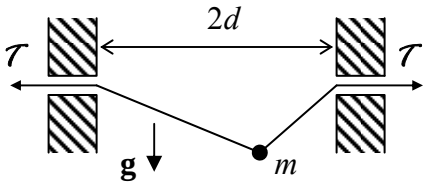

3.2. Calculate the functional dependence of period $\mathcal{T}$ of oscillations of a 1D particle of mass m in potential $U(q) = \alpha q^{2n}$ (where $\alpha > 0$, and n is a positive integer) on energy E. Explore the limit $n \to \infty$.

3.3. Explain why the term $mr^2\dot{\varphi}^2/2$, recast in accordance with Eq. (42), cannot be merged with $U(r)$ in Eq. (38), to form an effective 1D potential energy $U(r) - L_z^2/2mr^2$, with the second term's sign opposite to that given by Eq. (44). We have done an apparently similar thing for our testbed, bead-on-rotating-ring problem in the very end of Sec. 1 – see Eq. (3.6); why cannot the same trick work for the planetary problem? Besides a formal explanation, discuss the physics behind this difference.

3.4. A dumbbell, consisting of two equal masses m on a light rod of length l, can slide without friction along a vertical ring of radius R, rotated about its vertical diameter with constant angular velocity ω - see Fig. on the right. Derive the condition of stability of the lower horizontal position of the dumbbell.

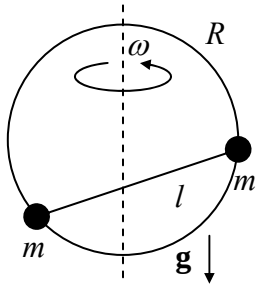

[24] This divergence, which persists at the quantum-mechanical treatment of the problem, is due to particles with large values of b, and disappears at an account, for example, of a finite concentration of the scattering centers.

3.5.[25] Analyze the dynamics of the so-called *spherical pendulum* - a point mass hung, in a uniform gravity field **g**, on a light cord of length l, with no motion's confinement to a vertical plane. In particular:

(i) find the integrals of motion and reduce the problem to a 1D one,
(ii) calculate the time period of the possible circular motion around the vertical axis,
(iii) explore small deviations from the circular motion. (Are the pendulum orbits closed?)

3.6. The orbits of Mars and Earth around the Sun may be well approximated as circles, with a radii ratio of 3/2. Use this fact, and the Earth year duration (which you should know :-), to calculate the time of travel to Mars spending least energy, neglecting the planets' size and the effects of their gravitational fields on the spacecraft.

3.7. Derive first-order and second-order differential equations for $u \equiv 1/r$ as a function of φ, describing the trajectory of particle's motion in a central potential $U(r)$. Spell out the latter equation for the particular case of the Coulomb potential (3.49) and discuss the result.

3.8. For motion in the central potential

$$U(r) = -\frac{\alpha}{r} + \frac{\beta}{r^2},$$

(i) find the orbit $r(\varphi)$, for positive α and β, and all possible ranges of energy E;
(ii) prove that in the limit $\beta \to 0$, and for energy $E < 0$, the orbit may be represented as a slowly rotating ellipse;
(iii) express the angular velocity of this slow orbit rotation via parameters α and β of the potential, particle's mass m, its energy E, and the angular momentum L_z.

3.9. A particle is moving in the field of an attractive central force, with potential

$$U(r) = -\frac{\alpha}{r^n}, \qquad \text{where } \alpha n > 0 .$$

For what values of n is a circular orbit stable?

3.10. Determine the condition for a particle of mass m, moving under the effect of a central attractive force

$$\mathbf{F} = -\alpha \frac{\mathbf{r}}{r^3} \exp\left\{-\frac{r}{R}\right\},$$

where C and R are positive constants, to have a stable circular orbit.

3.11. A particle of mass m, with angular momentum L_z, moves in the field of an attractive central force with a distance-independent magnitude F. If particle's energy E is slightly higher than the value $E_{\min}$ corresponding to the circular orbit of the particle, what is the time period of its radial oscillations? Compare the period with that of the circular orbit at $E = E_{\min}$.

[25] Solving this problem is a very good preparation for the analysis of symmetric top rotation in Sec. 6.5.

3.12. For particle scattering in a repulsive Coulomb field, calculate the minimum approach distance r_{min} and velocity v_{min} at that point, and analyze their dependence on the impact parameter b (see Fig. 3.8 of the lecture notes) and the initial velocity v_∞ of the particle.

3.13. A particle is launched from afar, with impact parameter b, toward an attracting center with central potential

$$U(r) = -\frac{\alpha}{r^n}, \quad \text{with } n > 2, \alpha > 0.$$

(i) Express the minimum distance between the particle and the center via b, if the initial kinetic energy E of the particle is barely sufficient for escaping the capture by the attracting center.

(ii) Calculate capture's full cross-section; explore the limit $n \to 2$.

3.14. A meteorite with initial velocity v_∞ approaches an atmosphere-free planet of mass M and radius R.

(i) Find the condition on the impact parameter b for the meteorite to hit planet's surface.

(ii) If the meteorite barely avoids the collision, what is its scattering angle?

3.15. Calculate the differential and full cross-sections of the classical, elastic scattering of small particles by a hard sphere of radius R.

3.16. The most famous[26] confirmation of Einstein's general relativity theory has come from the observation, by A. Eddington and his associates, of light's deflection by the Sun, during the May 1919 solar eclipse. Considering light photons as classical particles propagating with the light speed $v_0 \to c \approx 2.998\times10^8$m/s, and the astronomic data for Sun's mass, $M_S \approx 1.99\times10^{30}$kg, and radius, $R_S \approx 0.6957\times10^9$m, calculate the nonrelativistic mechanics' prediction for the angular deflection of the light rays grazing the Sun's surface.

[26] It was not the first confirmation, though. The first one came 4 years earlier from A. Einstein himself, who showed that his theory may qualitatively explain the difference between the rate of Mercury orbit's precession, known from earlier observations, and the nonrelativistic theory of this effect.

This page is intentionally left blank

Chapter 4. Oscillations

In this course, oscillations in 1D (and effectively 1D) systems are discussed in detail, because of their key importance for physics and engineering. We will start with the so-called "linear" oscillator whose differential equation of motion is linear and hence allows the full analytical solutions, and then proceed to "nonlinear" and parametric systems whose dynamics may be only explored by either approximate analytical or numerical methods.

4.1. Free and forced oscillations

In Sec. 3.2 we briefly discussed oscillations in a very important Hamiltonian system - a 1D *harmonic oscillator* described by a simple 1D Lagrangian[1]

$$L \equiv T(\dot{q}) - U(q) = \frac{m}{2}\dot{q}^2 - \frac{\kappa}{2}q^2, \tag{4.1}$$

whose Lagrangian equation of motion,

Harmonic oscillator's equation

$$m\ddot{q} + \kappa q = 0, \quad \text{i.e. } \ddot{q} + \omega_0^2 q = 0, \quad \text{with } \omega_0^2 \equiv \frac{\kappa}{m} \geq 0, \tag{4.2}$$

is a *linear homogeneous* differential equation. Its general solution is presented by Eq. (3.16), but it is frequently useful to recast it into another, amplitude-phase form:

Harmonic oscillator's motion

$$q(t) = u\cos\omega_0 t + v\sin\omega_0 t = A\cos(\omega_0 t - \varphi), \tag{4.3a}$$

where A is the *amplitude* and φ the *phase* of the oscillations, which are determined by the initial conditions. Mathematically, it is frequently easier to work with sinusoidal functions as complex exponents, by rewriting Eq. (3a) in one more form:[2]

$$q(t) = \mathrm{Re}\left[Ae^{-i(\omega_0 t - \varphi)}\right] = \mathrm{Re}\left[ae^{-i\omega_0 t}\right], \tag{4.3b}$$

Real and complex amplitudes

where a is the *complex amplitude* of the oscillations:

$$a \equiv Ae^{i\varphi}, \quad |a| = A, \quad \mathrm{Re}\,a = A\cos\varphi = u, \quad \mathrm{Im}\,a = A\sin\varphi = v. \tag{4.4}$$

Equations (3) represent the so-called *free oscillations* of the system, that are physically due to the initial energy of the system. At an account for dissipation, i.e. energy leakage out of the system, such oscillations decay with time. The simplest model of this effect is represented by an additional *viscosity force* that is proportional to the generalized velocity and directed opposite to it:

[1] For the notation simplicity, in this chapter I will drop indices "ef" in the energy components T and U, and parameters like m, κ, etc. However, the reader should still remember that T and U do not necessarily coincide with the real kinetic and potential energies (even if those energies may be uniquely identified) – see Sec. 3.1.

[2] Note that this is the so-called physics convention. Most engineering texts use the opposite sign in the imaginary exponent, $\exp\{-i\omega t\} \to \exp\{i\omega t\}$, with the corresponding sign implications for intermediate formulas, but (of course) similar final results for real variables.

$$F_v = -\eta\dot{q}\,, \tag{4.5}$$

where constant η is called the *viscosity coefficient*.[3] The inclusion of this force modifies the equation of motion (2) to become

$$m\ddot{q} + \eta\dot{q} + \kappa q = 0\,. \tag{4.6a}$$

This equation is frequently presented in the form

$$\ddot{q} + 2\delta\dot{q} + \omega_0^2 q = 0, \quad \text{with } \delta \equiv \frac{\eta}{2m}, \tag{4.6b}$$

Free oscillator with damping

where parameter δ is called the *damping coefficient*. Note that Eq. (6) is still a linear homogeneous second-order differential equation, and its general solution still has the form of the sum (3.13) of two exponents of the type $\exp\{\lambda t\}$, with arbitrary pre-exponential coefficients. Plugging such an exponent into Eq. (4), we get the following algebraic characteristic equation for λ:

$$\lambda^2 + 2\delta\lambda + \omega_0^2 = 0. \tag{4.7}$$

Solving this quadratic equation, we get

$$\lambda_\pm = -\delta \pm i\omega_0', \quad \text{where } \omega_0' \equiv \left(\omega_0^2 - \delta^2\right)^{1/2}, \tag{4.8}$$

so that for not very high damping ($\delta < \omega_0$)[4] we get the following generalization of Eq. (3):

$$q_{\text{free}}(t) = c_+ e^{\lambda_+ t} + c_- e^{\lambda_- t} = \left(u_0 \cos\omega_0' t + v_0 \sin\omega_0' t\right)e^{-\delta t} = A_0 e^{-\delta t}\cos\left(\omega_0' t - \varphi_0\right). \tag{4.9}$$

The result shows that, besides a certain correction to the free oscillation frequency (which is very small in the most interesting case of *low damping*, $\delta << \omega_0$), the energy dissipation leads to an exponential decay of oscillation amplitude with time constant $\tau = 1/\delta$:

$$A = A_0 e^{-t/\tau}, \quad \text{where } \tau \equiv \frac{1}{\delta} = \frac{2m}{\eta}. \tag{4.10}$$

Decaying free oscillations

A convenient, dimensionless measure of damping is the so-called *quality factor* Q (or just *Q-factor*) which is defined as $\omega_0/2\delta$, and may be rewritten in several other useful forms:

[3] Here I treat Eq. (5) as a phenomenological model, but in statistical mechanics such dissipative term may be *derived* as an average force exerted on a body by its environment whose numerous degrees of freedom are in random, though possibly thermodynamically-equilibrium states. Since such environmental force also has a random component, the dissipation is fundamentally related to *fluctuations*, and the latter effects may be neglected (as they are in this course) only if the oscillation energy is much higher than the energy scale of random fluctuations of the environment - in the thermal equilibrium at temperature T, the larger of $k_B T$ and $\hbar\omega_0/2$ - see, e.g., SM Chapter 5 and QM Chapter 7.

[4] Systems with very high damping ($\delta > \omega_0$) can hardly be called oscillators, and though they are used in engineering and physics experiment (e.g., for the shock, vibration, and sound isolation), for their discussion I have to refer the interested reader to special literature – see, e.g., C. Harris and A. Piersol, *Shock and Vibration Handbook*, 5th ed., McGraw Hill, 2002. Let me only note that at very high damping, $\delta >> \omega_0$, the system may be adequately described with just one parameter: the relaxation time $1/\lambda_+ \approx 2\delta/\omega_0^2 >> \omega_0$.

$$Q \equiv \frac{\omega_0}{2\delta} = \frac{m\omega_0}{\eta} = \frac{(m\kappa)^{1/2}}{\eta} = \pi\frac{\tau}{\mathcal{T}} = \frac{\omega_0\tau}{2}, \tag{4.11}$$

where $\mathcal{T} = 2\pi/\omega_0$ is the oscillation period in the absence of damping – see Eq. (3.29). Since the oscillation energy E is proportional to their amplitude squared, i.e. decays as $\exp\{-2t/\tau\}$, with time constant $\tau/2$, the last form of Eq. (11) may be used to rewrite the Q-factor in one more form:

$$Q = \omega_0 \frac{E}{(-\dot{E})} \equiv \omega_0 \frac{E}{\mathcal{P}}, \tag{4.12}$$

where $\mathcal{P}$ is the dissipation power. (Two other useful ways to measure Q will be discussed in a minute.) The range of Q-factors of important oscillators is very broad, all the way from $Q \sim 10$ for a human leg (with relaxed muscles), to $Q \sim 10^4$ of the quartz crystals used in "electronic" clocks and watches, all the way up to $Q \sim 10^{12}$ for microwave cavities with superconducting walls.

In contrast to the decaying free oscillations, the *forced oscillations*, induced by an external force $F(t)$, may maintain their amplitude infinitely, even at nonvanishing damping. This process may be described by a still linear but now *inhomogeneous* differential equation

Forced oscillator with damping

$$m\ddot{q} + \eta\dot{q} + \kappa q = F(t), \tag{4.13a}$$

or, more conveniently, by the following generalization of Eq. (6b):

$$\ddot{q} + 2\delta\dot{q} + \omega_0^2 q = f(t), \quad \text{where } f(t) \equiv F(t)/m. \tag{4.13b}$$

For a particle of mass m, confined to a straight line, Eq. (12a) is just an expression of the 2nd Newton law (or rather one of its Cartesian component). More generally, according to Eq. (1.41), Eq. (13) is valid for any dissipative 1D system whose Gibbs potential energy (1.39) has the form $U_G(q, t) = \kappa q^2/2 - F(t)q$.

The forced-oscillation solutions may be analyzed by two mathematically equivalent methods whose relative convenience depends on the character of function $f(t)$.

(i) Frequency domain. Let us present function $f(t)$ as a Fourier sum of sinusoidal harmonics:[5]

$$f(t) = \sum_{\omega} f_\omega e^{-i\omega t}. \tag{4.14}$$

Then, due to linearity of Eq. (13), its general solution may be presented as a sum of the decaying free oscillations (9) with frequency ω_0', independent of function $F(t)$, and forced oscillations due to each of the Fourier components of the force:[6]

General solution of Eq. (13)

$$q(t) = q_{\text{free}}(t) + q_{\text{forced}}(t), \quad q_{\text{forced}}(t) = \sum_{\omega} a_\omega e^{-i\omega t}. \tag{4.15}$$

Plugging Eq. (15) into Eq. (13), and requiring the factors before each $e^{-i\omega t}$ in both parts to be equal, we get

[5] Operator Re, used in Eq. (3), may be dropped here, because for any physical (real) force, the imaginary components of the sum compensate each other. This imposes the following condition on the complex Fourier amplitudes: $f_{-\omega} = f_\omega^*$, where the star means the complex conjugation.

[6] In physics, this mathematical property of linear equations is frequently called the *linear superposition principle*.

$$a_\omega = f_\omega \chi(\omega), \tag{4.16}$$

where complex function $\chi(\omega)$, in our particular case equal to

$$\chi(\omega) = \frac{1}{\left(\omega_0^2 - \omega^2\right) - 2i\omega\delta}, \tag{4.17}$$

is called either the *response function* or (especially for non-mechanical oscillators) the *generalized susceptibility*. From here, the real amplitude of oscillations under the effect of a sinusoidal force that may be represented by just one Fourier harmonic of the sum (15), is

$$A_\omega \equiv |a_\omega| = |f_\omega||\chi(\omega)|, \quad \text{with } |\chi(\omega)| = \frac{1}{\left[(\omega_0^2 - \omega^2)^2 + (2\omega\delta)^2\right]^{1/2}}. \tag{4.18}$$

Forced oscillation's amplitude

This formula describes, in particular, an increase of the oscillation amplitude A_ω at $\omega \to \omega_0$ - see Fig. 1. According to Eqs. (11) and (20), at the exact resonance,

$$|\chi(\omega)|_{\omega=\omega_0} = \frac{1}{2\omega_0\delta}, \tag{4.19}$$

so that, according to Eq. (11), the ratio of the oscillator response magnitudes at $\omega = \omega_0$ and at $\omega = 0$ ($|\chi(\omega)|_{\omega=0} = 1/\omega_0^2$) is exactly equal to the Q-factor. Thus, the response increase is especially strong in the low damping limit ($\delta << \omega_0$, i.e. $Q >> 1$); moreover at $Q \to \infty$ and $\omega \to \omega_0$ the response diverges. (This fact is very useful for the approximate methods to be discussed later in this chapter.) This is of course the classical description of the famous phenomenon of *resonance*, so ubiquitous in physics.

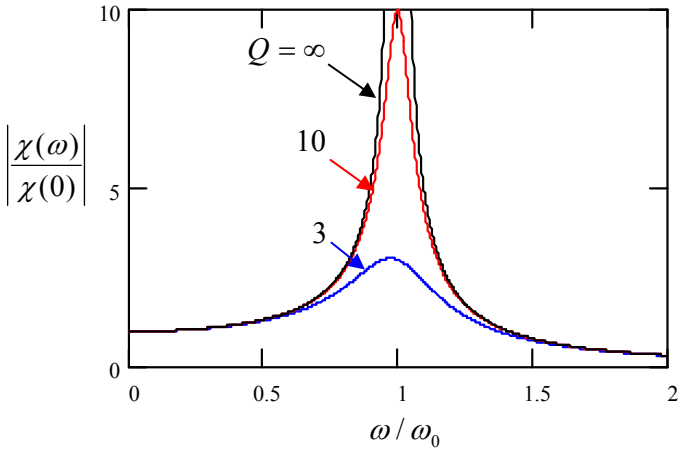

Fig. 4.1. Resonance in a harmonic oscillator (13), for several values of the Q-factor.

Due to the increase of the resonance peak height, its width is inversely proportional to Q. Quantitatively, in the most interesting low-damping limit, $Q >> 1$, the reciprocal Q-factor gives the normalized value of the so-called FWHM ("full-width at half-maximum") of the resonance curve:

$$\frac{\Delta\omega}{\omega_0} = \frac{1}{Q}. \tag{4.20}$$

Indeed, $\Delta\omega$ is defined as the difference ($\omega_+ - \omega_-$) between the two values of ω at that the square of oscillator response function, $|\chi(\omega)|^2$ (which is, in particular, proportional to the oscillation energy),

equals a half of its resonance value (19). In the low damping limit, both these points are very close to ω_0, so that in the first (linear) approximation in $(\omega - \omega_0) << \omega_0$, ω we can take $(\omega_0^2 - \omega^2) \equiv -(\omega+\omega_0)(\omega-\omega_0) \approx (-2\omega\xi) \approx (-2\omega_0\xi)$, where

$$\xi \equiv \omega - \omega_0 \tag{4.21}$$

is a convenient parameter called *detuning*. (We will repeatedly use it later in this chapter.) In this approximation, the second of Eqs. (18) is reduced to

$$\left|\chi(\omega)\right|^2 = \frac{1}{4\omega^2\left(\delta^2 + \xi^2\right)}. \tag{4.22}$$

As a result, points $\omega_\pm$ correspond to $\xi^2 = \delta^2$, i.e. $\omega_\pm = \omega_0 \pm \delta = \omega_0(1 \pm 1/2Q)$, so that $\Delta\omega \equiv \omega_+ - \omega_- = \omega_0/Q$, thus proving Eq. (20).

(ii) Time domain. Returning to the general problem of linear oscillations, one may argue that Eqs. (9), (15)-(17) provide a full solution of the forced oscillation problem. This is formally correct, but this solution may be very inconvenient if the external force is far from sinusoidal function of time. In this case, we should first calculate the complex amplitudes f_ω participating in the Fourier sum (14). In the general case of non-periodic $f(t)$, this is actually the Fourier integral,

$$f(t) = \int_{-\infty}^{+\infty} f_\omega e^{-i\omega t}\, dt, \tag{4.23}$$

so that f_ω should be calculated using the reciprocal Fourier transform,

$$f_\omega = \frac{1}{2\pi}\int_{-\infty}^{+\infty} f(t')e^{i\omega t'}\, dt'. \tag{4.24}$$

Now we can use Eq. (16) for each Fourier component of the resulting forced oscillations, and rewrite the last of Eqs. (15) as

$$\begin{aligned} q_{\text{forced}}(t) &= \int_{-\infty}^{+\infty} a_\omega e^{-i\omega t}\, d\omega = \int_{-\infty}^{+\infty} \chi(\omega) f_\omega e^{-i\omega t}\, d\omega = \int_{-\infty}^{+\infty} d\omega\, \chi(\omega)\frac{1}{2\pi}\int_{-\infty}^{+\infty} dt'\, f(t')e^{i\omega(t'-t)} \\ &= \int_{-\infty}^{+\infty} dt'\, f(t')\left[\frac{1}{2\pi}\int_{-\infty}^{+\infty} d\omega\, \chi(\omega)e^{i\omega(t'-t)}\right], \end{aligned} \tag{4.25}$$

with the response function $\chi(\omega)$ given, in our case, by Eq. (17). Besides requiring two integrations, Eq. (25) is conceptually uncomforting: it seems to indicate that the oscillator's coordinate at time t depends not only on the external force exerted at earlier times $t' < t$, but also in future times. This would contradict one of the most fundamental principles of physics (and indeed, science as a whole), the *causality*: no effect may precede its cause.

Fortunately, a straightforward calculation (left for reader's exercise) shows that the response function (17) satisfies the following rule:[7]

[7] This is true for all systems in which $f(t)$ represents a cause, and $q(t)$ its effect. Following tradition, I discuss the frequency-domain expression of this causality relation (called the *Kramers-Kronig relations*) in the *Classical Electrodynamics* part of this lecture series – see EM Sec. 7.3.

$$\int_{-\infty}^{+\infty} \chi(\omega) e^{-i\omega\tau} d\omega = 0, \qquad \text{for } \tau < 0. \tag{4.26}$$

This fact allows the last form of Eq. (25) to be rewritten in either of the following equivalent forms:

$$q_{\text{forced}}(t) = \int_{-\infty}^{t} f(t') G(t-t') dt' = \int_{0}^{\infty} f(t-\tau) G(\tau) d\tau, \tag{4.27}$$

Linear system's response

where $G(\tau)$, defined as the Fourier transform of the response function,

$$G(\tau) \equiv \frac{1}{2\pi} \int_{-\infty}^{+\infty} \chi(\omega) e^{-i\omega\tau} d\omega, \tag{4.28}$$

Temporal Green's function

is called the (*temporal*) *Green's function* of the system. According to Eq. (26), $G(\tau) = 0$ for all $\tau < 0$.

While the second form of Eq. (27) is more convenient for calculations, its first form is more clear conceptually. Namely, it expresses the linear superposition principle in time domain, and may be interpreted as follows: the full effect of force $f(t)$ on an oscillator (actually, any *linear system*[8]) may be described as a sum of effects of short pulses of duration dt' and magnitude $f(t')$:

$$q_{\text{forced}}(t) = \lim_{\Delta t' \to 0} \sum_{t'=-\infty}^{t} G(t-t') f(t') \Delta t'. \tag{4.29}$$

- see Fig. 2. The Green's function $G(\tau)$ thus describes the oscillator response to a unit pulse of force, measured at time $\tau = t - t'$ after the pulse.

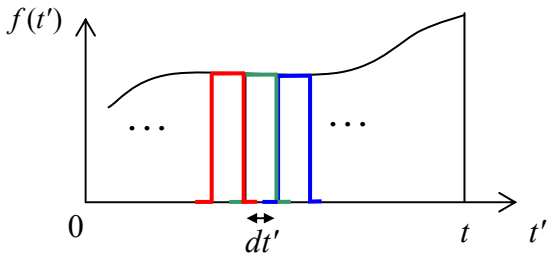

Fig. 4.2. Presentation of the force as a function of time as a sum of short pulses.

Mathematically, it is more convenient to go to the limit $dt' \to 0$ and describe the elementary, unit-area pulse by Dirac's δ-function,[9] thus returning to Eq. (27). This line of reasoning also gives a convenient way to calculate the Green's function. Indeed, for the particular case,

$$f(t) = \delta(t - t_0), \quad \text{with } t_0 < t, \tag{4.30}$$

Eq. (27) yields $q(t) = G(t - t_0)$. In particular, if $t > 0$, we may take $t_0 = 0$; then $q(t) = G(t)$. Hence the Green's function may be calculated as a solution of the differential equation of motion of the system, in our case, Eq. (13), with the δ-functional right-hand part:

$$\frac{d^2 G(\tau)}{d\tau^2} + 2\delta \frac{dG(\tau)}{d\tau} + \omega_0^2 G(\tau) = \delta(\tau), \tag{4.31}$$

[8] This is a very unfortunate, but common jargon, meaning "the system described by linear equations of motion".
[9] For a reminder of the basic properties of the δ-function, see MA Sec. 14.

and zero initial conditions:

$$G(-0) = \frac{dG}{d\tau}(-0) = 0, \tag{4.32}$$

where $t = -0$ means the instant immediately preceding $t = 0$.

This calculation may be simplified even further. Let us integrate both sides of Eq. (31) over a infinitesimal interval including the origin, e.g. $[-d\tau/2, +d\tau/2]$, and then follow the limit $d\tau \to 0$. Since Green's function has to be continuous because of its physical sense as the (generalized) coordinate, all terms in the left hand part but the first one vanish, while the first term yields $dG/d\tau\big|_{+0} - dG/d\tau\big|_{-0}$. Due to the second of Eqs. (32), the last of these two terms equals zero, while the right-hand part yields 1. Thus, $G(\tau)$ may be calculated for $\tau > 0$ (i.e. for all times when $G(\tau) \neq 0$) by solving the *homogeneous* version of system's equation of motion for $\tau > 0$, with the following special initial conditions:

$$G(0) = 0, \quad \frac{dG}{d\tau}(0) = 1. \tag{4.33}$$

This approach gives us a convenient way for calculation of Green's functions of linear systems. In particular for the oscillator with not very low damping ($\delta > \omega_0$, i.e. $Q > ½$), imposing boundary conditions (33) on the general free-oscillation solution (9), we immediately get[10]

Oscillator's Green's function

$$G(\tau) = \frac{1}{\omega_0'} e^{-\delta\tau} \sin \omega_0' \tau\,. \tag{4.34}$$

Equations (27) and (34) provide a very convenient recipe for solving most forced oscillations problems. As a very simple example, let us calculate the transient process in an oscillator under the effect of a constant force being turned on at $t = 0$:

$$f(t) = \begin{cases} 0, & t < 0, \\ f_0, & t > 0, \end{cases} \tag{4.35}$$

provided that at $t < 0$ the oscillator was at rest, so that $q_{\text{free}}(t) \equiv 0$. Then the second form of Eq. (27) yields

$$q(t) = \int_0^\infty f(t-\tau) G(\tau)\, d\tau = f_0 \int_0^t \frac{1}{\omega_0'} e^{-\delta\tau} \sin \omega_0' \tau \; d\tau. \tag{4.36}$$

The simplest way to work out such integrals is to present the sine function as the imaginary part of $\exp\{i\omega_0' t\}$, and merge the two exponents, getting

$$q(t) = f_0 \frac{1}{\omega_0'} \operatorname{Im}\left[\frac{1}{\delta + i\omega_0'} e^{-\delta\tau - i\omega_0'\tau} \right]_0^t = \frac{F_0}{k}\left[1 - e^{-\delta t}\left(\cos \omega_0' t + \frac{\delta}{\omega_0'} \sin \omega_0' t \right) \right]. \tag{4.37}$$

This result, plotted in Fig. 3, is rather natural: it describes nothing more than the transient from the initial equilibrium position $q = 0$ to the new equilibrium position $q_0 = f_0/\omega_0^2 = F_0/\kappa$, accompanied by

[10] The same result may be obtained from Eq. (28) with the response function $\chi(\omega)$ given by Eq. (19). This, more cumbersome, way is left for reader's exercise.

decaying oscillations. For this particular simple function $f(t)$, the same result might be also obtained by introducing a new variable $\tilde{q}(t) \equiv q(t) - q_0$ and solving the resulting *homogeneous* equation for $\tilde{q}$ (with appropriate initial condition $\tilde{q}(0) = -q_0$), but for more complicated functions $f(t)$ the Green's function approach is irreplaceable.

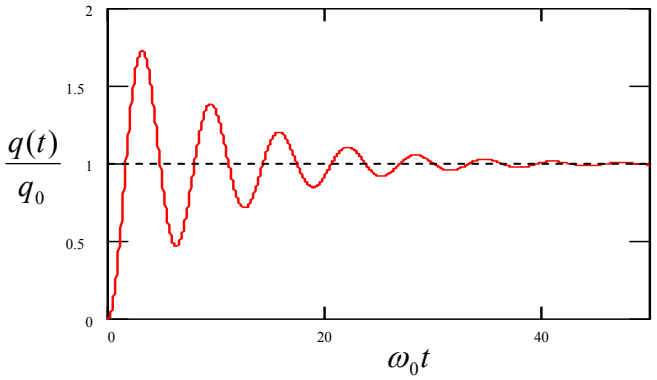

Fig. 4.3. Transient process in a linear oscillator, induced by a step-like force $f(t)$, for the particular case $\delta/\omega_0 = 0.1$ (i.e., $Q = 5$).

Note that for any particular linear system, its Green's function should be calculated only once, and then may be repeatedly used in Eq. (27) to calculate the system response to various external forces - either analytically or numerically. This property makes the Green's function approach very popular in many other fields of physics - with the corresponding generalization or re-definition of the function.[11]

4.2. Weakly nonlinear oscillations

In comparison with systems discussed in the last section, which are described by linear differential equations with constant coefficients and thus allow a complete and exact analytical solution, oscillations in nonlinear systems generally present a complex and, generally, analytically intractable problem. Let us start a discussion of such *nonlinear oscillations*[12] from an important case that may be explored analytically. In many important 1D oscillators, higher terms in the potential expansion (3.10) cannot be neglected, but are small and may be accounted for approximately. If, in addition, damping is low (or negligible), the equation of motion may be presented as a slightly modified Eq. (13):

$$\ddot{q} + \omega^2 q = f(t, q, \dot{q}, ...), \tag{4.38}$$

Weakly nonlinear oscillator

where $\omega \approx \omega_0$ is the anticipated frequency of oscillations (whose choice is to a certain extent arbitrary – see below), and the right-hand part f is small (say, scales as some small dimensionless parameter $\varepsilon << 1$), and may be considered as a *perturbation*.

Since at $\varepsilon = 0$ this equation has the sinusoidal solution given by Eq. (3), one might naïvely think that at nonvanishing but small ε, the approximate solution to Eq. (38) should be sought in the form

$$q(t) = q^{(0)} + q^{(1)} + q^{(2)} + ..., \quad \text{where } q^{(n)} \propto \varepsilon^n, \tag{4.39}$$

Formal perturbative solution

with $q^{(0)} = A \cos(\omega_0 t - \varphi) \propto \varepsilon^0$. This is a good example of an apparently impeccable mathematical reasoning that would lead to a very inefficient procedure. Indeed, let us apply it to the problem we

[11] See, e.g., EM Sec. 2.7, and QM Sec. 2.2.

[12] Again, "nonlinear oscillations" is a generally accepted slang term for oscillations in systems described by nonlinear equations of motion.

already know the exact solution for, namely the free oscillations in a linear but damped oscillator, for this occasion assuming the damping to be very low, $\delta/\omega_0 \sim \varepsilon << 1$. The corresponding equation of motion, Eq. (6), may be presented in form (38) if we take $\omega = \omega_0$ and

$$f = -2\delta\dot{q}, \quad \delta \propto \varepsilon . \tag{4.40}$$

The naïve approach described above would allow us to find *small* corrections, of the order of δ, to the free, non-decaying oscillations $A\cos(\omega_0 t - \varphi)$. However, we already know from Eq. (9) that the main effect of damping is a gradual decrease of the free oscillation amplitude to zero, i.e. a very *large* change of the amplitude, though at low damping, $\delta << \omega_0$, this decay takes large time $t \sim \tau >> 1/\omega_0$. Hence, if we want our approximate method to be productive (i.e. to work at all time scales, in particular for forced oscillations with established, constant amplitude and phase), we need to account for the fact that the *small* right-hand part of Eq. (38) may eventually lead to *essential* changes of oscillation amplitude A (and sometimes, as we will see below, also of oscillation phase φ) at large times, because of the *slowly accumulating* effects of the small perturbation.[13]

This goal may be achieved by the account of these slow changes already in the "0th approximation", i.e. the basic part of the solution in expansion (39):

0th order RWA solution

$$q^{(0)} = A(t)\cos[\omega t - \varphi(t)], \quad \text{with } \dot{A}, \dot{\varphi} \to 0 \quad \text{at } \varepsilon \to 0 . \tag{4.41}$$

The approximate methods based on Eqs. (39) and (41) have several varieties and several names,[14] but their basic idea and the results in the most important approximation (41) are the same. Let me illustrate this approach on a particular, simple but representative example of a dissipative (but high-Q) pendulum driven by a weak sinusoidal external force with a nearly-resonant frequency:

$$\ddot{q} + 2\delta\dot{q} + \omega_0^2 \sin q = f_0 \cos\omega t, \tag{4.42}$$

with $|\omega - \omega_0|$, $\delta << \omega_0$, and the force amplitude f_0 so small that $|q| << 1$ at all times. From what we know about the forced oscillations from Sec. 1, it is natural to identify ω in the left-hand part of Eq. (38) with the force frequency. Expanding $\sin q$ into the Taylor series in small q, keeping only the first two terms of this expansion, and moving all the small terms to the right-hand part, we can bring Eq. (42) to the canonical form (38):[15]

Duffing equation

$$\ddot{q} + \omega^2 q = -2\delta\dot{q} + 2\xi\omega q + \alpha q^3 + f_0 \cos\omega t \equiv f(t, q, \dot{q}) . \tag{4.43}$$

Here $\alpha = \omega_0^2/6$ in the case of the pendulum (though the calculations below will be valid for any α), and the second term in the right-hand part was obtained using the approximation already employed in Sec. 1:

---

[13] The same flexible approach is necessary to approximations used in quantum mechanics. The method discussed here is close in spirit (but not identical) to the *WKB approximation* (see, e.g., QM Sec. 2.4) rather to the *perturbation theory* varieties (QM Ch. 6).

[14] In various texts, one can meet references to either the *small parameter method* or *asymptotic methods*. The list of scientists credited for the development of this method and its variations notably includes J. Poincaré, B. van der Pol, N. Krylov, N. Bogolyubov, and Yu. Mitroplolsky. Expression (41) itself is frequently called the *Rotating-Wave Approximation* - RWA. (The origin of the term will be discussed in Sec. 6 below.) In the view of the pioneering role of B. van der Pol in the development of this approach, in some older textbooks the rotating-wave approximation is called the "van der Pol method".

[15] This equation is frequently called the *Duffing equation* (or the equation of the *Duffing oscillator*), after G. Duffing who was the first one to carry out its (rather incomplete) analysis in 1918.

$(\omega^2 - \omega_0^2)q \approx 2\omega(\omega - \omega_0)q = 2\omega\xi q$, where $\xi \equiv \omega - \omega_0$ is the detuning parameter that was already used earlier – see Eq. (21).

Now, following the general recipe expressed by Eqs. (39) and (41), in the 1st approximation in $f \propto \varepsilon$,[16] we may look for the solution to Eq. (43) in the form

$$q(t) = A\cos\Psi + q^{(1)}(t), \quad \text{where } \Psi \equiv \omega t - \varphi, \qquad q^{(1)} \sim \varepsilon. \tag{4.44}$$

Let us plug this assumed solution into both parts of Eq. (43), leaving only the terms of the first order in ε. Thanks to our (smart :-) choice of ω in the left-hand part of that equation, the two zero-order terms in that part cancel each other. Moreover, since each term in the right-hand part of Eq. (43) is already of the order of ε, we may drop $q^{(1)} \propto \varepsilon$ from the substitution into that part at all, because this would give us only terms $O(\varepsilon^2)$ or higher. As a result, we get the following approximate equation:

$$\ddot{q}^{(1)} + \omega^2 q^{(1)} = f^{(0)} \equiv -2\delta\frac{d}{dt}(A\cos\Psi) + 2\xi\omega A\cos\Psi + \alpha\left(A\cos\Psi\right)^3 + f_0\cos\omega t. \tag{4.45}$$

According to Eq. (41), generally A and φ should be considered as (slow) functions of time. However, let us leave the analyses of transient process and system stability until the next section, and use Eq. (45) to find stationary oscillations in the system, that are established after the initial transient. For that limited task, we may take A = const, φ = const, so that $q^{(0)}$ presents sinusoidal oscillations of frequency ω. Sorting the terms in the right-hand part according to their time dependence,[17] we see that it has terms with frequencies ω and 3ω:

$$f^{(0)} = (2\xi\omega A + \frac{3}{4}\alpha A^3 + f_0\cos\varphi)\cos\Psi + (2\delta\omega A - f_0\sin\varphi)\sin\Psi + \frac{1}{4}\alpha A^3\cos 3\Psi. \tag{4.46}$$

Now comes the main trick of the rotating-wave approximation: mathematically, Eq. (45) may be viewed as the equation of oscillations in a linear, dissipation-free harmonic oscillator of frequency ω (not ω_0!) under the action of an external force represented by the right-hand part of the equation. In our particular case, it has three terms: two *quadrature* components at that very frequency ω, and the third one at frequency 3ω. As we know from our analysis of this problem in Sec. 1, if any of the first two components is nonvanishing, $q^{(1)}$ grows to infinity – see Eq. (19) with $\delta = 0$. At the same time, by the very structure of the rotating-wave approximation, $q^{(1)}$ has to be finite - moreover, small! The only way out of this contradiction is to require that amplitudes of both quadrature components of $f^{(0)}$ with frequency ω are equal to zero:

$$2\xi\omega A + \frac{3}{4}\alpha A^3 + f_0\cos\varphi = 0, \qquad 2\delta\omega A - f_0\sin\varphi = 0. \tag{4.47}$$

These two *harmonic balance equations* enable us to find both parameters of the forced oscillations: their amplitude A and phase φ. In particular, the phase may be readily eliminated from this

[16] For a mathematically rigorous treatment of the higher approximations, see, e.g., Yu. Mitropolsky and N. Dao, *Applied Asymptotic Methods in Nonlinear Oscillations*, Springer, 2004. A more laymen (and somewhat verbose) discussion of various oscillatory phenomena may be found in the classical text A. Andronov, A. Vitt, and S. Khaikin, *Theory of Oscillators*, Dover, 2011.

[17] Using the second of Eqs. (44), $\cos\omega t$ may be rewritten as $\cos(\Psi + \varphi) \equiv \cos\Psi\cos\varphi - \sin\Psi\sin\varphi$. Then using the trigonometric identity $\cos^3\Psi = (3/4)\cos\Psi + (1/4)\cos 3\Psi$ - see, e.g., MA Eq. (3.4) results in Eq. (46).

system (most easily, by expressing $\sin\varphi$ and $\cos\varphi$ from the corresponding equations, and then requiring the sum $\sin^2\varphi + \cos^2\varphi$ to equal 1), and the solution for amplitude A presented in the following implicit but convenient form:

$$A^2 = \frac{f_0^2}{4\omega^2}\frac{1}{\xi^2(A)+\delta^2}, \quad \text{where } \xi(A) \equiv \xi + \frac{3}{8}\frac{\alpha A^2}{\omega} = \omega - \left(\omega_0 - \frac{3}{8}\frac{\alpha A^2}{\omega}\right). \tag{4.48}$$

This expression differs from Eq. (22) for the linear resonance in the low-damping limit only by the replacement of the detuning ξ with its effective amplitude-dependent value $\xi(A)$ or, equivalently, of the eigenfrequency ω_0 of the resonator with its effective, amplitude-dependent value

$$\omega_0(A) = \omega_0 - \frac{3}{8}\frac{\alpha A^2}{\omega}. \tag{4.49}$$

The physical meaning of $\omega_0(A)$ is simple: this is just the frequency of free oscillations of amplitude A in a similar nonlinear system, but with zero damping. Indeed, for $\delta = 0$ and $f_0 = 0$ we could repeat our calculations, assuming that ω is an amplitude-dependent eigenfrequency $\omega_0(A)$, to be found. Then the second of Eqs. (47) is trivially satisfied, while the second of them gives Eq. (49).

Expression (48) allows one to draw the curves of this *nonlinear resonance* just by bending the linear resonance plots (Fig. 1) according to the so-called *skeleton curve* expressed by Eq. (49). Figure 4 shows the result of this procedure. Note that at small amplitude, $\omega(A) \to \omega_0$, and we return to the usual, "linear" resonance (22).

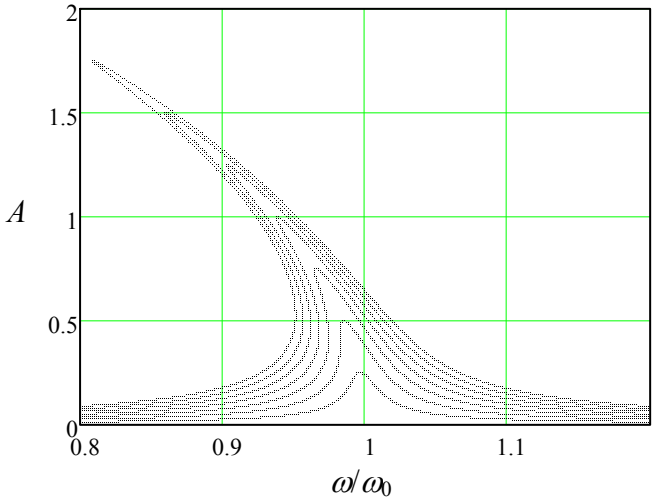

Fig. 4.4. Nonlinear resonance in the Duffing oscillator, as described by the rotating-wave approximation result (48), for the particular case $\alpha = \omega_0^2/6$, $\delta/\omega = 0.01$ (i.e. $Q = 50$), and seven values of parameter f_0/ω_0^2, increased by equal steps from 0 to 0.035.

To bring our solution to its logical completion, we should still find the first perturbation $q^{(1)}(t)$ from what is left of Eq. (45). Since the structure of this equation is similar to Eq. (13) with the force of frequency 3ω and zero damping, we may use Eqs. (16)-(17) to obtain

$$q^{(1)}(t) = -\frac{1}{32\omega^2}\alpha A^3 \cos 3(\omega t - \varphi). \tag{4.50}$$

Adding this perturbation (note the negative sign!) to the sinusoidal oscillation (41), we see that as the amplitude A of oscillations in a system with $\alpha > 0$ (e.g., a pendulum) grows, their waveform become a bit more "blunt" near the maximum deviations from the equilibrium.

Expression (50) also allows an estimate of the range of validity of the rotating-wave approximation: since it has been based on the assumption $|q^{(1)}| << |q^{(0)}| \le A$, for this particular problem we have to require $\alpha A^2/32\omega^2 << 1$. For a pendulum (with $\alpha = \omega_0^2/6$), this condition becomes $A^2 << 1/192$. Though numerical coefficients in such strong inequalities should be taken with a grain of salt, the smallness of this particular coefficient gives a good hint that the method should give very good results even for relatively large oscillations with $A \sim 1$. In Sec. 7 below, we will see that this is indeed the case.

From the mathematical viewpoint, the next step would be to calculate the next approximation

$$q(t) = A\cos\Psi + q^{(1)}(t) + q^{(2)}(t), \qquad q^{(2)} \sim \varepsilon^2, \tag{4.51}$$

and plug it into the Duffing equation (43), which (thanks to our special choice of $q^{(0)}$ and $q^{(1)}$) would retain only $\ddot{q}^{(2)} + \omega^2 q^{(2)}$ in its left-hand part. Again, requiring that amplitudes of two quadrature components of frequency ω in the right-hand part to be zero, we may get the second-order corrections to A and φ. Then we may use the remaining part of the equation to calculate $q^{(2)}$, and then go after the third-order terms, etc. However, for most purposes the sum $q^{(0)} + q^{(1)}$, and sometimes even just the crudest approximation $q^{(0)}$ alone, are completely sufficient. For example, according to Eq. (50), for a simple pendulum ($\alpha = \omega_0^2/6$) swinging as much as between the opposite horizontal positions ($A = \pi/2$), the 1st order correction $q^{(1)}$ is of the order of 0.5%. (Soon beyond this value, completely new dynamic phenomena start – see Sec. 7 below, but these phenomena cannot be covered by the rotating-wave approximation, at least in our current form.) Due to this reason, higher approximations are rarely pursued either in physics or engineering.

4.3. RWA equations

A much more important issue is the stability of solutions described by Eq. (48). Indeed, Fig. 4 shows that within a certain range of parameters, these equations give three different values for the oscillation amplitude (and phase), and it is important to understand which of these solutions are stable. Since these solutions are not the fixed points in the sense discussed in the Sec. 3.2 (each point in Fig. 4 represents a nearly-sinusoidal oscillation), their stability analysis needs a more general approach that would be valid for oscillations with amplitude and phase slowly evolving in time. This approach will also enable the analysis of non-stationary (especially the initial transient) processes that are of key importance for some dynamic systems.

First of all, let us formalize the way the harmonic balance equations, such as Eqs. (47), are obtained for the general case (38) – rather than for the particular Eq. (43) considered in the last section. After plugging in the 0th approximation (41) into the right-hand part of equation (38) we have to require the amplitudes of its both quadrature components of frequency ω to be zero. From the standard Fourier analysis we know that these requirements may be presented as

$$\boxed{\overline{f^{(0)}\sin\Psi} = 0, \quad \overline{f^{(0)}\cos\Psi} = 0,} \tag{4.52}$$

Harmonic balance equations

where symbol $\overline{...}$ means time averaging – in our current case, over the period $2\pi/\omega$ of the right-hand part of Eq. (52), with the arguments calculated in the 0th approximation:

$$f^{(0)} \equiv f(t, q^{(0)}, \dot{q}^{(0)}, ...) \equiv f\left(t, A\cos\Psi, -A\omega\sin\Psi, ...\right), \quad \text{with } \Psi = \omega t - \varphi\,. \tag{4.53}$$

Now, for a transient process the contribution of $q^{(0)}$ to left-hand part of Eq. (38) is not zero any longer, because both amplitude and phase may be slow functions of time – see Eq. (41). Let us calculate this contribution. The exact result would be

$$\ddot{q}^{(0)} + \omega^2 q^{(0)} \equiv \left(\frac{d^2}{dt^2} + \omega^2 \right) A\cos(\omega t - \varphi) = \left(\ddot{A} + 2\dot{\varphi}\omega A - \dot{\varphi}^2 A \right)\cos(\omega t - \varphi) - 2\dot{A}(\omega - \dot{\varphi})\sin(\omega t - \varphi). \tag{4.54}$$

However, in the first approximation in ε, we may neglect the second derivative of A, and also the squares and products of the first derivatives of A and φ (that are all of the second order in ε), so that Eq. (54) is reduced to

$$\ddot{q}^{(0)} + \omega^2 q^{(0)} \approx 2A\dot{\varphi}\omega\cos(\omega t - \varphi) - 2\dot{A}\omega\sin(\omega t - \varphi). \tag{4.55}$$

In the right-hand part of Eq. (52), we can neglect the time derivatives of the amplitude and phase at all, because this part is already proportional to the small parameter. Hence, in the first order in ε, Eq. (38) becomes

$$\ddot{q}^{(1)} + \omega^2 q^{(1)} = f_{\text{ef}}^{(0)} \equiv f^{(0)} - \left(2A\dot{\varphi}\omega\cos\Psi - 2\dot{A}\omega\sin\Psi \right). \tag{4.56}$$

Now, applying Eqs. (52) to function $f_{\text{ef}}^{(0)}$, and taking into account that the time averages of $\sin^2\Psi$ and $\cos^2\Psi$ are both equal to ½, while the time average of the product $\sin\Psi\cos\Psi$ vanishes, we get a pair of so-called *RWA equations* (alternatively called "the reduced equations" or sometimes "the van der Pol equations") for the time evolution of the amplitude and phase:

$$\dot{A} = -\frac{1}{\omega}\overline{f^{(0)}\sin\Psi}, \quad \dot{\varphi} = \frac{1}{\omega A}\overline{f^{(0)}\cos\Psi}. \tag{4.57a}$$

Extending the definition (4) of the complex amplitude of oscillations to their slow evolution in time, $a(t) \equiv A(t)\exp\{i\varphi(t)\}$, and differentiating this relation, we see that two equations (57a) may be also re-written in the form of either one equation for a:

Alternative forms of RWA equations

$$\dot{a} = \frac{i}{\omega}\overline{f^{(0)}e^{i(\Psi+\varphi)}} \equiv \frac{i}{\omega}\overline{f^{(0)}e^{i\omega t}}, \tag{4.57b}$$

or two equations for the real and imaginary parts of $a(t) = u(t) + iv(t)$:

$$\dot{u} = -\frac{1}{\omega}\overline{f^{(0)}\sin\omega t}, \quad \dot{v} = \frac{1}{\omega}\overline{f^{(0)}\cos\omega t}. \tag{4.57c}$$

The first-order harmonic balance equations (52) are evidently just the particular case of the RWA equations (57) for stationary oscillations ($\dot{A} = \dot{\varphi} = 0$).[18]

Superficially, the system (57a) of two coupled, first-order differential equations may look more complex than the initial, second-order differential equation (38), but actually it is usually much simpler.

[18] One may ask why cannot we stick to the just one, most compact, complex–amplitude form (57b) of the RWA equations. The main reason is that when function $f(q, \dot{q}, t)$ is nonlinear, we cannot replace its real arguments, such as $q = A\cos(\omega t - \varphi)$, with their complex-function representations like $a\exp\{-i\omega t\}$ (as could be done in the linear problems considered in Sec. 4.1), and need to use real variables, such as either $\{A, \varphi\}$ or $\{u, v\}$, anyway.

For example, let us spell them out for the easy case of free oscillations a linear oscillator with damping. For that, we may reuse the ready Eq. (46) with $\alpha = f_0 = 0$, turning Eqs. (4.57a) into

$$\dot{A} = -\frac{1}{\omega}\overline{f^{(0)}\sin\Psi} = -\frac{1}{\omega}\overline{(2\xi\omega A\cos\Psi + 2\delta\omega A\sin\Psi)\sin\Psi} = -\delta A, \tag{4.58a}$$

$$\dot{\varphi} = \frac{1}{\omega A}\overline{f^{(0)}\cos\Psi} = \frac{1}{\omega A}\overline{(2\xi\omega A\cos\Psi + 2\delta\omega A\sin\Psi)\cos\Psi} = \xi. \tag{4.58b}$$

The solution of Eq. (58a) gives us the same "envelope" law $A(t) = A(0)e^{-\delta t}$ as the exact solution (10) of the initial differential equation, while the elementary integration of Eq. (58b) yields $\varphi(t) = \xi t + \varphi(0) = \omega t - \omega_0 t + \varphi(0)$. This means that our approximate solution,

$$q^{(0)}(t) = A(t)\cos\bigl[\omega t - \varphi(t)\bigr] = A(0)e^{-\delta t}\cos\bigl[\omega_0 t - \varphi(0)\bigr], \tag{4.59}$$

agrees with the exact Eq. (9), and misses only correction (8) to the oscillation frequency, that is of the second order in δ, i.e. of the order of ε^2 – beyond the accuracy of our first approximation. It is remarkable how nicely do the RWA equations recover the proper frequency of free oscillations in this autonomous system - in which the very notion of ω is ambiguous.

The situation is different at forced oscillations. For example, for the (generally, nonlinear) Duffing oscillator described by Eq. (43) with $f_0 \neq 0$, Eqs. (57a) yield the RWA equations,

$$\dot{A} = -\delta A + \frac{f_0}{2\omega}\sin\varphi, \quad A\dot{\varphi} = \xi(A)A + \frac{f_0}{2\omega}\cos\varphi, \tag{4.60}$$

which are valid for an arbitrary function $\xi(A)$, provided that the nonlinear detuning remains much smaller than the oscillation frequency. Here (after a transient), the amplitude and phase tend to the stationary states described by Eqs. (47). This means that φ becomes a constant, so that $q^{(0)} \to A\cos(\omega t - \text{const})$, i.e. the RWA equations again automatically recover the correct frequency of the solution, in this case equal to that of the external force.

Note that each stationary oscillation regime, with certain amplitude and phase, corresponds to a fixed point of the RWA equations, so that the stability of those fixed points determine that of the oscillations. In what follows, we will carry out such an analysis for several simple systems of key importance for physics and engineering.

4.4. Self-oscillations and phase locking

The rotating-wave approximation was pioneered by B. van der Pol in the late 1920s for analysis of one more type of oscillatory motion: *self-oscillations*. Several systems, e.g., electronic rf amplifiers with positive feedback, and optical media with quantum level population inversion, provide convenient means for the compensation, and even over-compensation of the intrinsic energy losses in oscillators. Phenomenologically, this effect may be described as the change of sign of the damping coefficient δ from positive to negative. Since for small oscillations the equation of motion is still linear, we may use Eq. (9) to describe its general solution. This equation shows that at $\delta < 0$, even infinitesimal deviations from equilibrium (say, due to unavoidable fluctuations) lead to oscillations with exponentially growing amplitude. Of course, in any real system such growth cannot persist infinitely, and shall be limited by

this or that effect - e.g., in the above examples, respectively, by amplifier saturation or electron population exhaustion.

In many cases, the amplitude limitation may be described reasonably well by *nonlinear damping*:

$$2\delta\dot{q} \to 2\delta\dot{q} + \beta\dot{q}^3, \tag{4.61}$$

with $\beta > 0$. Let us analyze this phenomenon, applying the rotating-wave approximation to the corresponding homogeneous differential equation:

$$\ddot{q} + 2\delta\dot{q} + \beta\dot{q}^3 + \omega_0^2 q = 0. \tag{4.62}$$

Carrying out the dissipative and detuning terms to the right hand part as f, we can readily calculate the right-hand parts of the RWA equations (57a), getting[19]

$$\dot{A} = -\delta(A)\,A, \qquad \text{where } \delta(A) \equiv \delta + \frac{3}{8}\beta\omega^2 A^2, \tag{4.63a}$$

$$A\dot{\varphi} = \xi\,A. \tag{4.63b}$$

The second of these equations has exactly the same form as Eq. (58b) for the case of decaying oscillations and hence shows that the self-oscillations (if they happen, i.e. if $A \neq 0$) have frequency ω_0 of the oscillator itself – see Eq. (59). Equation (63a) is more interesting. If the initial damping δ is positive, it has only the trivial fixed point, $A_0 = 0$ (that describes the oscillator at rest), but if δ is negative, there is also another fixed point,

$$A_1 = \left(\frac{8|\delta|}{3\beta\omega^2}\right)^{1/2}, \tag{4.64}$$

which describes steady self-oscillations with a non-zero amplitude.

Let us apply the general approach discussed in Sec. 3.2, the linearization of equations of motion, to this RWA equation. For the trivial fixed point $A_0 = 0$, the linearization of Eq. (63a) is reduced to discarding the nonlinear term in the definition of the amplitude-dependent damping $\delta(A)$. The resulting linear equation evidently shows that the system's equilibrium point, $A = A_0 = 0$, is stable at $\delta > 0$ and unstable at $\delta < 0$. (We have already discussed this *self-excitation condition* above.) The linearization of Eq. (63a) near the non-trivial fixed point A_1 requires a bit more math: in the first order in $\widetilde{A} \equiv A - A_1 \to 0$, we get

$$\dot{\widetilde{A}} \equiv \dot{A} = -\delta(A_1 + \widetilde{A}) - \frac{3}{8}\beta\omega^2(A_1 + \widetilde{A})^3 \approx -\delta\,\widetilde{A} - \frac{3}{8}\beta\omega^2 3A_1^2\widetilde{A} = \left(-\delta + 3\delta\right)\widetilde{A} = 2\delta\widetilde{A}, \tag{4.65}$$

where Eq. (64) has been used to eliminate A_1. We see that fixed point A_1 (and hence the whole process) is stable as soon as it exists ($\delta < 0$) - similar to the situation in our "testbed problem" (Fig. 2.1).

Now let us consider another important problem: the effect of a external sinusoidal force on a self-excited oscillator. If the force is sufficiently small, its effects on the self-excitation condition and the oscillation amplitude are negligible. However, if frequency ω of such weak force is close to the

[19] For that, one needs to use the trigonometric identity $\sin^3\Psi = (3/4)\sin\Psi - (1/4)\sin 3\Psi$ - see, e.g., MA Eq. (3.4).

eigenfrequency ω_0 of the oscillator, it may lead to a very important effect of *phase-locking* (also called "synchronization"). At this effect, oscillator's frequency deviates from ω_0, and becomes exactly equal to the external force's frequency ω, within a certain range

$$-\Delta \le \omega - \omega_0 < +\Delta . \tag{4.66}$$

In order to prove this fact, and also to calculate the phase locking range width 2Δ, we may repeat the calculation of the right-hand parts of the RWA equations (57a), adding term $f_0 \cos \omega t$ to the right-hand part of Eq. (62) – cf. Eqs. (42)-(43). This addition modifies Eqs. (63) as follows:[20]

$$\dot{A} = -\delta(A)\, A + \frac{f_0}{2\omega}\sin\varphi, \tag{4.67a}$$

$$A\dot{\varphi} = \xi\, A + \frac{f_0}{2\omega}\cos\varphi. \tag{4.67b}$$

If the system is self-excited, and the external force is weak, its effect on the oscillation amplitude is small, and in the first approximation in f_0 we can take A to be constant and equal to the value A_1 given by Eq. (64). Plugging this approximation into Eq. (67b), we get a very simple equation[21]

$$\boxed{\dot{\varphi} = \xi + \Delta\cos\varphi\,,} \tag{4.68}$$

Phase locking equation

where in our current case

$$\Delta \equiv \frac{f_0}{2\omega A_1}. \tag{4.69}$$

Within the range $-|\Delta| < \xi < +|\Delta|$, Eq. (68) has two fixed points on each 2π-segment of variable φ:

$$\varphi_\pm = \pm\arccos\left(-\frac{\xi}{\Delta}\right) + 2\pi n\,. \tag{4.70}$$

It is easy to linearize Eq. (68) near each point to analyze their stability in our usual way; however, let me this case to demonstrate another convenient way to do this in 1D systems, using the so-called *phase plane* – the plot of the right-hand part of Eq. (68) as a function of φ - see Fig. 5.

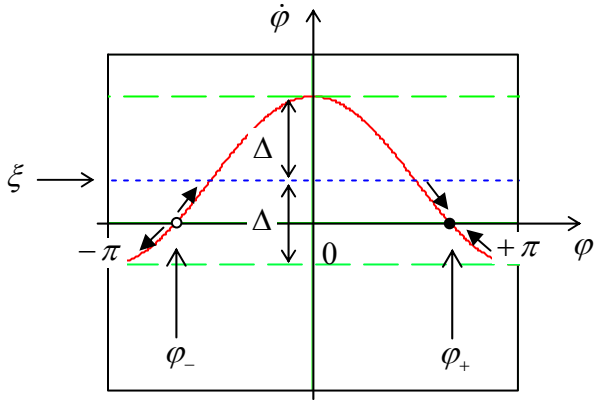

Fig. 4.5. Phase plane of a phase-locked oscillator, for the particular case $\xi = \Delta/2, f_0 > 0$.

[20] Actually, this result should be evident, even without calculations, from the comparison of Eqs. (60) and (63).

[21] This equation is ubiquitous in phase locking systems, including even some digital electronic circuits used for that purpose.

Since the positive values of this function correspond to the growth of φ in time, and vice versa, we may draw the arrows showing the direction of phase evolution. From this graphics, it is clear that one of these fixed points (for $f_0 > 0$, φ_+) is stable, while its counterpart is unstable. Hence the magnitude of Δ given by Eq. (69) is indeed the phase locking range (or rather it half) that we wanted to find. Note that the range is proportional to the amplitude of the phase locking signal - perhaps the most important feature of phase locking.

In order to complete our simple analysis, based on the assumption of fixed oscillation amplitude, we need to find the condition of validity of this assumption. For that, we may linearize Eq. (67a), for the stationary case, near value A_1, just as we have done in Eq. (65) for the transient process. The stationary result,

$$\tilde{A} \equiv A - A_1 = \frac{1}{2|\delta|}\frac{f_0}{2\omega}\sin\varphi_\pm \approx A_1\left|\frac{\Delta}{2\delta}\right|\sin\varphi_\pm , \tag{4.71}$$

shows that our assumption, $|\tilde{A}| << A_1$. and hence the final result (69), are valid if the phase locking range, 2Δ, is much smaller than $4|\delta|$.

4.5. Parametric excitation

In both problems solved in the last section, the stability analysis was easy because it could be carried out for just one slow variable, *either* amplitude *or* phase. Generally, such analysis of the RWA equations involves both these variables. The classical example of such situation is provided by one important physical phenomenon – the *parametric excitation* of oscillations. An elementary example of such oscillations is given by a pendulum with an externally-changed parameter, for example length $l(t)$ - see Fig. 6. Experiments (including those with playground swings :-) and numerical simulations show that if the length is changed (*modulated*) periodically, with frequency 2ω that is close to $2\omega_0$ and a sufficiently large swing Δl, the equilibrium position of the pendulum becomes unstable, and it starts swinging with frequency ω equal *exactly* to the half of the length modulation frequency (and hence only *approximately* equal to the average eigenfrequency ω_0 of the oscillator).

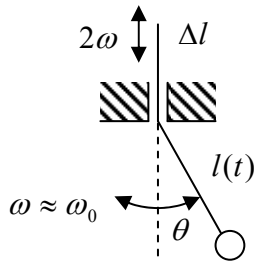

Fig. 4.6. Parametric excitation of pendulum oscillations.

For an elementary analysis of this effect we may consider the simplest case when the oscillations are small. At the lowest point ($\theta = 0$), where the pendulum moves with the highest velocity v_{max}, string's tension $\mathcal{T}$ is *higher* than mg by the centripetal force: $\mathcal{T}_{max} = mg + mv_{max}^2/l$. On the contrary, at the maximum deviation of the pendulum from the equilibrium, the force is *weakened* by string's tilt: $\mathcal{T}_{min} = mg\cos\theta_{max}$. Using the energy conservation, $E = mv_{max}^2/2 = mgl(1 - \cos\theta_{max})$, we may express these values as $\mathcal{T}_{max} = mg + 2E/l$ and $\mathcal{T}_{min} = mg - E/l$. Now, if during each oscillation period the string is pulled

up sharply and slightly by Δl ($|\Delta l| << l$) at each of its two passages through the lowest point, and is let to go down by the same amount at each of two points of the maximum deviation, the net work of the external force per period is positive:

$$W \approx 2(\mathcal{T}_{\max} - \mathcal{T}_{\min})\Delta l \approx 6\frac{\Delta l}{l}E, \tag{4.72}$$

and hence results in an increase of the oscillator's energy. If the so-called *modulation depth* $\Delta l/2l$ is sufficient, this increase may be sufficient to overcompensate the energy drained out by damping. Quantitatively, Eq. (10) shows that low damping ($\delta << \omega_0$) leads to the following energy decrease,

$$\Delta E \approx -4\pi\frac{\delta}{\omega_0}E, \tag{4.73}$$

per oscillation period. Comparing Eqs. (72) and (73), we see that the net energy flow into the oscillations is positive, $W + \Delta E > 0$, i.e. oscillation amplitude has to grow if[22]

$$\frac{\Delta l}{l} > \frac{2\pi\delta}{3\omega_0} \equiv \frac{\pi}{3Q}. \tag{4.74}$$

Since this result is independent on E, the growth of energy and amplitude is exponential (for sufficiently low E), so that Eq. (74) is the condition of parametric excitation - in this simple model.

However, this result does not account for the possible difference between the oscillation frequency ω and the eigenfrequency ω_0, and also does not clarify whether the best phase shift between the parametric oscillations and parameter modulation, assumed in the above calculation, may be sustained automatically. In order to address these issues, we may apply the rotating-wave approximation to a simple but reasonable linear equation

$$\ddot{q} + 2\delta\dot{q} + \omega_0^2(1 + \mu\cos 2\omega t)q = 0, \tag{4.75}$$

describing the parametric excitation for a particular case of sinusoidal modulation of $\omega_0^2(t)$. Rewriting this equation in the canonical form (38),

$$\ddot{q} + \omega^2 q = f(t, q, \dot{q}) = -2\delta\dot{q} + 2\xi\omega q - \mu\omega_0^2 q\cos 2\omega t, \tag{4.76}$$

and assuming that the dimensionless ratios δ/ω and $|\xi|/\omega$, and the modulation depth μ are all much less than 1, we may use general Eqs. (57a) to get the following RWA equations:

$$\begin{aligned} \dot{A} &= -\delta A - \frac{\mu\omega}{4}A\sin 2\varphi, \\ A\dot{\varphi} &= A\xi - \frac{\mu\omega}{4}A\cos 2\varphi. \end{aligned} \tag{4.77}$$

These equations evidently have a fixed point $A_0 = 0$, but its stability analysis (though possible) is not absolutely straightforward, because phase φ of oscillations is undetermined at that point. In order to

[22] A modulation of pendulum's mass (say, by periodic pumping water in and out of a suspended bottle) gives a qualitatively similar result. Note, however, that parametric oscillations cannot be excited by modulating *any* oscillator's parameter – for example, oscillator's damping coefficient (at least if it stays positive at all times), because its does not change system's energy, just the energy drain rate.

avoid this (technical rather than conceptual) technical difficulty, we may use, instead of the real amplitude and phase of oscillations, either their complex amplitude $a = A \exp\{i\varphi\}$, or its Cartesian components u and v – see Eqs. (4). Indeed, for our function f, Eq. (57b) gives

$$\dot{a} = (-\delta + i\xi)a - i\frac{\mu\omega}{4}a^*, \tag{4.78}$$

while Eqs. (57c) yield

RWA equations for parametric excitation

$$\boxed{\begin{aligned} \dot{u} &= -\delta u - \xi v - \frac{\mu\omega}{4}v, \\ \dot{v} &= -\delta v + \xi u - \frac{\mu\omega}{4}u. \end{aligned}} \tag{4.79}$$

We see that in contrast to Eqs. (77), in Cartesian coordinates $\{u, v\}$ the trivial fixed point $a_0 = 0$ (i.e. $u_0 = v_0 = 0$) is absolutely regular. Moreover, equations (78)-(79) are already linear, so they do not require any additional linearization. Thus we may use the same approach as was already used in Secs. 3.2 and 4.1, i.e. look for the solution of Eqs. (79) in the exponential form $\exp\{\lambda t\}$. However, now we are dealing with two variables, and should allow them to have, for each value of λ, a certain ratio u/v. For that, we should take the partial solution in the form

$$u = c_u e^{\lambda t}, \quad v = c_v e^{\lambda t}. \tag{4.80}$$

where constants c_u and c_v are frequently called the *distribution coefficients*. Plugging this solution into Eqs. (79), we get for them the following system of two linear algebraic equations:

$$\begin{aligned} (-\delta - \lambda)c_u + (-\xi - \frac{\mu\omega}{4})c_v &= 0, \\ (\xi - \frac{\mu\omega}{4})c_u + (-\delta - \lambda)c_v &= 0. \end{aligned} \tag{4.81}$$

The characteristic equation of this system,

$$\begin{vmatrix} -\delta - \lambda & -\xi - \frac{\mu\omega}{4} \\ \xi - \frac{\mu\omega}{4} & -\delta - \lambda \end{vmatrix} \equiv \lambda^2 + 2\delta\lambda + \delta^2 + \xi^2 - \left(\frac{\mu\omega}{4}\right)^2 = 0, \tag{4.82}$$

has two roots:

$$\lambda_\pm = -\delta \pm \left[\left(\frac{\mu\omega}{4}\right)^2 - \xi^2\right]^{1/2}. \tag{4.83}$$

Requiring the fixed point to be unstable, $\mathrm{Re}\lambda_+ > 0$, we get the parametric excitation condition

$$\frac{\mu\omega}{4} > \left(\delta^2 + \xi^2\right)^{1/2}. \tag{4.84}$$

Thus the parametric excitation may indeed happen without any artificial phase adjustment: the arising oscillations self-adjust their phase to pick up energy from the external source responsible for the parameter variation.

Our key result (84) may be compared with two other calculations. First, in the case of negligible damping ($\delta = 0$), Eq. (84) turns into condition $\mu\omega/4 > |\xi|$. This result may be compared with the well-developed theory of the so-called *Mathieu equation* whose canonical form is

$$\frac{d^2y}{dv^2} + (a - 2b\cos 2v)y = 0. \tag{4.85}$$

It is evident that with the substitutions $y \to q$, $v \to \omega t$, $a \to (\omega_0/\omega)^2$, $b \to -\mu/2$, this equation is just a particular case of Eq. (75) for $\delta = 0$. In terms of Eq. (85), the result of our approximate analysis may be re-written just as $b > |a - 1|$, and is supposed to be valid for $b << 1$. This condition is shown in Fig. 7 together with the numerically calculated[23] stability boundaries of the Mathieu equation.

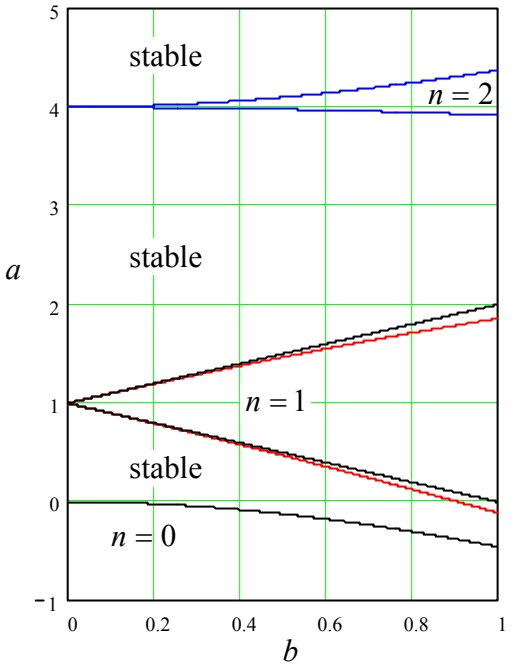

Fig. 4.7. Stability boundaries of the Mathieu equation (85), as calculated: numerically (curves) and using the rotating-wave approximation (dashed straight lines). In the regions numbered by various n the trivial solution $y = 0$ of the equation is unstable, i.e. its general solution $y(v)$ includes an exponentially growing term.

One can see that the rotating-wave approximation works just fine within its applicability limit (and beyond :-), though it fails to predict some other important features of the Mathieu equation, such as the existence of higher, more narrow regions of parametric excitation (at $a \approx n^2$, i.e. $\omega_0 \approx \omega/n$, for all integer n), and some spill-over of the stability region into the lower half-plane $a < 0$.[24] The reason of these failures is the fact that, as can be seen in Fig. 7, these phenomena do not appear in the first approximation in the parameter modulation amplitude $\mu \propto q$, that is the RWA applicability realm.

In the opposite case of finite damping but exact tuning ($\xi = 0$, $\omega \approx \omega_0$), Eq. (84) gives

$$\mu > \frac{4\delta}{\omega_0} \equiv \frac{2}{Q}. \tag{4.86}$$

[23] Such calculations may be substantially simplified by the use of the so-called *Floquet theorem*, which is also the mathematical basis for the discussion of wave propagation in periodic media – see the next chapter.

[24] This region describes, for example, the counter-intuitive stability of an inverted pendulum with the periodically modulated length, within a limited range of the modulation depth μ.

This condition may be compared with Eq. (74), taking $\Delta l/l = 2\mu$.. The comparison shows that though the structure of these conditions is similar, the numerical coefficients are different by a factor close to 2. The first reason of this difference is that the instant parameter change at optimal moments of time is more efficient then the smooth, sinusoidal variation described by (75). Even more significantly, the change of pendulum's length modulates not only its eigenfrequency ω_0, as Eq. (75) implies, but also its *mechanical impedance* $Z \equiv (g/l)^{1/2}$ – the notion to be discussed in detail in the next chapter. (Due to the time restrictions, I have to leave the analysis of the general case of the simultaneous modulation of ω_0 and Z for reader's exercise.)

Before moving on, let me summarize the most important differences between the parametric and forced oscillations:

(i) Parametric oscillations completely disappear outside of their excitation range, while the forced oscillations have a non-zero amplitude for any frequency and amplitude of the external force – see Eq. (18).

(ii) Parametric excitation may be described by a linear homogeneous equation - e.g., Eq. (75) - which cannot predict any finite oscillation amplitude within the excitation range, even at finite damping. In order to describe stationary parametric oscillations, some nonlinear effect has to be taken into account. (Again, I am leaving analyses of such effects for reader's exercises.)

One more important feature of the parametric oscillations will be discussed in the end of the next section.

4.6. Fixed point classification

RWA equations (79) give us a good pretext for a brief discussion of fixed points of a dynamic system described by *two* time-independent, *first-order* differential equations.[25] After their linearization near a fixed point, the equations for deviations can always be presented in the form similar to Eq. (79):

$$\begin{aligned} \dot{\tilde{q}}_1 &= M_{11}\tilde{q}_1 + M_{12}\tilde{q}_2, \\ \dot{\tilde{q}}_2 &= M_{21}\tilde{q}_1 + M_{22}\tilde{q}_2, \end{aligned} \tag{4.87}$$

where $M_{jj'}$ (with $j,j' = 1, 2$) are some real scalars that may be understood as elements of a 2×2 matrix M. Looking for an exponential solution of the type (80),

$$\tilde{q}_1 = c_1 e^{\lambda t}, \quad \tilde{q}_2 = c_2 e^{\lambda t}, \tag{4.88}$$

we get a more general system of two linear equations for the distribution coefficients $c_{1,2}$:

$$\begin{aligned} (M_{11} - \lambda)c_1 + M_{12}c_2 &= 0, \\ M_{21}c_1 + (M_{22} - \lambda)c_2 &= 0. \end{aligned} \tag{4.89}$$

These equations are consistent if

[25] Autonomous systems described by a *single second-order* differential equation, say $F(q, \dot{q}, \ddot{q}) = 0$, also belong to this class, because we may treat velocity $\dot{q} \equiv v$ as a new variable, and use this definition as one first-order differential equation, and the initial equation, in the form $F(q, v, \dot{v}) = 0$, as the second first-order equation.

$$\begin{vmatrix} M_{11}-\lambda & M_{12} \\ M_{21} & M_{22}-\lambda \end{vmatrix} = 0, \tag{4.90}$$

Characteristic equation of system (87)

giving us a quadratic characteristic equation

$$\lambda^2 - \lambda(M_{11}+M_{22}) + (M_{11}M_{22} - M_{12}M_{21}) = 0. \tag{4.91}$$

Its solution,[26]

$$\lambda_{\pm} = \frac{1}{2}(M_{11}+M_{22}) \pm \frac{1}{2}\left[(M_{11}-M_{22})^2 + 4M_{12}M_{21}\right]^{1/2}, \tag{4.92}$$

shows that the following situations are possible:

A. The expression under the square root, $(M_{11}- M_{22})^2 + 4M_{12}M_{21}$, is positive. In this case, both characteristic exponents $\lambda_{\pm}$ are real, and we can distinguish three sub-cases:

(i) Both λ_+ and λ_- are negative. In this case, the fixed point is evidently stable. Because of generally different magnitudes of exponents $\lambda_{\pm}$, the process presented on the phase plane $[\tilde{q}_1, \tilde{q}_2]$ (Fig. 8a) may be seen as consisting of two stages: first, a faster (with rate $|\lambda_+|$) relaxation to a linear *asymptote*,[27] and then a slower decline, with rate $|\lambda_-|$, along this line, i.e. at the virtually fixed ratio of the variables. Such fixed point is called the *stable node*.

(ii) Both λ_+ and λ_- are positive. This case (rarely met in actual physical systems) of the *unstable node* differs from the previous one only by the direction of motion along the phase plane trajectories (see dashed arrows in Fig. 8a). Here the variable ratio is also approaching a constant soon, but now the one corresponding to the larger of the rates λ

(iii) Finally, in the case of a *saddle* ($\lambda_+ > 0$, $\lambda_- < 0$) the system dynamics is different (Fig. 8b): after the rate-$|\lambda_+|$ relaxation to the λ_--asymptote, the perturbation starts to grow, with rate λ_-, along one of two opposite directions. (The direction is determined on which side of another straight line, called *separatrix*, the system has been initially.) It is evident that the saddle[28] is an unstable fixed point.

B. The expression under the square root, $(M_{11}- M_{22})^2 + 4\, M_{12}M_{21}$, is negative. In this case the square root in Eq. (92) is imaginary, making the real parts of both roots equal, $\mathrm{Re}\lambda_{\pm} = (M_{11} + M_{22})/2$, and their imaginary parts equal but sign-opposite. As a result, here there can be just two types of fixed points:

(i) S*table focus*, at $(M_{11} + M_{22}) < 0$. The phase plane trajectories are spirals going to the center (i.e. toward the fixed point) – see Fig. 8c with solid arrow.

(ii) *Unstable focus*, taking place at $(M_{11} + M_{22}) > 0$, differs from the stable one only by the direction of motion along the phase trajectories – see the dashed arrow in Fig. 8c.

---

[26] In terms of linear algebra, $\lambda_{\pm}$ are the *eigenvalues*, and the corresponding sets $[c_1, c_2]_{\pm}$, the *eigenvectors* of matrix M with elements $M_{jj'}$.

[27] The asymptote direction may be found by plugging the value λ_+ back into Eq. (89) and finding the corresponding ratio c_1/c_2.

[28] The term "saddle" is due to the fact that system's dynamics in this case is qualitatively similar to those of particle's motion in the 2D potential $U(\tilde{q}_1, \tilde{q}_2)$ having the shape of a horse saddle (or a mountain pass).

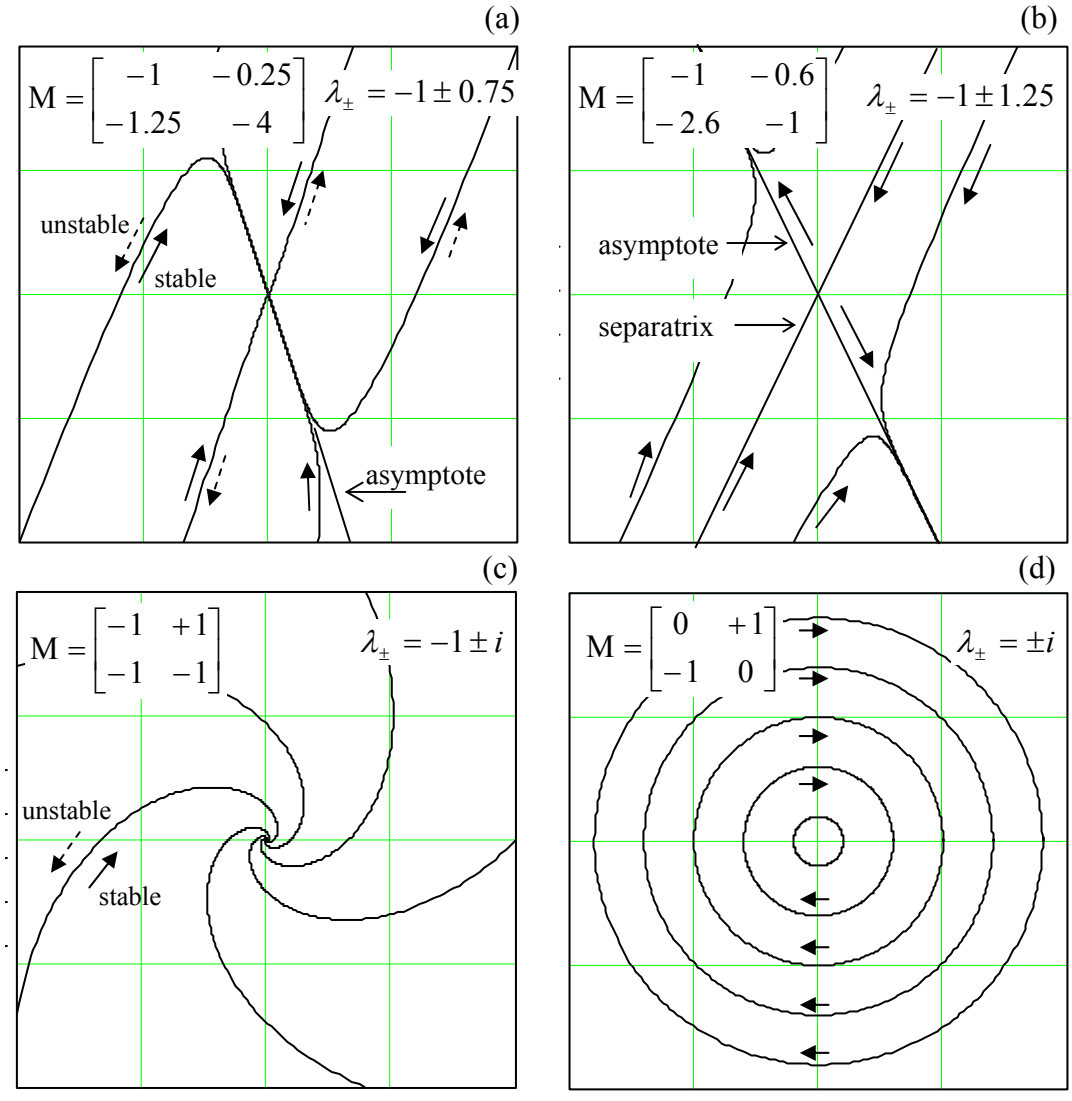

Fig. 4.8. Typical trajectories on the phase plane $[\tilde{q}_1, \tilde{q}_2]$ near fixed points of various types: (a) node, (b) saddle, (c) focus, and (d) center. The particular values of the matrix M used in the first three panels correspond to the RWA equations (81) for parametric oscillators with $\xi = \delta$, and three different values of parameter $\mu\omega/4\delta$: (a) 1.25, (b) 1.6 and (c) 0.

C. Sometimes the border case, $M_{11} + M_{22} = 0$, is also distinguished, and the corresponding fixed point is refereed to as the *center* (Fig. 8d). Considering centers a special category makes sense because such fixed points are typical for Hamiltonian systems whose first integral of motion may be frequently presented as the distance of the from a fixed point. For example, a harmonic oscillator without dissipation may be described by the system

$$\dot{q} = \frac{p}{m}, \quad \dot{p} = -m\omega_0^2 q, \tag{4.94}$$

that is evidently a particular case of Eq. (87) with $M_{11} = M_{22} = 0$, $M_{12}M_{21} = -\omega_0^2 < 0$, and hence $(M_{11}-M_{22})^2 + 4M_{12}M_{21} = -4\omega_0^2 < 0$, and $M_{11} + M_{22} = 0$. The phase plane of the system may be symmetrized by plotting q vs. the properly normalized momentum $p/m\omega_0$. On the symmetrized plane, sinusoidal oscillations of amplitude A are represented by a circle of radius A about the center-type fixed point $A = 0$. Such a circular trajectory correspond to the conservation of the oscillator's energy

$$E = \frac{m\dot{q}^2}{2} + \frac{m\omega_0^2 q^2}{2} = \frac{m\omega_0^2}{2}\left[\left(\frac{p}{m\omega_0}\right)^2 + q^2\right]. \tag{4.95}$$

This is a convenient moment for a brief discussion of the so-called *Poincaré* (or "slow-variable", or "stroboscopic") *plane*.[29] From the point of view of the rotating-wave approximation, sinusoidal oscillations $q(t) = A\cos(\omega t - \varphi)$, in particular those described by a circular trajectory on the real (or "fast") phase plane (Fig. 8c) correspond to a fixed point $\{A, \varphi\}$, which may conveniently presented by a steady geometrical point on a plane with these polar coordinates (Fig. 9a). (As follows from Eq. (4), the Cartesian coordinates on that plane are u and v.) The quasi-sinusoidal process (41), with slowly changing A and φ, may be represented by a slow motion of that point on this Poincaré plane.

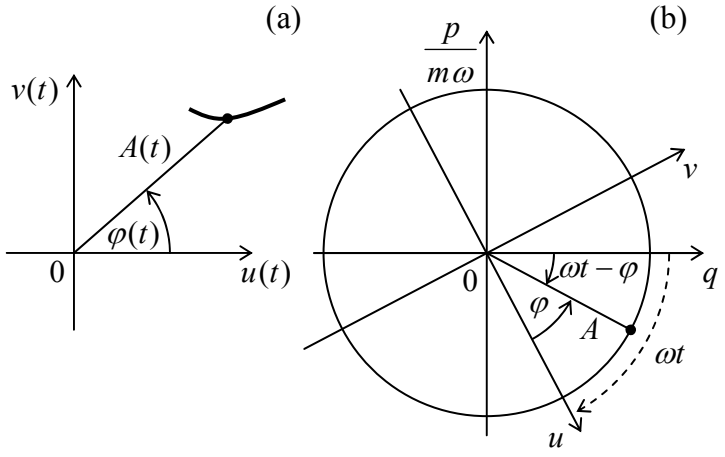

Fig. 4.9. (a) Presentation of a sinusoidal oscillation (point) and a slow transient (line) on the Poincaré plane, and (b) transfer from the "fast" phase plane to the "slow" (Poincaré) plane.

Figure 9b shows one possible way to visualize the relation between the "real" phase plane of an oscillator, with symmetrized Cartesian coordinates q and $p/m\omega_0$, and the Poincaré plane with Cartesian coordinates u and v: the latter reference frame rotates relative to the former one about the origin clockwise, with angular velocity ω.[30] Another, "stroboscopic" way to generate the Poincaré plane pattern is to have a fast glance at the "real" phase plane just once during the oscillation period $T = 2\pi/\omega$.

In many cases, such presentation is more convenient than that on the "real" phase plane. In particular, we have already seen that the RWA equations for such important phenomena as phase locking and parametric oscillations, whose original differential equations include time explicitly, are time-independent – cf., e.g., (75) and (79) describing the latter effect. This simplification brings the

[29] Named after J. H. Poincaré (1854-1912) who is credited, among many other achievements, for his contributions to special relativity (see, e.g., EM Chapter 9) and the idea of deterministic chaos (to be discussed in Chapter 9 below).

[30] This notion of phase plane rotation is the basis for the rotating-wave approximation's name. (Word "wave" has sneaked in from this method's wide application in classical and quantum optics.)

equations into the category considered in this section, and enables the classification of their fixed points, which may shed additional light on their dynamic properties.

In particular, Fig. 10 shows the classification of the trivial fixed point of a parametric oscillator, which follows from Eq. (83). As the parameter modulation depth μ is increased, the type of the trivial fixed point $A_1 = 0$ on the Poincaré plane changes from a stable focus (typical for a simple oscillator with damping) to a stable node and then to a saddle describing the parametric excitation. In the last case, the two directions of the perturbation growth, so prominently featured in Fig. 8b, correspond to the two possible values of the oscillation phase φ, with the phase choice determined by initial conditions.

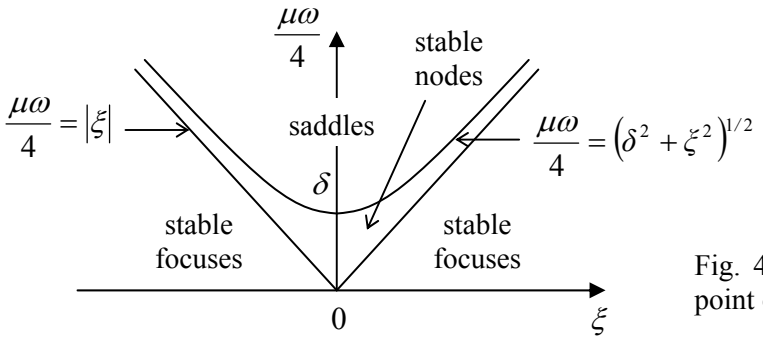

Fig. 4.10. Types of the trivial fixed point of a parametric oscillator.

This double degeneracy of the parametric oscillation's phase could already be noticed from Eqs. (77), because they are evidently invariant with respect to replacement $\varphi \to \varphi + \pi$. Moreover, the degeneracy is not an artifact of the rotating-wave approximation, because the initial Eq. (75) is already invariant with respect to the corresponding replacement $q(t) \to q(t - \pi/\omega)$. This invariance means that all other characteristics (e.g., the amplitude) of the parametric oscillations excited with either of two phases are *absolutely* similar. At the dawn of the computer age (in the late 1950s and early 1960s), there were substantial attempts, especially in Japan, to use this property for storage and processing digital information coded in the phase-binary form.

4.7. Numerical approach

If the amplitude of oscillations, by whatever reason, becomes so large that the nonlinear terms in the equation describing a system are comparable to its linear terms, numerical methods are virtually the only avenue available for their study. In Hamiltonian 1D systems, such methods may be applied directly to integral (3.26), but dissipative and/or parametric systems typically lack first integrals of motion similar to Eq. (3.24), so that the initial differential equation has to be solved.

Let us discuss the general idea of such methods on the example of what mathematicians call the *Cauchy problem* (finding the solution for all moments of time, starting from known initial conditions) for first-order differential equation

$$\dot{q} = f(t, q). \tag{4.96}$$

(The generalization to a set of several such equations is straightforward.) Breaking the time axis into small, equal steps h (Fig. 9) we can reduce the equation integration problem to finding the function value in the next time point, $q_{n+1} \equiv q(t_{n+1}) = q(t_n + h)$ from the previously found value $q_n = q(t_n)$ - and, if

necessary, the values of q at other previous time steps. In the generic approach (called the *Euler method*), q_{n+1} is found using the following formula:

$$\begin{aligned} q_{n+1} &= q_n + k, \\ k &\equiv h f(t_n, q_n). \end{aligned} \tag{4.97}$$

It is evident that this approximation is equivalent to the replacement of the genuine function $q(t)$, on the segment $[t_n, t_{n+1}]$, with the two first terms of its Taylor expansion in point t_n:

$$q(t_n + h) \approx q(t_n) + \dot{q}(t_n)h \equiv q(t_n) + hf(t_n, q_n). \tag{4.98}$$

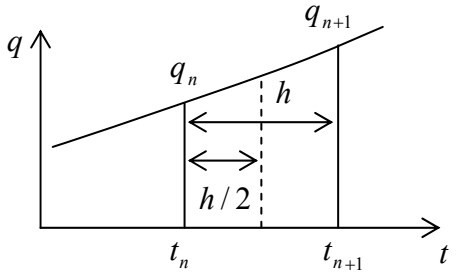

Fig. 4.11. The basic notions used at numerical integration of ordinary differential equations.

Such approximation has an error proportional to h^2. One could argue that making the step h sufficiently small the Euler's method error might be done arbitrary small, but even with the number-crunching power of modern computers, the computation time necessary to reach sufficient accuracy may be too high for large problems.[31] Besides that, the increase of the number of time steps, which is necessary at $h \to 0$, increases the total rounding errors, and eventually may cause an increase, rather than the reduction of the overall error of the computed result.

A more efficient way is to modify Eq. (97) to include the terms of the second order in h. There are several ways to do this, for example using the *2nd-order Runge-Kutta* method:

$$\begin{aligned} q_{n+1} &= q_n + k_2, \\ k_2 &\equiv h f\left(t_n + \frac{h}{2}, q_n + \frac{k_1}{2}\right), \quad k_1 \equiv h f(t_n, q_n). \end{aligned} \tag{4.99}$$

One can readily check that this method gives the exact result if function $q(t)$ is a quadratic polynomial, and hence in the general case its errors are of the order of h^3. We see that the main idea here is to first break the segment $[t_n, t_{n+1}]$ in half (Fig. 11), then evaluate the right-hand part of the differential equation (96) at the point intermediate (in both t and q) between points n and $(n + 1)$, and then use this information to predict q_{n+1}.

The advantage of the Runge-Kutta approach is that it can be readily extended to the 4th order, without an additional breaking of the interval $[t_n, t_{n+1}]$.:

[31] In addition, the Euler method is not time-reversible - the handicap which may be essential for integration of Hamiltonian systems described by systems of second-order differential equations. However, this drawback may be readily overcome by the so-called *leapfrogging* – the overlap of time steps h for a generalized coordinate and the corresponding generalized velocity.

$$q_{n+1} = q_n + \frac{1}{6}(k_1 + 2k_2 + 2k_3 + k_4),$$
$$k_4 \equiv h f(t_n + h, q_n + k_3),\ k_3 \equiv h f(t_n + \frac{h}{2}, q_n + \frac{k_2}{2}),\ k_2 \equiv h f(t_n + \frac{h}{2}, q_n + \frac{k_1}{2}),\ k_1 \equiv h f(t_n, q_n). \quad (4.100)$$

This method reaches much lower error, $O(h^5)$, without being not too cumbersome. These features have made the 4th-order Runge-Kutta the default method in most numerical libraries. Its extension to higher orders is possible but requires more complex formulas and is justified only for some special cases, e.g., very abrupt functions $q(t)$.[32] The most frequent enhancement of the method is the automatic adjustment of step h to reach the specified accuracy.

Figure 12 shows a typical example of application of that method to the very simple problem of a damped linear oscillator, for two values of fixed time step h (expressed in terms of the number N of such steps per oscillation period). Black lines connect the points obtained by the 4th-order Runge-Kutta method, while the points connected by green straight lines present the exact analytical solution (22). A few-percent errors start to appear only at as few as ~10 time steps per period, so that the method is indeed very efficient. I will illustrate the convenience and handicaps of the numerical approach to the solution of dynamics problems on the discussion of the following topic.

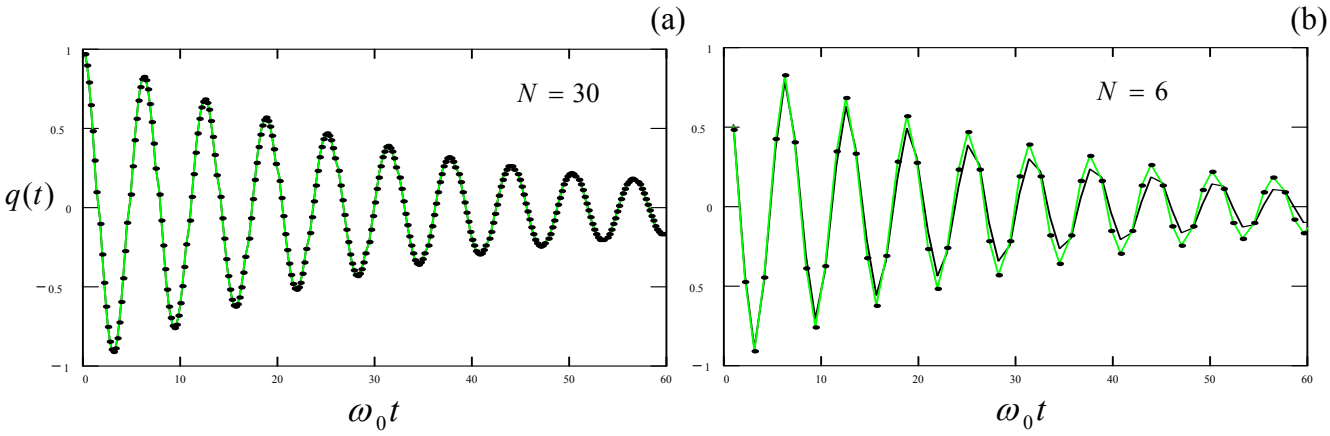

Fig. 4.12. Results of the fixed-point Runge-Kutta solution to the equation of linear oscillator with damping (with $\delta/\omega_0 = 0.03$) for: (a) 30 and (b) 6 points per oscillation period. The results are shown by points; lines are only the guide for the eye.

4.8. Higher harmonic and subharmonic oscillations

Figure 13 shows the numerically calculated[33] transient process and stationary oscillations in a linear oscillator and a very representative nonlinear system, the pendulum described by Eq. (42), both with the same resonance frequency ω_0 for small oscillations. Both systems are driven by a sinusoidal

[32] The most popular approaches in such cases are the *Richardson extrapolation*, the *Bulirsch-Stoer algorithm*, and a set of *prediction-correction techniques*, e.g. the *Adams-Bashforth-Moulton method* – see the literature recommended in MA Sec. 16 (iii).

[33] All numerical results shown in this section have been obtained by the 4th-order Runge-Kutta method with the automatic step adjustment which guarantees the relative error of the order of 10^{-4} – much smaller than the pixel size in the plots.

external force of the same amplitude and frequency - in this illustration, equal to the small-oscillation eigenfrequency ω_0 of both systems. The plots show that despite a very substantial amplitude of the pendulum oscillations (an angle amplitude of about one radian) their waveform remains almost exactly sinusoidal.[34] On the other hand, the nonlinearity affects the oscillation amplitude very substantially. These results illustrate that the validity of the small-parameter method and its RWA extension far exceeds what might be expected from the formal requirement $|q| << 1$.

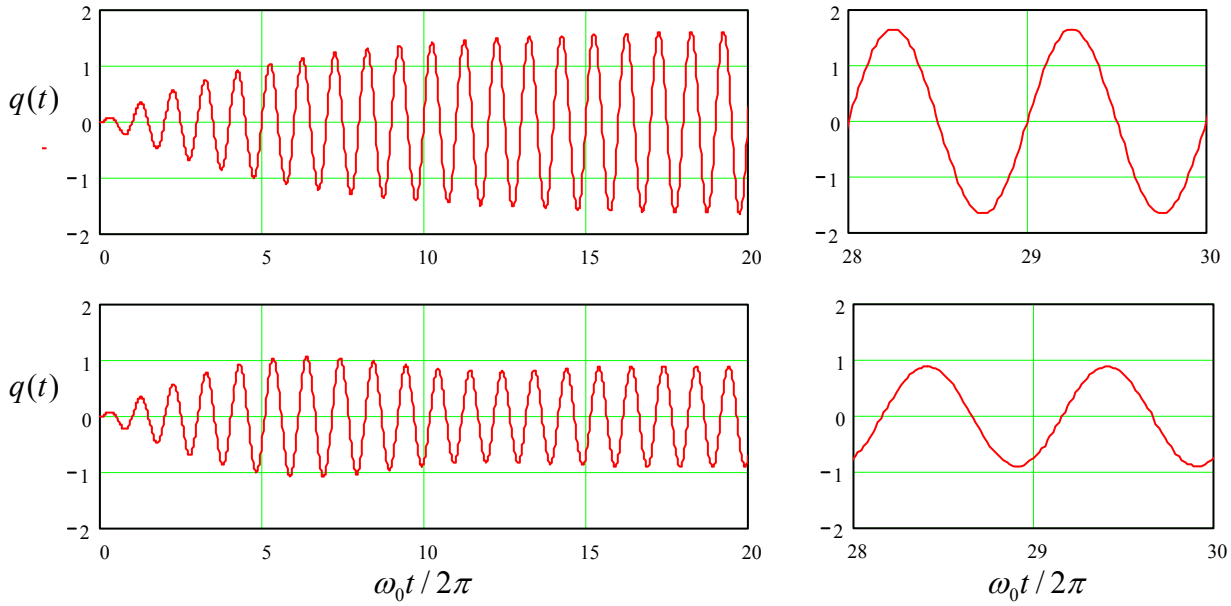

Fig. 4.13. Oscillations induced by a similar sinusoidal external force (turned on at $t = 0$) in two systems with the same small-oscillation frequency ω_0 and low damping – a linear oscillator (two top panels) and a pendulum (two bottom panels). $\delta/\omega_0 = 0.03$, $f_0 = 0.1$, and $\omega = \omega_0$.

The higher harmonic contents in the oscillation waveform may be sharply increased[35] by reducing the external force frequency to $\sim\omega_0/n$, where integer n is the number of the desirable harmonic. For example, Fig. 14a shows oscillations in a pendulum described by the same Eq. (42), but driven at frequency $\omega_0/3$. One can see that the 3rd harmonic amplitude may be comparable with that of the basic harmonic, especially if the external frequency is additionally lowered (Fig. 14b) to accommodate for the deviation of the effective frequency $\omega_0(a)$ of own oscillations from its small-oscillation value ω_0 – see Eq. (49), Fig. 4 and their discussion in Sec. 2 above.

Generally, the higher harmonic generation by nonlinear systems might be readily anticipated. Indeed, the Fourier theorem tells us that any non-sinusoidal periodic function of time, e.g., an initially sinusoidal waveform of frequency ω, distorted by nonlinearity, may be presented as a sum of its basic harmonic and higher harmonics with frequencies $n\omega$. Note that an effective generation of higher

[34] In this particular case, the higher harmonic contents is about 0.5%, dominated by the 3rd harmonic whose amplitude and phase are in a very good agreement with Eq. (50).

[35] This method is used in practice, for example, for the generation of electromagnetic waves with frequencies in the terahertz range (10^{12}-10^{13} Hz) which still lacks efficient electronic self-oscillators.

harmonics is only possible with adequate nonlinearity of the system. For example, consider the nonlinear term αq^3 used in equations explored in Secs. 2 and 3. If the waveform $q(t)$ is approximately sinusoidal, such term can create only the basic and 3rd harmonics. The "pendulum nonlinearity" $\sin q$ cannot produce, without a constant component is process $q(t)$, any even (e.g., the 2nd) harmonic. The most efficient generation of harmonics may be achieved using systems with the sharpest nonlinearities – e.g., semiconductor diodes whose current may follow an exponential dependence on the applied voltage through several orders of magnitude.

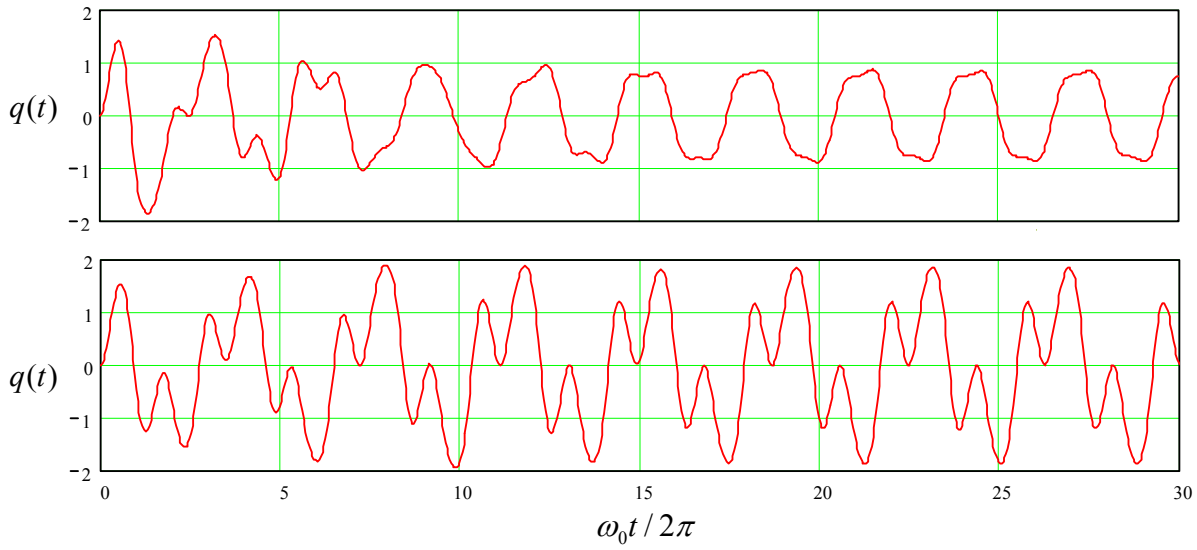

Fig. 4.14. Oscillations induced in a pendulum with damping $\delta/\omega_0 = 0.03$, driven by a sinusoidal external force of amplitude $f_0 = 0.75$, and frequency $\omega_0/3$ (top panel) and $0.8\omega_0/3$ (bottom panel).

However, numerical modeling of nonlinear oscillators, as well as experiments with their physical implementations, bring more surprises. For example, the bottom panel of Fig. 15 shows oscillations in a pendulum under effect of a strong sinusoidal force with a frequency close to $3\omega_0$. One can see that at some parameter values and initial conditions the system's oscillation spectrum is heavily contributed (almost dominated) by the 3rd *sub*harmonic, i.e. a component that is synchronous with the driving force of frequency 3ω, but has the frequency ω that is close to the eigenfrequency ω_0 of the system.

This counter-intuitive phenomenon may be explained as follows. Let us assume that the subharmonic oscillations of frequency $\omega \approx \omega_0$ have somehow appeared, and coexist with the forced oscillations of frequency 3ω:

$$q(t) \approx A\cos\Psi + A_{\text{sub}}\cos\Psi_{\text{sub}}, \quad \text{where } \Psi \equiv 3\omega t - \varphi, \quad \Psi_{\text{sub}} \equiv \omega t - \varphi_{\text{sub}}. \tag{4.101}$$

Then, the first nonlinear term αq^3 of the Taylor expansion of pendulum's nonlinearity $\sin q$ yields

$$\begin{aligned} q^3 &= (A\cos\Psi + A_{\text{sub}}\cos\Psi_{\text{sub}})^3 \\ &= A^3\cos^3\Psi + 3A^2A_{\text{sub}}\cos^2\Psi\cos\Psi_{\text{sub}} + 3AA_{\text{sub}}^2\cos\Psi\cos^2\Psi_{\text{sub}} + A_{\text{sub}}^3\cos^3\Psi_{\text{sub}}. \end{aligned} \tag{4.102}$$

While the first and the last terms of this expression depend only of amplitudes of the individual components of oscillations, the two middle terms are more interesting because they produce so-called *combinational frequencies* of the two components. For our case, the third term,

$$3A A_{\rm sub}^2 \cos\Psi \cos^2 \Psi_{\rm sub} = \frac{3}{4} A A_{\rm sub}^2 \cos(\Psi - 2\Psi_{\rm sub}) + \dots , \tag{4.103}$$

of a special importance, because it produces, besides other combinational frequencies, the subharmonic component with the total phase

$$\Psi - 2\Psi_{\rm sub} = \omega t - \varphi + 2\varphi_{\rm sub} . \tag{4.104}$$

Thus, within a certain range of the mutual phase shift between the Fourier components, this nonlinear contribution is synchronous with the subharmonic oscillations, and describes the interaction that can deliver to it the energy from the external force, so that the oscillations may be self-sustained. Note, however, that the amplitude of the term (103) describing this energy exchange is proportional to the square of $A_{\rm sub}$, and vanishes at the linearization of the equations of motion near the trivial fixed point. This means that the point is always stable, i.e., the 3rd subharmonic cannot be self-excited and always need an initial "kick-off" – compare the two panels of Fig. 15. The same is evidently true for higher subharmonics.

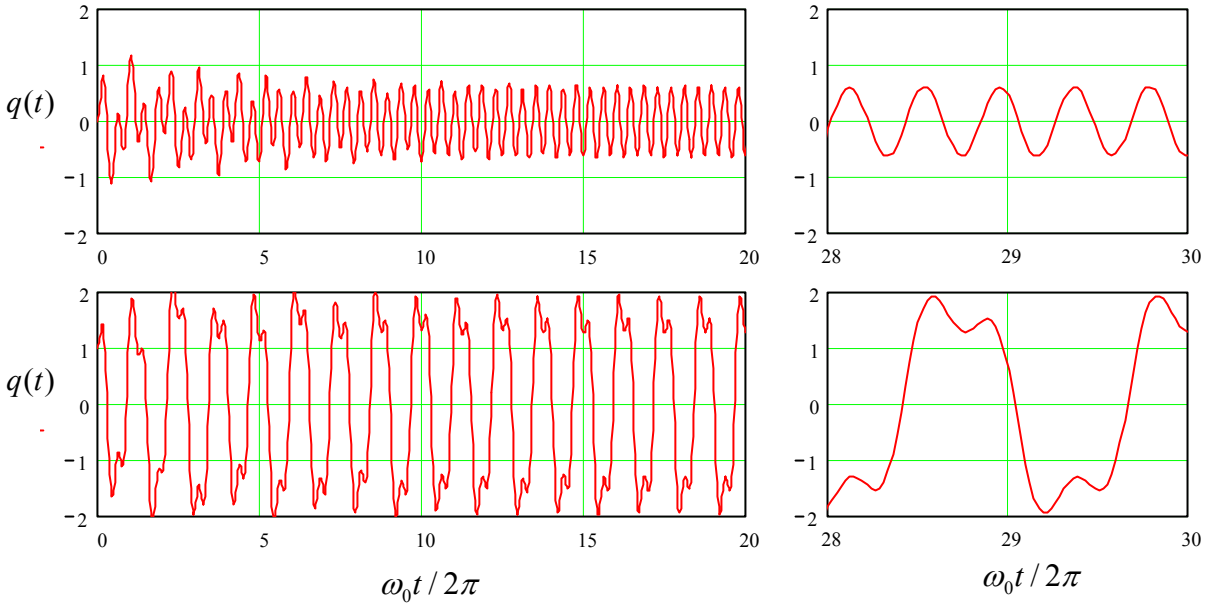

Fig. 4.15. Oscillations induced in a pendulum with $\delta/\omega_0 = 0.03$ by a sinusoidal external force of amplitude $f_0 = 3$ and frequency $3\omega_0 \times 0.8$, with initial conditions $q(0) = 0$ (the top row) and $q(0) = 1$ (the bottom row).

Only the second subharmonic presents a special case. Indeed, let us make a calculation similar to Eq. (102), by replacing Eq. (101) with

$$q(t) \approx A\cos\Psi + A_{\rm sub}\cos\Psi_{\rm sub}, \quad \text{where } \Psi \equiv 2\omega t - \varphi, \quad \Psi_{\rm sub} \equiv \omega t - \varphi_{\rm sub}, \tag{4.105}$$

for a nonlinear term proportional to q^2:

$$q^2 = (A\cos\Psi + A_{\rm sub}\cos\Psi_{\rm sub})^2 = A^2\cos^2\Psi + 2AA_{\rm sub}\cos\Psi\cos\Psi_{\rm sub} + A_{\rm sub}^2\cos^2\Psi_{\rm sub}. \quad (4.106)$$

Here the combinational-frequency term capable of supporting the 2nd subharmonic,

$$2AA_{\rm sub}\cos\Psi\cos\Psi_{\rm sub} = AA_{\rm sub}\cos(\Psi - \Psi_{\rm sub}) = AA_{\rm sub}\cos(\omega t - \varphi + \varphi_{\rm sub}) + \ldots, \quad (4.107)$$

is linear in the subharmonic amplitude, i.e. survives the equation linearization near the trivial fixed point. This mean that the second subharmonic may arise spontaneously, from infinitesimal fluctuations.

Moreover, such excitation of the second subharmonic is very similar to the parametric excitation that was discussed in detail in Sec. 5, and this similarity is not coincidental. Indeed, let us redo expansion (4.106) at a somewhat different assumption that the oscillations are a sum of the forced oscillations at the external force frequency 2ω, and an *arbitrary but weak* perturbation:

$$q(t) = A\cos(2\omega t - \varphi) + \tilde{q}(t), \quad |\tilde{q}| << A. \quad (4.108)$$

Then, neglecting the small term proportional to $\tilde{q}^2$, we get

$$q^2 \approx A^2\cos^2(2\omega t - \varphi) + 2\tilde{q}(t)A\cos(2\omega t - \varphi). \quad (4.109)$$

Besides the inconsequential phase φ, the second term in the last formula is *exactly* similar to the term describing the parametric effects in Eq. (75). This fact means that for a weak perturbation, a system with a quadratic nonlinearity in the presence of a strong "pumping" signal of frequency 2ω is equivalent to a system with parameters changing in time with frequency 2ω. This fact is broadly used for the parametric excitation at high (e.g., optical) frequencies where the mechanical means of parameter modulation (see, e.g., Fig. 5) are not practicable. The necessary quadratic nonlinearity at optical frequencies may be provided by a *noncentrosymmetric nonlinear crystal*, e.g., the β-phase barium borate (BaB_2O_4).

Before finishing this chapter, let me elaborate a bit on a general topic: the relation between the numerical and analytical approaches to problems of dynamics (and physics as a whole). We have just seen that sometimes numerical solutions, like those shown in Fig. 15b, may give vital clues for previously unanticipated phenomena such as the excitation of subharmonics. (The phenomenon of deterministic chaos, which will be discussed in Chapter 9 below, presents another example of such "numerical discoveries".) One might also argue that in the absence of exact analytical solutions, numerical simulations may be the main theoretical tool for the study of such phenomena. These hopes are, however, muted by the problem that is frequently called the *curse of dimensionality*,[36] in which the last word refers to the number of input parameters of the problem to be solved.[37]

Indeed, let us have another look at Fig. 15. OK, we have been lucky to find a new phenomenon, the 3rd subharmonic generation, for a particular set of parameters - in that case, five of them: $\delta/\omega_0 = 0.03$, $3\omega/\omega_0 = 2.4$, $f_0 = 3$, $q(0) = 1$, and $dq/dt\ (0) = 0$. Could we tell anything about how common this effect is? Are subharmonics with different n possible in the system? The only way to address these

[36] This term had been coined in 1957 by R. Bellman in the context of the optimal control theory (where the dimensionality typically means the number of parameters affecting the system under control), but gradually has spread all over quantitative sciences using numerical methods.

[37] In EM Sec. 1.2, I discuss implications of the curse implications for a different case, when both analytical and numerical solutions to the same problem are possible.

questions computationally is to carry out similar numerical simulations in many points of the d-dimensional (in this case, $d = 5$) space of parameters. Say, we have decided that breaking the reasonable range of each parameter to $N = 100$ points is sufficient. (For many problems, even more points are necessary – see, e.g., Sec. 9.1.) Then the total number of numerical experiments to carry out is $N^d = (10^2)^5 = 10^{10}$ – not a simple task even for the powerful modern computing facilities. (Besides the pure number of required CPU cycles, consider storage and analysis of the results.) For many important problems of nonlinear dynamics, e.g., turbulence, the parameter dimensionality d is substantially larger, and the computer resources necessary for one numerical experiment, are much greater.

In the view of the curse of dimensionality concerns, approximate analytical considerations, like those outlined above for the subharmonic excitation, are invaluable. More generally, physics used to stand on two legs, experiment and (analytical) theory. The enormous progress of computer performance during a few last decades has provided it with one more point of support (a tail? :-) – numerical simulation. This does not mean we can afford to cut and throw away any of the legs we are standing on.

4.9. Exercise problems

4.1.* Prove Eq. (26) for the response function given by Eq. (17).

Hint: You may like to use the *Cauchy integral theorem* for analytical functions of complex variable.[38]

4.2. A square-wave pulse of force (see Fig. on the right) is exerted on a linear oscillator with eigenfrequency ω_0 (no damping), initially at rest. Calculate the law of motion $q(t)$, sketch it, and interpret the result.

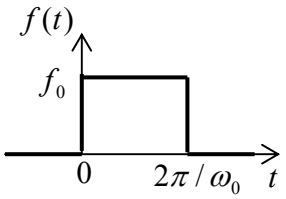

4.3. At $t = 0$, a sinusoidal external force $F(t) = F_0 \cos \omega t$, with constant A and ω, is applied to a linear oscillator with eigenfrequency ω_0 and damping δ, which was at rest at $t \le 0$.

(i) Calculate the general expression for the time evolution of the oscillator's coordinate, and interpret the result.

(ii) Spell out your result for the case of the resonance ($\omega = \omega_0$) in a system with low damping ($\delta << \omega_0$), and, in particular, explore the limit $\delta \to 0$.

4.4. A pulse of external force $F(t)$, with a finite duration $\mathcal{T}$, is exerted on a harmonic oscillator, initially at rest in the equilibrium position. Neglecting dissipation, calculate the change of oscillator's energy, using two different methods, and compare the results.

4.5.* For a system with the following Lagrangian function:

$$L = \frac{m}{2}\dot{q}^2 - \frac{\kappa}{2}q^2 + \frac{\varepsilon}{2}\dot{q}^2 q^2,$$

calculate the frequency of free oscillations as a function of their amplitude A, at $A \to 0$, using two different approaches.

[38] See, e.g., MA Eq. (15.1).

4.6. For a system with the Lagrangian function

$$L = \frac{m}{2}\dot{q}^2 - \frac{\kappa}{2}q^2 + \varepsilon\dot{q}^4,$$

with small parameter ε, use the rotating-wave approximation to find the frequency of free oscillations as a function of their amplitude.

4.7. Find the regions of real, time-independent parameters a_1 and a_2, in which the fixed point of the following system of equations,

$$\dot{q}_1 = a_1(q_2 - q_1),$$
$$\dot{q}_2 = a_2 q_1 - q_2,$$

is unstable. On the $[a_1, a_2]$ plane, sketch the regions of each fixed point type - stable and unstable nodes, focuses, etc.

4.8. Solve Problem 4.3(ii) using the rotating-wave approximation, and compare the result with the exact solution.

4.9. Use the rotating-wave approximation to analyze forced oscillations in an oscillator with weak nonlinear damping, described by equation

$$\ddot{q} + 2\delta\dot{q} + \omega_0^2 q + \beta\dot{q}^3 = f_0\cos\omega t,$$

with $\omega \approx \omega_0$; β, $\delta > 0$; and $\beta\omega A^2 << 1$. In particular, find the stationary amplitude of forced oscillations and analyze their stability. Discuss the effect(s) of the nonlinear term on the resonance.

4.10.* Analyze stability of the forced nonlinear oscillations described by Eq. (43). Relate the result to the slope of resonance curves (Fig. 4).

4.11. Use the rotating-wave approximation to analyze parametric excitation of an oscillator with weak nonlinear damping, described by equation

$$\ddot{q} + 2\delta\dot{q} + \beta\dot{q}^3 + \omega_0^2(1 + \mu\cos 2\omega t)q = 0,$$

with $\omega \approx \omega_0$; β, $\delta > 0$; and μ, $\beta\omega A^2 << 1$. In particular, find the amplitude of stationary oscillations and analyze their stability.

4.12. Adding nonlinear term αq^3 to the left-hand part of Eq. (76),

(i) find the corresponding addition to the RWA equations,
(ii) find the stationary amplitude A of parametric oscillations,
(iii) sketch and discuss the $A(\xi)$ dependence,
(iv) find the type and stability of each fixed point of the RWA equations,
(v) sketch the Poincaré phase plane of the system in main parameter regions.

4.13. Use the rotating-wave approximation to find the conditions of parametric excitation in an oscillator with weak modulation of both the effective mass $m(t) = m_0(1 + \mu_m\cos 2\omega t)$ and spring constant $\kappa(t) = \kappa_0[1 + \mu_\kappa\cos(2\omega t - \psi)]$, with the same frequency $2\omega \approx 2\omega_0$, but arbitrary modulation depths ratio

μ_m/μ_k and phase shift ψ. Interpret the result in terms of modulation of the instantaneous frequency $\omega(t) \equiv [\kappa(t)/m(t)]^{1/2}$ and mechanical impedance $Z(t) \equiv [\kappa(t)m(t)]^{1/2}$ of the oscillator.

4.14.* Find the condition of parametric excitation of a nonlinear oscillator described by equation

$$\ddot{q} + 2\delta\dot{q} + \omega_0^2 q + \gamma q^2 = f_0 \cos 2\omega t,$$

with sufficiently small δ, γ, f_0, and $\xi \equiv \omega - \omega_0$.

Chapter 5. From Oscillations to Waves

In this chapter, the discussion of oscillations is extended to systems with two and more degrees of freedom. This extension naturally leads to another key notion - waves. The discussion of waves (*at this stage*, *in 1D systems*) *is focused at such key phenomena as their dispersion and reflection from interfaces/boundaries.*

5.1. Two coupled oscillators

Let us move on to discuss oscillations in systems with more than one degree of freedom, starting from the simplest case of two linear, dissipation-free oscillators. If the Lagrangian of the system may be presented as a sum of those for two harmonic oscillators,

$$L = L_1 + L_2, \quad L_{1,2} = T_{1,2} - U_{1,2} = \frac{m_{1,2}}{2}\dot{q}_{1,2}^2 - \frac{\kappa_{1,2}}{2}q_{1,2}^2, \tag{5.1}$$

(plus arbitrary, inconsequential constants if you like), then according to Eq. (2.19), the equations of motion of the oscillators are independent of each other, and each one is similar to Eq. (1.1), with its *partial frequency* $\Omega_{1,2}$ equal to

$$\Omega_{1,2}^2 = \frac{\kappa_{1,2}}{m_{1,2}}. \tag{5.2}$$

This means that in this simplest case, the arbitrary motion of the system is just a sum of independent sinusoidal oscillations at two frequencies equal to the partial frequencies (2).

Hence, in order to describe the oscillator *coupling* (i.e. interaction), the full Lagrangian L should contain an additional *mixed* term L_{int} depending on both generalized coordinates q_1 and q_2 and/or generalized velocities. The simplest, and most frequently met type of such interaction term is the following *bilinear form* $U_{\text{int}} = -\kappa q_1 q_2$, where κ is a constant, giving $L_{\text{int}} = -U_{\text{int}} = \kappa q_1 q_2$. Figure 1 shows the simplest example of system with such interaction.[1] In it, three springs, keeping two massive particles between two stiff walls, have generally different spring constants.

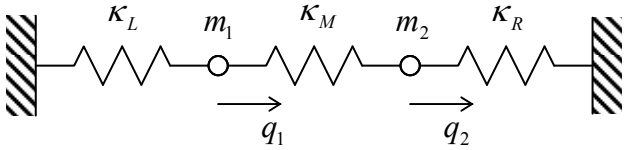

Fig. 5.1. Simple system of two coupled harmonic oscillators.

Indeed, in this case the kinetic energy is still separable, $T = T_1 + T_2$, but the total potential energy, consisting of elastic energies of three springs, is not:

$$U = \frac{\kappa_L}{2}q_1^2 + \frac{\kappa_M}{2}(q_1 - q_2)^2 + \frac{\kappa_R}{2}q_2^2, \tag{5.3a}$$

[1] Here it is assumed that the particles are constrained to move in only one dimension (shown horizontal).

where $q_{1,2}$ are the horizontal displacements of particles from their equilibrium positions. It is convenient to rewrite this expression as

$$U = \frac{\kappa_1}{2} q_1^2 + \frac{\kappa_2}{2} q_2^2 - \kappa q_1 q_2, \quad \text{where } \kappa_1 \equiv \kappa_L + \kappa_M, \quad \kappa_2 \equiv \kappa_R + \kappa_M, \quad \kappa \equiv \kappa_M, \tag{5.3b}$$

showing that the Lagrangian $L = T - U$ of this system indeed contains a bilinear interaction term:

$$L = L_1 + L_2 + L_{\text{int}}, \quad L_{\text{int}} = \kappa q_1 q_2. \tag{5.4}$$

The resulting Lagrange equations of motion are

$$\boxed{\begin{aligned} m_1 \ddot{q}_1 + m_1 \Omega_1^2 q_1 &= \kappa q_2, \\ m_2 \ddot{q}_2 + m_2 \Omega_2^2 q_2 &= \kappa q_1. \end{aligned}} \tag{5.5}$$

Linearly coupled oscillators

Thus the interaction energy describes effective generalized force κq_2 exerted on subsystem 1 by subsystem 2, and the reciprocal effective force κq_1. Note that in contrast to real physical forces (these effective forces (such as $F_{12} = -F_{21} = \kappa_M(q_2 - q_1)$ for the system shown in Fig. 1) the effective forces in the right-hand part of Eqs. (5) do obey the 3rd Newton law. Note also that they are proportional to the same coefficient κ; this feature is a result of the general bilinear structure (4) of the interaction energy rather than of any special symmetry.

We already know how to solve Eqs. (5), because it is still a system of linear and homogeneous differential equations, so that its general solution is a sum of particular solutions of the form similar to Eqs. (4.88),

$$q_1 = c_1 e^{\lambda t}, \quad q_2 = c_2 e^{\lambda t}. \tag{5.6}$$

for all possible values of λ. These values may be found by plugging Eq. (6) into Eqs. (5), and requiring the resulting system of two linear algebraic equations for the distribution coefficients $c_{1,2}$,

$$\begin{aligned} m_1 \lambda^2 c_1 + m_1 \Omega_1^2 c_1 &= \kappa c_2, \\ m_2 \lambda^2 c_2 + m_2 \Omega_2^2 c_2 &= \kappa c_1, \end{aligned} \tag{5.7}$$

to be self-consistent. In our particular case, we get a characteristic equation,

$$\begin{vmatrix} m_1(\lambda^2 + \Omega_1^2) & -\kappa \\ -\kappa & m_2(\lambda^2 + \Omega_2^2) \end{vmatrix} = 0, \tag{5.8}$$

that is quadratic in λ^2, and thus allows a simple solution:

$$\begin{aligned} (\lambda^2)_\pm &= -\frac{1}{2}(\Omega_1^2 + \Omega_2^2) \mp \left[\frac{1}{4}(\Omega_1^2 + \Omega_2^2)^2 - \Omega_1^2 \Omega_2^2 + \frac{\kappa^2}{m_1 m_2} \right]^{1/2} \\ &= -\frac{1}{2}(\Omega_1^2 + \Omega_2^2) \mp \left[\frac{1}{4}(\Omega_1^2 - \Omega_2^2)^2 + \frac{\kappa^2}{m_1 m_2} \right]^{1/2}. \end{aligned} \tag{5.9}$$

According to Eqs. (2) and (3b), for any positive values of spring constants, product $\Omega_1\Omega_2 = (\kappa_L + \kappa_M)(\kappa_R + \kappa_M)/(m_1 m_2)^{1/2}$ is always larger than $\kappa/(m_1 m_2)^{1/2} = \kappa_M/(m_1 m_2)^{1/2}$, so that the square root in Eq. (9) is always less than $(\Omega_1^2 + \Omega_2^2)/2$. As a result, both values of λ^2 are negative, i.e. the general solution to Eq.

(5) is a sum of four terms, each proportional to $\exp\{\pm i\omega_\pm t\}$, where both *eigenfrequencies* $\omega_\pm \equiv i\lambda_\pm$ are real:

Anticrossing description

$$\omega_\pm^2 \equiv -\lambda_\pm^2 = \frac{1}{2}\left(\Omega_1^2 + \Omega_2^2\right) \pm \left[\frac{1}{4}\left(\Omega_1^2 - \Omega_2^2\right)^2 + \frac{\kappa^2}{m_1 m_2}\right]^{1/2}. \qquad (5.10)$$

A plot of these eigenfrequencies as a function of one of the partial frequencies Ω (say, Ω_1), with the other partial frequency fixed, gives the famous *anticrossing* (also called "avoided crossing" or non-crossing") *diagram* (Fig. 2). One can see that at weak coupling, frequencies $\omega_\pm$ are close to the partial frequencies everywhere besides a narrow range near the anticrossing point $\Omega_1 = \Omega_2$. Most remarkably, at passing through this region, ω_+ smoothly "switches" from following Ω_2 to following Ω_1 and vice versa.

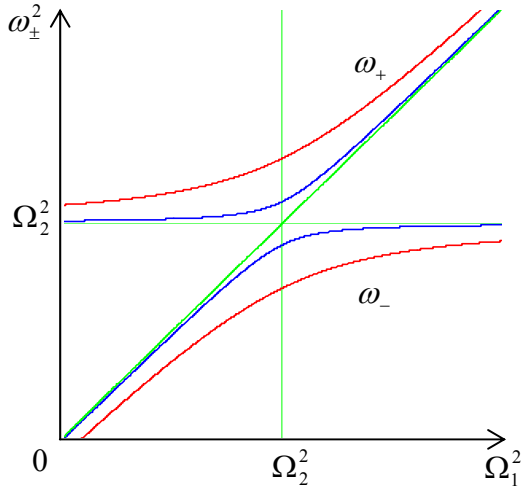

Fig. 5.2. Anticrossing diagram for two values of the oscillator coupling strength $\kappa/(m_1 m_2)^{1/2}\Omega_2^2$: 0.3 (red lines) and 0.1 (blue lines). In this plot, Ω_1 is assumed to be changed by varying κ_1 rather than m_1, but in the opposite case the diagram is qualitatively similar.

The reason for this counterintuitive behavior may be found by examining the distribution coefficients $c_{1,2}$ corresponding to each branch of the diagram, which may be obtained by plugging the corresponding value of $\lambda_\pm = -i\omega_\pm$ back into Eqs. (7). For example, at the anticrossing point $\Omega_1 = \Omega_2 \equiv \Omega$, Eq. (10) is reduced to

$$\omega_\pm^2 = \Omega^2 \pm \frac{\kappa}{(m_1 m_2)^{1/2}} = \Omega^2\left(1 \pm \frac{\kappa}{(\kappa_1 \kappa_2)^{1/2}}\right). \qquad (5.11)$$

Plugging this expression back into any of Eqs. (7), we see that for the two branches of the anticrossing diagram, the distribution coefficient ratio is the same by magnitude but opposite by sign: [2]

$$\left(\frac{c_1}{c_2}\right)_\pm = \mp\left(\frac{m_2}{m_1}\right)^{1/2}, \quad \text{at } \Omega_1 = \Omega_2. \qquad (5.12)$$

In particular, if the system is symmetric ($m_1 = m_2$, $\kappa_L = \kappa_R$), then at the upper branch, corresponding to $\omega_+ > \omega_-$, $c_1 = -c_2$. This means that in this *hard mode*,[3] masses oscillate in anti-phase: $q_1(t) \equiv -q_2(t)$. The

[2] It is useful to rewrite Eq. (12) as $Z_1 c_1 = \pm Z_2 c_2$, where $Z_{1,2} \equiv (\kappa_{1,2} m_{1,2})^{1/2}$ are of the partial oscillator *impedances* - the notion already mentioned in Chapter 4, and to be discussed in more detail in Sec. 4 below.

resulting substantial extension/compression of the middle spring yields additional returning force which increases the oscillation frequency. On the contrary, on the lower branch, corresponding to ω_-, the particle oscillations are in phase: $c_1 = c_2$, $q_1(t) \equiv q_2(t)$, so that the middle spring is never stretched at all. As a result, the *soft mode* oscillation frequency ω_- is lower than ω_+ and does not depend on κ:

$$\omega_-^2 = \Omega^2 - \frac{\kappa}{m} = \frac{\kappa_L}{m} = \frac{\kappa_R}{m} \ . \tag{5.13}$$

Note that for both modes, the oscillations equally engage both particles.

Far from the anticrossing point, the situation is completely different. Indeed, an absolutely similar calculation of $c_{1,2}$ shows that on each branch of the diagram, one of the distribution coefficients is much larger (by magnitude) than its counterpart. Hence, in this limit any particular mode of oscillations involves virtually only one particle. A slow change of system parameters, bringing it through the anticrossing, results, first, in a maximal delocalization of each mode, and then in the restoration of the localization, but in a different partial degree of freedom.

We could readily carry out similar calculations for the case when the systems are coupled via their velocities, $L_{\text{int}} = m\dot{q}_1\dot{q}_2$, where m is a coupling coefficient – not necessarily a certain physical mass. (In mechanics, with $q_{1,2}$ standing for actual particle displacements, such coupling is hard to implement, but there are many dynamic systems of non-mechanical nature in which such coupling is the most natural one.) The results are generally similar to those discussed above, again with the maximum level splitting at $\Omega_1 = \Omega_2 \equiv \Omega$:

$$\omega_\pm^2 = \frac{\Omega^2}{1 \mp |m|/(m_1 m_2)^{1/2}} \approx \Omega^2 \left(1 \pm \frac{|m|}{(m_1 m_2)^{1/2}} \right), \tag{5.14}$$

the last relation being valid for weak coupling. The generalization to the case of both coordinate and velocity coupling is also straightforward - see the next section.

The anticrossing diagram shown in Fig. 2 may be met not only in classical mechanics. It is even more ubiquitous quantum mechanics, because, due to the time-oscillatory character of the Schrödinger equation solutions, weak coupling of any two quantum states leads to a qualitatively similar behavior of eigenfrequencies $\omega_\pm$ and hence of the eigenenergies ("energy levels") $E_\pm = \hbar\omega_\pm$.[4]

5.2. *N* coupled oscillators

The calculations of the previous section may be readily generalized to the case of arbitrary number (say, N) coupled harmonic oscillators, with arbitrary type of coupling. It is evident that in this case Eq. (4) should be replaced with

[3] In physics, term "mode" is typically used for a particular type of variable distribution in space (in our current case, a certain set of distribution coefficients $c_{1,2}$), that sustains oscillations at a single frequency.

[4] One more property of weakly coupled oscillators, a periodic slow transfer of energy from one oscillator to the other and back, is more important for quantum rather than for classical mechanics. This is why I refer the reader to QM Secs. 2.5 and 5.1 for a detailed discussion of this phenomenon.

$$L = \sum_{j=1}^{N} L_j + \sum_{j,j'=1}^{N} L_{jj'}. \tag{5.15}$$

Moreover, we can generalize the above relations for the mixed terms $L_{jj'}$, taking into account their possible dependence not only on the generalized coordinates, but on the generalized velocities, in a bilinear form similar to Eq. (4). The resulting Lagrangian may be presented in a compact form,

$$L = \sum_{j,j'=1}^{N} \left(\frac{m_{jj'}}{2} \dot{q}_j \dot{q}_{j'} - \frac{\kappa_{jj'}}{2} q_j q_{j'} \right), \tag{5.16}$$

where the off-diagonal terms are index-symmetric: $m_{jj'} = m_{j'j}$, $\kappa_{jj'} = \kappa_{j'j}$, and the factors ½ compensate the double counting of each term with $j \neq j'$, taking place at the summation over two independently running indices. One may argue that Eq. (16) is quite general is we still want the equations of motion to be linear - as they have to be if the oscillations are small enough.

Plugging Eq. (16) into the general form (2.19) of the Lagrange equation, we get N equations of motion of the system, one for each value of index $j' = 1, 2, \ldots, N$:

$$\sum_{j=1}^{N} \left(m_{jj'} \ddot{q}_j + \kappa_{jj'} q_j \right) = 0. \tag{5.17}$$

Just as in the previous section, let us look for a particular solution to this system in the form

$$q_j = c_j e^{\lambda t}. \tag{5.18}$$

As a result, we are getting a system of N linear, homogeneous algebraic equations,

$$\sum_{j=1}^{N} \left(m_{jj'} \lambda^2 + \kappa_{jj'} \right) c_j = 0, \tag{5.19}$$

for the set of N distribution coefficients c_j. The condition that this system is self-consistent is that the determinant of its matrix equals zero:

$$\mathrm{Det}\left(m_{jj'} \lambda^2 + \kappa_{jj'} \right) = 0. \tag{5.20}$$

This characteristic equation is an algebraic equation of degree N for λ^2, and so has N roots $(\lambda^2)_n$. For any Hamiltonian system with stable equilibrium, matrices $m_{jj'}$ and $\kappa_{jj'}$ ensure that all these roots are real and negative. As a result, the general solution to Eq. (17) is the sum of $2N$ terms proportional to $\exp\{\pm i\omega_n t\}$, $n = 1, 2, \ldots, N$, where all N eigenfrequencies ω_n are real.

Plugging each of these $2N$ values of $\lambda = \pm i\omega_n$ back into the set of linear equations (17), one can find the corresponding set of distribution coefficients $c_{j\pm}$. Generally, the coefficients are complex, but in order to keep $q_j(t)$ real, the coefficients c_{j+} corresponding to $\lambda = +i\omega_n$ and c_{j-} corresponding to $\lambda = -i\omega_n$ have to be complex conjugate of each other. Since the sets of the distribution coefficients may be different for each λ_n, they should be marked with two indices, j and n. Thus, at general initial conditions, the time evolution of j-th coordinate may be presented as

$$q_j = \frac{1}{2} \sum_{n=1}^{N} \left(c_{jn} \exp\{+i\omega_n t\} + c_{jn}^* \exp\{-i\omega_n t\} \right) = \mathrm{Re} \sum_{n=1}^{N} c_{jn} \exp\{i\omega_n t\}. \tag{5.21}$$

This formula shows very clearly again the physical sense of the distribution coefficients c_{jn}: a set of these coefficients, with different values of index j but the same n, gives the complex amplitudes of oscillations of the coordinates for the special choice of initial conditions, that ensures purely sinusoidal motion of the system, with frequency ω_n. Moreover, these coefficients show how exactly such special initial conditions should be selected – within a common constant factor.

Calculation of the eigenfrequencies and distribution coefficients of a coupled system with many degrees of freedom from Eq. (20) is a task that frequently may be only done numerically.[5] Let us discuss just two particular but very important cases. First, let all the coupling coefficients be small ($|m_{jj'}| << m_j \equiv m_{jj}$ and $|\kappa_{jj'}| << \kappa_j \equiv \kappa_{jj}$, for all $j \neq j$), and all partial frequencies $\Omega_j \equiv (\kappa_j/m_j)^{1/2}$ be not too close to each other:

$$\frac{\left|\Omega_j^2 - \Omega_{j'}^2\right|}{\Omega_j^2} >> \frac{\left|\kappa_{jj'}\right|}{\kappa_j}, \frac{\left|m_{jj'}\right|}{m_j}, \quad \text{for all } j \neq j'. \tag{5.22}$$

(Such situation frequently happens if parameters of the system are "random" in the sense that they do not follow any special, simple rule.) Results of the previous section imply that in this case the coupling does not produce a noticeable change of oscillation frequencies: $\{\omega_n\} \approx \{\Omega_j\}$. In this situation, oscillations at each eigenfrequency are heavily concentrated in one degree of freedom, i.e. in each set of the distribution coefficients c_{jn} (for a given n), one coefficient's magnitude is much larger than all others.

Now let the conditions (22) be valid for all but one pair of partial frequencies, say Ω_1 and Ω_2, while these two frequencies are so close that coupling of the corresponding partial oscillators becomes essential. In this case the approximation $\{\omega_n\} \approx \{\Omega_j\}$ is still valid for all other degrees of freedom, and the corresponding terms may be neglected in Eqs. (19) for $j = 1$ and 2. As a result, we return to Eqs. (7) (perhaps generalized for velocity coupling) and hence to the anticrossing diagram (Fig. 2) discussed in the previous section. As a result, an extended change of only one partial frequency (say, Ω_1) of a weakly coupled system produces a series of eigenfrequency anticrossings – see Fig. 3.

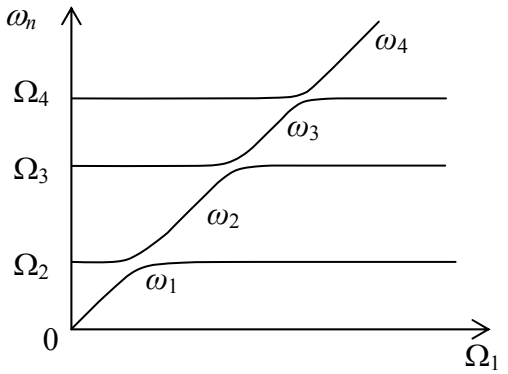

Fig. 5.3. Level anticrossing in a system of N weakly coupled oscillators – schematically.

[5] Fortunately, very effective algorithms have been developed for this *matrix diagonalization* task – see, e.g., references in MA Sec. 16(iii)-(iv). For example, the popular MATLAB package was initially created for this purpose. ("MAT" in its name stands for "matrix" rather than "mathematics".)

5.3. 1D waves in periodic systems

For coupled systems with considerable degree of symmetry, the general results of the last section may be simplified, some with very profound implications. Perhaps the most important of them are *waves*. Figure 4 shows a classical example of a wave-supporting system – a long 1D chain of massive particles, with the elastic next-neighbor coupling.

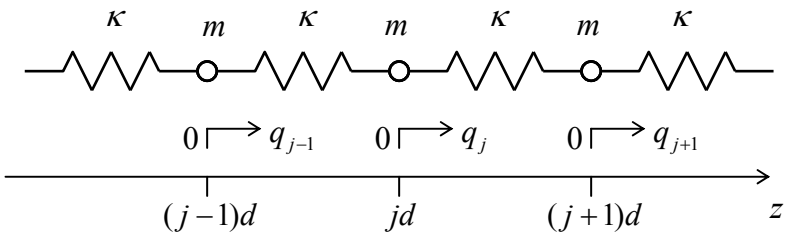

Fig. 5.4. Uniform 1D chain of elastically coupled particles.

Let us start from the case when the system is so long (formally, infinite) that the boundary effects may be neglected; then its Lagrangian may be represented by an infinite sum of similar terms, each including the kinetic energy of *j*-th particle, and the potential energy of the spring on one (say, right) side of it:

$$L = \sum_j \left[\frac{m}{2}\dot{q}_j^2 - \frac{\kappa}{2}\left(q_{j+1} - q_j\right)^2 \right]. \tag{5.23}$$

From here, the Lagrange equations of motion (2.19) have the same form for each particle:

$$m\ddot{q}_j - \kappa(q_{j+1} - q_j) + \kappa(q_j - q_{j-1}) = 0. \tag{5.24}$$

Apart from the (formally) infinite size of the system, this is evidently just a particular case of Eq. (17), and thus its particular solution may be looked in the form (18), with $\lambda^2 \to -\omega^2 < 0$. With this substitution, Eq. (24) gives the following simple form of the general system (17) for the distribution coefficients c_j:

$$\left(-m\omega^2 + 2\kappa\right)c_j - \kappa c_{j+1} - \kappa c_{j-1} = 0. \tag{5.25}$$

Now comes the most important conceptual step toward the wave theory: the translational symmetry of Eq. (23), i.e. its invariance to the replacement $j \to j + 1$, allows it to have a particular solution of the following form:

$$c_j = ae^{i\alpha j}, \tag{5.26}$$

where coefficient α may depend on ω (and system's parameters), but not on the particle number *j*. Indeed, plugging Eq. (26) into Eq. (25) and cancelling the common factor $e^{i\alpha j}$, we see that it is identically satisfied, if α obeys the following algebraic equation:

$$\left(-m\omega^2 + 2\kappa\right) - \kappa e^{+i\alpha} - \kappa e^{-i\alpha} = 0. \tag{5.27}$$

The physical sense of solution (26) becomes clear if we use it and Eq. (18) with $\lambda = \mp i\omega$ to write

$$q_j(t) = \mathrm{Re}\left[ae^{i(kz_j \mp \omega t)}\right] = \mathrm{Re}\left[ae^{ik\left(z_j \mp v_{\mathrm{ph}} t\right)}\right], \tag{5.28}$$

1D traveling wave

where *wave number* k is defined as $k \equiv \alpha/d$, and $z_j = jd$ is the equilibrium position of j-th particle - the notion that should not be confused with particle's displacement q_j from that equilibrium position – see Fig. 4. Relation (28) describes nothing else than a *sinusoidal traveling wave* of particle displacements (and hence of spring extensions/constrictions), that propagates, depending on the sign before v_{ph}, to the right or to the left along the particle chain with *phase velocity*

$$v_{\mathrm{ph}} \equiv \frac{\omega}{k}. \tag{5.29}$$

Phase velocity

Perhaps the most important characteristic of a wave is the so-called *dispersion relation*, i.e. the relation between its frequency ω and wave number k – essentially between the temporal and spatial frequencies of the wave. For our current system, this relation is given by Eq. (27) with $\alpha \equiv kd$. Taking into account that $(2 - e^{+i\alpha} - e^{-i\alpha}) = 2(1 - \cos\alpha) = 4\sin^2(\alpha/2)$, it may be rewritten in a simpler form:

$$\omega = \pm\omega_0 \sin\frac{\alpha}{2} = \pm\omega_0 \sin\frac{kd}{2}, \qquad \text{where } \omega_0 \equiv 2\left(\frac{\kappa}{m}\right)^{1/2}. \tag{5.30}$$

This result, frequently called the *Debye dispersion relation*,[6] is sketched in Fig. 5, and is rather remarkable in several aspects.

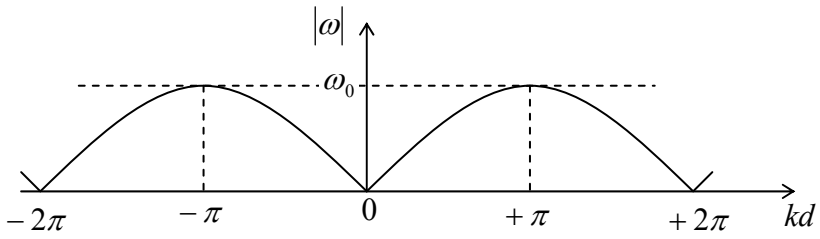

Fig. 5.5. The Debye dispersion relation.

First, if the wavelength $\lambda \equiv 2\pi/|k|$ is much larger than the spatial period a of the structure, i.e. if $|kd| << 1$ (so that $|\omega| << \omega_0$), the dispersion relation is approximately linear:

$$\omega = \pm\omega_0 \frac{kd}{2} = \pm vk, \tag{5.31}$$

where parameter v is frequency-independent:

$$v \equiv \frac{\omega_0 d}{2} = \left(\frac{\kappa}{m}\right)^{1/2} d\,. \tag{5.32}$$

Comparison of Eq. (31) with Eq. (28) shows that this constant plays, in the low-frequency region, the role of phase velocity for any frequency component of a waveform created in the system - say, by initial conditions. As a result, low-frequency waves of arbitrary form can propagate in the system without

[6] Named after P. Debye who developed this theory in 1912, in the context of specific heat of solids at low temperatures (beating nobody else than A. Einstein on the way :-) – see, e.g., SM Sec. 2.6.

deformation (called *dispersion*). Such waves are called *acoustic*,[7] and are the general property of *any* elastic continuous medium.

Indeed, the limit $|kd| << 1$ means that distance d between adjacent particles is much smaller than wavelength $\lambda = 2\pi/|k|$, i.e. that the differences $q_{j+1}(t) - q_j(t)$ and $q_j(t) - q_{j-1}(t)$, participating in Eq. (24), are relatively small and may be approximated with $\partial q/\partial j = \partial q/\partial(z/d) = d(\partial q/\partial z)$, with the derivatives taken at middle points between the particles: respectively, $z_+ \equiv (z_{j+1} - z_j)/2$ and $z_- \equiv (z_j - z_{j-1})/2$. Here z is now considered as a continuous argument (and hence the system, as a 1D *continuum*), and $q(z,t)$, as a continuous function of space and time. In this approximation, the sum of the last two terms of Eq. (24) is equal to $-\kappa d[\partial q/\partial z(z_+) - \partial q/\partial z(z_-)]$, and may be similarly approximated by $-\kappa d^2(\partial^2 q/\partial z^2)$, with the second derivative taken at point $(z_+ - z_-)/2 = z_j$, i.e. exactly at the same point as the time derivative. As the result, the *ordinary* differential equation (24) is reduced to a *partial* differential equation

$$m\frac{\partial^2 q}{\partial t^2} - \kappa d^2 \frac{\partial^2 q}{\partial z^2} = 0 . \tag{5.33a}$$

Using Eqs. (30) and (32), we may present this equation in a more general form

1D wave equation

$$\left(\frac{1}{v^2}\frac{\partial^2}{\partial t^2} - \frac{\partial^2}{\partial z^2}\right) q(z,t) = 0 , \tag{5.33b}$$

which describes a scalar acoustic wave (of any physical nature) in a 1D linear, dispersion-free continuum – cf. Eq. (1.2). In our current simple model (Fig. 4), direction z of the wave propagation coincides with the direction of particle displacements q; such acoustic waves are called *longitudinal*. However, in Chapter 7 we will see that 3D elastic media may also support different, *transverse* waves that also obey Eq. (33b), but with a different acoustic velocity v.

Second, when the wavelength *is* comparable with the structure period d (i.e. the product kd is *not* small), the dispersion relation is *not* linear, and the system is *dispersive*. This means that as a wave, whose Fourier spectrum has several essential components with frequencies of the order of ω_0, travels along the structure, its *waveform* (which may be defined as the shape of a snapshot of all q_j, at the same time) changes.[8] This effect may be analyzed by presenting the general solution of Eq. (24) as the sum (more generally, an integral) of components (28) with different complex amplitudes a:

1D wave packet

$$q_j(t) = \mathrm{Re}\int_{-\infty}^{+\infty} a_k e^{i\left[kz_j - \omega(k)t\right]} dk . \tag{5.34}$$

This notation emphasizes the dependence of the partial wave amplitudes a_k and frequencies on the wave number k. While the latter dependence is given by the dispersion relation, in our current case by Eq. (30), function a_k is determined by the initial conditions. For applications, the case when a_k is substantially different from zero only is a narrow interval, of width $\Delta k << k_0$ around some central value k_0, is of special importance. (The Fourier transform reciprocal to Eq. (34) shows that this is true, in particular for a so-called *wave packet* - a sinusoidal wave modulated by an *envelope* with a large width

[7] This term is purely historical. Though the usual sound waves in air belong to this class, the waves we are discussing may have frequency both well below and well above human ear's sensitivity range.

[8] The waveform deformation due to *dispersion* (which we are considering now) should be clearly distinguished from its possible change due to *attenuation*, i.e. energy loss - which is *not* taken into account is our energy-conserving model (23) – cf. Sec. 5 below.

$\Delta z \sim 1/\Delta k >> 1/k_0$ – see Fig. 6.) Using that strong inequality, the wave packet propagation may be analyzed by expending the dispersion relation $\omega(k)$ into the Taylor series at point k_0, and, in the first approximation in $\Delta k/k_0$, restricting the expansion by its first two terms:

$$\omega(k) \approx \omega_0 + \left.\frac{d\omega}{dk}\right|_{k=k_0} \tilde{k}, \quad \text{where } \omega_0 \equiv \omega(k_0), \text{ and } \tilde{k} \equiv k - k_0. \tag{5.35}$$

In this approximation, Eq. (34) yields

$$\begin{aligned} q_j(t) &\approx \mathrm{Re} \int_{-\infty}^{+\infty} a_k \exp\left\{ i\left[\left(k_0 + \tilde{k}\right) z_j - \left(\omega_0 + \left.\frac{d\omega}{dk}\right|_{k=k_0} \tilde{k} \right) t \right] \right\} dk \\ &= \mathrm{Re}\left[\exp\left\{ i\left(k_0 z_j - \omega_0 t\right) \right\} \int_{-\infty}^{+\infty} a_k \exp\left\{ i\tilde{k}\left(z_j - \left.\frac{d\omega}{dk}\right|_{k=k_0} t \right) \right\} dk \right]. \end{aligned} \tag{5.36}$$

Comparing this expression with the initial form of the wave packet,

$$q_j(0) = \mathrm{Re} \int_{-\infty}^{+\infty} a_k e^{ikz_j} dk = \mathrm{Re}\left[\exp\left\{ ik_0 z_j \right\} \int_{-\infty}^{+\infty} a_k \exp\left\{ i\tilde{k} z_j \right\} dk \right], \tag{5.37}$$

and taking into account that the phase factors before the integrals in the last forms of Eqs. (36) and (37) do not affect its envelope, we see that in this approximation[9] the envelope sustains its initial form and propagates along the system with the so-called *group velocity*

$$\boxed{v_{\mathrm{gr}} \equiv \left.\frac{d\omega}{dk}\right|_{k=k_0}}. \tag{5.38}$$

Group velocity

Note that, with the exception of the acoustic wave limit (31), this velocity (that characterizes the propagation of waveform's envelope), is different from the phase velocity (28) that describes the propagation of the "carrier" sine wave – for example, one of its zeros – see Fig. 6.

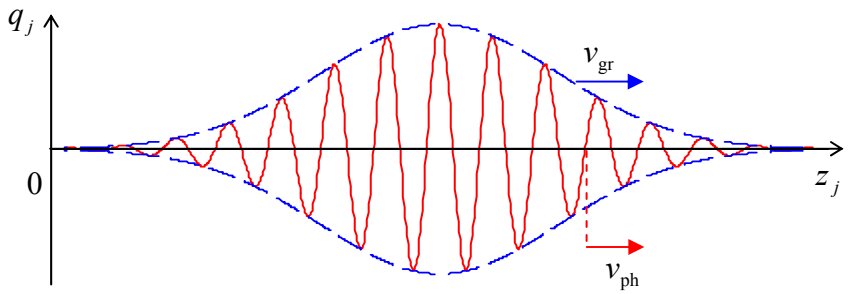

Fig. 5.6. Phase and group velocities of a wave packet.

Next, at the Debye dispersion law (30), the difference between v_{ph} and v_{gr} increases as the average frequency ω approaches ω_0, with the group velocity tending to zero, while the phase velocity staying virtually constant. The existence of such a maximum for the wave propagation frequency

[9] Taking into account the next term in the Taylor expansion of function $\omega(q)$, proportional to $d^2\omega/dq^2$, we would find that actually the dispersion leads to a gradual change of the envelope form. Such changes play an important role in quantum mechanics, so that I discuss them in that part of my notes (see QM Sec. 2.1).

presents one more remarkable feature of this system. It physics may be readily understood by noticing that according to Eq. (30), at $\omega = \omega_0$, the wave number k equals $n\pi/d$, where n is an odd integer, and hence the phase shift $\alpha \equiv kd$ is an odd multiple of π. Plugging this value into Eq. (28), we see that at the Debye frequency, oscillations of two adjacent particles are in anti-phase, for example:

$$q_0(t) = a\exp\{-i\omega t\}, \quad q_1(t) = a\exp\{i(\pi - \omega t)\} = -a\exp\{-i\omega t\} = -q_0(t). \tag{5.39}$$

It is clear from Fig. 4 that at such phase shift, all the springs are maximally stretched/compressed (just as in the hard mode of the two coupled oscillators analyzed in Sec. 1), so that it is natural that this mode has the highest frequency.

This invites a natural question what happens with the system if it is excited at a frequency $\omega > \omega_0$, say by an external force applied at the system's boundary. While the boundary phenomena will be considered in the next section, the most essential part of the answer may be obtained immediately from Eqs. (26) and (30). Indeed, reviewing the calculations that have led to these results, we see that they are valid not only for real but also any complex values of α. In particular, at $\omega > \omega_0$ the dispersion relation (30) gives

$$\alpha = n\pi \pm i\frac{d}{\Lambda}, \quad \text{where } \Lambda \equiv \frac{d}{2\text{arccosh}(\omega/\omega_0)}. \tag{5.40}$$

Plugging this relation into Eq. (26), we see that the wave's amplitude becomes an exponential function of position:

$$\left|q_j\right| = \left|a\right|e^{\pm j\,\text{Im}\,\alpha} \propto e^{\pm z_j/\Lambda}. \tag{5.41}$$

Physically this means that the wave decays penetrating into the structure (from the excitation point), dropping by a factor of $e \approx 3$ on the so-called *penetration depth* Λ. (According to Eq. (40), this depth decreases with frequency, but rather slowly, always remaining of the order of the distance between the adjacent particles.) Such a limited penetration is a very common property of various waves, including the electromagnetic waves in plasmas and superconductors, and quantum-mechanical "de Broglie waves" (wavefunctions) in the classically-forbidden regions. Note that this effect of "wave expulsion" from the media they cannot propagate in does not require any energy dissipation.

Finally, one more fascinating feature of the dispersion relation (30) is that if it is satisfied by some wave number $k_0(\omega)$, it is also satisfied at any $k_n(\omega) = k_0(\omega) + 2\pi n/d$, where n is any integer. This property is independent of the particular dynamics of the system: it follows already from Eq. (27), before its substitution into Eq. (25), because such a wave number translation by $2\pi/d$, i.e. the addition of 2π to phase shift α, is equivalent to the multiplication of $q_j(t)$ by $\exp\{i2\pi\} = 1$. Thus, such $(2\pi/d)$-periodicity in the wave number space is a common property of all systems that are d-periodic in the usual ("direct") space.[10]

Besides dispersion, one more key characteristic of any wave-supporting system is its *wave impedance* - the notion strangely missing from many physics (but not engineering) textbooks. It may be

[10] This property has especially important implications for quantum properties of periodic structures, e.g., crystals. It means, in particular, that the product $\hbar k$ cannot present the actual momentum of the particle (which is not conserved in periodic systems), but rather serves as its *quasi-momentum* (or "crystal momentum") – see, e.g., QM Sec. 2.5.

revealed by calculating the forces in the sinusoidal wave (28). For example, the force exerted by *j*-th particle on its right neighbor, given by the second term in Eq. (24), equals

$$F_{j+}(t) = \kappa\left[q_j(t) - q_{j+1}(t)\right] = \mathrm{Re}\left[\kappa\left(1 - e^{ikd}\right)ae^{i(kz_j \mp \omega t)}\right] \to \mathrm{Re}\left[-ikd\kappa ae^{i(kz_j \mp \omega t)}\right], \quad (5.42)$$

where the last form is valid in the most important acoustic wave limit, $kd \to 0$. Let us compare this expression for the wave of forces with that for the corresponding wave of particle velocities:

$$\dot{q}_j(t) = \mathrm{Re}\left[\mp i\omega ae^{i(\alpha j \mp \omega t)}\right]. \quad (5.43)$$

We see that these to waves have the same phase, and hence their ratio does not depend on either time or the particle number. Moreover, this ratio,

$$\frac{F_+}{\dot{q}} = \pm\frac{kd\kappa}{\omega} = \pm\frac{d\kappa}{v} = \pm Z, \quad (5.44)$$

is a real constant independent even on wave's frequency. Its magnitude is called the *wave impedance*:

$$Z \equiv \frac{d\kappa}{v} = (\kappa m)^{1/2}, \quad (5.45)$$

Wave impedance

and characterizes the dynamic "stiffness" of the system for the propagating waves.

In particular, the impedance scales the power carried by the wave. Indeed, the direct time averaging of the instantaneous power $\mathcal{P}_j(t) \equiv F_j(t)dq_j/dt$ transferred through particle *j* to the subsystem on the right of it, using Eqs. (42)-(43), yields a position-independent result

$$\overline{\mathcal{P}_j} \equiv \overline{[F_j(t)\dot{q}_j(t)]_\pm} = \pm\frac{\omega^2 Z}{2}aa^* \equiv \pm\frac{\omega^2 Z}{2}A^2, \quad (5.46)$$

Traveling wave's power

where $A \equiv |a|$ is the real amplitude of the wave, and, as before, the positive sign corresponds to the wave propagating to the right (and vice versa). Note that $\mathcal{P}$ is the *power flow* in the acoustic wave, and its spatial and temporal independence means that wave's energy is conserved - as could be expected from our Hamiltonian system we are considering.[11] Hence, the wave impedance *Z* characterizes the energy *transfer* along the system rather than its *dissipation*.

5.4. Interfaces and boundaries

The importance of the wave impedance notion becomes even more evident when we consider waves in non-uniform and finite-size systems. Indeed, our previous analysis assumed that the 1D system supporting the waves (Fig. 4) is exactly periodic, i.e. macroscopically uniform, and extends all the way from -∞ to +∞. Now let us examine what happens when this is not true. The simplest (and very important) example of such nonuniform systems is an *interface*, i.e. a point at which system parameters experience a change. Figure 7 shows a simple and representative example of such a sharp interface, for the same 1D wave system that was analyzed in the last section.

[11] The direct calculation of the energy (per unit length) is a simple but useful exercise, left for the reader.

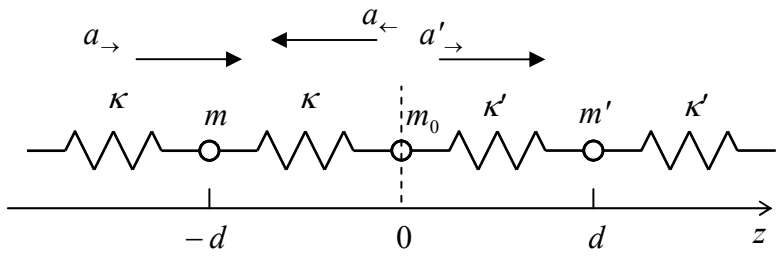

Fig. 5.7. 1D system with a sharp interface at $z = 0$, and the wave components at the partial reflection of a wave incident from the left.

Since the parameters κ and m are still constant on each side of the interface (put, for convenience, at $z_j = 0$), equations of motion (24) are is still valid for $j < 0$ and $j > 0$ (in the latter case, with the primed parameters), and show that at a fixed frequency ω, they can sustain sinusoidal waves of the type (28). However, the final jump of parameters at the interface ($m' \neq m$, $\kappa' \neq \kappa$) leads to a partial *reflection* of the incident wave from the interface, so that at least on the side of incidence (say, $z_j \leq 0$), we need to assume two such waves, one describing the incident wave and another, the reflected wave:

$$q_j(t) = \mathrm{Re}\begin{cases} a_{\rightarrow}e^{i\left(kz_j - \omega t\right)} + a_{\leftarrow}e^{i\left(-kz_j - \omega t\right)}, & \text{for } j \leq 0, \\ a'_{\rightarrow}e^{i\left(k'z_j - \omega t\right)}, & \text{for } j \geq 0. \end{cases} \tag{5.47}$$

In order to obtain boundary conditions for "stitching" these waves (i.e. getting relations between their complex amplitudes) at $j = 0$, i.e. $z_j = 0$, we need to take into account, first, that displacement $q_0(t)$ of the interface particle has to be the same whether it is considered a part of the left or right sub-system, and hence participates in Eqs. (24) for both $j \leq 0$ and $j \geq 0$. This gives us the first boundary condition,

$$a_{\rightarrow} + a_{\leftarrow} = a'_{\rightarrow}. \tag{5.48}$$

Second, writing the equation of motion for the special particle with $j = 0$,

$$m_0\ddot{q}_0 - \kappa'(q_1 - q_0) + \kappa(q_0 - q_{-1}) = 0. \tag{5.49}$$

and plugging into it the solution (47), we get the second boundary condition

$$-\omega^2 m_0 a'_{\rightarrow} - \kappa' a'_{\rightarrow}\left(e^{ik'd} - 1\right) + \kappa\left[a_{\rightarrow}\left(1 - e^{-ikd}\right) + a_{\leftarrow}\left(1 - e^{ikd}\right)\right] = 0. \tag{5.50}$$

The system of two linear equations (48) and (50) allows one to express both $a_{\leftarrow}$ and $a'_{\rightarrow}$ via amplitude $a_{\rightarrow}$ of the incident wave, and hence find the *reflection* (R) *and transmission* (T) *coefficients* of the interface:[12]

$$R \equiv \frac{a_{\leftarrow}}{a_{\rightarrow}}, \quad T \equiv \frac{a'_{\rightarrow}}{a_{\rightarrow}}. \tag{5.51}$$

The general result for R and T is a bit bulky, but may be simplified in the most important acoustic wave limit: $k'd$, $kd \rightarrow 0$. Indeed, in this limit all three parentheses participating in Eq. (50) may be approximated by the first terms of their Taylor expansions, e.g., $\exp\{ik'd\} - 1 \approx ik'd$, etc. Moreover, in this limit, the first term of Eq. (50) is of the second order in small parameter $\omega/\omega_0 \sim ka << 1$ (unless the

[12] Sorry, one more traditional usage of letter T. I do not think there any chance to confuse it with the kinetic energy.

interface particle mass m_0 is much larger than both m and m'), and hence may be neglected. As a result, Eq. (50) takes a very simple form[13]

$$\kappa k\left(a_{\rightarrow}-a_{\leftarrow}\right)=\kappa' k' a'_{\rightarrow}. \tag{5.52a}$$

According to Eqs. (31), (32) and (45), in the acoustic limit the ratio of factors κk of the waves (with the same frequency ω!) propagating at $z < 0$ and $z > 0$ is equal to that of the wave impedances Z of the corresponding parts of the system, so that Eq. (52a) may be rewritten as

$$Z\left(a_{\rightarrow}-a_{\leftarrow}\right)=Z' a'_{\rightarrow}. \tag{5.52b}$$

Now, solving the simple system of linear equations (48) and (52a), we get very important formulas,

$$R=\frac{Z-Z'}{Z+Z'},\quad T=\frac{2Z}{Z+Z'}, \tag{5.53}$$

Reflection and transmission coefficients

which are valid for any waves in 1D continua - with the corresponding re-definition of impedance.[14] Note that coefficients R and T characterize the ratios of wave amplitudes rather than their power. Using Eq. (46), for the time-averaged power flows we get relations

$$\frac{\mathcal{P}_{\leftarrow}}{\mathcal{P}_{\rightarrow}}=\left(\frac{Z-Z'}{Z+Z'}\right)^2,\quad \frac{\mathcal{P}'_{\rightarrow}}{\mathcal{P}_{\rightarrow}}=\frac{4ZZ'}{\left(Z+Z'\right)^2}. \tag{5.54}$$

(Note that $\mathcal{P}_{\leftarrow}+\mathcal{P}'_{\rightarrow}=\mathcal{P}_{\rightarrow}$, again reflecting the energy conservation.)

The first important result of this calculation that wave is fully transmitted through the interface if the so-called *impedance matching condition* $Z' = Z$ is satisfied, even if the wave velocities v (32) are different on the left and the right sides of the interface. On the contrary, the equality of the acoustic velocities in two media does *not* guarantee the full transmission of their interface. Again, this is a very general result.

Now let us consider the two limits in which Eq. (53) predicts a *total wave reflection*, $\mathcal{P}_{\leftarrow}/\mathcal{P}_{\rightarrow}\rightarrow 0$: $Z'/Z\rightarrow\infty$ (when $R = -1$) and $Z'/Z\rightarrow 0$ (when $R = 1$). According to Eq. (45), the former limit corresponds to the infinite product $\kappa' m'$, so that particles on the right side of the interface cannot move at all. This means that this particular case also describes a perfectly rigid boundary (Fig. 8a) for arbitrary ω, i.e. not necessarily in the acoustic wave limit. The negative sign of R in the relation $R = -1$ means that in the reflected wave, the phase of particle oscillations is shifted by π relative to the initial wave, $a = a_{\leftarrow} = -a_{\rightarrow}$, so that the sum of these two *traveling waves* may be also viewed as a single *standing wave*

$$q_{j\le 0}(t)=\mathrm{Re}\left[ae^{i\left(kz_j-\omega t\right)}-ae^{i\left(-kz_j-\omega t\right)}\right]=\mathrm{Re}\left[2iae^{-i\omega t}\sin kz_j\right]=2A\sin\left(\omega t-\varphi\right)\sin kz_j, \tag{5.55}$$

where $a\equiv a_{\rightarrow}=A\,e^{i\varphi}$. At the boundary ($z_j = 0$) this expression yields $q_0(t)\equiv 0$, i.e., a *node* of particle displacements. On the contrary, the corresponding standing wave of spring forces, described by Eq. (42), has a maximum at $z = 0$.

---

[13] This equation could be also obtained using Eq. (42), as the condition of balance of the forces exerted on the interface particle with $j = 0$ from the left and right - again, neglecting the inertia of that particle.

[14] See, e.g., corresponding parts of my lecture notes: QM Sec. 2.3 and EM Sec. 7.4. In 2D and 3D systems, Eqs. (53) are valid for the normal wave incidence only, otherwise they have to be modified – see, e.g., EM Sec. 7.4.

A similar standing wave forms in the opposite limit $Z'/Z \to 0$, that describes an "open" boundary shown in Fig. 8b. However, in this limit (with $R = +1$), the standing wave of displacements has a maximum at $z_j = 0$,

$$q_{j\le 0}(t) = \mathrm{Re}\left[ae^{i\left(kz_j - \omega t\right)} + ae^{i\left(-kz_j - \omega t\right)} \right] = \mathrm{Re}\left[2ae^{-i\omega t}\cos kz_j \right] = 2A\cos\left(\omega t - \varphi\right)\cos kz_j, \quad (5.56)$$

while the corresponding wave of forces has a node at that point. Most importantly, for both boundaries shown in Fig. 8, the standing waves are formed at any ratio ω/ω_0.

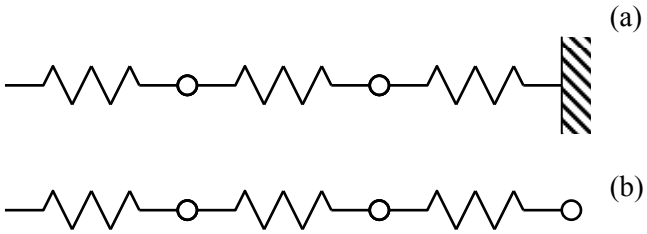

Fig. 5.8. (a) Rigid and (b) open boundaries of a 1D chain.

If the opposite boundary of a finite-length chain also provides a total wave reflection, the system may only support standing waves with certain wave numbers k_n, and hence certain eigenfrequencies ω_n that may be found from the set of k_n and the dispersion relation $\omega_n \equiv \omega(k_n)$, in our case given by Eq. (30). For example, if both boundaries of a chain with length L are rigid (Fig. 8a), then the standing wave (54) should have nodes at them both, giving the wave number *quantization condition*[15]

$$\sin k_n L = 0, \quad \text{i.e. } k_n = \frac{\pi n}{L}, \quad (5.57a)$$

where n is an integer. In order to count the number of different modes in a chain with a finite number N of oscillating particles, let us take into account, first, that adding one period $\Delta k = 2\pi/d$ of the dispersion relation to any k_n leads to the same mode. Moreover, changing the sign of k_n in standing wave (55) is equivalent to changing the sign of its amplitude. Hence, there are only N different modes, for example with

$$n = 1, 2, ..., N, \quad \text{i.e. } k_n = \frac{\pi}{L}, 2\frac{\pi}{L}, ..., N\frac{\pi}{L}. \quad (5.57b)$$

This fact is of course just a particular case of the general result obtained in Sec. 2.

According to Eq. (56), if both boundaries are open (Fig. 8b), the oscillation modes are different, but their wave numbers form the same set (57). Finally, if the types of boundary conditions on the chain's ends are opposite, the wave number set is somewhat different,

$$k_n = \frac{\pi}{L}\left(n - \frac{1}{2}\right), \quad (5.58)$$

[15] This result should be very familiar to the reader from freshmen-level "guitar string"-type problems. Note, however, that Eqs. (54)-(56) are valid not only for continuous 1D systems like a string, but also for (uniform) chains with a finite and arbitrary number N of particles – the fact we will use below.

but since the distance between the adjacent values of k_n is still the same (π/Nd), the system still has exactly N such values within each period $2\pi/d$ of the dispersion law, and hence, again, exactly N different oscillation modes.

This insensitivity of the number of modes and their equal spacing (called *equidistance*) on the k axis, enables the following useful (and very popular) trick. In many applications, it is preferable to speak about the number of different *traveling*, rather than *standing* waves in a system of a large but finite size, with coordinates z_0 and z_N describing the same particle. One can plausibly argue that the local dynamics of the chain of $N >> 1$ particles should not be affected if it is gradually bent into a large closed loop of length $L = Nd >> d$. Such a loop may sustain traveling waves, if they satisfy the following periodic *Born-Karman condition*: $q_0(t) \equiv q_N(t)$. (A popular vivid image is that the wave "catches its own tail with its teeth".) According to Eq. (27), this condition is equivalent to

$$e^{ik_n L} = 1, \qquad \text{i.e. } k_n = \frac{2\pi}{L} n . \tag{5.59}$$

Possible traveling wave number values

This equation gives a set of wave numbers twice more sparse than that described by Eqs. (57). However, now we can use N values of n, giving k_n, for example, from $-N$ to $+N$ (strictly speaking, excluding one of the boundary values to avoid double counting of the identical modes with $n = \pm N$), because traveling waves (28) with equal but opposite values of k_n propagate in opposite directions and hence present different modes. As a result, the total number of different traveling-wave modes is the same (N) as that of different standing-wave modes, and they are similarly (uniformly) distributed along the wave number axis. Since for $N >> 1$ the exact values of k_n are not important, the Born-Carman boundary conditions and the resulting set (59) of wave numbers are frequently used even for multi-dimensional systems whose bending into a ring along each axis is hardly physically plausible.

5.5. Dissipative, parametric, and nonlinear phenomena

In conclusion, let us discuss more complex effects in oscillatory systems with more than one degree of freedom. Starting from linear systems, energy dissipation may be readily introduced, just as for a single oscillator, by adding terms proportional to $\eta_j \dot{q}_j$, to the equations of motion such as Eqs. (5), (17), or (24). In arbitrary case, viscosity coefficients η_j are different for different particles; however, in many uniform systems like that shown in Fig. 4, the coefficients are naturally equal, turning Eq. (24) into

$$m\ddot{q}_j + \eta\dot{q}_j - \kappa(q_{j+1} - q_j) + \kappa(q_j - q_{j-1}) = 0 . \tag{5.60}$$

In the most important limit of acoustic waves, we may now repeat the arguments that have led to the wave equation (33) to get its generalization

$$\left(\frac{1}{v^2}\frac{\partial^2}{\partial t^2} + \frac{2\delta}{v^2}\frac{\partial}{\partial t} - \frac{\partial^2}{\partial z^2} \right) q(x,t) = 0, \quad \text{with } \delta \equiv \frac{\eta}{2m} . \tag{5.61}$$

Dissipative wave equation

Such dissipative equation may describe two major particular effects. First, it describes the decay *in time* of the standing waves in an autonomous wave system (say, of a finite length L) that have been caused by some initial push, described by non-trivial initial conditions, say, $q(z,0) \neq 0$. In order to analyze these decaying oscillations, one may look for the solution of Eq. (61) in the form of a sum of standing wave modes (that satisfy the given boundary conditions), each with its own, time-dependent

amplitude $A_n(t)$. For example, for rigid boundary conditions ($q = 0$) at $z = 0$ and $z = L$, we can use Eq. (55) as a hint to write

$$q(z,t) = \sum_{n=1}^{N} A_n(t) \sin k_n z \,, \tag{5.62}$$

where the set of q_n is given by Eq. (57). Plugging this solution into Eq. (61),[16] we get

$$\frac{1}{v^2} \sum_{n=1}^{N} \left(\ddot{A}_n + 2\delta \dot{A}_n + \omega_n^2 A_n \right) \sin k_n z = 0, \quad \text{with } k_n = \frac{\pi}{L} n. \tag{5.63}$$

Since functions $\sin k_n z$ are mutually orthogonal, Eq. (63) may be only satisfied if all N expressions in parentheses are equal to zero. As the result, the amplitude of each mode satisfies an ordinary differential equation absolutely similar to that studied in Sec. 4.1, with a similar solution describing the free oscillation decay with the relaxation constant (4.23). Here the wave character of the system gives nothing new, besides that different modes have different Q-factors: $Q_n = \omega_n/2\delta$.

More wave-specific is a different situation when the waves are due to their persisting excitation by some actuator at one of the ends (say, $z = 0$) of a very long structure. In this case, an initial transient process settles to a wave with a time-independent waveform limited by certain envelope $A(z)$ that decays at $z \to \infty$. In order to find the envelope, for the simplest case of sinusoidal excitation of frequency ω, one may look for a particular solution to Eq. (61) in a form very different from Eq. (60):

$$q(z,t) = \mathrm{Re}\left[a(z) e^{-i\omega t} \right], \tag{5.64}$$

generally with complex $a(z)$. Plugging this solution into Eq. (61), we see that this is indeed a valid solution, provided that $q(0,t) = a(0)\exp\{-i\omega t\}$ satisfies the boundary condition (now describing the wave excitation), and $a(z)$ obeys an following ordinary differential equation that describes wave's evolution in space rather than in time:[17]

$$\left(\frac{d^2}{dz^2} + k^2 \right) a = 0, \quad \text{with } k^2 \equiv \left(\frac{\omega}{v} \right)^2 + 2i \frac{\delta \omega}{v^2}. \tag{5.65}$$

The general solution to such differential equation is

$$a(x) = a_+ e^{ikz} + a_- e^{-ikz}, \tag{5.66}$$

with k now having both real and imaginary parts, $k = k' + ik''$, so that the wave (64) is

$$q(z,t) = a_+ e^{i(k'z - \omega t)} e^{-k''z} + a_- e^{i(-k'z - \omega t)} e^{k''z}. \tag{5.67}$$

If our boundary conditions correspond to the wave propagating to the right, we have to keep only the first term of this expression, with positive k''. The first exponent of that term describes the wave propagating from the boundary into the system (at low damping, with velocity virtually equal to v), while the second exponent describes an exponential decay of the wave's amplitude in space:

---

[16] Actually, this result may be also obtained from Eq. (60) and hence is valid for an arbitrary ratio ω_n/ω_0.

[17] Equation (65), as well as its multi-dimensional generalizations, is frequently called the *Helmholtz equation*, named after H. von Helmholtz (1821-1894).

$$A(z) \equiv |a(z)| = A(0)e^{-\alpha z/2}, \quad \frac{\alpha}{2} \equiv -k'' \approx \frac{\delta}{v}, \tag{5.68}$$

Wave attenuation

where the last, approximate relation is valid in the weak damping limit ($\delta << \omega$, i.e. $\delta/v << k'$). Constant α is called the *attenuation coefficient*, and in more general wave systems may depend on frequency ω. Physically, $2/\alpha$ is the scale of wave penetration into a dissipative system.[18] Note that our simple solution (68) is only valid if the system length L is much larger than $2/\alpha$; otherwise we would need to use the second term in Eq. (67) to describe wave reflection from the second end.

Now let me discuss (because of the lack of time, on a semi-quantitative level only), nonlinear and parametric phenomena in oscillatory systems with more than one degree of freedom. One important new effect here is the *mutual phase locking* of (two or more) weakly coupled self-excited oscillators with close frequencies: if the eigenfrequencies of the oscillators are sufficiently close, their oscillation frequencies "stick together" to become exactly equal. Though its dynamics of this process is very close to that of the phase locking of a single oscillator by external signal, that was discussed in Sec. 4.4, it is rather counter-intuitive in the view of the results of Sec. 1, and in particular the anticrossing diagram shown in Fig. 2. The analysis of the effect using the rotating-wave approximation (that is highly recommend to the reader) shows that the origin of the difference is oscillator's nonlinearity, which makes oscillation amplitude virtually independent of phase evolution – see Eq. (4.68) and its discussion.

One more new effect is the so-called *non-degenerate parametric excitation*. It may be illustrated of the example of just two coupled oscillators – see Sec. 1 above. Let us assume that the coupling constant κ, participating in Eqs. (5), is not constant, but oscillates in time - say with frequency ω_p. In this case the forces acting on each oscillator from its counterpart, described by the right-hand parts of Eqs. (5), will be proportional to $\kappa q_{2,1}(1 + \mu \cos\omega_p t)$. Assuming that oscillations of q_1 and q_2 are close to sinusoidal, with frequencies $\omega_{1,2}$, we see that the force acting on each oscillator will contain the so-called *combinational frequencies*

$$\omega_p \pm \omega_{2,1}. \tag{5.69}$$

If one of these frequencies in the right-hand part of each equation coincides with its own oscillation frequency, we can expect a substantial parametric interaction between the oscillators (on the top of the constant coupling effects discussed in Sec. 1). According to Eq. (69), this may happen in two cases:

$$\omega_p = \omega_1 \pm \omega_2, \tag{5.70}$$

Parametric interaction condition

The quantitative analysis (also highly recommended for reader's exercise) shows that in the positive sign case, the parameter modulation indeed leads to energy "pumping" into oscillations. As a result, sufficiently large μ, at sufficiently low damping coefficients $\delta_{1,2}$ and effective detuning

$$\xi \equiv \omega_p - (\Omega_1 + \Omega_2), \tag{5.71}$$

may lead to the simultaneous excitation of two frequency components $\omega_{1,2}$. These frequencies, while being close to corresponding eigenfrequencies of the system, are related to the *pumping frequency* ω_p by exact relation (70), but otherwise are arbitrary, e.g., incommensurate (Fig. 9a), thus justifying the term

[18] In engineering, the attenuation coefficient of wave-carrying systems is most frequently characterized by a logarithmic measure called *decibel per meter* (or just dB/m): $\alpha_{dB/m} \equiv 10 \log_{10} \alpha$.

non-degenerate parametric excitation. (The parametric excitation of a single oscillator, that was analyzed in Sec. 4.5, is a particular, *degenerate* case of such excitation, with $\omega_1 = \omega_2 = \omega_p/2$.) On the other hand, for the case described by Eq. (70) with the negative sign, parameter modulation always pumps energy from the oscillations, effectively increasing system's damping.

Somewhat counter-intuitively, this difference between two cases (70) may be simpler interpreted using the notions of quantum mechanics. Namely, equality $\omega_p = \omega_1 + \omega_2$ enables a decay of an external photon of energy $\hbar\omega_p$ into two photons of energies $\hbar\omega_1$ and $\hbar\omega_2$ going into the oscillatory system. (The complementary relation, $\omega_1 = \omega_p + \omega_2$, results in the oscillation photon decay.)

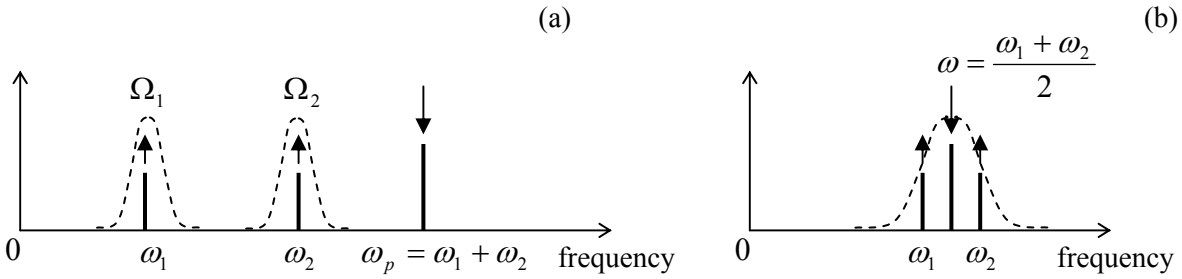

Fig. 5.9. Spectra of oscillations at (a) the non-degenerate parametric excitation, and (b) four-wave mixing. The arrow directions symbolize the power flows into and out of the system.

Proceeding to nonlinear phenomena, let us note, first of all, that the simple reasoning, that accompanied Eq. (4.109), is also valid in the case when oscillations consist of two (or more) sinusoidal components with incommensurate frequencies. Replacing notation 2ω for ω_p, we see that non-degenerate parametric excitation of the type (70a) is possible to implement in a system of two coupled oscillators with a quadratic nonlinearity (of the type γq^2), "pumped" by an intensive external signal at frequency $\omega_p \approx \Omega_1 + \Omega_2$. In optics, it is often more convenient to have all signals within the same, relatively narrow frequency range. A simple calculation, similar to the one made in Eqs. (4.108)-(4.109), shows that this may be done using the cubic nonlinearity[19] of the type αq^3, which allows the similar parametric energy exchange at frequency relation (Fig. 9b)

Four-wave mixing

$$2\omega = \omega_1 + \omega_2, \qquad \text{with } \omega \approx \omega_1 \approx \omega_2 . \tag{5.72a}$$

This process is often called the *four-wave mixing* (FWM), because it may be interpreted quantum-mechanically as the transformation of *two* externally-delivered photons, each with energy $\hbar\omega_p$, into two other photons of energies $\hbar\omega_1$ and $\hbar\omega_2$. Word "wave" in this term stems from the fact that at optical frequencies, it is hard to couple a sufficient volume of a nonlinear medium with lumped-type resonators. It is easier to implement the parametric excitation of light (as well as other nonlinear phenomena like the higher harmonic generation) in *distributed systems* of a linear size much larger than the involved wavelengths. In such systems, the energy transfer from the incoming wave of frequency ω to generated waves of frequencies ω_1 and ω_2 is gradually accumulated at their joint propagation along the system. From the analogy between Eq. (65) (describing the evolution of wave's amplitude *in space*),

[19] In optics, the nonlinearity is implemented using transparent crystals such as lithium niobate ($LiNbO_3$), with the cubic-nonlinear dependence of the electric polarization as a function of the applied electric field: $\mathcal{P} \propto \mathcal{E} + \alpha\mathcal{E}^3$.

and the usual equation of the harmonic oscillator (describing its evolution *in time*), it is clear that this energy transfer accumulation requires not only the frequencies ω, but also wave numbers k be in similar relations. For example, the four-wave mixing requires that not only the frequency balance (72a), but also a similar relation

$$2k = k_1 + k_2, \tag{5.72b}$$

to be *exactly* fulfilled. Since all three frequencies are close, this is easy to arrange if the dispersion relation $\omega(k)$ of the media is not too steep. Unfortunately, due to the lack of time/space, for more discussion of this interesting subject, *nonlinear optics*, I have to refer the reader to special literature.[20]

Note that even if the frequencies ω_1 and ω_2 of the parametrically excited oscillations are incommensurate, the oscillations are highly correlated. Indeed, the quantum mechanical theory of this effect[21] shows that the generated photons are *entangled*. This fact makes the parametric excitation very popular for a broad class of experiments in several currently active fields including quantum computation and encryption, and Bell inequality / local reality studies.[22]

It may look like a dispersion-free media, with $\omega/k = v = \text{const}$, is the perfect solution for arranging the parametric interaction of waves, because in such media, for example, Eq. (72b) automatically follows from Eq. (72a). However, in such media not only the desirable three parametrically interacting waves, but also all their harmonics, have the same velocity. At these conditions, energy transfer rates between all harmonics are of the same order. Perhaps the most important result of such multi-harmonic interaction is that intensive waves, interacting with nonlinear media, may develop sharply non-sinusoidal waveforms, in particular those with an almost instant change of the field at a certain moment. Such *shock waves*, especially those of mechanical nature, present large interest for certain applications - some not quite innocent, e.g., the explosion of usual and nuclear bombs. I will only briefly return to shock waves in Sec. 8.5.[23]

5.6. Exercise problems

5.1. For the system of two elastically coupled pendula, confined to a vertical plane, with the parameters shown in Fig. on the right (cf. Problem 1.3), find possible frequencies of small sinusoidal oscillations and the corresponding distribution coefficients. Sketch the oscillation modes.

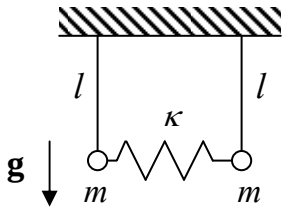

5.2. The same task as in Problem 1, for the double pendulum, confined to the vertical plane containing the support point (considered in Problem 2.1), with $m' = m$ and $l = l'$ - see Fig. on the right.

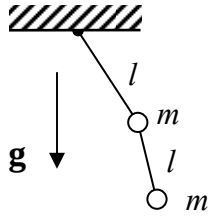

[20] See, e.g., the classical monograph by N. Bloembergen, *Nonlinear Optics*, 4th ed., World Scientific, 1996, or a more modern treatment by R. W. Boyd, *Nonlinear Optics*, 3rd ed., Academic Press, 2008.

[21] Which is, surprisingly, not much more complex than the classical theory – see, e.g., QM Sec.5.5.

[22] See, e.g., QM Secs. 8.5 and 10.1, correspondingly.

[23] The classical (and perhaps still the best) monograph on the subject is Ya. Zeldovich, *Physics of Shock Waves and High-Temperature Phenomena,* Dover, 2002.

5.3.* The same tasks as in Problem 5.1, for the triple pendulum shown in Fig. on the right, with the motion confined to a vertical plane containing the support point.

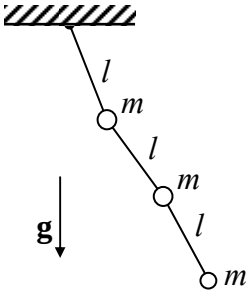

Hint: You may use any (e.g., numerical) method to calculate the characteristic equation roots.

5.4.*

(i) Explore an approximate way to analyze waves in a continuous 1D system with parameters slowly varying along its length.[24]

(ii) Apply this method to calculate eigenfrequencies of transverse standing waves on a freely hanging heavy rope of length L, with constant mass per unit length – see Fig. on the right.

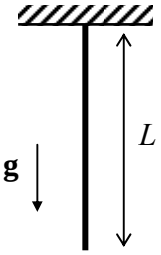

(iii) For three lowest standing wave modes, compare the results with those obtained in the solution of Problem 5.3 for the triple pendulum.

5.5. The same tasks as in Problem 1, for a linear, symmetric system of 3 particles, shown in Fig. on the right. Assume that the connections between the particles not only act as usual elastic springs (as described by their potential energies $U = \kappa \tilde{l}^2/2$), but also resist system's bending, giving an additional potential energy $U' = \kappa' l^2 \theta^2/2$, where θ is the (small) bending angle.[25]

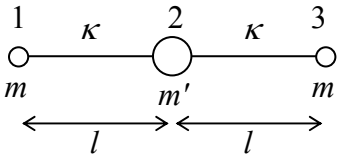

5.6. Three similar beads, which may slide along a circle of radius R without friction, are connected with similar springs with elastic constants κ and equilibrium lengths l_0 – see Fig. on the right. Analyze stability of the symmetric stationary state of the system, and calculate the frequencies and modes of its small oscillations about this state.

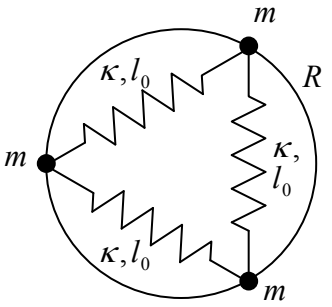

5.7. An external force $F(t)$ is applied to the right particle of system of shown in Fig. 5.1 of the lecture notes, with $\kappa_L = \kappa_R = \kappa'$ and $m_1 = m_2 \equiv m$ (see Fig. on the right), and the response $q_1(t)$ of the left particle to this force is being measured.

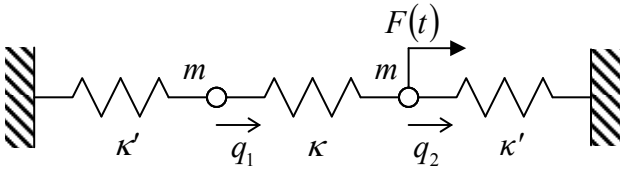

5.8. Calculate the spatial distributions of the kinetic and potential energies in a standing, sinusoidal, 1D acoustic wave, and analyze its evolution in time.

---

[24] The reader familiar with the WKB approximation in quantum mechanics (see, e.g., QM Sec. 2.4) is welcome to adapt it for this classical application. Another possible starting point is the rotating-wave approximation (RWA), discussed in Sec. 4.3 above, which should be translated from the time domain to the space domain.

[25] This is a good model for small oscillations of linear molecules such as CO_2 (for which the values of elastic constants κ and κ' are well known).

5.9. Calculate the dispersion law $\omega(k)$ and the maximum frequency of small longitudinal waves in an infinite line of similar, spring-coupled pendula - see Fig. on the right.

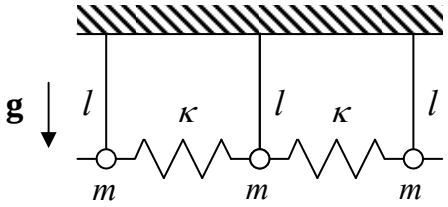

5.10. Calculate and analyze the dispersion relation $\omega(k)$ for longitudinal waves in an infinite 1D chain of coupled oscillators with alternating masses - see Fig. on the right. In particular, find and discuss dispersion relation's period Δk.

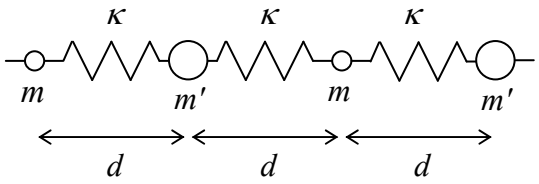

5.11. Calculate the longitudinal wave reflection from a "point inhomogeneity": a single particle with a different mass $m_0 \neq m$, in an otherwise uniform 1D chain - see Fig. on the right. Analyze the result.

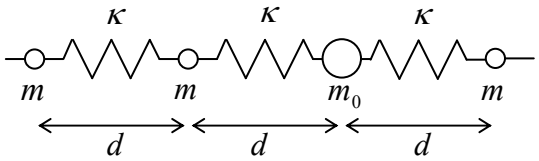

5.12.* Use the rotating-wave approximation to analyze the mutual phase locking of two weakly coupled self-oscillators with the dissipative nonlinearity, for the cases of:

(i) direct coordinate coupling, described by Eq. (5.5) of the lecture notes, and
(ii) linear but otherwise arbitrary coupling of two similar oscillators.

5.13.* Extend the second task of the previous problem to the mutual phase locking of N similar oscillators. In particular, explore the in-phase mode's stability for the case of the so-called *global coupling* via a single force F contributed equally by all oscillators.

5.14.* Find the condition of non-degenerate parametric excitation in a system of two coupled oscillators, described by Eqs. (5) with time-dependent coupling: $\kappa \to \kappa(1 + \mu\cos\omega_p t)$, with $\omega_p \approx \Omega_1 + \Omega_2$, and $\Omega_2 - \Omega_1 >> k/m$.

Hint: Assuming the modulation depth μ, static coupling κ, and detuning $\xi \equiv \omega_p - (\Omega_1 + \Omega_2)$ sufficiently small, use the rotating-wave approximation for each of the coupled oscillators.

5.15. Show that the cubic nonlinearity of the type αq^3 indeed enables the parametric interaction ("four-wave mixing") of oscillations with incommensurate frequencies related by Eq. (72a).

Chapter 6. Rigid Body Motion

This chapter discusses the motion of rigid bodies, with a focus on their rotation. Some byproduct results of this analysis will enable us to discuss, in the end of the chapter, the description of motion of point particles in non-inertial reference frames.

6.1. Angular velocity vector

Our study of 1D waves in the past chapter has prepared us to for a discussion of 3D systems of particles. We will start it with a (relatively :-) simple limit when the changes of distances $r_{kk'} \equiv |\mathbf{r}_k - \mathbf{r}_{k'}|$ between particles of the system are negligibly small. Such an abstraction is called the (*absolutely*) *rigid body*, and is a reasonable approximation in many practical problems, including the motion of solids. In this model we neglect *deformations* - that will be the subject of the next two chapters.

The rigid body approximation reduces the number of degrees of freedom of the system from $3N$ to just 6 - for example, 3 Cartesian coordinates of one point (say, O), and 3 angles of the system rotation about 3 mutually perpendicular axes passing through this point. (An alternative way to arrive at the same number 6 is to consider 3 points of the body, which uniquely define its position. If movable independently, the points would have 9 degrees of freedom, but since 3 distances $r_{kk'}$ between them are now fixed, the resulting 3 constraints reduce the number of degrees of freedom to 6.)

Let us show that an arbitrary elementary displacement of such a rigid body may be always considered as a sum of a translational motion and a rotation. Consider a "moving" reference frame, firmly bound to the body, and an arbitrary vector **A** – see Fig. 1.

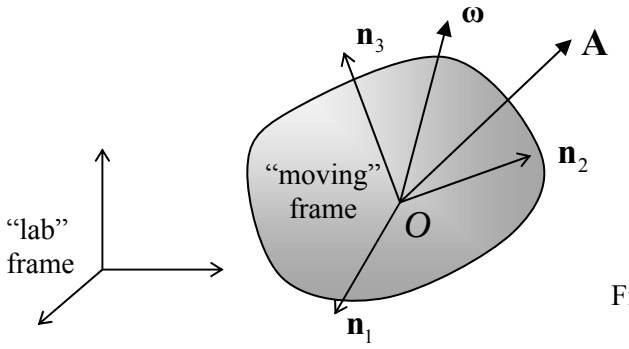

Fig. 6.1. Deriving Eq. (8).

The vector may be represented by its Cartesian components A_j in that reference frame:

$$\mathbf{A} = \sum_{j=1}^{3} A_j \mathbf{n}_j \,. \tag{6.1}$$

Let us calculate its time derivative in an arbitrary, possibly different ("lab") frame, taking into account that if the body rotates relative to this frame, then the directions of the unit vectors $\mathbf{n}_j$ change in time. Hence, we have to differentiate both operands in each product contributing to sum (1):

$$\frac{d\mathbf{A}}{dt}\Big|_{\text{in lab}} = \sum_{j=1}^{3} \frac{dA_j}{dt} \mathbf{n}_j + \sum_{j=1}^{3} A_j \frac{d\mathbf{n}_j}{dt} \,. \tag{6.2}$$

In this expression, the first sum evidently describes the change of vector **A** as observed from the moving frame. Each of the infinitesimal vectors $d\mathbf{n}_j$ participating in the second sum may be presented by its Cartesian components in the moving frame:

$$d\mathbf{n}_j = \sum_{j'=1}^{3} d\varphi_{jj'}\mathbf{n}_{j'} . \tag{6.3}$$

In order to find more about the set of scalar coefficients $d\varphi_{jj'}$, let us scalar-multiply each part of this relation by an arbitrary unit vector $\mathbf{n}_{j''}$, and take into account the evident orthogonality condition:

$$\mathbf{n}_{j'} \cdot \mathbf{n}_{j''} = \delta_{j'j''} . \tag{6.4}$$

As a result, we get

$$d\varphi_{jj''} = d\mathbf{n}_j \cdot \mathbf{n}_{j''} . \tag{6.5}$$

Now let us use Eq. (5) to calculate the first differential of Eq. (4):

$$d\mathbf{n}_{j'} \cdot \mathbf{n}_{j''} + \mathbf{n}_{j'} \cdot d\mathbf{n}_{j''} = d\varphi_{j'j''} + d\varphi_{j''j'} = 0; \quad \text{in particular,} \quad 2d\mathbf{n}_j \cdot \mathbf{n}_j = 2d\varphi_{jj} = 0 . \tag{6.6}$$

These relations, valid for any choice of indices j, j', and j'' of the set {1, 2, 3}, mean that the matrix of elements $d\varphi_{jj'}$ is antisymmetric; in other words, there are not 9, but just 3 independent coefficients $d\varphi_{jj'}$, all with $j \neq j'$. Hence it is natural to renumber them in a simpler way: $d\varphi_{jj'} = -\,d\varphi_{j'j} \equiv d\varphi_{j''}$, where indices j, j', and j'' follow in a "correct" order - either {1,2,3}, or {2,3,1}, or {3,1,2}. Now it is easy to check (say, just by a component-by-component comparison) that in this new notation, Eq. (3) may be presented just as a vector product:

$$\boxed{d\mathbf{n}_j = d\boldsymbol{\varphi} \times \mathbf{n}_j ,} \tag{6.7}$$

Elementary rotation

where $d\boldsymbol{\varphi}$ is the infinitesimal vector defined by its Cartesian components $d\varphi_j$ (in the moving frame).

Relation (7) is the basis of all rotation kinematics. Using it, Eq. (2) may be rewritten as

$$\boxed{\left.\frac{d\mathbf{A}}{dt}\right|_{\text{in lab}} = \left.\frac{d\mathbf{A}}{dt}\right|_{\text{in mov}} + \sum_{j=1}^{3} A_j \frac{d\boldsymbol{\varphi}}{dt} \times \mathbf{n}_j = \left.\frac{d\mathbf{A}}{dt}\right|_{\text{in mov}} + \boldsymbol{\omega} \times \mathbf{A}, \quad \text{where } \boldsymbol{\omega} \equiv \frac{d\boldsymbol{\varphi}}{dt}.} \tag{6.8}$$

Vector's evolution in time

In order to interpret the physical sense of vector $\boldsymbol{\omega}$, let us apply Eq. (8) to the particular case when **A** is the radius-vector **r** of a point of the body, and the lab frame is selected in a special way: its origin moves with the same velocity as that of the moving frame in the particular instant under consideration. In this case the first term in the right-hand part of Eq. (8) is zero, and we get

$$\left.\frac{d\mathbf{r}}{dt}\right|_{\text{in special lab frame}} = \boldsymbol{\omega} \times \mathbf{r} , \tag{6.9}$$

were vector **r** is the same in both frames. According to the vector product definition, the particle velocity described by this formula has a direction perpendicular to vectors $\boldsymbol{\omega}$ and **r** (Fig. 2), and magnitude $\omega r \sin\theta$. As Fig. 2 shows, this expression may be rewritten as $\omega\rho$, where $\rho = r\sin\theta$ is the distance from the line that is parallel to vector $\boldsymbol{\omega}$ and passes through point *O*. This is of course just the pure *rotation* about that line (called the *instantaneous axis of rotation*), with angular velocity ω. Since, according to Eqs. (3) and (8), the *angular velocity vector* $\boldsymbol{\omega}$ is defined by the time evolution of the moving frame alone, it is the same for all points **r**, i.e. for the rigid body as a whole. Note that nothing in

our calculations forbids not only the magnitude but also the direction of vector **ω**, and thus of the instantaneous axis of rotation, to change in time (and in many cases it does); hence the name.

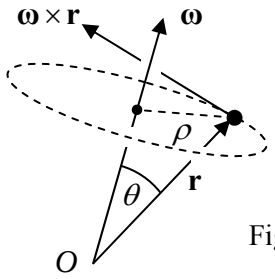

Fig. 6.2. Instantaneous axis of rotation.

Now let us generalize our result a step further, considering two laboratory reference frames that do not rotate versus each other: one arbitrary, and another one selected in the special way described above, so that for it Eq. (9) is valid in it. Since their relative motion of these two reference frames is purely translational, we can use the simple velocity addition rule given by Eq. (1.8) to write

Body point's velocity

$$\mathbf{v}\big|_{\text{in lab}} = \mathbf{v}_O\big|_{\text{in lab}} + \mathbf{v}\big|_{\text{in special lab frame}} = \mathbf{v}_O\big|_{\text{in lab}} + \boldsymbol{\omega}\times\mathbf{r}, \tag{6.10}$$

where **r** is the radius-vector of a point is measured in the body-bound ("moving") frame *O*.

6.2. Inertia tensor

Since the dynamics of each point of a rigid body is strongly constrained by conditions $r_{kk'} = \text{const}$, this is one of the most important fields of application of the Lagrangian formalism that was discussed in Chapter 2. The first thing we need to know for using this approach is the kinetic energy of the body in an inertial reference frame. It is just the sum of kinetic energies of all its points, so that we can use Eq. (10) to write:[1]

$$T = \sum \frac{m}{2}\mathbf{v}^2 = \sum \frac{m}{2}\left(\mathbf{v}_O + \boldsymbol{\omega}\times\mathbf{r}\right)^2 = \sum \frac{m}{2}v_O^2 + \sum m\mathbf{v}_O\cdot(\boldsymbol{\omega}\times\mathbf{r}) + \sum \frac{m}{2}(\boldsymbol{\omega}\times\mathbf{r})^2. \tag{6.11}$$

Let us apply to the right-hand part of Eq. (11) two general vector analysis formulas, listed in the Math Appendix: the operand rotation rule MA Eq. (7.6) to the second term, and MA Eq. (7.7b) to the third term. The result is

$$T = \sum \frac{m}{2}v_O^2 + \sum m\mathbf{r}\cdot(\mathbf{v}_O\times\boldsymbol{\omega}) + \sum \frac{m}{2}\left[\omega^2 r^2 - (\boldsymbol{\omega}\cdot\mathbf{r})^2\right]. \tag{6.12}$$

This expression may be further simplified by making a specific choice of point *O* (from the radius-vectors **r** of all particles are measured), namely if we use for this point the center of mass of the body. As was already mentioned in Sec. 3.4, radius-vector **R** of this point is defined as

$$M\mathbf{R} \equiv \sum m\mathbf{r}, \quad M \equiv \sum m, \tag{6.13}$$

[1] Actually, all symbols for particle masses, coordinates and velocities should carry the particle index, say *k*, over which the summation is carried out. However, for the sake of notation simplicity, this index is just implied.

where M is just the total mass of the body. In the reference frame centered as that point, $\mathbf{R} = 0$, so that in that frame the second sum in Eq. (12) vanishes, so that the kinetic energy is a sum of two terms:

$$T = T_{\text{tran}} + T_{\text{rot}}, \quad T_{\text{tran}} \equiv \frac{M}{2}V^2, \quad T_{\text{rot}} \equiv \sum \frac{m}{2}\left[\omega^2 r^2 - (\boldsymbol{\omega}\cdot\mathbf{r})^2\right], \tag{6.14}$$

where $\mathbf{V} \equiv d\mathbf{R}/dt$ is the center-of-mass velocity in our inertial reference frame, and all particle positions $\mathbf{r}$ have to be measured in the center-of-mass frame. Since the angular velocity vector $\boldsymbol{\omega}$ is common for all points of a rigid body, it is more convenient to rewrite the rotational energy in a form in which the summation over the components of this vector is clearly separated from the summation over the points of the body:

$$T_{\text{rot}} = \frac{1}{2}\sum_{j,j'=1}^{3} I_{jj'}\omega_j\omega_{j'}, \tag{6.15}$$

Kinetic energy of rotation

where the 3×3 matrix with elements

$$I_{jj'} \equiv \sum m\left(r^2\delta_{jj'} - r_j r_{j'}\right) \tag{6.16}$$

Inertia tensor

is called the *inertia tensor* of the body.

Actually, the term "tensor" for the matrix has to be justified, because in physics this name implies a certain reference-frame-independent notion, so that its elements have to obey certain rules at the transfer between reference frames. In order to show that the inertia tensor deserves its title, let us calculate another key quantity, the total angular momentum $\mathbf{L}$ of the same body.[2] Summing up the angular momenta of each particle, defined by Eq. (1.31), and using Eq. (10) again, in our inertial reference frame we get

$$\mathbf{L} \equiv \sum \mathbf{r}\times\mathbf{p} = \sum m\mathbf{r}\times\mathbf{v} = \sum m\mathbf{r}\times\left(\mathbf{v}_O + \boldsymbol{\omega}\times\mathbf{r}\right) = \sum m\mathbf{r}\times\mathbf{v}_O + \sum m\mathbf{r}\times\left(\boldsymbol{\omega}\times\mathbf{r}\right). \tag{6.17}$$

We see that the momentum may be presented as a sum of two terms. The first one,

$$\mathbf{L}_O \equiv \sum m\mathbf{r}\times\mathbf{v}_O = M\mathbf{R}\times\mathbf{v}_O, \tag{6.18}$$

describes possible rotation of the center of mass about the inertial frame origin. This term evidently vanishes if the moving reference frame's origin O is positioned at the center of mass. In this case we are left with only the second term, which describes the rotation of the body about its center of mass:

$$\mathbf{L} = \mathbf{L}_{\text{rot}} \equiv \sum m\mathbf{r}\times\left(\boldsymbol{\omega}\times\mathbf{r}\right). \tag{6.19}$$

Using one more vector algebra formula, the "bac minis cab" rule,[3] we may rewrite this expression as

$$\mathbf{L} = \sum m\left[\boldsymbol{\omega}r^2 - \mathbf{r}\left(\mathbf{r}\cdot\boldsymbol{\omega}\right)\right]. \tag{6.20}$$

Let us spell out an arbitrary Cartesian component of this vector:

[2] Hopefully, there is a little chance of confusion between the angular momentum $\mathbf{L}$ (a vector) and its Cartesian components L_j (scalars with an index) on one hand, and the Lagrange function L (a scalar without an index) on the other hand.

[3] See, e.g., MA Eq. (7.5).

$$L_j = \sum m\left[\omega_j r^2 - r_j \sum_{j'=1}^{3} r_{j'}\omega_{j'}\right] = \sum m \sum_{j'=1}^{3} \omega_{j'}\left(r^2\delta_{jj'} - r_j r_{j'}\right). \tag{6.21}$$

Changing the order of summations, and comparing the result with Eq. (16), we see that the angular momentum may be conveniently expressed via the same matrix elements $I_{jj'}$ as the rotational kinetic energy:

Angular momentum

$$\boxed{L_j = \sum_{j'=1}^{3} I_{jj'}\omega_{j'}\ .} \tag{6.22}$$

Since **L** and **ω** are both legitimate vectors (meaning that they describe physical vectors independent on the reference frame choice), their connection, the matrix of elements $I_{jj'}$, is a legitimate tensor. This fact, and the symmetry of the tensor ($I_{jj'} = I_{j'j}$), which is evident from its definition (16), allow the tensor to be further simplified. In particular, mathematics tells us that by a certain choice of the axis orientation, any symmetric tensor may be reduced to a diagonal form

$$I_{jj'} = I_j \delta_{jj'}, \tag{6.23}$$

where, in our case

Principal moments of inertia

$$\boxed{I_j = \sum m\left(r^2 - r_j^2\right) = \sum m\left(r_{j'}^2 + r_{j''}^2\right) = \sum m\rho_j^2\ ,} \tag{6.24}$$

ρ_j being the distance of the particle from the j-th axis, i.e. the length of the perpendicular dropped from the point to that axis. The axes of such special coordinate system are called the *principal axes*, while the diagonal elements I_j given by Eq. (24), the *principal moments of inertia* of the body. In such a special reference frame, Eqs. (15) and (22) are reduced to very simple forms:

Rotational energy and angular momentum in principal axes

$$\boxed{T_{\text{rot}} = \sum_{j=1}^{3} \frac{I_j}{2}\omega_j^2\ ,} \tag{6.25}$$

$$\boxed{L_j = I_j \omega_j .} \tag{6.26}$$

Both these results remind the corresponding relations for the translational motion, $T_{\text{tran}} = MV^2/2$ and $\mathbf{P} = M\mathbf{V}$, with the angular velocity **ω** replacing the "linear" velocity **V**, and the tensor of inertia playing the role of scalar mass M. However, let me emphasize that even in the specially selected coordinate system, with axes pointing in principal directions, the analogy is incomplete, and rotation is generally more complex than translation, because the measures of inertia, I_j, are generally different for each principal axis.

Let me illustrate this fact on a simple but instructive system of three similar massive particles fixed in the vertices of an equilateral triangle (Fig. 3).

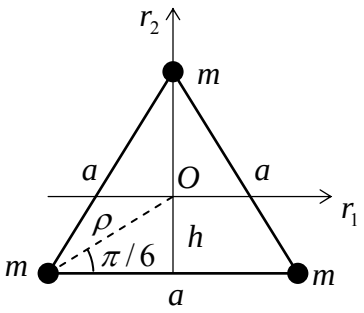

Fig. 6.3. Principal moments of inertia: a simple case study.

Due to symmetry of the configuration, one of the principal axes has to pass through the center of mass *O*, perpendicular to the plane of the triangle. For the corresponding principal moment of inertia, Eq. (24) readily yields $I_3 = 3m\rho^2$. If we want to express the result in terms of the triangle side *a*, we may notice that due to system's symmetry, the angle marked in Fig. 3 equals $\pi/6$, and from the corresponding right triangle, $a/2 = \rho\cos(\pi/6) \equiv \rho\sqrt{3}/2$, giving $\rho = a/\sqrt{3}$, so that, finally, $I_3 = ma^2$.

Another way to get the same result is to use the following general *axis shift theorem*, which may be rather useful - especially for more complex cases. Let us relate the inertia tensor components $I_{jj'}$ and $I'_{jj'}$, calculated in two reference frames - one in the center of mass *O*, and another one displaced by a certain vector **d** (Fig. 4a), so that for an arbitrary point, $\mathbf{r}' = \mathbf{r} + \mathbf{d}$. Plugging this relation into Eq. (16), we get

$$\begin{aligned} I'_{jj'} &= \sum m\left[(\mathbf{r}+\mathbf{d})^2\delta_{jj'} - (r_j + d_j)(r_{j'} + d_{j'})\right] \\ &= \sum m\left[(r^2 + 2\mathbf{r}\cdot\mathbf{d} + d^2)\delta_{jj'} - (r_j r_{j'} + r_j d_{j'} + r_{j'} d_j + d_j d_{j'})\right]. \end{aligned} \tag{6.27}$$

Since in the center-of-mass frame, all sums $\sum m r_j$ equal zero, we may use Eq. (16) to finally obtain

$$\boxed{I'_{jj'} = I_{jj'} + M(\delta_{jj'} d^2 - d_j d_{j'})}. \tag{6.28}$$

Rotation axis shift

In particular, this equation shows that if the shift vector **d** is perpendicular to one (say, *j*-th) of the principal axes (Fig. 4b), i.e. $d_j = 0$, then Eq. (28) is reduced to a very simple formula:

$$\boxed{I'_j = I_j + Md^2}. \tag{6.29}$$

Principal axis shift

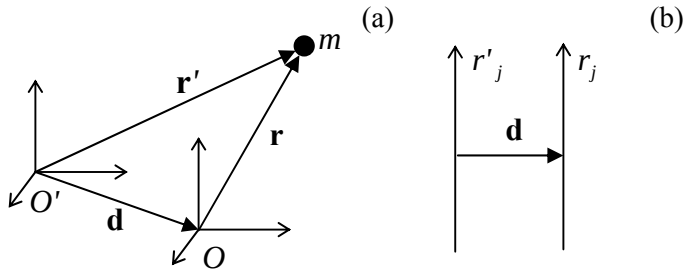

Fig. 6.4. (a) General reference frame shift from the center of mass, and (b) a shift perpendicular to one of the principal axes.

Returning to the system shown in Fig. 3, let us perform such a shift so that the new ("primed") axis passes through the location of one of the particles, still perpendicular to particles' plane. Then the contribution of that particular mass to the primed moment of inertia vanishes, and $I'_3 = 2ma^2$. Now, returning to the center of mass and applying Eq. (29), we get $I_3 = I'_3 - M\rho^2 = 2ma^2 - (3m)(a/\sqrt{3})^2 = ma^2$, i.e. the same result as above.

The symmetry situation inside the triangle plane is somewhat less evident, so let us start with calculating the moments of inertia for the axes shown vertical and horizontal in Fig. 3. From Eq. (24) we readily get:

$$I_1 = 2mh^2 + m\rho^2 = m\left[2\left(\frac{a}{2\sqrt{3}}\right)^2 + \left(\frac{a}{\sqrt{3}}\right)^2\right] = \frac{ma^2}{2}, \qquad I_2 = 2m\left(\frac{a}{2}\right)^2 = \frac{ma^2}{2}, \tag{6.30}$$

where I have taken into account the fact that the distance h from the center of mass and any side of the triangle is $h = \rho\sin(\pi/6) = \rho/2 = a/2\sqrt{3}$. We see that $I_1 = I_2$, and mathematics tells us that in this case *any* in-plane axis (passing through the center of mass O) may be considered as principal, and has the same moment of inertia. A rigid body with this property, $I_1 = I_2 \neq I_3$, is called the *symmetric top*. (The last direction is called the *main principal axis* of the system.)

Symmetric top: definition

Despite the name, the situation may be even more symmetric in the so-called *spherical tops*, i.e. highly symmetric systems whose principal moments of inertia are all equal,

$$I_1 = I_2 = I_3 \equiv I\,, \tag{6.31}$$

Spherical top: definition and description

Mathematics says that in this case the moment of inertia for rotation about *any* axis (but still passing through the center of mass) is equal to the same I. Hence Eqs. (25) and (26) are further simplified for any direction of vector $\boldsymbol{\omega}$:

$$T_{\text{rot}} = \frac{I}{2}\omega^2\,, \quad \mathbf{L} = I\boldsymbol{\omega}\,, \tag{6.32}$$

thus making the analogy of rotation and translation complete. (As will be discussed in the next section, the analogy is also complete if the rotation axis is fixed by external constraints.)

An evident example of a spherical top is a uniform sphere or spherical shell; a less obvious example is a uniform cube - with masses either concentrated in vertices, or uniformly spread over the faces, or uniformly distributed over the volume. Again, in this case *any* axis passing through the center of mass is principal, and has the same principal moment of inertia. For a sphere, this is natural; for a cube, rather surprising – but may be confirmed by a direct calculation.

6.3. Fixed-axis rotation

Now we are well equipped for a discussion of rigid body's rotational dynamics. The general equation of this dynamics is given by Eq. (1.38), which is valid for dynamics of any system of particles – either rigidly connected or not:

$$\dot{\mathbf{L}} = \boldsymbol{\tau}\,, \tag{6.33}$$

where $\boldsymbol{\tau}$ is the net torque of external forces. Let us start exploring this equation from the simplest case when the axis of rotation, i.e. the direction of vector $\boldsymbol{\omega}$, is fixed by some external constraints. Let us direct axis z along this vector; then $\omega_x = \omega_y = 0$. According to Eq. (22), in this case, the z-component of the angular momentum,

$$L_z = I_{zz}\omega_z\,, \tag{6.34}$$

where I_{zz}, though not necessarily one of the principal momenta of inertia, still may be calculated using Eq. (24):

$$I_{zz} = \sum m\rho_z^2 = \sum m\left(x^2 + y^2\right), \tag{6.35}$$

with ρ_z being the distance of each particle from the rotation axis z. According to Eq. (15), the rotational kinetic energy in this case is just

$$T_{\text{rot}} = \frac{I_{zz}}{2}\omega_z^2 . \tag{6.36}$$

Moreover, it is straightforward to use Eqs. (12), (17), and (28) to show that if the rotation axis is fixed, Eqs. (34)-(36) are valid even if the axis does not pass through the center of mass – if only distances ρ_z are now measured from that axis. (The proof is left for reader's exercise.)

As a result, we may not care about other components of vector **L**,[4] and use just one component of Eq. (33),

$$\dot{L}_z = \tau_z , \tag{6.37}$$

because it, when combined with Eq. (34), completely determines the dynamics of rotation:

$$I_{zz}\dot{\omega}_z = \tau_z , \quad \text{i.e. } I_{zz}\ddot{\theta}_z = \tau_z , \tag{6.38}$$

where θ_z is the angle of rotation about the axis, so that $\omega_z = \dot{\theta}$. Scalar relations (34), (36) and (38), describing rotation about a fixed axis, are completely similar to the corresponding formulas of 1D motion of a single particle, with ω_z corresponding to the usual ("linear") velocity, the angular momentum component L_z - to the linear momentum, and I_z - to particle's mass.

The resulting motion about the axis is also frequently similar to that of a single particle. As a simple example, let us consider what is called the *physical pendulum* (Fig. 5) - a rigid body free to rotate about a fixed horizontal axis *A* that does not pass through the center of mass *O*, in the uniform gravity field **g**.

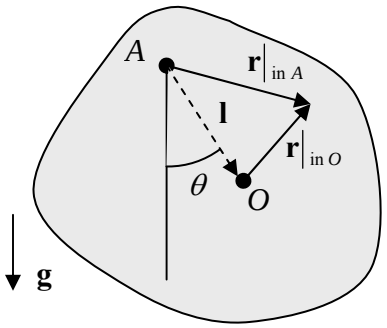

Fig. 6.5. Physical pendulum. The fixed (horizontal) rotation axis *A* is perpendicular to the plane of drawing.

Let us drop a perpendicular from point *O* to the rotation axis, and call the corresponding vector **l** (Fig. 5). Then the torque (relative to axis *A*) of the forces exerted by the axis constraint is zero, and the only contribution to the net torque is due to gravity alone:

$$\boldsymbol{\tau}\big|_{\text{in } A} \equiv \sum \mathbf{r}\big|_{\text{in } A} \times \mathbf{F} = \sum \left(\mathbf{l} + \mathbf{r}\big|_{\text{in } O}\right) \times m\mathbf{g} = \sum m\left(\mathbf{l} \times \mathbf{g}\right) + \sum m\mathbf{r}\big|_{\text{in } O} \times \mathbf{g} = M\mathbf{l} \times \mathbf{g} . \tag{6.39}$$

(For the last transition, I have used the facts that point *O* is the center of mass, and that vectors **l** and **g** are the same for all particles of the body.) This result shows that the torque is directed along the rotation

[4] Note that according to Eq. (22), other Cartesian components of the angular momentum, $L_x = I_{xz}\omega_z$ and $L_y = I_{yz}\omega_z$ may be different from zero, and even evolve in time. (Indeed, if axes *x* and *y* are fixed in lab frame, I_{xz} and I_{yz} may change due to body's rotation.) The corresponding torques $\tau_x^{(\text{ext})}$ and $\tau_y^{(\text{ext})}$, which obey Eq. (33), are automatically provided by external forces which keep the rotation axis fixed.

axis, and its (only) component τ_z is equal to $-Mgl\sin\theta$, where θ is the angle between vectors **l** and **g**, i.e. the angular deviation of the pendulum from the position of equilibrium. As a result, Eq. (38) takes the form,

$$I_A\ddot{\theta} = -Mgl\sin\theta, \tag{6.40}$$

where, I_A is the moment of inertia for rotation about axis A rather about the center of mass. This equation is identical to that of the point-mass (sometimes called "mathematical") pendulum, with the small-oscillation frequency

Physical pendulum's frequency

$$\Omega = \left(\frac{Mgl}{I_A}\right)^{1/2}. \tag{6.41}$$

As a sanity check, in the simplest case when the linear size of the body is much smaller than the suspension length l, Eq. (35) yields $I_A = Ml^2$, and Eq. (41) reduces to the well-familiar formula $\Omega = (g/l)^{1/2}$ for the mathematical pendulum.

Now let us discuss the situations when a body not only rotates, but also moves as the whole. As we already know from our introductory chapter, the total momentum of the body,

$$\mathbf{P} \equiv \sum m\mathbf{v} = \sum m\dot{\mathbf{r}} = \frac{d}{dt}\sum m\mathbf{r}, \tag{6.42}$$

satisfies the 2nd Newton law in the form (1.30). Using the definition (13) of the center of mass, the momentum may be presented as

$$\mathbf{P} = M\dot{\mathbf{R}} = M\mathbf{V}, \tag{6.43}$$

so Eq. (1.30) may be rewritten as

C.o.m.'s law of motion

$$M\dot{\mathbf{V}} = \mathbf{F}, \tag{6.44}$$

where **F** is the vector sum of all external forces. This equation shows that the center of mass of the body moves exactly as a point particle of mass M, under the effect of the net force **F**. In many cases this fact makes the translational dynamics of a rigid body absolutely similar to that of a point particle.

The situation becomes more complex if some of the forces contributing to the vector sum **F** depend on rotation of the same body, i.e. if its rotational and translational motions are coupled. Analysis of such coupled motion is rather straightforward if the *direction* of the rotation axis does not change in time, and hence Eqs. (35)-(36) are still valid. Possibly the simplest example is a round cylinder (say, a wheel) rolling on a surface without slippage (Fig. 6).

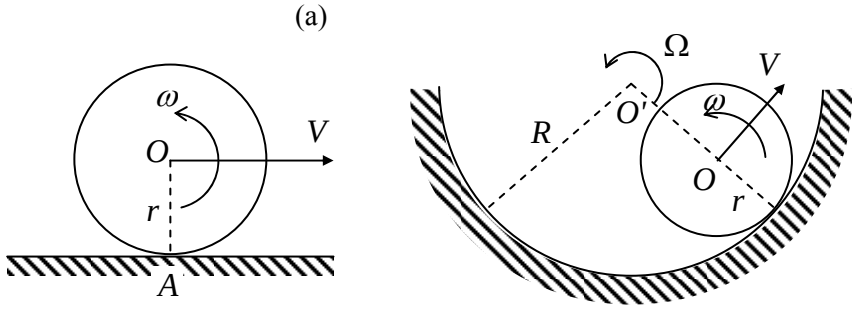

Fig. 6.6. Round cylinder rolling over (a) plane surface and (b) concave surface.

The no-slippage condition may be presented as the requirement of zero net velocity of the particular wheel point *A* that touches the surface – in the reference frame connected to the surface. For the simplest case of plane surface (Fig. 6a), the application of Eq. (10) shows that this requirement gives the following relation between the angular velocity ω of the wheel and the linear velocity V of its center:

$$V + r\omega = 0. \tag{6.45}$$

Such kinematic relations are essentially holonomic constraints, which reduce the number of degrees of freedom of the system. For example, without condition (45) the wheel on a plane surface has to be considered as a system with two degrees of freedom, so that its total kinetic energy (14) is a function of two independent generalized velocities, say V and ω:

$$T = T_{\text{tran}} + T_{\text{rot}} = \frac{M}{2}V^2 + \frac{I}{2}\omega^2. \tag{6.46}$$

Using Eq. (45) we may eliminate, for example, the linear velocity and reduce Eq. (46) to

$$T = \frac{M}{2}(\omega r)^2 + \frac{I}{2}\omega^2 = \frac{I_{\text{ef}}}{2}\omega^2, \quad \text{where} \quad I_{\text{ef}} \equiv I + Mr^2. \tag{6.47}$$

This result may be interpreted as the kinetic energy of pure rotation of the wheel about the instantaneous axis *A*, with I_{ef} being the moment of inertia about that axis, satisfying Eq. (29).

Kinematic relations are not always as simple as Eq. (45). For example, if the wheel is rolling on a concave surface (Fig. 6b), we need relate the angular velocities of the wheel rotation about its axis *O* (denoted ω) and that of its axis' rotation about the center *O*' of curvature of the surface (Ω). A popular error here is to write $\Omega = -(r/R)\omega$ [WRONG!]. A prudent way to get the correct relation is to note that Eq. (45) holds for this situation as well, and on the other hand the same linear velocity of wheel's center may be expressed as $V = (R - r)\Omega$. Combining these equations, we get a (not quite evident) relation

$$\Omega = -\frac{r}{R - r}\omega. \tag{6.48}$$

Another famous example of the relation between the translational and rotational motion is given by the "sliding ladder" problem (Fig. 7). Let us analyze it for the simplest case of negligible friction, and ladder's thickness small in comparison with its length l.

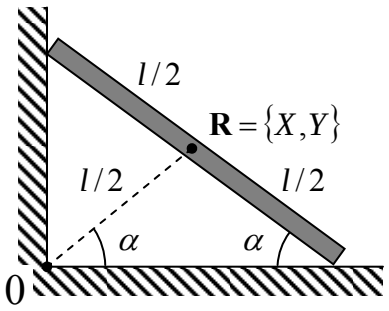

Fig. 6.7. Sliding ladder problem.

In order to use the Lagrangian formalism, we may write the kinetic energy of the ladder as the sum (14) of the translational and rotational parts:

$$T = \frac{M}{2}\left(\dot{X}^2 + \dot{Y}^2\right) + \frac{I}{2}\dot{\alpha}^2, \tag{6.49}$$

where X and Y are the Cartesian coordinates of its center of mass in an inertial reference frame, and I is the moment of inertia for rotation about the z-axis passing through the center of mass. (For the uniformly-distributed mass, an elementary integration of Eq. (35) yields $I = Ml^2/12$). In the reference frame with the center in the corner O, both X and Y may be simply expressed via angle α:

$$X = \frac{l}{2}\cos\alpha, \quad Y = \frac{l}{2}\sin\alpha. \tag{6.50}$$

(The easiest way to obtain these relations is to notice that the dashed line in Fig. 7 has slope α and length $l/2$.) Plugging these expressions into Eq. (49), we get

$$T = \frac{I_{\text{ef}}}{2}\dot{\alpha}^2, \quad I_{\text{ef}} \equiv I + M\left(\frac{l}{2}\right)^2 = \frac{1}{3}Ml^2. \tag{6.51}$$

Since the potential energy of the ladder in the gravity field may be also expressed via the same angle,

$$U = MgY = Mg\frac{l}{2}\sin\alpha, \tag{6.52}$$

α may be conveniently used as the (only) generalized coordinate of the system. Even without writing the Lagrangian equation of motion for that coordinate explicitly, we may notice that since the Lagrangian function ($T - U$) does not depend on time explicitly, and the kinetic energy (51) is a quadratic-homogeneous function of the generalized velocity $\dot{\alpha}$, the full mechanical energy,

$$E \equiv T + U = \frac{I_{\text{ef}}}{2}\dot{\alpha}^2 + Mg\frac{l}{2}\sin\alpha = \frac{Mgl}{2}\left(\frac{l\dot{\alpha}^2}{3g} + \sin\alpha\right), \tag{6.53}$$

is conserved and gives us the first integral of motion. Moreover, Eq. (53) shows that the system's energy (and hence dynamics) is identical to that of a physical pendulum with an unstable fixed point $\alpha_1 = \pi/2$, stable fixed point at $\alpha_2 = -\pi/2$, and frequency

$$\Omega = \left(\frac{3g}{2l}\right)^{1/2} \tag{6.54}$$

of small oscillations near the latter point. (Of course, that fixed point cannot be reached in the simple geometry shown in Fig. 7, where ladder's hitting the floor would change its equations of motion).

6.4. Free rotation

Now let us proceed to more complex case when the rotation axis is *not* fixed. A good illustration of the complexity arising is this case comes from the simplest case of a rigid body left alone, i.e. not subjected to external forces and hence its potential energy U is constant. Since in this case, according to Eq. (44), the center of mass moves (as measured from any inertial reference frame) with a constant velocity, we can always use an convenient inertial reference frame with the center at that point. From the point of view of such frame, the body's motion is a pure rotation, and $T_{\text{tran}} = 0$. Hence, the system's Lagrangian equals just the rotational energy (15), which is, first, a quadratic-homogeneous function of

components ω_j (that may be taken for generalized velocities), and, second, does not depend on time explicitly. As we know from Chapter 2, in this case the energy is conserved. For the components of vector $\boldsymbol{\omega}$ in the principal axes, this means

$$T_{\rm rot} = \sum_{j=1}^{3} \frac{I_j}{2} \omega_j^2 = \text{const}. \qquad (6.55)$$

Rotational energy's conservation

Next, as Eq. (33) shows, in the absence of external forces the angular momentum $\mathbf{L}$ of the body is conserved as well. However, though we can certainly use Eq. (26) to present this fact as

$$\mathbf{L} = \sum_{j=1}^{3} I_j \omega_j \mathbf{n}_j = \text{const}, \qquad (6.56)$$

Angular momentum's conservation

where $\mathbf{n}_j$ are the principal axes of inertia, this does not mean that components ω_j of the angular velocity vector $\boldsymbol{\omega}$ are constant, because the principal axes are fixed relative to the rigid body, and hence may rotate with it.

Before going after these complications, let us briefly mention two conceptually trivial, but practically very important, particular cases. The first is a spherical top ($I_1 = I_2 = I_3 = I$). In this case Eqs. (55) and (56) imply that all components of vector $\boldsymbol{\omega} = \mathbf{L}/I$, i.e. both the magnitude and the direction of the angular velocity are conserved, for any initial spin. In other words, the body conserves its rotation speed and axis direction, as measured in an inertial frame.

The most obvious example is a spherical planet. For example, our Mother Earth, rotating about its axis with angular velocity $\omega = 2\pi/(1\ \text{day}) \approx 7.3\times10^{-5}\ \text{s}^{-1}$, keeps its axis at a nearly constant angle of 23°27' to the *ecliptic pole*, i.e. the axis normal to the plane of its motion around the Sun. (In Sec. 6 below, we will discuss some very slow motions of this axis, due to gravity effects.)

Spherical tops are also used in the most accurate gyroscopes, usually with gas or magnetic suspension in vacuum. If done carefully, such systems may have spectacular stability. For example, the gyroscope system of the Gravity Probe B satellite experiment, flown in 2004-2005, was based on quartz spheres - round with precision of about 10 nm and covered by superconducting thin films (which have enabled their magnetic suspension and SQUID monitoring). The whole system was stable enough to measure that the so-called *geodetic effect* in general relativity (essentially, the space curving by Earth's mass), resulting in the axis precession by just 6.6 arcseconds per year, i.e. with a precession frequency of just $\sim10^{-11}\text{s}^{-1}$, agrees with theory with a record ~0.3% accuracy.[5]

The second simple case is that of the "symmetric top" ($I_1 = I_2 \neq I_3$), with the initial vector $\mathbf{L}$ aligned with the main principal axis. In this case, $\boldsymbol{\omega} = \mathbf{L}/I_3 = \text{const}$, so that the rotation axis is conserved.[6] Such tops, typically in the shape of a flywheel (rotor) supported by a "gimbal" system (Fig. 8), are broadly used in more common gyroscopes, core parts of automatic guidance systems, for

[5] Such beautiful experimental physics does not come cheap: the total Gravity Probe B project budget was about $750M. Even at this price tag, the declared main goal of the project, an accurate measurement of a more subtle relativistic effect, the so-called *frame-dragging drift* (or "the Schiff precession"), predicted to be about 0.04 arc seconds per year, has not been achieved.

[6] This is also true for an asymmetric top, i.e. an arbitrary body (with, say, $I_1 < I_2 < I_3$), but in this case the alignment of vector $\mathbf{L}$ with axis $\mathbf{n}_2$, corresponding to the intermediate moment of inertia, is unstable.

example, in ships, airplanes, missiles, etc. Even if the ship's hull wobbles, the suspended gyroscope sustains its direction relative to Earth (which is sufficiently inertial for these applications).[7]

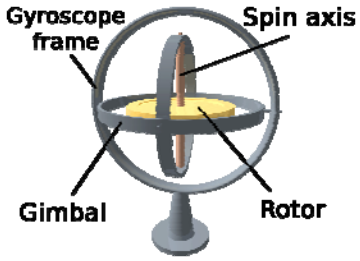

Fig. 6.8. Typical gyroscope. (Adapted from http://en.wikipedia.org/wiki/Gyroscope.)

However, in the general case with no such special initial alignment, the dynamics of symmetric tops is more complex. In this case, vector **L** is still conserved, including its direction, but vector **ω** is not. Indeed, let us direct axis $\mathbf{n}_2$ perpendicular to the common plane of vectors **L** and the instantaneous direction $\mathbf{n}_3$ of the main principal axis (in Fig. 9, the plane of drawing); then, in that particular instant, $L_2 = 0$. Now let us recall that in a symmetric top, axis $\mathbf{n}_2$ is a principal one. According to Eq. (26) with $j = 2$, the corresponding component ω_2 has to be equal to L_2/I_2, so it vanishes. This means that vector **ω** lies in this plane (the common plane of vectors **L** and $\mathbf{n}_3$) as well – see Fig. 9a.

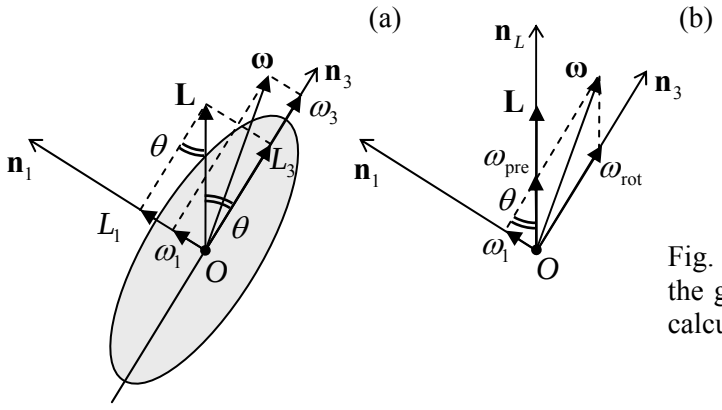

Fig. 6.9. Free rotation of a symmetric top: (a) the general configuration of vectors, and (b) calculating the free precession frequency.

Now consider any point of the body, located on axis $\mathbf{n}_3$, and hence within plane [$\mathbf{n}_3$, **L**]. Since **ω** is the instantaneous axis of rotation, according to Eq. (9), the point has instantaneous velocity $\mathbf{v} = \boldsymbol{\omega}\times\mathbf{r}$ directed normally to that plane. Since this is true for each point of the main axis (besides only one, with $\mathbf{r} = 0$, i.e. the center of mass, which does not move), this axis as a whole has to move perpendicular to the common plane of vectors **L**, **ω**, and $\mathbf{n}_3$. Since such conclusion is valid for any moment of time, it means that vectors **ω** and $\mathbf{n}_3$ rotate about the space-fixed vector **L** together, with some angular velocity ω_{pre}, at each moment staying in one plane. This effect is usually called the *free precession* (or "torque-

[7] Much more compact (and much less accurate) gyroscopes used, e.g., in smartphones and tablet computers, are based on the effect of rotation on oscillator frequency, and implemented as micro-electromechanical systems (MEMS) on silicon chip surface – see, e.g., Chapter 22 in V. Kaajakari, *Practical MEMS*, Small Gear Publishing, 2009.

free", or "regular") *precession*, and has to be clearly distinguished it from the completely different effect of the *torque-induced precession* which will be discussed in the next section.

In order to calculate ω_{pre}, let us present the instant vector $\boldsymbol{\omega}$ as a sum of not its Cartesian coordinates (as in Fig. 9a), but rather of two non-orthogonal vectors directed along $\mathbf{n}_3$ and $\mathbf{L}$ (Fig. 9b):

$$\boldsymbol{\omega} = \omega_{rot}\mathbf{n}_3 + \omega_{pre}\mathbf{n}_L, \quad \mathbf{n}_L \equiv \frac{\mathbf{L}}{L}. \tag{6.57}$$

It is clear from Fig. 9b that ω_{rot} has the meaning of the angular velocity of body rotation of the body about its main principal axis, while ω_{pre} is the angular velocity of rotation of that axis about the constant direction of vector **L,** i.e. the frequency of precession. Now the latter frequency may be readily calculated from the comparison of two panels of Fig. 9, by noticing that the same angle θ between vectors **L** and $\mathbf{n}_3$ participates in two relations:

$$\sin\theta = \frac{L_1}{L} = \frac{\omega_1}{\omega_{pre}}. \tag{6.58}$$

Since axis $\mathbf{n}_1$ is principal, we may use Eq. (26) for $j = 1$, i.e. $L_1 = I_1\omega_1$, to eliminate ω_1 from Eq. (58), and get a very simple formula

$$\boxed{\omega_{pre} = \frac{L}{I_1}.} \tag{6.59}$$

Free precession frequency

This result shows that the precession *frequency* is constant and independent of the alignment of vector **L** with the main principal axis $\mathbf{n}_3$, while the *amplitude* of this motion (characterized by angle θ) does depend on the alignment, and vanishes if **L** is parallel to $\mathbf{n}_3$.[8] Note also that if all principal moments of inertia are of the same order, ω_{pre} is of the same order as the total angular velocity $\omega = |\boldsymbol{\omega}|$ of rotation.

Now, let us briefly discuss the free precession in the general case of an "asymmetric top", i.e. a body with $I_1 \neq I_2 \neq I_3$. In this case the effect is more complex because here not only the *direction* but also the *magnitude* of the instantaneous angular velocity $\boldsymbol{\omega}$ may evolve in time. If we are only interested in the relation between the instantaneous values of ω_j and L_j, i.e. the "trajectories" of vectors $\boldsymbol{\omega}$ and **L** as observed from the reference frame $\{\mathbf{n}_1,\mathbf{n}_2,\mathbf{n}_3\}$ of the principal axes of the body (rather than an explicit law of their time evolution), they may be found directly from the conservation laws. (Let me emphasize again that vector **L**, being constant in an inertial frame, generally evolves in the frame rotating with the body.) Indeed, Eq. (55) may be understood as the equation of an ellipsoid in Cartesian coordinates $\{\omega_1, \omega_2, \omega_3\}$, so that for free body, vector $\boldsymbol{\omega}$ has to stay on the surface of that ellipsoid.[9] On the other hand, since the reference frame rotation preserves the length of any vector, the *magnitude* (but not direction!) of vector **L** is also an integral of motion in the moving frame, and we can write

$$L^2 \equiv \sum_{j=1}^{3} L_j^2 = \sum_{j=1}^{3} I_j^2\omega_j^2 = \text{const}. \tag{6.60}$$

[8] For Earth, the free precession amplitude it so small (below 10 m of linear displacement on the Earth surface) that this effect is of the same order as other, irregular motions of the rotation axis, resulting from the turbulent fluid flow effects in planet's interior and its atmosphere.

[9] It is frequently called the *Poinsot ellipsoid*, after L. Poinsot (1777-1859) who have made several key contributions to the rigid body mechanics.

Hence the trajectory of vector $\boldsymbol{\omega}$ follows the closed curve formed by the intersection of two ellipsoids, (55) and (60). It is evident that this trajectory is generally "taco-edge-shaped", i.e. more complex than a plane circle but never very complex either.

The same argument may be repeated for vector **L**, for whom the first form of Eq. (60) descries a sphere, and Eq. (55), another ellipsoid:

$$T_{\text{rot}} = \sum_{j=1}^{3} \frac{1}{2I_j} L_j^2 = \text{const}. \tag{6.61}$$

On the other hand, if we are interested in the trajectory of vector $\boldsymbol{\omega}$ in an inertial frame (in which vector **L** stays still), we may note that the general relation (15) for the same rotational energy T_{rot} may also be rewritten as

$$T_{\text{rot}} = \frac{1}{2} \sum_{j=1}^{3} \omega_j \sum_{j'=1}^{3} I_{jj'} \omega_{j'}. \tag{6.62}$$

But according to the Eq. (22), the second sum in the right-hand part is nothing more than L_j, so that

$$T_{\text{rot}} = \frac{1}{2} \sum_{j=1}^{3} \omega_j L_j = \frac{1}{2} \boldsymbol{\omega} \cdot \mathbf{L}. \tag{6.63}$$

This equation shows that for a free body (T_{rot} = const, **L** = const), even is vector $\boldsymbol{\omega}$ changes in time, its end point should stay within a plane perpendicular to angular momentum **L**. (Earlier, we have seen that for the particular case of the symmetric top – see Fig. 9b, but for an asymmetric top, the trajectory of the end point may not be circular.)

If we are interested not only in the trajectory of vector $\boldsymbol{\omega}$, but also its explicit evolution in time, it may be calculated using the general Eq. (33) presented in principal components ω_j. For that, we have to recall that Eq. (33) is only valid in an inertial reference frame, while the frame $\{\mathbf{n}_1, \mathbf{n}_2, \mathbf{n}_3\}$ may rotate with the body and hence is generally not inertial. We may handle this problem by applying to vector **L** the general relation (8):

$$\left.\frac{d\mathbf{L}}{dt}\right|_{\text{in lab}} = \left.\frac{d\mathbf{L}}{dt}\right|_{\text{in mov}} + \boldsymbol{\omega} \times \mathbf{L}. \tag{6.64}$$

Combining it with Eq. (33), in the moving frame we get

$$\frac{d\mathbf{L}}{dt} + \boldsymbol{\omega} \times \mathbf{L} = \boldsymbol{\tau}, \tag{6.65}$$

where $\boldsymbol{\tau}$ is the external torque. In particular, for the principal-axis components L_j, related to components ω_j by Eq. (26), Eq. (65) is reduced to a set of three scalar *Euler equations*

Euler equations

$$\boxed{I_j \dot{\omega}_j + (I_{j''} - I_{j'}) \omega_{j'} \omega_{j''} = \tau_j}, \tag{6.66}$$

where the set of indices $\{j, j', j''\}$ has to follow the usual "right" order - e.g., {1, 2, 3}, etc.[10]

[10] These equations are of course valid in the simplest case of the fixed rotation axis as well. For example, if $\boldsymbol{\omega} = \mathbf{n}_z \omega$, i.e. $\omega_x = \omega_y = 0$, Eq. (66) is reduced to Eq. (38).

In order to get a feeling how do the Euler equations work, let us return to the case of a free symmetric top ($\tau_1 = \tau_2 = \tau_3 = 0$, $I_1 = I_2 \neq I_3$). In this case, $I_1 - I_2 = 0$, so that Eq. (66) with $j = 3$ yields $\omega_3 = \text{const}$, while the equations for $j = 1$ and $j = 2$ take the simple form

$$\dot{\omega}_1 = -\Omega_{\text{pre}}\omega_2, \quad \dot{\omega}_2 = \Omega_{\text{pre}}\omega_1, \tag{6.67}$$

where Ω_{pre} is a constant determined by the system parameters and initial conditions:

$$\Omega_{\text{pre}} \equiv \omega_3 \frac{I_3 - I_1}{I_1}. \tag{6.68}$$

Obviously, Eqs. (67) have a sinusoidal solution with frequency Ω_{pre}, and describe uniform rotation of vector $\boldsymbol{\omega}$, with that frequency, about the main axis $\mathbf{n}_3$. This is just another presentation of the torque-free precession analyzed above, this time as observed from the rotating body. Evidently, Ω_{pre} is substantially different from the frequency ω_{pre} (59) of the precession as observed from the lab frame; for example, the former frequency vanishes for the spherical top (with $I_1 = I_2 = I_3$), while the latter frequency tends to the rotation frequency.

Unfortunately, for the rotation of an asymmetric top (i.e., an arbitrary rigid body), when no component ω_j is conserved, the Euler equations (66) are strongly nonlinear even in the absence of the external torque, and a discussion of their solutions would take more time than I can afford.[11]

6.5. Torque-induced precession

The dynamics of rotation becomes even more complex in the presence of external forces. Let us consider the most important and counter-intuitive effect of *torque-induced precession*, for the simplest case of an axially-symmetric body (which is a particular case of the symmetric top, $I_1 = I_2 \neq I_3$) rapidly spinning about his symmetry axis, and supported at some point A of that axis, that does not coincide with the center of mass O – see Fig. 10. Without external forces, such top would retain the direction of its rotation axis that would always coincide with the direction of the angular momentum:

$$\mathbf{L} = I_3\boldsymbol{\omega} = I_3\omega_{\text{rot}}\mathbf{n}_3. \tag{6.69}$$

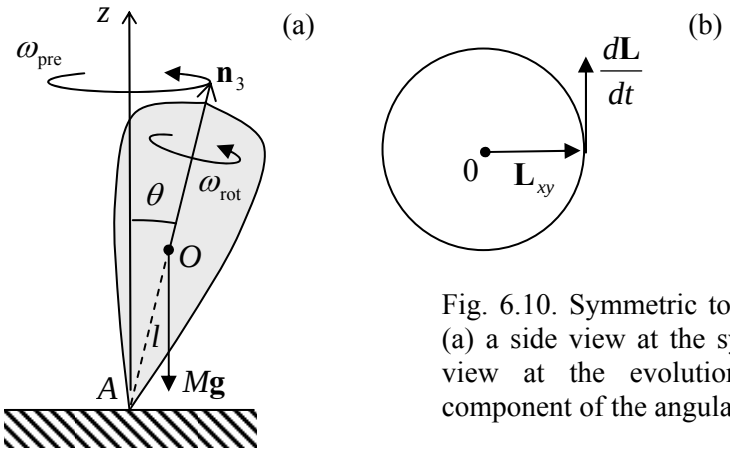

Fig. 6.10. Symmetric top in the gravity field: (a) a side view at the system and (b) the top view at the evolution of the horizontal component of the angular momentum vector.

[11] Such discussion may be found, e.g. in Sec. 37 of L. Landau and E. Lifshitz, *Mechanics*, 3rd ed., Butterworth-Heinemann, 1976.

The uniform gravity field creates bulk-distributed forces that, as we know from the analysis of the physical pendulum in Sec. 3, are equivalent to a single force $M\mathbf{g}$ applied in the center of mass – in Fig. 10, point O. The torque of the force relative to the support point A is

$$\boldsymbol{\tau} = \mathbf{r}_O\big|_{\text{in } A} \times M\mathbf{g} = Ml\mathbf{n}_3 \times \mathbf{g}. \tag{6.70}$$

Hence the general equation (33) of the angular momentum (valid in the inertial "lab" frame, in which point A rests) becomes

Precession: equation

$$\dot{\mathbf{L}} = Ml\mathbf{n}_3 \times \mathbf{g}. \tag{6.71}$$

Despite the apparent simplicity of this (exact!) equation, its analysis is straightforward only in the limit of relatively high rotation velocity ω_{rot} or, alternatively, very small torque. In this limit, we may, in the 0^{th} approximation, still use Eq. (69) for $\mathbf{L}$. Then Eq. (71) shows that vector $\dot{\mathbf{L}}$ is perpendicular to both $\mathbf{n}_3$ (and hence $\mathbf{L}$) and $\mathbf{g}$, i.e. lies within the horizontal plane, and is perpendicular to the horizontal component $\mathbf{L}_{xy}$ of vector $\mathbf{L}$ – see Fig. 10b. Since the magnitude of this vector is constant, $|\dot{\mathbf{L}}| = mgl\sin\theta$, vector $\mathbf{L}$ (and hence the body's main axis) rotates about the vertical axis with angular velocity

Precession: frequency

$$\omega_{\text{pre}} = \frac{|\dot{\mathbf{L}}|}{L_{xy}} = \frac{Mgl\sin\theta}{L\sin\theta} = \frac{Mgl}{L} = \frac{Mgl}{I_3\omega_{\text{rot}}}. \tag{6.72}$$

Thus, very counter-intuitively, the fast-rotating top "does not want to" follow the external, vertical force and, in addition to fast spinning about the symmetry axis $\mathbf{n}_3$, also performs a revolution, called the *torque-induced precession*, about the vertical axis. Note that, similarly to the free-precession frequency (59), the torque-induced precession frequency (72) does not depend on the initial (and sustained) angle θ. However, the torque-induced precession frequency is inversely (rather than directly) proportional to ω, and is typically much lower. This relative slowness is also required for the validity of our simple theory of this effect. Indeed, in our approximate treatment we have used Eq. (69), i.e. neglected precession's contribution to the angular momentum vector $\mathbf{L}$. This is only possible if the contribution is relatively small, $I\omega_{\text{pre}} << I_3\omega_{\text{rot}}$, where I is a certain effective moment of inertia for the precession (to be worked out later). Using our result (72), this condition may be rewritten as

$$\omega_{\text{rot}} >> \left(\frac{MglI}{I_3^2}\right)^{1/2}. \tag{6.73}$$

For a body of not too extreme proportions, i.e. with all linear dimensions of the order of certain length l, all inertia moments are of the order of Ml^2, so that the right-hand part of Eq. (73) is of the order of $(g/l)^{1/2}$, i.e. comparable with the eigenfrequency of the same body as the physical pendulum, i.e. at the absence of fast rotation.

In order to develop a qualitative theory that could take us beyond such approximate treatment, the Euler equations (66) may be used, but are not very convenient. A better approach, suggested by the same L. Euler, is to introduce a set of three independent angles between the principal axes $\{\mathbf{n}_1,\mathbf{n}_2,\mathbf{n}_3\}$ bound to the rigid body, and axes $\{\mathbf{n}_x,\mathbf{n}_y,\mathbf{n}_z\}$ of an inertial reference frame (Fig. 11), and then express the basic equation (33) of rotation, via these angles. There are several possible options for the definition of

such angles;[12] Fig. 11 shows the set of *Euler angels*, most convenient for discussion of fast rotation. As one can see at the figure, the first Euler angle, θ, is the usual polar angle measured from axis $\mathbf{n}_z$ to axis $\mathbf{n}_3$. The second one is the azimuthal angle φ, measured from axis $\mathbf{n}_x$ to the so-called *line of nodes* formed by the intersection of planes $[\mathbf{n}_x,\mathbf{n}_y]$ and $[\mathbf{n}_1,\mathbf{n}_2]$. The last Euler angle, ψ, is measured within plane $[\mathbf{n}_1,\mathbf{n}_2]$, from the line of nodes to axis $\mathbf{n}_1$. In the simple picture of the force-induced precession of a symmetric top, which was derived above, angle θ is constant, angle ψ changes very rapidly, with the rotation velocity ω_{rot}, while angle φ grows with the precession frequency ω_{pre} (72).

Euler angles

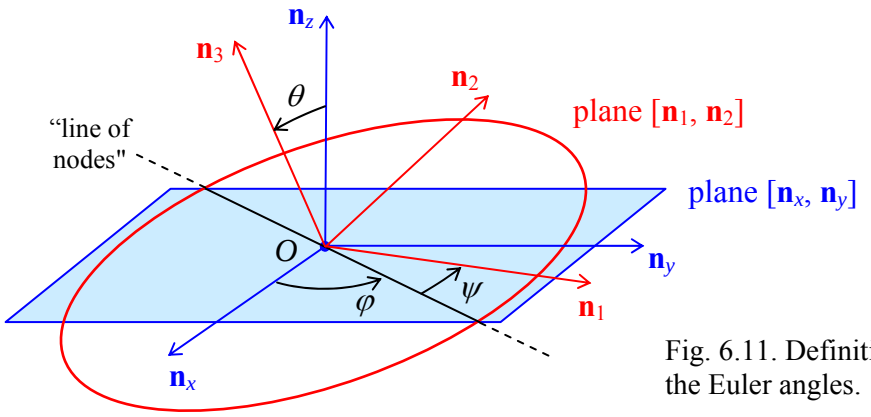

Fig. 6.11. Definition of the Euler angles.

Now we can express the principal-axes components of the instantaneous angular velocity vector, ω_1, ω_2, and ω_3, as measured in the lab reference frame, in terms of the Euler angles. It may be easily done calculating, from Fig. 11, the contributions to the change of Euler angles to each principal axis, and then adding them up. The result is

$$\begin{aligned} \omega_1 &= \dot{\varphi}\sin\theta\sin\psi + \dot{\theta}\cos\psi, \\ \omega_2 &= \dot{\varphi}\sin\theta\cos\psi - \dot{\theta}\sin\psi, \\ \omega_3 &= \dot{\varphi}\cos\theta + \dot{\psi}. \end{aligned} \tag{6.74}$$

Components of ω via Euler angles

These formulas allow the expression of the kinetic energy of rotation (25) and the angular momentum components (26) in terms of the generalized coordinates θ, φ, and ψ, and use then powerful Lagrangian formalism to derive their equations of motion. This is especially simple to do in the case of symmetric tops (with $I_1 = I_2$), because plugging Eqs. (74) into Eq. (25) we get an expression,

$$T_{\text{rot}} = \frac{I_1}{2}\left(\dot{\theta}^2 + \dot{\varphi}^2\sin^2\theta\right) + \frac{I_3}{2}\left(\dot{\varphi}\cos\theta + \dot{\psi}\right)^2, \tag{6.75}$$

which does not include explicitly either φ or ψ. (This reflects the fact that for a symmetric top we can always select axis $\mathbf{n}_1$ to coincide with the line of nodes, and hence take $\psi = 0$ at the considered moment of time. Note that this trick does *not* mean we can take $\dot{\psi} = 0$, because axis $\mathbf{n}_1$, as observed from the inertial reference frame, moves!) Now we should not forget that at the torque-induced precession, the center of mass moves as well (see Fig. 10), so that according to Eq. (14), the total kinetic energy of the body is the sum of two terms,

[12] Of the several choices more convenient in the absence of fast rotation, the most common is the set of so-called *Tait-Brian angles* (called the *yaw*, *pitch*, and *roll*) that are broadly used in airplane and maritime navigation.

$$T = T_{\rm rot} + T_{\rm tran}, \quad T_{\rm tran} = \frac{M}{2}V^2 = \frac{M}{2}l^2\left(\dot\theta^2 + \dot\varphi^2 \sin^2\theta\right), \tag{6.76}$$

while the potential energy is just

$$U = Mgl\cos\theta + \text{const}. \tag{6.77}$$

Now we could readily write the Lagrangian equations of motion for the Euler angles, but it is better to immediately notice that according to Eqs. (75)-(77), the Lagrangian function, $T - U$, does not depend explicitly on "cyclic" coordinates φ and ψ, so that the corresponding generalized momenta are conserved:

$$p_\varphi \equiv \frac{\partial T}{\partial \dot\varphi} = I_A\dot\varphi\sin^2\theta + I_3(\dot\varphi\cos\theta + \dot\psi)\cos\theta = \text{const}, \tag{6.78}$$

$$p_\psi \equiv \frac{\partial T}{\partial \dot\psi} = I_3(\dot\varphi\cos\theta + \dot\psi) = \text{const}, \tag{6.79}$$

where, according to Eq. (29), $I_A \equiv I_1 + Ml^2$ is just the body's moment of inertia for rotation about a horizontal axis passing through the support point *A*. According to the last of Eqs. (74), p_ψ is just L_3, the angular momentum's component along the *rotating* axis $\mathbf{n}_3$. On the other hand, by its definition p_φ is L_z, the same vector $\mathbf{L}$'s component along the *static* axis *z*. (Actually, we could foresee in advance the conservation of both these components of $\mathbf{L}$, because vector (70) of the external torque is perpendicular to both $\mathbf{n}_3$ and $\mathbf{n}_z$.) Using these notions, and solving the simple system of linear equations (78)-(79) for the angle derivatives, we get

$$\dot\varphi = \frac{L_z - L_3\cos\theta}{I_A\sin^2\theta}, \quad \dot\psi = \frac{L_3}{I_3} - \frac{L_z - L_3\cos\theta}{I_A\sin^2\theta}\cos\theta. \tag{6.80}$$

One more conserved quantity in this problem is the full mechanical energy[13]

$$E \equiv T + U = \frac{I_A}{2}\left(\dot\theta^2 + \dot\varphi^2\sin^2\theta\right) + \frac{I_3}{2}\left(\dot\varphi\cos\theta + \dot\psi\right)^2 + Mgl\cos\theta. \tag{6.81}$$

Plugging Eqs. (80) into Eq. (81), we get a first-order differential equation for angle θ, which may be presented in the following physically transparent form:

$$\frac{I_A}{2}\dot\theta^2 + U_{\rm ef}(\theta) = E, \qquad U_{\rm ef}(\theta) \equiv \frac{(L_z - L_3\cos\theta)^2}{2I_A\sin^2\theta} + \frac{L_3^2}{2I_3} + Mgl\cos\theta + \text{const}. \tag{6.82}$$

Thus, similarly to the planetary problems considered in Sec. 3.5, the symmetric top precession has been reduced (without any approximations!) to a 1D problem of motion of one of its degrees of freedom, the polar angle θ, in an effective potential $U_{\rm ef}(\theta)$, which is the sum of the real potential energy U (77) and a contribution from the kinetic energy of motion along two other angles. In the absence of rotation about axes $\mathbf{n}_z$ and $\mathbf{n}_3$ (i.e., $L_z = L_3 = 0$), Eq. (82) is reduced to the first integral of the equation (40) of motion of a physical pendulum. If the rotation is present, then (besides the case of special initial

[13] Indeed, since the Lagrangian does not depend on time explicitly, H = const, and since the full kinetic energy T is a quadratic-homogeneous function of the generalized velocities, $E = H$.

conditions when $\theta(0) = 0$ *and* $L_z = L_3$),[14] the first contribution to $U_{ef}(\theta)$ diverges at $\theta \to 0$ and π, so that the effective potential energy has a minimum at some finite value θ_0 of the polar angle θ.

If the initial angle $\theta(0)$ equals this θ_0, i.e. if the initial effective energy is equal to its minimum value $U_{ef}(\theta_0)$, the polar angle remains constant through the motion: $\theta(t) = \theta_0$. This corresponds to the pure torque-induced precession whose angular velocity is given by the first of Eqs. (80):

$$\omega_{pre} \equiv \dot{\varphi} = \frac{L_z - L_3 \cos\theta_0}{I_A \sin^2\theta_0}. \tag{6.83}$$

The condition for finding θ_0, $dU_{ef}/d\theta = 0$, is a transcendent algebraic equation that cannot be solved analytically for arbitrary parameters. However, in the high spinning speed limit (73), this is possible. Indeed, in this limit the potential energy contribution to U_{ef} is small, and we may analyze its effect by successive approximations. In the 0^{th} approximation, i.e. at $Mgl = 0$, the minimum of U_{ef} is evidently achieved at $\cos\theta_0 = L_z/L_3$, giving zero precession frequency (83). In the next, 1^{st} approximation, we may require that at $\theta = \theta_0$, the derivative of first term in the right-hand part of Eq. (82) for U_{ef} over $\cos\theta$, equal to $-L_z(L_z - L_3\cos\theta)/I_A\sin^2\theta$,[15] is cancelled with that of the gravity-induced term, equal to Mgl. This immediately yields $\omega_{pre} = (L_z - L_3\cos\theta_0)/I_A\sin^2\theta_0 = Mgl/L_3$, so that taking $L_3 = I_3\omega_{rot}$ (as we may in the high spinning speed limit), we recover the simple expression (72).

The second important result that readily follows from Eq. (82) is the exact expression the threshold value of the spinning speed for a vertically rotating top ($\theta = 0$, $L_z = L_3$). Indeed, in the limit $\theta \to 0$ this expression may be readily simplified:

$$U_{ef}(\theta) \approx \text{const} + \left(\frac{L_3^2}{8I_A} - \frac{Mgl}{2}\right)\theta^2. \tag{6.84}$$

This formula shows that if $\omega_3 = L_3/I_3$ (i.e. the angular velocity that was called ω_{rot} in the approximate theory) is higher than the following threshold value,

$$\omega_{th} \equiv 2\left(\frac{MglI_A}{I_3^2}\right)^{1/2}, \tag{6.85}$$

Threshold angular velocity

then the coefficient at θ^2 in Eq. (84) is positive, so that U_{ef} has a stable minimum at $\theta_0 = 0$. On the other hand, if ω_3 is decreased below ω_{th}, the fixed point becomes unstable, so that the top falls down. Note that if we take $I = I_A$ in condition (73) of the approximate treatment, it acquires a very simple sense: $\omega_{rot} >> \omega_{th}$.

Finally, Eqs. (82) give a natural description of one more phenomenon. If the initial energy is larger than $U_{ef}(\theta_0)$, angle θ oscillates between two classical turning points on both sides of the fixed point θ_0. The law and frequency of these oscillations may be found exactly as in Sec. 3.3 – see Eqs. (3.27) and (3.28). At $\omega_3 >> \omega_{th}$, this motion is a fast rotation of the symmetry axis $\mathbf{n}_3$ of the body about its average position performing the slow precession. These oscillations are called *nutations*, but

[14] In that simple case the body continues to rotate about the vertical symmetry axis: $\theta(t) = 0$. Note, however, that such motion is stable only if the spinning speed is sufficiently high – see below.

[15] Indeed, the derivative of the fraction $1/2I_A\sin^2\theta$, taken at the point $\cos\theta = L_z/L_3$, is multiplied by the nominator, $(L_z - L_3\cos\theta)^2$, which at this point vanishes.

physically they are absolutely similar to the free precession that was analyzed in the previous section, and the order of magnitude of their frequency is still given by Eq. (59).

It may be proved that small energy dissipation (not taken into account in our analysis) leads first to a decay of nutations, then to a slower drift of the precession angle θ_0 to zero and, finally, to a gradual decay of the spinning speed ω_3 until it reaches the threshold (85) and the top falls down.

6.6. Non-inertial reference frames

Before moving on to the next chapter, let us use the results of our discussion of rotation kinematics in Sec. 1 to complete the analysis of transfer between two reference frames, started in the introductory Chapter 1 – see Fig. 1.2. Indeed, the differentiation rule described by Eq. (8) and derived for an arbitrary vector **A** enables us to relate not only radius-vectors, but also the velocities and accelerations of a particle as measured in two reference frames: the "lab" frame *O'* (which will be later assumed inertial) and the "moving" (possibly rotating) frame *O* – see Fig. 12.

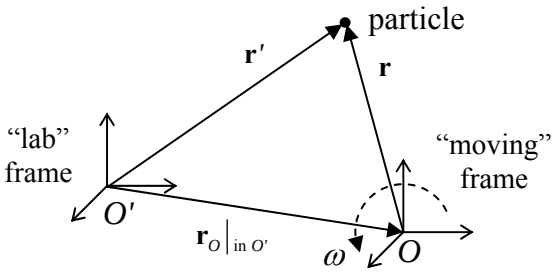

Fig. 6.12. General case of transfer between two reference frames.

As this picture shows, even if frame *O* rotates relative to the lab frame, the radius-vectors are still related, at any moment of time, by the simple Eq. (1.7). In the notation of Fig. 12 it reads

$$\mathbf{r}'\big|_{\text{in lab}} = \mathbf{r}_O\big|_{\text{in lab}} + \mathbf{r}\big|_{\text{in lab}} . \tag{6.86}$$

However, as was discussed in Sec. 1, for velocities the general addition rule is already more complex. In order to find it, let us differentiate Eq. (86) over time:

$$\frac{d}{dt}\mathbf{r}'\big|_{\text{in lab}} = \frac{d}{dt}\mathbf{r}_O\big|_{\text{in lab}} + \frac{d}{dt}\mathbf{r}\big|_{\text{in lab}} . \tag{6.87}$$

The left-hand part of this relation is evidently particle's velocity as measured in the lab frame, and the first term in the right-hand part of Eq. (87) is the velocity of point *O*, as measured in the same frame. The last term is more complex: we need to differentiate vector **r** that connects point *O* with the particle (Fig. 12), considering how its evolution looks from the *lab* frame. Due to the possible mutual rotation of frames *O* and *O'*, that term may not be zero even if the particle does not move relative to frame *O*.

Fortunately, we have already derived the general Eq. (8) to analyze situations exactly like this one. Taking **A** = **r**, we may apply it to the last term of Eq. (87), to get

Transformation of velocity

$$\mathbf{v}\big|_{\text{in lab}} = \mathbf{v}_O\big|_{\text{in lab}} + (\mathbf{v} + \boldsymbol{\omega} \times \mathbf{r}), \tag{6.88}$$

where $\boldsymbol{\omega}$ is the instantaneous angular velocity of an imaginary rigid body connected to the moving reference frame (or we may say, of the frame as such), an $\mathbf{v}$ is $d\mathbf{r}/dt$, as measured in the *moving* frame O, (Here and later in this section, all vectors without indices imply their observation from the moving frame.) Relation (88), on one hand, is a natural generalization of Eq. (10) for $\mathbf{v} \neq 0$; on the other hand, if $\boldsymbol{\omega} = 0$, it is reduced to simple Eq. (1.8) for the translational motion of frame O.

Now, in order to calculate acceleration, me may just repeat the trick: differentiate Eq. (88) over time, and then use Eq. (8) again, now for vector $\mathbf{A} = \mathbf{v} + \boldsymbol{\omega}\times\mathbf{r}$. The result is

$$\mathbf{a}\big|_{\text{in lab}} \equiv \mathbf{a}_O\big|_{\text{in lab}} + \frac{d}{dt}(\mathbf{v} + \boldsymbol{\omega}\times\mathbf{r}) + \boldsymbol{\omega}\times(\mathbf{v} + \boldsymbol{\omega}\times\mathbf{r}). \tag{6.89}$$

Carrying out the differentiation in the second term, we finally get the goal equation,

Transformation of acceleration

$$\boxed{\mathbf{a}\big|_{\text{in lab}} \equiv \mathbf{a}_O\big|_{\text{in lab}} + \mathbf{a} + \dot{\boldsymbol{\omega}}\times\mathbf{r} + 2\boldsymbol{\omega}\times\mathbf{v} + \boldsymbol{\omega}\times(\boldsymbol{\omega}\times\mathbf{r}),} \tag{6.90}$$

where $\mathbf{a}$ is particle's acceleration, as measured in the moving frame. Evidently, Eq. (90) is a natural generalization of the simple Eq. (1.9) to the rotating frame case.

Now let the lab frame O' be inertial; then the 2nd Newton law for a particle of mass m is

$$m\mathbf{a}\big|_{\text{in lab}} = \mathbf{F}, \tag{6.91}$$

where $\mathbf{F}$ is the vector sum of all forces action on the particle. This is simple and clear; however, in many cases it is much more convenient to work in a non-inertial reference frames. For example, describing most phenomena on Earth's surface, in is rather inconvenient to use a reference frame resting on the Sun (or in the galactic center, etc.). In order to understand what we should pay for the convenience of using the moving frame, we may combine Eqs. (90) and (91) to write

2nd Newton law in non-inertial reference frame

$$\boxed{m\mathbf{a} = \mathbf{F} - m\mathbf{a}_O\big|_{\text{in lab}} - m\boldsymbol{\omega}\times(\boldsymbol{\omega}\times\mathbf{r}) - 2m\boldsymbol{\omega}\times\mathbf{v} - m\dot{\boldsymbol{\omega}}\times\mathbf{r}.} \tag{6.92}$$

This result may be interpreted in the following way: if we want to use the 2nd Newton law's analog in a non-inertial reference frame, we have to add, to the real net force $\mathbf{F}$ acting on a particle, four *pseudo-force* terms, called *inertial forces*, all proportional to particle's mass. Let us analyze them, while always remembering that these are just mathematical terms, not real forces. (In particular, it would be futile to seek for the 3rd Newton law's counterpart for an inertial force.)

The first term, $-m\mathbf{a}_O|_{\text{in lab}}$, is the only one not related to rotation, and is well known from the undergraduate mechanics. (Let me hope the reader remembers all these weight-in-the-moving-elevator problems.) Despite its simplicity, this term has subtle and interesting consequences. As an example, let us consider a planet, such as our Earth, orbiting a star and also rotating about its own axis – see Fig. 13. The bulk-distributed gravity forces, acting on a planet from its star, are not quite uniform, because they obey the $1/r^2$ gravity law (1.16a), and hence are equivalent to a single force applied to a point A slightly offset from the planet's center of mass O toward the star. For a spherically-symmetric planet, points O and A would be exactly aligned with the direction toward the star. However, real planets are not absolutely rigid, so that, due to the centrifugal "force" (to be discussed shortly), their rotation about their own axis makes them slightly elliptic – see Fig. 13. (For our Earth, this *equatorial bulge* is about 10 km in each direction.) As a result, the net gravity force does create a small torque relative to the center of mass O. On the other hand, repeating all the arguments of this section for a body (rather than a point), we may see that, in the reference frame moving with the planet, the inertial "force" $-M\mathbf{a}_O$ (which is of

course equal to the total gravity force and directed from the star) is applied exactly to the center of mass and does not create a torque. As a result, this pair of forces creates a torque $\boldsymbol{\tau}$ perpendicular to both the direction toward the star and the vector connecting points *O* and *A*. (In Fig. 13, the torque vector is perpendicular to the plane of drawing). If angle δ between the planet's "polar" axis of rotation and the direction towards the star was fixed, then, as we have seen in the previous section, this torque would induce a slow axis precession about that direction. However, as a result of orbital motion, angle δ oscillates in time much faster (once a year) between values $(\pi/2 + \varepsilon)$ and $(\pi/2 - \varepsilon)$, where ε is the axis tilt, i.e. angle between the polar axis (direction of vectors **L** and $\boldsymbol{\omega}_{\text{rot}}$) and the normal to the *ecliptic plane* of the planet's orbit. (For the Earth, $\varepsilon \approx 23.4°$.) A straightforward averaging over these fast oscillations[16] shows that the torque leads to the polar axis precession about the axis *perpendicular* to the ecliptic plane, keeping angle ε constant. For the Earth, the period, $T_{\text{pre}} = 2\pi/\omega_{\text{pre}}$, of this *precession of the equinoxes* (or "precession of the equator"), corrected to the substantial effect of Moon's gravity, is close to 26,000 years.

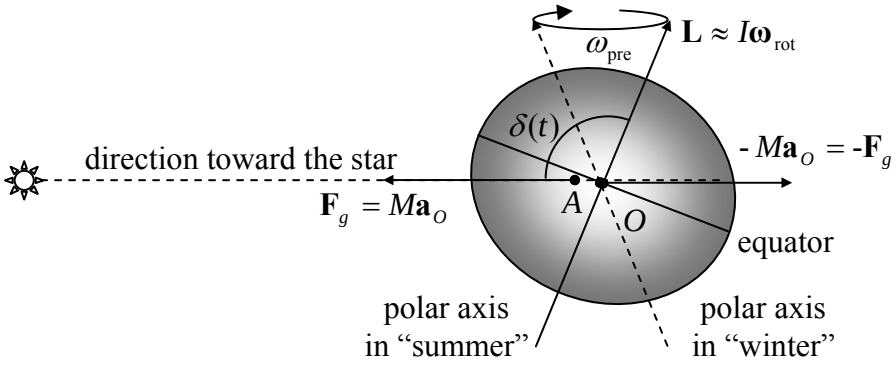

Fig. 6.13. Axial precession of a planet (with the equatorial bulge and the force line offset strongly exaggerated).

Returning to Eq. (92), the direction of the second term of its right-hand part, $\mathbf{F}_c = -m\boldsymbol{\omega}\times(\boldsymbol{\omega}\times\mathbf{r})$, called the *centrifugal force*, is always perpendicular to, and directed out of the instantaneous rotation axis – see Fig. 14.

Centrifugal force

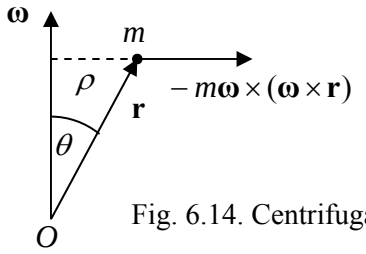

Fig. 6.14. Centrifugal "force".

Indeed, vector $\boldsymbol{\omega}\times\mathbf{r}$ is perpendicular to both $\boldsymbol{\omega}$ and **r** (in Fig. 14, normal to the picture plane and directed from the reader) and has magnitude $\omega r\sin\theta = \omega\rho$, where ρ is the distance of the particle from the rotation axis. Hence the outer vector product, with the account of the minus sign, is normal to the rotation axis $\boldsymbol{\omega}$, directed out from the axis, and equal to $\omega^2 r\sin\theta = \omega^2\rho$. The "centrifugal force" is of

[16] Details of this calculation may be found, e.g., in Sec. 5.8 of the textbook by H. Goldstein, C. Poole, and J. Safko, *Classical Mechanics*, 3rd ed., Addison Wesley, 2002.

course just the result of the fact that the centripetal acceleration $\omega^2\rho$, explicit in the inertial reference frame, disappears in the rotating frame. For a typical location of the Earth ($\rho \sim R_E \approx 6\times10^6$ m), with its angular velocity $\omega_E \approx 10^{-4}$ s^{-1}, the acceleration is rather considerable, of the order of 3 cm/s^2, i.e. ~0.003 g, and is responsible, in particular, for the largest part of the equatorial bulge mentioned above.

As an example of using the centrifugal "force" concept, let us return again to our "testbed" problem on the bead sliding along a rotating ring – see Figs. 1.5 and 2.1. In the non-inertial reference frame attached to the ring, we have to add, to real forces $m\mathbf{g}$ and $\mathbf{N}$ acting on the bead, the horizontal centrifugal "force"[17] directed out of the rotation axis, with magnitude $m\omega^2\rho$. In the notations of Fig. 2.1, its component tangential to the ring equals $m\omega^2\rho\cos\theta = m\omega^2 R\sin\theta\cos\theta$, and hence the Cartesian component of Eq. (92) along this direction is

$$ma = -mg\sin\theta + m\omega^2 R\sin\theta\cos\theta . \qquad (6.93)$$

With $a = R\ddot{\theta}$, this gives us the equation of motion equivalent to Eq. (2.25), which had been derived in Sec. 2.2 (in the inertial frame) using the Lagrangian formalism.

The third term in the right-hand part of Eq. (92) is the so-called *Coriolis force*,[18] which exists only if the particle moves in the rotating reference frame. Its physical sense may be understood by considering a projectile fired horizontally, say from the North Pole. From the point of view of the Earth-based observer, it will a subject of an additional Coriolis force $\mathbf{F}_C = -2m\boldsymbol{\omega}\times\mathbf{v}$, directed westward, with magnitude $2m\omega_E v$, where $\mathbf{v}$ is the main, southward component of the velocity. This force would cause the westward acceleration $a = 2\omega_E v$, and the resulting eastward deviation growing with time as $d = at^2/2 = \omega_E v t^2$ – see Fig. 15. (This formula is exact only if d is much smaller than the distance $r = vt$ passed by the projectile.) On the other hand, from the point of view of the inertial-frame observer, the projectile trajectory in the horizontal plane is a straight line, but during the flight time t, the Earth surface slips eastward from under the trajectory by distance $d = r\varphi = (vt)(\omega_E t) = \omega_E v t^2$ where $\varphi = \omega_E t$ is the azimuthal angle of the Earth rotation during the flight). Thus, both approaches give the same result.

Coriolis force

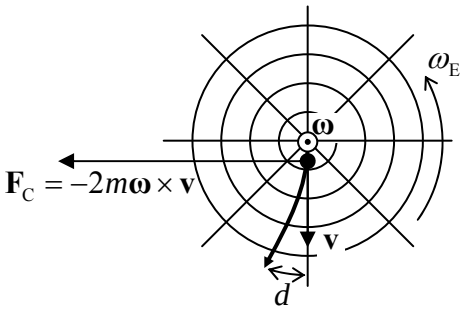

Fig. 6.15. Trajectory of a projectile fired horizontally from the North Pole, from the point of view of an Earth-bound observer looking down. Circles show parallels, straight lines mark meridians.

Hence, the Coriolis "force" is just a fancy (but frequently very convenient) way of description of a purely geometric effect pertinent to rotation, from the point of view of the observer participating in it. This force is responsible, in particular, for the higher right banks of rivers in the Northern hemisphere, regardless of the direction of their flow – see Fig. 16. Despite the smallness of the Coriolis force (for a

[17] For this problem, all other inertial "forces", besides the Coriolis force (see below) vanish, while the latter force is directed perpendicular to the ring and does not affect the bead's motion along it.

[18] Named after G.-G. Coriolis (1792-1843), who is also credited for the first unambiguous definitions of mechanical work and kinetic energy.

typical velocity of the water in a river, $v \sim 1$ m/s, it is equivalent to acceleration $a_C \sim 10^{-2}$ cm/s$^2 \sim 10^{-5}$ g), its multi-century effects may be rather prominent.[19]

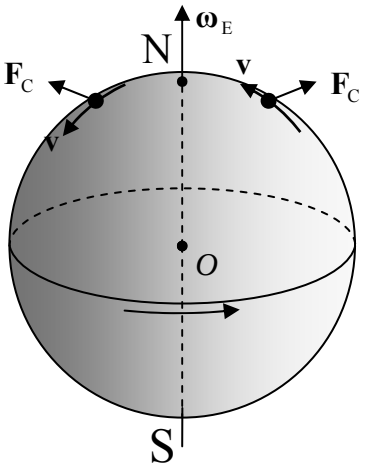

Fig. 6.16. Coriolis "forces" due to Earth's rotation, in the Northern hemisphere.

The last, fourth term of Eq. (92), $-m\dot{\boldsymbol{\omega}}\times\mathbf{r}$, exists only when the rotation frequency changes in time, and may be interpreted as a local-position-specific addition to the first term.

Equation (92), derived above from the Newton equation (91), may be alternatively obtained from the Lagrangian approach, which also gives some important insights on energy at rotation. Let us use Eq. (88) to present the kinetic energy of the particle in an *inertial* frame in terms of **v** and **r** measured in a *rotating* frame:

$$T = \frac{m}{2}\left[\mathbf{v}_O\big|_{\text{in lab}} + (\mathbf{v}+\boldsymbol{\omega}\times\mathbf{r})\right]^2, \tag{6.94}$$

and use this expression to calculate the Lagrangian function. For the relatively simple case of particle motion in the field of potential forces, measured from a reference frame that performs pure rotation (so that $\mathbf{v}_O|_{\text{in lab}} = 0$) with a constant angular velocity $\boldsymbol{\omega}$, the result is

$$L \equiv T - U = \frac{m}{2}v^2 + m\mathbf{v}\cdot(\boldsymbol{\omega}\times\mathbf{r}) + \frac{m}{2}(\boldsymbol{\omega}\times\mathbf{r})^2 - U = \frac{m}{2}v^2 + m\mathbf{v}\cdot(\boldsymbol{\omega}\times\mathbf{r}) - U_{\text{ef}}, \tag{6.95}$$

where the effective potential energy,[20]

$$U_{\text{ef}} \equiv U - \frac{m}{2}(\boldsymbol{\omega}\times\mathbf{r})^2, \tag{6.96}$$

is just the sum of the real potential energy U of the particle and the so-called *centrifugal potential energy* associated with the centrifugal "inertial force":

[19] The same force causes also the counter-clockwise circulation inside our infamous "Nor'easter" storms, in which velocity **v**, caused by lower atmospheric pressure in the middle of the cyclone, is directed toward its center.

[20] Note again the difference between the negative sign before the (always positive) second term, and the positive sign before the similar positive second term in Eq. (3.44). As was already discussed in Chapter 3, this difference hinges on different background physics: in the planetary problem, the angular momentum (and hence its component L_z) is fixed, while the corresponding angular velocity $\dot{\varphi}$ is not. On the opposite, in our current discussion, the angular velocity $\boldsymbol{\omega}$ (of the reference frame) is fixed, i.e. is independent on particle's motion.

$$\mathbf{F}_c \equiv -m\boldsymbol{\omega}\times(\boldsymbol{\omega}\times\mathbf{r}) = -\nabla\left[-\frac{m}{2}(\boldsymbol{\omega}\times\mathbf{r})^2\right]. \tag{6.97}$$

Of course, the Lagrangian equations of motion derived from Eq. (95), considering the Cartesian components of **r** and **v** as generalized coordinates and velocities, coincide with Eq. (92) (with $\mathbf{a}_O|_{\text{in lab}} = \dot{\boldsymbol{\omega}} = 0$, and $\mathbf{F} = -\nabla U$), but it is very informative to have a look at a by-product of this derivation, the generalized momentum corresponding to particle's coordinate **r** as measured in the rotating reference frame,[21]

$$\boldsymbol{p} \equiv \frac{\partial L}{\partial \mathbf{v}} = m(\mathbf{v}+\boldsymbol{\omega}\times\mathbf{r}). \tag{6.98}$$

Canonical momentum at rotation

According to Eq. (88), with $\mathbf{v}_O|_{\text{in lab}} = 0$, the expression in parentheses is just $m\mathbf{v}|_{\text{in lab}}$. However, from the point of view of the moving frame, i.e. not knowing about the physical sense of vector $\boldsymbol{p} = m\mathbf{v}|_{\text{in lab}}$, we would have a reason to speak about two different momenta of the same particle, the so-called *kinetic momentum* $\mathbf{p} = m\mathbf{v}$ and the *canonical momentum* $\boldsymbol{p} = \mathbf{p} + m\boldsymbol{\omega}\times\mathbf{r}$. [22]

Now let us calculate the Hamiltonian function H and energy E as functions of the same moving-frame variables:

$$H \equiv \sum_{j=1}^{3}\frac{\partial L}{\partial v_j}v_j - L = \boldsymbol{p}\cdot\mathbf{v} - L = m\mathbf{v}\cdot(\mathbf{v}+\boldsymbol{\omega}\times\mathbf{r}) - \left[\frac{m}{2}v^2 + m\mathbf{v}\cdot(\boldsymbol{\omega}\times\mathbf{r}) - U_{\text{ef}}\right] = \frac{mv^2}{2} + U_{\text{ef}}, \tag{6.99}$$

$$E \equiv T + U = \frac{m}{2}v^2 + m\mathbf{v}\cdot(\boldsymbol{\omega}\times\mathbf{r}) + \frac{m}{2}(\boldsymbol{\omega}\times\mathbf{r})^2 + U = \frac{m}{2}v^2 + U_{\text{ef}} + m\mathbf{v}\cdot(\boldsymbol{\omega}\times\mathbf{r}) + m(\boldsymbol{\omega}\times\mathbf{r})^2. \tag{6.100}$$

These expressions clearly show that E and H are *not* equal. In hindsight, this is not surprising, because the kinetic energy (94), expressed in the moving-frame variables, includes a term linear in **v,** and hence is not a quadratic-homogeneous function of this generalized velocity. The difference of these functions may be presented as

$$E - H = m\mathbf{v}\cdot(\boldsymbol{\omega}\times\mathbf{r}) + m(\boldsymbol{\omega}\times\mathbf{r})^2 = m(\mathbf{v}+\boldsymbol{\omega}\times\mathbf{r})\cdot(\boldsymbol{\omega}\times\mathbf{r}) = m\mathbf{v}\big|_{\text{in lab}}\cdot(\boldsymbol{\omega}\times\mathbf{r}). \tag{6.101}$$

Now using the operand rotation rule again, we may transform this expression into a even simpler form:[23]

$$E - H = \boldsymbol{\omega}\cdot\left(\mathbf{r}\times m\mathbf{v}\big|_{\text{in lab}}\right) = \boldsymbol{\omega}\cdot(\mathbf{r}\times\boldsymbol{p}) = \boldsymbol{\omega}\cdot\mathbf{L}\big|_{\text{in lab}}. \tag{6.102}$$

E and *H* at rotation

Let us evaluate this difference for our testbed problem – see Fig. 2.1. In this case, vector $\boldsymbol{\omega}$ is aligned with axis z, so that of all Cartesian components of vector **L**, only component L_z is important for the scalar product (102). This component evidently equals $I_z\omega = m\rho^2\omega = m\omega R^2\sin^2\theta$, so that

$$E - H = m\omega^2 R^2\sin^2\theta, \tag{6.103}$$

[21] $\partial L/\partial\mathbf{v}$ is just a shorthand for a vector with Cartesian components $\partial L/\partial v_j$. In a different language, this is the gradient of L in the velocity space.

[22] A very similar situation arises at the motion of a particle with electric charge q in magnetic field **B**. In that case the role of the additional term $\boldsymbol{p} - \mathbf{p} = m\boldsymbol{\omega}\times\mathbf{r}$ is played by product $q\mathbf{A}$, where **A** is the vector-potential of the field ($\mathbf{B} = \nabla\times\mathbf{A}$) – see, e.g., EM Sec. 9.7, and in particular Eqs. (9.183) and (9.192).

[23] Note that by definition (1.36), angular momenta **L** of particles merely add up. As a result, Eq. (102) is valid for an arbitrary system of particles.

i.e. the same result that follows from the direct subtraction of Eqs. (2.40) and (2.41).

The last form of Eq. (99) shows that in the rotating frame, the Hamiltonian function of a particle has a very simple physical sense. It is conserved, and hence may serve as an integral of motion, in many important situations when **L**, and hence E, are not – our testbed problem is again a very good example.

6.7. Exercise problems

6.1. Calculate the principal moments of inertia for the following rigid bodies:

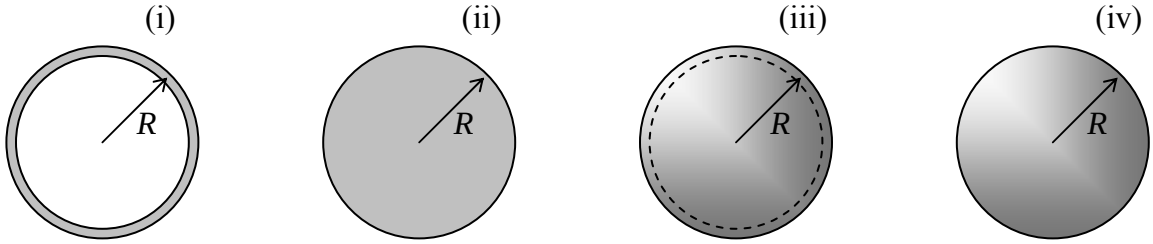

(i) a thin, plane round hoop,
(ii) a flat uniform round disk,
(iii) a thin spherical shell, and
(iv) a uniform solid sphere.

Compare the results assuming that all the bodies have the same radius R and mass M.

6.2. Calculate the principal moments of inertia for the following rigid bodies (see Fig. below):

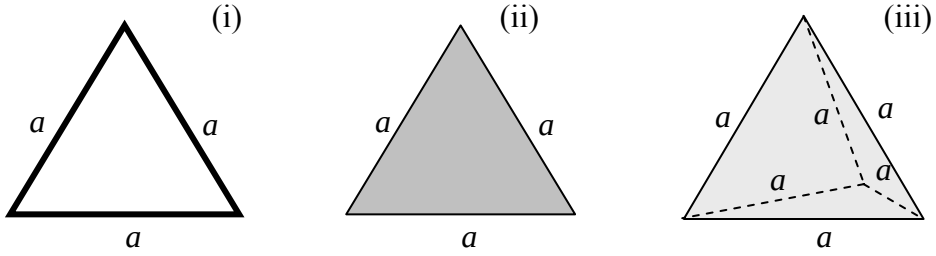

(i) an equilateral triangle made of thin rods with a uniform linear mass density μ,
(ii) a thin plate in the shape of an equilateral triangle, with a uniform areal mass density σ, and
(iii) a tetrahedral pyramid made of a heavy material with a uniform bulk mass density ρ.

Assuming that the total mass of the three bodies is the same, compare the results and give an interpretation of their difference.

6.3. Prove that Eqs. (34)-(36) are valid for rotation about a fixed axis, even if it does not pass through the center of mass, if all distances ρ_z are measured from that axis.

6.4. The end of a uniform, thin, heavy rod of length $2l$ and mass m, initially at rest, is hit by a bullet of mass m', flying with velocity v_0, which gets stuck in the stick - see Fig. on the right. Use two different approaches to calculate the velocity of the opposite end of the rod right after the collision.

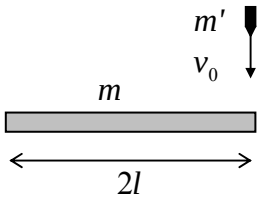

6.5. A uniform ball is placed on a horizontal plane, while rotating with an angular velocity ω_0, but having no initial linear velocity. Calculate the angular velocity after ball's slippage stops, assuming the usual simple approximation of the kinetic friction force: $F_f = \mu N$, where N is a pressure between the surfaces, and μ is a velocity-independent coefficient.

6.6. A body may rotate about fixed horizontal axis A - see Fig. 5. Find the frequency of its small oscillations, in a uniform gravity field, as a function of distance l of the axis from body's center of mass O, and analyze the result.

6.7. A thin uniform bar of mass M and length l is hung on a light thread of length l' (like a "chime" bell – see Fig. on the right). Find:

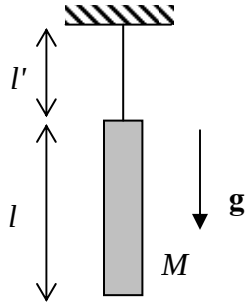

(i) the equations of motion of the system (within the plane of drawing);
(ii) the eigenfrequencies of small oscillations near the equilibrium;
(iii) the distribution coefficients for each oscillation mode.

Sketch the oscillation modes for the particular case $l = l'$.

6.8. A solid, uniform, round cylinder of mass M can roll, without slipping, over a concave, round cylindrical surface of a block of mass M', in a uniform gravity field – see Fig. on the right. The block can slide without friction on a horizontal surface. Using the Lagrangian formalism,

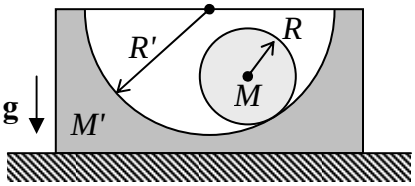

(i) find the frequency of small oscillations of the system near the equilibrium, and
(ii) sketch the oscillation mode for the particular case $M' = M$, $R' = 2R$.

6.9. A uniform solid hemisphere of radius R is placed on a horizontal plane – see Fig. on the right. Find the frequency of its small oscillations within a vertical plane, for two ultimate cases:

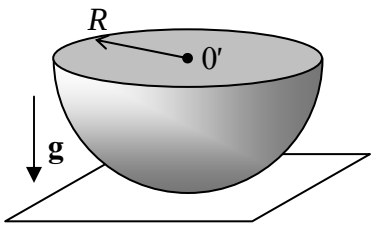

(i) there is no *friction* between the hemisphere and plane surfaces, and
(ii) the static friction is so strong that there is no *slippage* between these surfaces.

6.10. For the "sliding ladder" problem started in Sec. 3 (see Fig. 7), find the critical value α_c of angle α at which the ladder loses contact with the vertical wall, assuming that it starts sliding from the vertical position with a negligible initial velocity.

6.11.* A rigid, straight, uniform rod of length l, with the lower end on a pivot, falls in a uniform gravity field – see Fig. on the right. Neglecting friction, calculate the distribution of the bending torque τ along its length, and analyze the result.

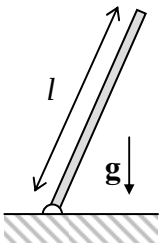

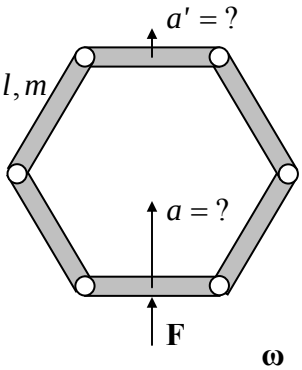

6.12. Six similar, uniform rods of length l and mass m are connected by light joints so that they may rotate, without friction, versus each other, forming a planar polygon. Initially, the polygon was at rest, and had the correct hexagon shape - see Fig. on the right. Suddenly, an external force **F** is applied to the middle of one rod, in the direction of hexagon's symmetry center. Calculate the accelerations: of the rod to which the force is applied (a), and of the opposite rod (a'), immediately after the application of the force.

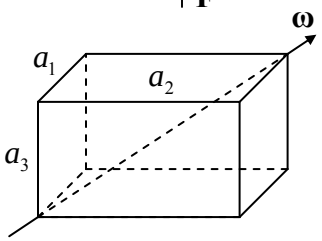

6.13. A rectangular cuboid (parallelepiped) with sides a_1, a_2, and a_3, made of a material with constant density ρ, is rotated, with a constant angular velocity ω, about one of its space diagonals – see Fig. on the right. Calculate the torque τ necessary to sustain such rotation.

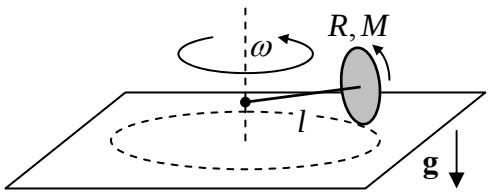

6.14. One end of a light shaft of length l is firmly attached to the center of a uniform solid disk of radius $R << l$ and mass M, whole plane is perpendicular to the shaft. Another end of the shaft is attached to a vertical axis (see Fig. on the right) so that the shaft may rotate about the axis without friction. The disk rolls, without slippage, over a horizontal surface, so that the whole system rotates about the vertical axis with a constant angular velocity ω. Calculate the (vertical) supporting force exerted on the disk by the surface.

6.15. An air-filled balloon is placed inside a container filled with water that moves in space, in a negligible gravity field. Suddenly, force **F** is applied to the container, pointing in a certain direction. What direction would the balloon move relative to the container?

6.16. Calculate the height of solar tides on a large ocean, using the following simplifying assumptions: the tide period (½ of Earth's day) is much longer than the period of all ocean waves, the Earth (of mass M_E) is a sphere of radius R_E, and its distance r_S from the Sun (of mass M_S) is constant and much larger than R_E.

6.17.* A satellite is on a circular orbit, of radius R, around the Earth.

(i) Write the equations of motion of a small body as observed from the satellite, and simplify them for the case when body's motion is limited to a close vicinity of the satellite.

(ii) Use the equations to prove that at negligible external forces (in particular, negligible gravitational attraction to the satellite) the body may be placed on an elliptical trajectory around satellite's center of mass, within its plane of rotation about Earth. Calculate the ellipse's orientation and eccentricity.

6.18.* A non-spherical shape of an artificial satellite may ensure its stable angular orientation relative to Earth's surface, advantageous for many practical goals. Modeling the satellite as a strongly elongated, axially-symmetric body, moving around the Earth on a circular orbit of radius R, find its

stable orientation, and analyze possible small oscillations of the satellite's symmetry axis around this equilibrium position.

6.19. A coin of radius or radius r is rolled, with velocity V, on a horizontal surface without slippage. What should be coin's tilt angle θ (see Fig. on the right) for it to roll on a circle of radius $R >> r$? Modeling the coin as a very thin, uniform disk, and assuming that angle θ is small, solve this problem in:

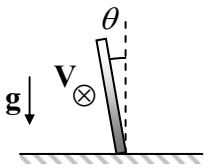

6.20. Two planets are on the circular orbit around their common center of mass. Calculate the effective potential energy of a much lighter mass (say, a spaceship) rotating with the same angular velocity, on the line connecting the planets. Sketch the plot of function the radial dependence of U_{ef} and find out the number of so-called *Lagrange points* is which the potential energy has local maxima. Calculate their position approximately in the limit when one of the planets is much more massive than the other one.

6.21. A small body is dropped down to the surface of Earth from height $h << R_E$, without initial velocity. Calculate the magnitude and direction of its deviation from the vertical, due to the Earth rotation. Estimate the effect's magnitude for a body dropped from the Empire State Building.

6.22. Use Eq. (94) to calculate the generalized momentum and derive the Lagrange equation of motion of a particle, considering L a function of $\mathbf{r}$ and $\mathbf{v}$ as measured in a non-inertial but non-rotating reference frame.

Chapter 7. Deformations and Elasticity

The objective of this chapter is a brief discussion of small deformations of 3D continuous media, with a focus on elastic properties of solids. The reader will see that deformation of solids is nontrivial even in the absence of motion, so that several key problems of statics will need to be discussed before proceeding to such dynamic phenomena as elastic waves in infinite media and thin rods.

7.1. Strain

Rigid bodies discussed in the previous chapter are just a particular case of *continuous media.* As has already been mentioned, these are systems of particles so close to each other that the system discreteness may be neglected, so that the particle displacement **q** may be considered as a continuous function of space and time. The subject of this chapter is small deviations from the rigid-body approximation discussed in Chapter 6, i.e. small *deformations*. The deformation smallness allows one to consider the displacement vector **q** as a function of the initial (pre-deformation) position of the particle **r**, and time t – just as was done in the Secs. 5.3-5.5 for 1D waves.

The first task of the deformation theory is to exclude from consideration the types of motion considered in Chapter 6, namely the translation and rotation unrelated to deformations. This means, first of all, the variables describing deformations should not depend on the part of displacement **q** that does not depend on position **r** (i.e. is common for the whole media), because that part corresponds to a translational shift rather than to a deformation (Fig. 1a). Moreover, even certain non-uniform displacements do not contribute to deformation. For example, Eq. (6.7) (with $d\mathbf{r}$ replaced with $d\mathbf{q}$ to comply with our current notation) shows that a small displacement of the type

$$d\mathbf{q}|_{\text{rotation}} = d\boldsymbol{\varphi}\times\mathbf{r}, \tag{7.1}$$

where $d\boldsymbol{\varphi} = \boldsymbol{\omega}dt$ is an infinitesimal vector common for the whole continuum, corresponds to its rotation about the direction of that vector, and has nothing to do with the body deformation (Fig. 1b).

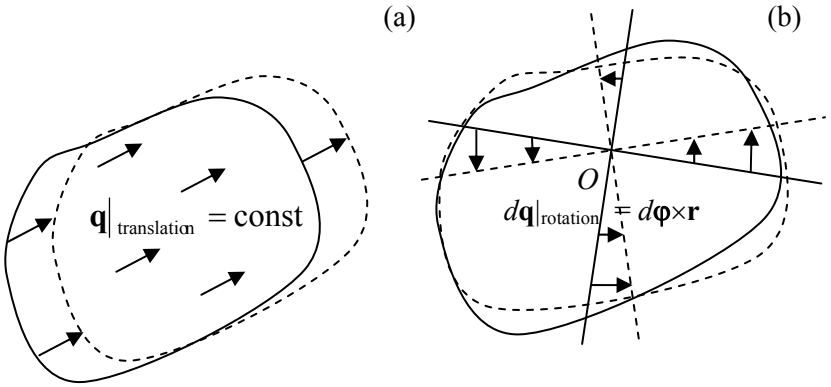

Fig. 7.1. Two types of displacement vector distributions that are unrelated to deformation: (a) translation and (b) rotation.

This is why in order to develop an adequate quantitative characterization of deformation, we should start with finding suitable appropriate functions of the spatial distribution of displacements, $\mathbf{q}(\mathbf{r})$, that exist only due to deformations. One of such measures is the change of distance $dl = |d\mathbf{r}|$ between two close points:

$$(dl)^2\big|_{\text{after deformation}} - (dl)^2\big|_{\text{before deformation}} = \sum_{j=1}^{3}(dr_j + dq_j)^2 - \sum_{j=1}^{3}(dr_j)^2 \ , \tag{7.2}$$

where dq_j is the j^{th} Cartesian component of the difference $d\mathbf{q}$ between the displacements $\mathbf{q}$ of the two points. If the deformation is small in the sense $|d\mathbf{q}| << |d\mathbf{r}| = dl$, we may keep in Eq. (2) only the terms proportional to the first power of the infinitesimal vector $d\mathbf{q}$:

$$(dl)^2\big|_{\text{after deformation}} - (dl)^2\big|_{\text{before deformation}} = \sum_{j=1}^{3}\left[2dr_j dq_j + (dq_j)^2\right] \approx 2\sum_{j=1}^{3} dr_j dq_j \ . \tag{7.3}$$

Since q_j is a function of 3 independent scalar arguments r_j, its differential may be presented as

$$dq_j = \sum_{j'=1}^{3} \frac{\partial q_j}{\partial r_{j'}} dr_{j'}. \tag{7.4}$$

Coefficients $\partial q_j/\partial r_{j'}$ may be considered as elements of a tensor[1] providing a linear relation between vectors d$\mathbf{r}$ and d$\mathbf{q}$. Plugging Eq. (4) into Eq. (2), we get

$$(dl)^2\big|_{\text{after deformation}} - (dl)^2\big|_{\text{before deformation}} = 2\sum_{j,j'=1}^{3} \frac{\partial q_j}{\partial r_{j'}} dr_j dr_{j'} \ . \tag{7.5}$$

A convenience of tensor $\partial q_j/\partial r_{j'}$ for characterizing deformations is that it automatically excludes the translation displacement (Fig. 1a) that is independent of r_j. Its drawback is that its particular components are still affected by the rotation of the body (though the sum (5) is not). Indeed, according to the vector product definition, Eq. (1) may be presented in Cartesian coordinates as

$$dq_j\big|_{\text{rotation}} = \left(d\varphi_{j'} r_{j''} - d\varphi_{j''} r_{j'}\right)\varepsilon_{jj'j''}, \tag{7.6}$$

where $\varepsilon_{jj'j''}$ is the *Levi-Civita symbol*[2] equal to (+1) if all indices j, j', and j'' are different and run in a "right" order - {1, 2, 3}, etc., and (-1) otherwise, so that for any order of non-equal indices, $\varepsilon_{jj'j''} = -\varepsilon_{j'jj''}$. Differentiating Eq. (6) over a particular Cartesian coordinate of vector $\mathbf{r}$, and taking into account that this partial differentiation (∂) is independent of (and hence may be swapped with) the differentiation (d) over the rotation angle φ, we get the amounts,

$$d\left(\frac{\partial q_j}{\partial r_{j'}}\right)_{\text{rotation}} = -\varepsilon_{jj'j''} d\varphi_{j''} \ , \quad d\left(\frac{\partial q_{j'}}{\partial r_j}\right)_{\text{rotation}} = -\varepsilon_{j'jj''} d\varphi_{j''} = \varepsilon_{jj'j''} d\varphi_{j''}, \tag{7.7}$$

which may differ from 0. However, notice that the *sum* of these two differentials equals zero for any $d\boldsymbol{\varphi}$, which is possible only if

$$\left(\frac{\partial q_{j'}}{\partial r_j} + \frac{\partial q_j}{\partial r_{j'}}\right)_{\text{rotation}} = 0, \quad \text{for } j \neq j', \tag{7.8}$$

[1] Since both $d\mathbf{q}$ and $d\mathbf{r}$ are legitimate physical vectors (whose Cartesian components are properly transformed as the transfer between reference frames), the 3×3 matrix with elements $\partial q_j/\partial r_{j'}$ is indeed a legitimate physical tensor – see the discussion in Sec. 6.2.

[2] See, e.g., MA Eq. (13.2).

so that the full sum (5), that includes 3 such partial sums, is not affected by rotation – as we already know. This is why it is convenient to rewrite Eq. (5) in a mathematically equivalent form

$$(dl)^2\big|_{\text{after deformation}} - (dl)^2\big|_{\text{before deformation}} = 2\sum_{j,j'=1}^{3} s_{jj'}dr_j dr_{j'}, \tag{7.9a}$$

where $s_{jj'}$ are the elements of the so-called *symmetrized strain tensor* defined as

Strain tensor

$$s_{jj'} \equiv \frac{1}{2}\left(\frac{\partial q_j}{\partial r_{j'}} + \frac{\partial q_{j'}}{\partial r_j}\right). \tag{7.9b}$$

(Note that this modification does not affect the diagonal elements: $s_{jj} = \partial q_j/\partial r_j$.). The advantage of symmetrized tensor (9b) over the initial tensor $\partial q_j/\partial r_{j'}$ is that according to Eq. (8), at pure rotation all elements of the symmetrized strain tensor vanish.

Now let us discuss the physical meaning of this tensor. At was already mentioned in Sec. 6.2, any symmetric tensor may be diagonalized by an appropriate selection of the reference frame axes. In such principal axes, $s_{jj'} = s_{jj}\delta_{jj'}$, so that Eq. (4) takes the simple form

$$dq_j = \frac{\partial q_j}{\partial r_j} dr_j = s_{jj} dr_j. \tag{7.10}$$

We may use this expression to calculate the change of each side of an infinitesimal cuboid (parallelepiped) with sides dq_j parallel to the principal axes:

$$dr_j\big|_{\text{after deformation}} - dr_j\big|_{\text{before deformation}} \equiv dq_j = s_{jj} dr_j\ , \tag{7.11}$$

and of cuboid's volume $dV = dr_1 dr_2 dr_3$:

$$dV\big|_{\text{after deformation}} - dV\Big|_{\text{before deformation}} = \prod_{j=1}^{3}(dr_j + s_{jj}dr_j) - \prod_{j=1}^{3} dr_j = dV\left[\prod_{j=1}^{3}(1+s_{jj}) - 1\right], \tag{7.12}$$

Since all our analysis is only valid in the linear approximation in small $s_{jj'}$, Eq. (12) is reduced to

$$dV\big|_{\text{after deformation}} - dV\big|_{\text{before deformation}} \approx dV\sum_{j=1}^{3} s_{jj} \equiv dV\,\mathrm{Tr}(\mathrm{s}), \tag{7.13}$$

where Tr (*trace*)[3] of any matrix (in particular, tensor) is the sum of its diagonal elements; in our case[4]

$$\mathrm{Tr}\,(\mathrm{s}) \equiv \sum_{j=1}^{3} s_{jj}\ . \tag{7.14}$$

So, the diagonal components of the tensor characterize medium's compression/extension; then what is the meaning of the off-diagonal components of the tensor? It may be illustrated on the simplest example of a purely *shear deformation*, shown in Fig. 2 (the geometry is assumed to be uniform along axis z). In this case, all displacements (assumed small) have just one Cartesian component, in Fig. 2

[3] The traditional European notation for Tr is Sp (from German *Spur* meaning "trace" or "track").
[4] Actually, the tensor theory shows that the trace does not depend on the particular choice of the coordinate axes.

along axis x: $\mathbf{q} = \mathbf{n}_x \alpha y$ (with $\alpha << 1$), so that the only nonvanishing component of the initial strain tensor $\partial q_j/\partial r_{j'}$ is $\partial q_x/\partial y = \alpha$, and the symmetrized tensor (9b) is

$$s = \begin{pmatrix} 0 & \alpha/2 & 0 \\ \alpha/2 & 0 & 0 \\ 0 & 0 & 0 \end{pmatrix}. \tag{7.15}$$

Evidently, the change (13) of volume vanishes in this case. Thus, off-diagonal elements of tensor s characterize shear deformations.

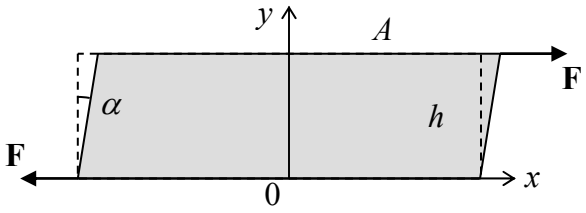

Fig. 7.2. Example of a pure shear.

To conclude this section, let me note that Eq. (9) is only valid in Cartesian coordinates. For the solution of some important problems, especially those with a spherical or axial symmetry, it is frequently convenient to express six different components of the symmetric strain tensor via three components of the displacement vector **q** in either spherical or cylindrical coordinates. A straightforward differentiation, using the definition of such coordinates,[5] yields, in particular, the following formulas for the diagonal elements of the tensor in the local mutually orthogonal coordinates that are directed along unit vectors – either $\{\mathbf{n}_r, \mathbf{n}_\theta, \mathbf{n}_\varphi\}$ or $\{\mathbf{n}_\rho, \mathbf{n}_\varphi, \mathbf{n}_z\}$ - at the given point:

(i) in the spherical coordinates:

$$s_{rr} = \frac{\partial q_r}{\partial r}, \quad s_{\theta\theta} = \frac{q_r}{r} + \frac{1}{r}\frac{\partial q_\theta}{\partial \theta}, \quad s_{\varphi\varphi} = \frac{q_r}{r} + \frac{q_\theta}{r}\frac{\cos\theta}{\sin\theta} + \frac{1}{r\sin\theta}\frac{\partial q_\varphi}{\partial \varphi}; \tag{7.16}$$

(ii) in the cylindrical coordinates:

$$s_{\rho\rho} = \frac{\partial q_\rho}{\partial \rho}, \quad s_{\varphi\varphi} = \frac{q_\rho}{\rho} + \frac{1}{\rho}\frac{\partial q_\varphi}{\partial \varphi}, \quad s_{zz} = \frac{\partial q_z}{\partial z}. \tag{7.17}$$

These expressions, that will be used below for solution of some problems for symmetrical geometries, may be a bit counter-intuitive. Indeed, Eq. (16) shows that even for a purely radial, spherically-symmetric deformation, $\mathbf{q} = \mathbf{n}_r q(r)$, diagonal angular components of strain do not vanish: $s_{\theta\theta} = s_{\varphi\varphi} = q/r$. (According to Eq. (17), in cylindrical coordinates, the same effect is exhibited by the only angular component of the tensor.) Note, however, that these relations describe a very simple geometric effect: the change of the lateral distance $rd\gamma << r$ between two close points with the same distance r from a central point, at a small change of r that keeps the angle $d\gamma$ between their radius-vectors **r** constant.

[5] See, e.g., MA Eqs. (10.1) and (10.7).

7.2. Stress

Now let us discuss the forces that cause deformations. Internal forces acting inside (i.e. between arbitrarily defined parts of) a continuous media may be also characterized by a tensor. This *stress tensor,*[6] with elements $\sigma_{jj'}$, relates components of the elementary vector $d\mathbf{F}$ of the force acting on an elementary area dA of an (possibly, imaginary) interface between two parts of a continuous media with elementary vector $d\mathbf{A} = \mathbf{n}dA$ normal to the area (Fig. 3):

Stress tensor

$$dF_j = \sum_{j'=1}^{3} \sigma_{jj'} dA_{j'} . \qquad (7.18)$$

The usual sign convention here is to take the outer normal $d\mathbf{n}$, i.e. to direct $d\mathbf{A}$ out of "our" part of the continuum, i.e. the part on which the calculated force $d\mathbf{F}$ is exerted.

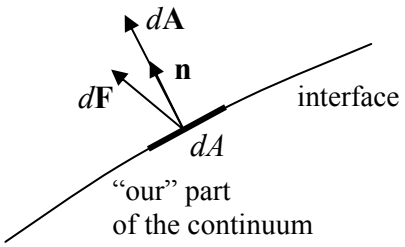

Fig. 7.3. Definition of vectors $d\mathbf{A}$ and $d\mathbf{F}$.

In some cases the stress tensor's structure is very simple. For example, as will be discussed in detail in the next chapter, static or frictionless fluids may only provide a force normal to any surface and usually directed toward "our" part of the body, so that

Pressure

$$d\mathbf{F} = -P d\mathbf{A}, \quad \text{i.e.}\ \sigma_{jj'} = -P\delta_{jj'}, \qquad (7.19)$$

where scalar P (in most cases positive) is called *pressure*, and generally depends on both the spatial position and time. This type of stress, with $P > 0$, is frequently called the *hydrostatic compression* - even if it takes place in solids.

However, in the general case the stress tensor also has off-diagonal terms, which characterize shear stress. For example, if the shear strain shown in Fig. 2 is caused by a pair of forces $\pm\mathbf{F}$, they create internal forces $F_x\mathbf{n}_x$, with $F_x > 0$ if we speak about the force acting upon a part of the sample below the imaginary horizontal interface we are discussing. In order to avoid horizontal acceleration of each horizontal slice of the sample, the forces should not depend on y, i.e. $F_x = \text{const} = F$. Superficially, it may look that this is the only nonvanishing component of the stress tensor is $dF_x/dA_y = F/A = \text{const}$, so that tensor is asymmetric, in contrast to the strain tensor (15) of the same system. Note, however, that the pair of forces $\pm\mathbf{F}$ creates not only the shear stress, but also a nonvanishing rotating torque $\boldsymbol{\tau} = -Fh\mathbf{n}_z = -(dF_x/dA_y)Ah\mathbf{n}_z = -(dF_x/dA_y)V\mathbf{n}_z$, where $V = Ah$ is sample's volume. So, if we want to perform a static stress experiment, i.e. avoid sample's rotation, we need to apply some other forces, e.g., a pair of vertical forces creating an equal and opposite torque $\boldsymbol{\tau}' = (dF_y/dA_x)V\mathbf{n}_z$, implying that $dF_y/dA_x = dF_x/dA_y = F/A$. As a result, the stress tensor becomes symmetric, and similar in structure to the symmetrized strain tensor (15):

[6] It is frequently called the *Cauchy stress tensor*, partly to honor A.-L. Cauchy (1789-1857) who introduced it, and partly to distinguish it from and other possible definitions of the stress tensor, including the 1st and 2nd *Piola-Kirchhoff tensors*. (For the infinitesimal deformations discussed in this course, all these notions coincide.)

$$\sigma = \begin{pmatrix} 0 & F_0/A & 0 \\ F_0/A & 0 & 0 \\ 0 & 0 & 0 \end{pmatrix}. \tag{7.20}$$

In many situations, the body may be stressed not only by forces applied to their surfaces, but also by some volume-distributed (*bulk*) forces $d\mathbf{F} = \mathbf{f}dV$, whose certain effective *bulk density* $\mathbf{f}$. (The most evident example of such forces is gravity. If its field is uniform as described by Eq. (1.16b), then $\mathbf{f} = \rho\mathbf{g}$, where ρ is the mass density.) Let us derive the key formula describing the correct summation of the surface and bulk forces. For that, consider again an infinitesimal cuboid with sides dr_j parallel to the corresponding coordinates axes (Fig. 4) - now not necessarily the principal axes of the stress tensor.

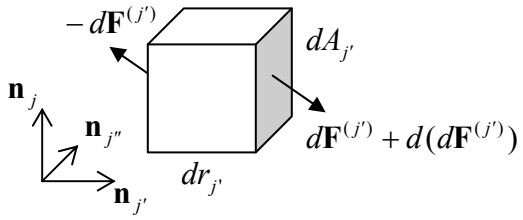

Fig. 7.4. Deriving Eq. (23).

If elements $\sigma_{jj'}$ of the tensor do not depend on position, the force $d\mathbf{F}^{(j')}$ acting on *j'*-th face of the cuboid is exactly balanced by the equal and opposite force acting on the opposite face, because vectors $d\mathbf{A}^{(j')}$ of these faces are equal and opposite. However, if $\sigma_{jj'}$ is a function of $\mathbf{r}$, then the net force $d(d\mathbf{F}^{(j')})$ does not vanish. Using the expression for to the *j'* th contribution to sum (18), in the first order in $d\mathbf{r}$, the j^{th} components of this vector is

$$d(dF_j^{(j')}) = d\left(\sigma_{jj'}dA_{j'}\right) = \frac{\partial\sigma_{jj'}}{\partial r_{j'}}dr_{j'}dA_{j'} = \frac{\partial\sigma_{jj'}}{\partial r_{j'}}dV, \tag{7.21}$$

where cuboid's volume $dV = dr_{j'}dA_{j'}$ does not depend on *j'*. The addition these force components for all three pairs of cuboid faces, i.e. the summation of Eqs. (21) for all 3 values of the upper index *j'*, yields the following relation for the j^{th} component of the net force exerted on the cuboid:

$$d(dF_j) = \sum_{j'=1}^{3} d(dF_j^{(j')}) = \sum_{j'=1}^{3} \frac{\partial\sigma_{jj'}}{\partial r_{j'}}dV \ . \tag{7.22}$$

Since any volume may be broken into such infinitesimal cuboids, Eq. (22) shows that the space-varying stress is equivalent to a volume-distributed force $d\mathbf{F}_{\text{ef}} = \mathbf{f}_{\text{ef}}dV$, whose *effective* (not real!) bulk density $\mathbf{f}_{\text{ef}}$ has the following Cartesian components

$$\left(f_{\text{ef}}\right)_j = \sum_{j'=1}^{3} \frac{\partial\sigma_{jj'}}{\partial r_{j'}}, \tag{7.23}$$

so that in the presence of genuinely bulk forces $d\mathbf{F} = \mathbf{f}dV$, densities $\mathbf{f}_{\text{ef}}$ and $\mathbf{f}$ just add up.

Let us use this addition rule to spell out the 2nd Newton law for a unit volume of a continuous medium:

$$\rho \frac{\partial^2 \mathbf{q}}{\partial t^2} = \mathbf{f}_{\text{ef}} + \mathbf{f}. \tag{7.24}$$

Using Eq. (23), the j^{th} Cartesian component of Eq. (24) may be presented as

Medium dynamics equation

$$\rho \frac{\partial^2 q_j}{\partial t^2} = \sum_{j'=1}^{3} \frac{\partial \sigma_{jj'}}{\partial r_{j'}} + f_j. \tag{7.25}$$

This is the key equation of medium's dynamics, which will be repeatedly used below.

For solution of some problems, it is also convenient to have a general expression for work δW of the stress forces at a virtual deformation $\delta\mathbf{q}$ - understood in the same variational sense as the virtual displacement $\delta\mathbf{r}$ in Sec. 2.1. Using the equivalence between the stress forces and the effective bulk forces with density $\mathbf{f}_{\text{ef}}$, for any volume V of the media we may write

$$\delta W = \int_V \mathbf{f}_{\text{ef}} \cdot \delta\mathbf{q} dV = \sum_{j=1}^{3} \int_V (f_{\text{ef}})_j \delta q_j dV = \sum_{j,j'=1}^{3} \int_V \frac{\partial \sigma_{jj'}}{\partial r_{j'}} \delta q_j d^3 r. \tag{7.28}$$

Let us take this integral by parts for a volume so large that deformations δq_j on its surface are negligible. Then, swapping the operations of variations and spatial differentiation (just like it was done with the time derivative in Sec. 2.1), we get

$$\delta W = -\sum_{j,j'=1}^{3} \int_V \sigma_{jj'} \delta \frac{\partial q_j}{\partial r_{j'}} d^3 r. \tag{7.29}$$

Assuming that tensor $\sigma_{jj'}$ is symmetric, we may rewrite this expression as

$$\delta W = -\frac{1}{2} \sum_{j,j'=1}^{3} \int_V \left(\sigma_{jj'} \delta \frac{\partial q_j}{\partial r_{j'}} + \sigma_{j'j} \delta \frac{\partial q_j}{\partial r_{j'}} \right) d^3 r. \tag{7.30}$$

Now, swapping indices j and j' in the second expression, we finally get

$$\delta W = -\frac{1}{2} \sum_{j,j'=1}^{3} \int_V \delta \left(\frac{\partial q_j}{\partial r_{j'}} \sigma_{jj'} + \frac{\partial q_{j'}}{\partial r_j} \sigma_{jj'} \right) d^3 r = -\sum_{j,j'=1}^{3} \int_V \sigma_{jj'} \delta s_{jj'} d^3 r, \tag{7.31}$$

where $s_{jj'}$ are the components of strain tensor (9b). It is natural to rewrite this important formula as

Work of stress forces

$$\delta W = \int_V \delta w(\mathbf{r}) d^3 r, \quad \text{where } \delta w(\mathbf{r}) \equiv -\sum_{j,j'=1}^{3} \sigma_{jj'} \delta s_{j'j}, \tag{7.32}$$

and interpret the locally-defined scalar function $\delta w(\mathbf{r})$ as the work of stress forces per unit volume, due to the small variation of the deformation.

7.3. Hooke's law

In order to form a complete system of equations describing media dynamics, one needs to complement Eq. (25) with an appropriate *material equation* describing the relation between the stress tensor $\sigma_{jj'}$ and the deformation $\mathbf{q}$ described (in the small deformation limit) by the strain tensor $s_{jj'}$. This

relation depends on the medium, and generally may be rather complex. Even leaving alone various anisotropic solids (e.g., crystals) and macroscopically-inhomogeneous materials (like ceramics or sand), strain typically depends not only on the current value of stress (possibly in a nonlinear way), but also on the previous history of stress application. Indeed, if strain exceeds a certain *plasticity threshold*, atoms (or nanocrystals) may slip to their new positions and never come back even if the strain is reduced. As a result, deformations become irreversible – see Fig. 5.

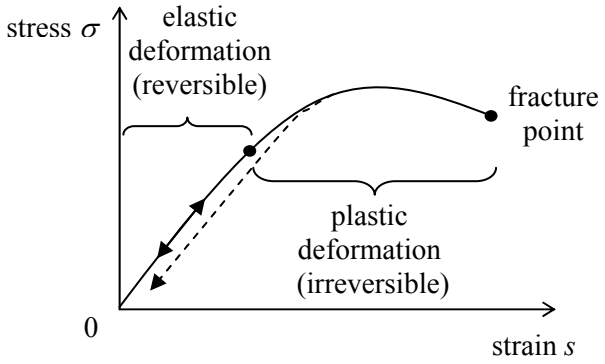

Fig. 7.5. Typical relation between stress and strain in solids (schematically).

Only below the thresholds of nonlinearity and plasticity (which are typically close to each other), strain is nearly proportional to stress, i.e. obeys the famous *Hooke's law*.[7] However, even in this *elastic range* the law is not quite simple, and even for an isotropic medium is described not by one but by two constants, called *elastic moduli*. The reason for that is that most elastic materials resist the strain accompanied by the volume change (say, the hydrostatic compression) differently from how they resist the shear deformation. In order to describe this difference, let us first present the symmetrized strain tensor (9b) in the mathematically equivalent form

$$s_{jj'} = \left(s_{jj'} - \frac{1}{3}\delta_{jj'}\mathrm{Tr}\,(\mathrm{s}) \right) + \left(\frac{1}{3}\delta_{jj'}\mathrm{Tr}\,(\mathrm{s}) \right). \tag{7.33}$$

According to Eq. (13), the *traceless tensor* in the first parentheses of Eq. (33) does not give any contribution to the volume change, e.g., may be used to characterize purely shear deformation, while the second one describes the hydrostatic compression alone. Hence we may expect that the stress tensor may be presented (again, in the elastic deformation range only!) as

$$\sigma_{jj'} = 2\mu\left(s_{jj'} - \frac{1}{3}\mathrm{Tr}\,(\mathrm{s})\delta_{jj'} \right) + 3K\left(\frac{1}{3}\mathrm{Tr}\,(\mathrm{s})\delta_{jj'} \right), \tag{7.34}$$

Hooke's law

where K and μ are some constants.[8] Indeed, experiments show that Hooke's law in this form is followed, at small strain, by all isotropic elastic materials. In accordance with the above discussion, constant μ (in some texts, denoted as G) is called the *shear modulus*, while constant K (sometimes called B), the *bulk modulus*. Two columns of Table 1 below show the approximate values of these moduli for typical representatives of several major classes of materials.[9]

[7] Named after R. Hooke (1635-1703) who was first to describe the law in its simplest, 1D version.

[8] The inclusion of coefficients 2 and 3 into Eq. (34) is justified by the simplicity of some of its corollaries – see, e.g., Eqs. (38) and (43) below.

[9] Since the strain tensor elements, defined by Eq. (5), are dimensionless, while the strain defined by Eq. (18) has the dimensionality of pressure (force by unit area), so do the elastic moduli K and μ.

To better appreciate these values, let us first discuss the physical meaning of K and μ, using two simple examples of elastic deformation. For that it is convenient first to solve the set of 9 (or rather 6 different) linear equations (34) for $s_{jj'}$. This is easy to do, due to the simple structure of these equations: they relate components $\sigma_{jj'}$ and $s_{jj'}$ with the same indices, besides the involvement of the tensor trace. This slight complication may be readily overcome by noticing that according to Eq. (34),

$$\mathrm{Tr}(\sigma) \equiv \sum_{j=1}^{3} \sigma_{jj} = 3K\,\mathrm{Tr}(s), \quad \text{i.e.} \quad \mathrm{Tr}(s) = \frac{1}{3K}\mathrm{Tr}(\sigma). \tag{7.35}$$

Plugging this result into Eq. (34) and solving it for $s_{jj'}$, we readily get the reciprocal relation, which may be presented in a similar form:

$$s_{jj'} = \frac{1}{2\mu}\left(\sigma_{jj'} - \frac{1}{3}\mathrm{Tr}(\sigma)\delta_{jj'}\right) + \frac{1}{3K}\left(\frac{1}{3}\mathrm{Tr}(\sigma)\delta_{jj'}\right). \tag{7.36}$$

Table 7.1. Elastic moduli, density, and sound velocities of a few representative materials (approximate values)

Material	K (GPa)	μ (GPa)	E (GPa)	σ	ρ (kg/m^3)	v_l (m/s)	v_t (m/s)
Diamond[(a)]	600	450	1,100	0.20	3,500	1,830	1,200
Hardened steel	170	75	200	0.30	7,800	5,870	3,180
Water[(b)]	2.1	0	0	0.5	1,000	1,480	0
Air[(b)]	0.00010	0	0	0.5	1.2	332	0

[(a)] Averages over crystallographic directions (~10% anisotropy).
[(b)] At the so-called *ambient conditions* (T = 20°C, P = 1 bar ≡ 10^{-5} Pa).

Now let us apply Hooke's law, in the form of Eqs. (34) or (36), to two simple situations in which the strain and stress tensors may be found without formulating the exact differential equations of the elasticity theory and boundary conditions for them. (That will be the subject of the next section.) The first experiment is the hydrostatic compression when the stress tensor is diagonal, and all its diagonal components are equal – see Eq. (19).[10] For this case Eq. (36) yields

$$s_{jj'} = -\frac{P}{3K}\delta_{jj'}, \tag{7.37}$$

which means that regardless of the shear modulus, the strain tensor is also diagonal, with all diagonal components equal. According to Eqs. (11) and (13), this means that all linear dimensions of the body are reduced by a similar fraction, so that its shape is preserved, while the volume is reduced by

[10] It may be proved that such situation may be implemented not only in a fluid with pressure P, but also by placing a solid sample of an *arbitrary* shape into a compressed fluid.

$$\frac{\Delta V}{V} = \sum_{j=1}^{3} s_{jj} = -\frac{P}{K}. \tag{7.38}$$

This equation clearly shows the physical sense of the bulk modulus K as the *reciprocal compressibility*.

As Table 1 shows, the values of K may be dramatically different for various materials, and that even for such "soft stuff" as water this modulus in actually rather high. For example, even at the bottom of the deepest, 10-km ocean well ($P \approx 10^3$ bar ≈ 0.1 GPa), water density increases by just about 5%. As a result, in most human-scale experiments, water may be treated as *incompressible* – a condition that will be widely used in the next chapter. Many solids are even much less compressible – see the first two rows of Table 1.

The most compressible media are gases. For a gas, certain background pressure P is necessary just for containing it within certain volume V, so that Eq. (38) is only valid for small increments of pressure, ΔP:

$$\frac{\Delta V}{V} = -\frac{\Delta P}{K}. \tag{7.39}$$

Moreover, gas compression also depends on thermodynamic conditions. (For most condensed media, the temperature effects are very small.) For example, at ambient conditions most gases are reasonably well described by the equation of state for the model called the *ideal classical gas*:

$$PV = Nk_{\rm B}T, \quad \text{i.e.}\, P = \frac{Nk_{\rm B}T}{V}. \tag{7.40}$$

where N is the number of molecules in volume V, and $k_{\rm B} \approx 1.38\times10^{-23}$ J/K is the Boltzmann constant.[11] For a small volume change ΔV at constant temperature, this equation gives

$$\Delta P\big|_{T=\text{const}} = -\frac{Nk_B T}{V^2}\Delta V = -\frac{P}{V}\Delta V, \quad \text{i.e.}\, \frac{\Delta V}{V}\Big|_{T=\text{const}} = -\frac{\Delta P}{P}. \tag{7.41}$$

Comparing this expression with Eq. (37), we get a remarkably simple result for the isothermal compression of gases,

$$K\big|_{T=\text{const}} = P, \tag{7.42}$$

which means in particular that the bulk modulus listed in Table 1 is actually valid, at the ambient conditions, for almost any gas. Note, however, that the change of thermodynamic conditions (say, from isothermal to adiabatic[12]) may affect gas' compressibility.

Now let us consider the second, rather different, fundamental experiment: a pure shear deformation shown in Fig. 2. Since the traces of matrices (15) and (20), which describe this experiment, are equal to 0, for their off-diagonal elements Eq. (34) gives simply $\sigma_{jj'} = 2\mu s_{jj'}$, so that the deformation angle α (see Fig. 2) is just

$$\alpha = \frac{1}{\mu}\frac{F}{A}. \tag{7.43}$$

[11] For the derivation and detailed discussion of Eq. (40) see, e.g., SM Sec. 3.1

[12] See, e.g., SM Sec. 1.3.

Notice that the angle does not depend on thickness h of the sample, though of course the maximal linear deformation $q_x = \alpha h$ is proportional to the thickness. Naturally, as Table 1 shows, for all fluids (liquids and gases) $\mu = 0$, because they cannot resist static shear stress.

However, not all experiments, even the apparently simple ones, involve just either K or μ. Let us consider stretching a long elastic rod of a small and uniform cross-section of area A – the so-called *tensile stress experiment* shown in Fig. 6.[13]

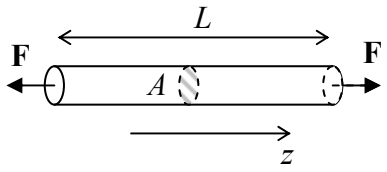

Fig. 7.6. Tensile stress experiment.

Though the deformation of the rod near its clamped ends depends on the exact way forces **F** are applied (we will discuss this issue later on), we may expect that over most of its length the tension forces are directed virtually along the rod, $d\mathbf{F} = F_z\mathbf{n}_z$, and hence, with the coordinate choice shown in Fig. 6, $\sigma_{xj} = \sigma_{yj} = 0$ for all j, including the diagonal elements σ_{xx} and σ_{yy}. Moreover, due to the open lateral surfaces, on which, evidently, $dF_x = dF_y = 0$, there cannot be an internal stress force of *any* direction, acting on any elementary internal boundary parallel to these surfaces. This means that $\sigma_{zx} = \sigma_{zy} = 0$. So, of all components of the stress tensor only one, σ_{zz}, is not equal to zero, and for a uniform sample, $\sigma_{zz} = \text{const} = F/A$. For this case, Eq. (36) shows that the strain tensor is also diagonal, but with different diagonal elements:

$$s_{zz} = \left(\frac{1}{9K} + \frac{1}{3\mu}\right)\sigma_{zz}, \tag{7.44}$$

$$s_{xx} = s_{yy} = \left(\frac{1}{9K} - \frac{1}{6\mu}\right)\sigma_{zz}. \tag{7.45}$$

Since the tensile stress is most common in engineering (and physical experiment) practice, both combinations of the elastic moduli participating in these two relations have deserved their own names. In particular, the constant in Eq. (44) is usually denoted as $1/E$ (but in many texts, as $1/Y$), where E is called the *Young's modulus*:

Young's modulus

$$\frac{1}{E} \equiv \frac{1}{9K} + \frac{1}{3\mu}, \quad \text{i.e. } E \equiv \frac{9K\mu}{3K+\mu}. \tag{7.46}$$

As Fig. 6 shows, in the tensile stress geometry $s_{zz} \equiv \partial q_z/\partial z = \Delta L/L$, so that the Young's modulus scales the linear relation between the relative extension of the rod and the force applied per unit area:[14]

$$\frac{\Delta L}{L} = \frac{1}{E}\frac{F}{A}. \tag{7.47}$$

[13] Though the analysis of compression in this situation gives similar results, in practical experiments a strong compression may lead to the loss of horizontal stability – the so-called *buckling* - of the rod.

[14] According to Eq. (47), E may be thought of as the force per unit area, which would double sample's length, if only our theory was valid for deformations that large.

The third column of Table 1 shows the values of this modulus for two well-known solids: diamond (with the highest known value of E of all bulk materials[15]) and the steel (physically, a solid solution of ~10% of carbon in iron) used in construction. Again, for fluids the Young's modulus vanishes - as it follows from Eq. (46) with $\mu = 0$.

I am confident that the reader of these notes has been familiar with Eq. (44), in the form of Eq. (47), from his or her undergraduate studies. However, most probably this cannot be said about its counterpart, Eq. (45), which shows that at the tensile stress, rod's cross-section dimension also change. This effect is usually characterized by the following dimensionless *Poisson's ratio*:[16]

$$-\frac{s_{xx}}{s_{zz}} = -\frac{s_{yy}}{s_{zz}} = -\left(\frac{1}{9K} - \frac{1}{6\mu}\right)\Big/\left(\frac{1}{9K} + \frac{1}{3\mu}\right) = \frac{1}{2}\frac{3K - 2\mu}{3K + \mu} \equiv \sigma, \tag{7.48}$$

Poisson ratio

According to this formula, for realistic materials with $K > 0$, $\mu \geq 0$, values of σ may vary from (-1) to (+½) , but for the vast majority of materials,[17] they are between 0 and ½ - see Table 1. The lower limit is reached in porous materials like cork whose *lateral dimensions* almost do not change at the tensile stress. Some soft materials like rubber present the opposite case: $\sigma \approx$ ½. Since according to Eqs. (13), (44) and (45), the volume change is

$$\frac{\Delta V}{V} = s_{xx} + s_{yy} + s_{zz} = \frac{1}{E}\frac{F}{A}(1 - 2\sigma), \tag{7.49}$$

such materials virtually do not change their *volume* at the tensile stress. The ultimate limit of this trend, $\Delta V/V = 0$, is provided by fluids and gases, because their Poisson ratio σ is exactly equal to ½. (This follows from Eq. (48) with $\mu = 0$.) However, for most practicable construction materials such as steel (see Table 1) the change (49) of volume is as high as ~40% of that of the length.

Due to the clear physical sense of coefficients E and σ, they are frequently used as a pair of independent elastic moduli, instead of K and μ. Solving Eqs. (46) and (48) for K and μ, we get

$$K = \frac{E}{3(1 - 2\sigma)}, \quad \mu = \frac{E}{2(1 + \sigma)}. \tag{7.50}$$

Using these formulas, the two (equivalent) formulations of Hooke's law, expressed by Eqs. (34) and (36), may be rewritten as

$$\sigma_{jj'} = \frac{E}{1 + \sigma}\left(s_{jj'} + \frac{\sigma}{1 - 2\sigma}\mathrm{Tr}\,(s)\delta_{jj'}\right), \tag{7.51a}$$

$$s_{jj'} = \frac{1 + \sigma}{E}\left(\sigma_{jj'} - \frac{\sigma}{1 + \sigma}\mathrm{Tr}\,(\sigma)\delta_{jj'}\right). \tag{7.51b}$$

Hooke's law with E and σ

[15] It is probably somewhat higher (up to 2,000 GPa) in such nanostructures as carbon nanotubes and monoatomic sheets (*graphene*), though there is still a substantial uncertainty in experimental values of elastic moduli of these structures – see, e.g., C. Lee *et al*, *Science* **321**, 5887 (2008) and J.-U. Lee *et al.*, *Nano Lett*. **12**, 4444 (2012).

[16] Unfortunately, the dominating tradition is to use for the Poisson ratio the same letter (σ) as for the stress tensor components, but they may be always distinguished by the presence or absence of component indices.

[17] The only known exceptions are certain exotic media with very specific internal microstructure – see, e.g., R. Lakes, *Science* **235**, 1038 (1987) and references therein.

The linear relation between the strain and stress tensor allows one to calculate the potential energy U of an elastic medium due to its elastic deformation. Indeed, to each infinitesimal part of this strain increase, we may apply Eq. (32), with the work δW of the surface forces equal to $-\delta U$. Let us slowly increase the deformation from a completely unstrained state (in which we may take $U = 0$) to a certain strained state, in the absence of bulk forces $\mathbf{f}$, keeping the deformation type, i.e. the relation between the elements of the stress tensor intact. In this case, all elements of tensor $\sigma_{jj'}$ are proportional to the same single parameter characterizing the stress (say, the total applied force), and according to Hooke's law, all elements of tensor $s_{j'j}$ are proportional to that parameter as well. In this case, integration over the variation yields the final value[18]

Elastic deformation energy

$$U = \int_V u(\mathbf{r}) d^3 r, \quad u(\mathbf{r}) = \frac{1}{2} \sum_{j,j'=1}^{3} \sigma_{jj'} s_{j'j} \ . \tag{7.52}$$

Evidently, $u(\mathbf{r})$ may be interpreted as the volume density of the potential energy of the elastic deformation.

7.4. Equilibrium

Now we are fully equipped to discuss dynamics of elastic deformations, but let us start with statics. The static (equilibrium) state may be described by requiring the right-hand part of Eq. (25) to vanish. In order to find the elastic deformation, we need to plug $\sigma_{jj'}$ from the Hooke's law (51a), and then express elements $s_{jj'}$ via the displacement distribution – see Eq. (9). For a uniform material, the result is[19]

$$\frac{E}{2(1+\sigma)} \sum_{j'=1}^{3} \frac{\partial^2 q_j}{\partial r_{j'}^2} + \frac{E}{2(1+\sigma)(1-2\sigma)} \sum_{j'=1}^{3} \frac{\partial^2 q_{j'}}{\partial r_j \partial r_{j'}} + f_j = 0. \tag{7.53}$$

Taking into account that the first sum in Eq. (53) is just the j^{th} component of $\nabla^2 \mathbf{q}$, while the second sum is the j^{th} component of $\nabla(\nabla \cdot \mathbf{q})$, we see that all three equations (53) for three Cartesian components (j = 1, 2 and 3) of the deformation vector $\mathbf{q}$, may be conveniently merged into one vector equation

$$\frac{E}{2(1+\sigma)} \nabla^2 \mathbf{q} + \frac{E}{2(1+\sigma)(1-2\sigma)} \nabla(\nabla \cdot \mathbf{q}) + \mathbf{f} = 0. \tag{7.54}$$

Equation of elastic equilibrium

For some applications, it is more convenient to recast this equation to another form, using vector identity[20] $\nabla^2 \mathbf{q} = \nabla(\nabla \cdot \mathbf{q}) - \nabla \times (\nabla \times \mathbf{q})$. The result is

$$\frac{E(1-\sigma)}{(1+\sigma)(1-2\sigma)} \nabla(\nabla \cdot \mathbf{q}) - \frac{E}{2(1+\sigma)} \nabla \times (\nabla \times \mathbf{q}) + \mathbf{f} = 0. \tag{7.55}$$

It is interesting that in problems without volume-distributed forces ($\mathbf{f} = 0$), the Young's modulus E cancels! Even more fascinating, in this case the equation may be re-written in a form not involving the

[18] For clarity, let me reproduce a similar integration for the 1D motion of a particle on a spring. In this case, $\delta U = -\delta W = -F\delta x$, and if spring's force is elastic, $F = -\kappa x$, the integration yields $U = \kappa x^2/2 = Fx/2$.

[19] As follows from Eqs. (50), the coefficient before the first sum in Eq. (53) is just the shear modulus μ, while that before the second sum is equal to $(K + \mu/3)$.

[20] See, e.g., MA Eq. (11.3).

Poisson ratio σ either. Indeed, acting by operator ∇ on the remaining terms of Eq. (55), we get a surprisingly simple equation

$$\nabla^2(\nabla\cdot\mathbf{q})=0. \tag{7.56}$$

A natural question here is how do the elastic moduli affect the deformation distribution if they do not participate in the differential equation describing it. The answer is two-fold. If what is fixed at the body boundary are deformations, then the moduli are irrelevant, because the deformation distribution through the body does not depend on them. On the other hand, if the boundary conditions fix stress (or a combination of stress and strain), then the elastic constants creep into the solution via the recalculation of these conditions into the strain.

As a simple but representative example, let us find the deformation distribution in a (generally, thick) spherical shell under the effect of different pressures fixed inside and outside it (Fig. 7a).

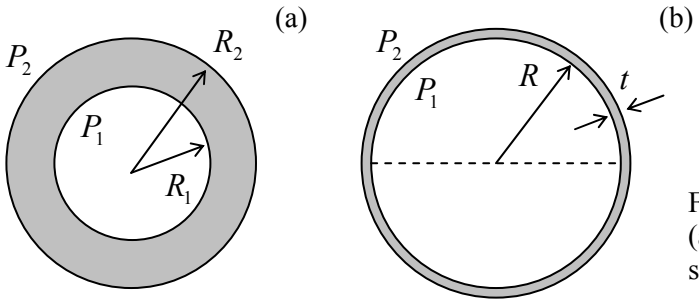

Fig. 7.7. Spherical shell problem: (a) the general case and (b) the thin shell limit.

Due to the spherical symmetry of the problem, the deformation is obviously spherically-symmetric and radial, $\mathbf{q} = q(r)\mathbf{n}_r$, i.e. is completely described by one scalar function $q(r)$. Since the curl of such a radial vector field is zero,[21] Eq. (55) is reduced to

$$\nabla(\nabla\cdot\mathbf{q})=0, \tag{7.57}$$

This equation means that the divergence of function $q(r)$ is constant within the shell. In spherical coordinates this means[22]

$$\frac{1}{r^2}\frac{d}{dr}\left(r^2 q\right)=\text{const}. \tag{7.58}$$

Naming this constant $3a$ (with the numerical factor chosen for later notation convenience), and integrating Eq. (58), we get its solution,

$$q(r)=ar+\frac{b}{r^2}, \tag{7.59}$$

that also includes another integration constant b.

To complete the analysis, we have to determine constants a and b from the boundary conditions. According to Eq. (19),

[21] If this is not immediately evident, have a look at MA Eq. (10.11) with $\mathbf{f} = f_r(r)\mathbf{n}_r$.
[22] See, e.g., MA Eq. (10.10) with $\mathbf{f} = q(r)\mathbf{n}_r$

$$\sigma_{rr} = \begin{cases} -P_1, & r = R_1, \\ -P_2, & r = R_2. \end{cases} \tag{7.60}$$

In order to relate this stress to strain, let us use Hooke's law, but for that, we first need to calculate the strain tensor components for the deformation distribution (59). Using Eqs. (16), we get

$$s_{rr} = \frac{\partial q}{\partial r} = a - 2\frac{b}{r^3}, \quad s_{\theta\theta} = s_{\varphi\varphi} = \frac{q}{r} = a + \frac{b}{r^3}, \tag{7.61}$$

so that Tr (s) = 3a. Plugging these relations into Eq. (51a) for σ_{rr}, we get

$$\sigma_{rr} = \frac{E}{1+\sigma}\left[\left(a - 2\frac{b}{r^3}\right) + \frac{\sigma}{1-2\sigma}3a\right]. \tag{7.62}$$

Now plugging this relation into Eqs. (60), we get a system of two linear equations for coefficients a and b. Solving this system, we get:

$$a = \frac{1-2\sigma}{E}\frac{P_1R_1^3 - P_2R_2^3}{R_2^3 - R_1^3}, \quad b = \frac{1+\sigma}{2E}\frac{(P_1 - P_2)R_1^3R_2^3}{R_2^3 - R_1^3}. \tag{7.63}$$

Formulas (59) and (63) give a complete solution of our problem. It is rich in contents and deserves at least some analysis. First of all, note that according to Eq. (50), coefficient (1 - 2σ)/E in the expression for a is just 1/3K, so that the first term in Eq. (59) for deformation is just the hydrostatic compression. In particular, the second of Eqs. (63) shows that if $R_1 = 0$, then $b = 0$. Thus for a solid sphere we have only the hydrostatic compression that was discussed in the previous section. Perhaps less intuitively, making two pressures equal gives the same result (hydrostatic compression) for arbitrary $R_2 > R_1$.

However, in the general case $b \neq 0$, so that the second term in the deformation distribution (59), which describes the shear deformation,[23] is also substantial. In particular, let us consider the important thin-shell limit $R_2 - R_1 \equiv t \ll R_{1,2} \equiv R$ - see Fig. 7b. In this case, $q(R_1) \approx q(R_2)$ is just the change of the shell radius R, for which Eqs. (59) and (63) (with $R_2^3 - R_1^3 \approx 3R^2t$) give

$$\Delta R \equiv q(R) \approx aR + \frac{b}{R^2} \approx \frac{(P_1 - P_2)R^2}{3t}\left(\frac{1-2\sigma}{E} + \frac{1+\sigma}{2E}\right) = (P_1 - P_2)\frac{R^2}{t}\frac{1-\sigma}{2E}. \tag{7.64}$$

Naively, one could think that at least in this limit the problem could be analyzed by elementary means. For example, the total force exerted by the pressure difference (P_1 - P_2) on the diametrical cross-section of the shell (see, e.g., the dashed line in Fig. 7b) is $F = \pi R^2(P_1 - P_2)$, giving the stress,

$$\sigma = \frac{F}{A} = \frac{\pi R^2(P_1 - P_2)}{2\pi Rt} = (P_1 - P_2)\frac{R}{2t}, \tag{7.65}$$

directed along shell's walls. One can check that this simple formula may be indeed obtained, in this limit, from the strict expressions for $\sigma_{\theta\theta}$ and $\sigma_{\varphi\varphi}$, following from the general treatment carried out above. However, if we try now to continue this approach by using the simple relation (47) to find the small change Rs_{zz} of sphere's radius, we would arrive at a result with the structure of Eq. (64), but

[23] Indeed, according to Eq. (50), the material-dependent factor in the second of Eqs. (63) is just 1/4μ.

without factor $(1 - \sigma) < 1$ in the nominator. The reason for this error (which may be as significant as ~30% for typical construction materials – see Table 1) is that Eq. (47), while being valid for thin *rods* of arbitrary cross-section, is invalid for thin *broad sheets*, and in particular the thin shell in our problem. Indeed, while at the tensile stress both lateral dimensions of a thin rod may contract freely, in our problem all dimensions of the shell are under stress – actually, under much more tangential stress than the radial one.[24]

7.5. Rod bending

The general approach to the static deformation analysis, outlined in the beginning of previous section, may be simplified not only for symmetric geometries, but also for the uniform thin structures such as thin plates ("membranes" or "sheets") and thin rods. Due to the shortage of time, in this course I will demonstrate typical approaches to such systems only on the example of thin rods. (The theory of membrane deformation is very much similar.) Besides the tensile stress analyzed in Sec. 3, two other major deformations of rods are *bending* and *torsion*. Let us start from a "local" analysis of bending caused by a pair of equal and opposite external torques $\boldsymbol{\tau} = \pm \mathbf{n}_y \tau_y$ perpendicular to the rod axis z (Fig. 8), assuming that the rod is "quasi-uniform", i.e. that on the scale of this analysis (comparable with linear scale a of the cross-section) its material parameters and cross-section A do not change substantially.

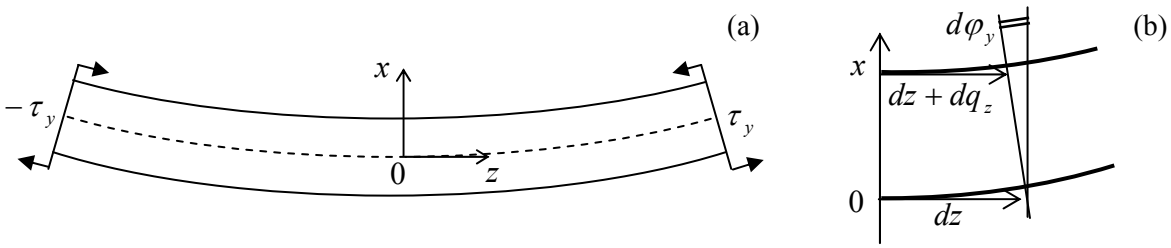

Fig. 7.8. This rod bending, in a local reference frame (specific for each cross-section).

Just as in the tensile stress experiment (Fig. 6), at bending the components of the stress forces $d\mathbf{F}$, normal to the rod length, have to equal zero on the surface of the rod. Repeating the arguments made for the tensile stress discussion, we arrive at the conclusion that only one diagonal component of the tensor (in Fig. 8, σ_{zz}) may differ from zero:

$$\sigma_{jj'} = \delta_{jz}\sigma_{zz}. \tag{7.66}$$

However, in contrast to the tensile stress, at pure static bending the net force along the rod has to vanish:

$$F_z = \int_A \sigma_{zz} d^2 r = 0, \tag{7.67}$$

so that σ_{zz} has to change sign at some point of axis x (in Fig. 8, selected to lay in the plane of the bent rod). Thus, the bending deformation may be viewed as a combination of stretching some layers of the rod (bottom layers in Fig. 8) with compression of other (top) layers.

Since it is hard to find more about the stress distribution from these general considerations, let us turn over to strain, assuming that the rod's cross-section is virtually constant on the length of the order

[24] Strictly speaking, this is only true if the pressure difference is not too small, namely, if $|P_1 - P_2| >> P_{1,2}t/R$.

of its cross-section size. From the above presentation of bending as a combination of stretching and compression, it evident that the longitudinal deformation q_z has to vanish along some *neutral line* on the rod's cross-section - in Fig. 8, represented by the dashed line.[25] Selecting the origin of coordinate x on this line, and expanding the relative deformation in the Taylor series in x, due to the cross-section smallness, we may limit ourselves to the linear term:

$$s_{zz} \equiv \frac{dq_z}{dz} = -\frac{x}{R}. \tag{7.68}$$

Here constant R has the sense of the *curvature radius* of the bent rod. Indeed, on a small segment dz the cross-section turns by a small angle $d\varphi_y = -dq_z/x$ (Fig. 8b). Using Eq. (68), we get $d\varphi_y = dz/R$, which is the usual definition of the curvature radius R in the differential geometry, for our special choice of the coordinate axes.[26]

Expressions for other components of the strain tensor are harder to guess (like at the tensile stress, not all of them are equal to zero!), but what we already know about σ_{zz} and s_{zz} is already sufficient to start formal calculations. Indeed, plugging Eq. (66) into the Hooke's law in the form (51b), and comparing the result for s_{zz} with Eq. (68), we find

$$\sigma_{zz} = -E\frac{x}{R}. \tag{7.69}$$

From the same Eq. (51b), we could also find the transverse components of the strain tensor, and see that they are related to s_{zz} exactly as at the tensile stress:

$$s_{xx} = s_{yy} = -\sigma s_{zz}, \tag{7.70}$$

and then, integrating these relations along the cross-section of the rod, find the deformation of the cross-section shape. More important for us, however, is the calculation of the relation between rod's curvature and the net torque acting on a given cross-section (of area A and orientation $dA_z > 0$):

$$\tau_y \equiv \int_A (\mathbf{r}\times d\mathbf{F})_y = -\int_A x\sigma_{zz}d^2r = \frac{E}{R}\int_A x^2 d^2r = \frac{EI_y}{R}, \tag{7.71}$$

where I_y is a geometric constant defined as

$$I_y \equiv \int_A x^2 dxdy. \tag{7.72}$$

Note that this factor, defining the bending rigidity of the rod, grows as fast as a^4 with the linear scale a of the cross-section.[27]

In these expressions, x has to be counted from the neutral line. Let us see where exactly does this line pass through rod's cross-section. Plugging result (69) into Eq. (67), we get the condition defining the neutral line:

---

[25] Strictly speaking, that dashed line is the intersection of the *neutral surface* (the continuous set of such neutral lines for all cross-sections of the rod) with the plane of drawing.

[26] Indeed, for $(dx/dz)^2 << 1$, the general formula MA Eq. (4.3) for curvature (with the appropriate replacements $f \to x$ and $x \to z$) is reduced to $1/R = d^2x/dz^2 = d(dx/dz)/dz = d(\tan\varphi_y)/dz \approx d\varphi_y/dz$.

[27] In particular, this is the reason why the usual electric wires are made not of a solid copper core, but rather a twisted set of thinner sub-wires, which may slip relative to each other, increasing the wire flexibility.

$$\int_A xdxdy = 0. \tag{7.73}$$

This condition allows a simple interpretation. Imagine a thin sheet of some material, with a constant mass density σ per unit area, cut in the form of rod's cross-section. If we place a reference frame into its center of mass, then, by its definition,

$$\sigma \int_A \mathbf{r} dxdy = 0. \tag{7.74}$$

Comparing this condition with Eq. (73), we see that one of neutral lines has to pass through the center of mass of the sheet, which may be called the "center of mass of the cross-section". Using the same analogy, we see that integral I_y (72) may be interpreted as the moment of inertia of the same imaginary sheet of material, with σ formally equal to 1, for its rotation about the neutral line – see Eq. (6.24). This analogy is so convenient that the integral is usually called the *moment of inertia of the cross-section* and denoted similarly – just as has been done above. So, our basic result (71) may be re-written as

$$\boxed{\frac{1}{R} = \frac{\tau_y}{EI_y}}. \tag{7.75}$$

Rod bending curvature vs. torque

This relation is only valid if the deformation is small in the sense $R >> a$. Still, since the deviations of the rod from its unstrained shape may accumulate along its length, Eq. (75) may be used for calculations of global deviations arbitrary on the scale of a. In order to describe such deformations, this equation has to be complemented by conditions of balance of the bending forces and torques. Unfortunately, this requires a bit more of differential geometry than I have time for, and I will only discuss this procedure for the simplest case of *relatively small* deviations $q \equiv q_x$ of the rod from its initial straight shape, which will be used for axis z (Fig. 9a), by some bulk-distributed force $\mathbf{f} = \mathbf{n}_x f_x(z)$. (The simplest example is a uniform gravity field, for which $f_x = -\rho g = \text{const}$.) Note that in the forthcoming discussion the reference frame will be global, i.e. common for the whole rod, rather than local (pertaining to each cross-section) as in the previous analysis – cf. Fig. 8.

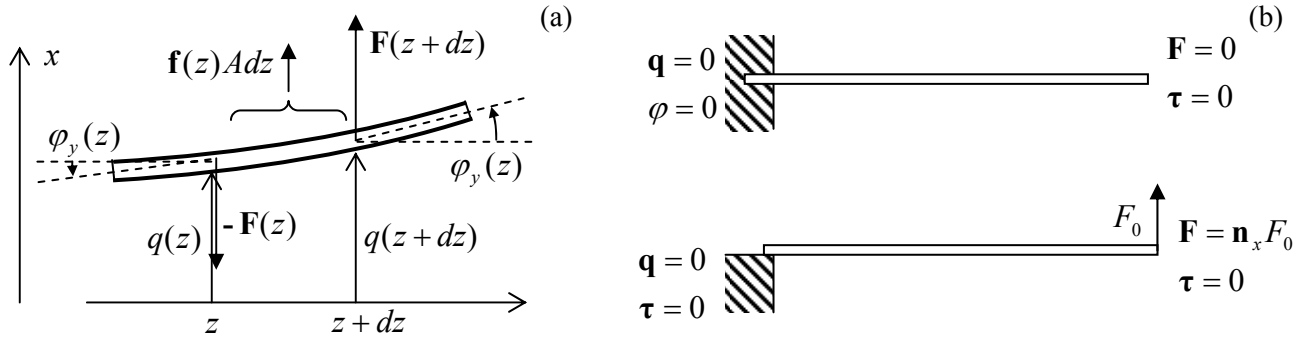

Fig. 7.9. Global picture of rod bending: (a) forces acting on a small fragment of a rod and (b) two bending problem examples, each with two typical, different boundary conditions.

First of all, we may write an evident differential equation for the average vertical force $\mathbf{F} = \mathbf{n}_x F_x(z)$ acting of the part of the rod located to the left of its cross-section located at point z. This equation expresses the balance of vertical forces acting on a small fragment dz of the rod (Fig. 9a), necessary for the absence of its linear acceleration: $F_x(z + dz) - F_x(z) + f_x(z)Adz = 0$, giving

$$\frac{dF_x}{dz} = -f_x A . \tag{7.76}$$

Note that this vertical component of the internal forces has been neglected at our derivation of Eq. (75), and hence our final results will be valid only if the ratio F_x/A is much less than the magnitude of σ_{zz} described by Eq. (69). However, these *lateral* forces create the very torque $\boldsymbol{\tau} = \mathbf{n}_y \tau_y$ that causes the bending, and thus have to be taken into account at the analysis of the global picture. This re-calculation is expressed by the balance of torque components acting on the same rod fragment of length dz, necessary for the absence of its angular acceleration:

$$\frac{d\tau_y}{dz} = -F_x . \tag{7.77}$$

These two equations of dynamics (or rather statics) should be complemented by two geometric relations. The first of them is $d\varphi_y/dz = 1/R$, which has already been discussed. We may immediately combine it with the basic result (75) of the local analysis, getting:

$$\frac{d\varphi_y}{dz} = \frac{\tau_y}{EI_y} . \tag{7.78}$$

The final equation is the geometric relation evident from Fig. 9a:

$$\frac{dq_x}{dz} = \varphi_y \tag{7.79}$$

which is (as all expressions of our simple analysis) only valid for small bending angles, $|\varphi_y| \ll 1$.

Four differential equations (76)-(79) are sufficient for the full solution of the weak bending problem, if complemented by appropriate boundary conditions. Figure 9b shows four most frequently met conditions. Let us solve, for example, the problem shown on the top panel of Fig. 9b: bending of a rod, clamped in a wall on one end, under its own weight. Considering, for the sake of simplicity, a uniform rod,[28] we may integrate equations (70), (72)-(74) one by one, each time using the appropriate boundary conditions. To start, Eq. (76), with $f_x = -\rho g$, yields

$$F_x = \rho g A z + \text{const} = \rho g A (z - L), \tag{7.80}$$

where the integration constant has been selected to satisfy the right-end boundary condition: $F_x = 0$ at $z = L$. As a sanity check, at the left wall ($z = 0$), $F_x = -\rho g A L = -mg$, meaning that the whole weight of the rod is exerted on the wall – fine.

Next, plugging Eq. (80) into Eq. (77) and integrating, we get

$$\tau_y = -\frac{\rho g A}{2}\left(z^2 - 2Lz\right) + \text{const} = -\frac{\rho g A}{2}\left(z^2 - 2Lz + L^2\right) = -\frac{\rho g A}{2}(z - L)^2 , \tag{7.81}$$

where the integration constant's choice ensures the second right-boundary condition: $\tau_y = 0$ at $z = L$. Proceeding in the same fashion to Eq. (78), we get

[28] As clear from their derivation, Eqs. (76)-(79) are valid for any distribution of parameters A, E, I, and ρ over the rod's length, provided that the rod is *quasi-uniform*, i.e. its parameters' changes are so slow that the local relation (78) is still valid at any point.

$$\varphi_y = -\frac{\rho g A}{2EI_y}\frac{(z-L)^3}{3} + \text{const} = -\frac{\rho g A}{6EI_y}\left[(z-L)^3 + L^3\right], \tag{7.82}$$

where the integration constant is selected to satisfy the *clamping condition* at the left end of the rod: $\varphi_y = 0$ at $z = 0$. (Note that this is different from the *support condition*, illustrated on the lower panel of Fig. 9b, which allows the *angle* at $z = 0$ to be finite but requires the *torque* to vanish.) Finally, integrating Eq. (79) with φ_y given by Eq. (82), we get rod's global deformation law,

$$q_x(z) = -\frac{\rho g A}{6EI_y}\left[\frac{(z-L)^4}{4} + L^3 z + \text{const}\right] = -\frac{\rho g A}{6EI_y}\left[\frac{(z-L)^4}{4} + L^3 z - \frac{L^4}{4}\right], \tag{7.83}$$

where the integration constant is zero again to satisfy the second left-boundary condition $q = 0$ at $x = 0$. So, the bending law is sort of complex even in this very simple problem. It is also remarkable how fast does the end's displacement grow with the increase of rod's length:

$$q_x(L) = -\frac{\rho g A L^4}{8EI_y}. \tag{7.84}$$

To conclude the solution, let us discuss the validity of this result. First, the geometric relation (79) is only valid if $|\varphi_y(L)| << 1$, and hence if $|q_x(L)| << L$. Next, the local formula Eq. (78) is valid if $1/R = \tau(L)/EI_y << 1/a \sim A^{-1/2}$. Using results (81) and (84), we see that the latter condition is equivalent to $|q_x(L)| << L^2/a$, i.e. is weaker, because all our analysis has been based on the assumption that $L >> a$.

Another point of concern may be that the off-diagonal stress component $\sigma_{xz} \sim F_x/A$, that is created by the vertical gravity forces, has been ignored in our local analysis. For that approximation to be, this component must be much smaller than the diagonal component $\sigma_{zz} \sim aE/R = a\tau/I_y$ taken into account in that analysis. Using Eqs. (80) and (81), we are getting the following estimates: $\sigma_{xz} \sim \rho g L$, $\sigma_{zz} \sim a\rho g A L^2/I_y \sim a^3 \rho g L^2/I_y$. According to its definition (72), I_y may be crudely estimated as a^4, so that we finally get the following simple condition: $a << L$, which has been assumed from the very beginning.

7.6. Rod torsion

One more class of analytically solvable elasticity problems is torsion of quasi-uniform, straight rods by a couple of axially-oriented torques $\boldsymbol{\tau} = \mathbf{n}_z \tau_z$ (Fig. 10).

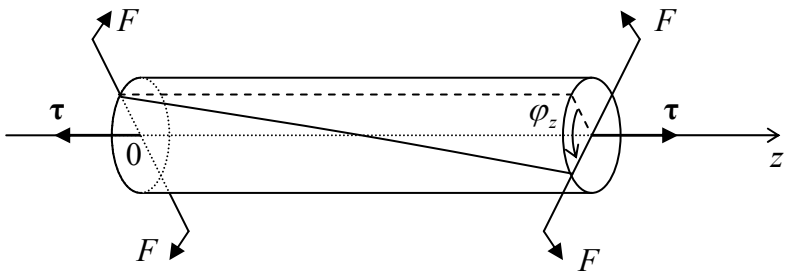

Fig. 7.10. Rod torsion.

Here the main goal of the local analysis is to relate torque τ_z to parameter κ in the relation

$$\frac{d\varphi_z}{dz} = \kappa. \tag{7.85}$$

If the deformation is elastic and small (in the sense $\kappa a << 1$, where a is again the characteristic size of rod's cross-section), κ is proportional to τ_z, and their ratio,

Torsional rigidity C

$$C \equiv \frac{\tau_z}{\kappa} = \frac{\tau_z}{d\varphi_z / dz}, \tag{7.86}$$

is called the *torsional rigidity* of the rod. Our task is to calculate the rigidity.

As the first guess (as we will see below, of a limited validity), one may assume that the torsion does not change the shape or size of the cross-section, but leads just to the mutual rotation of cross-sections about certain central line. Using a reference frame with the origin on that line, this assumption immediately allows the calculation of components of the displacement vector $d\mathbf{q}$, by using Eq. (6) with $d\boldsymbol{\varphi} = \mathbf{n}_z d\varphi_z$:

$$dq_x = -y d\varphi_z = -\kappa y dz, \quad dq_y = x d\varphi_z = \kappa x dz, \quad dq_z = 0. \tag{7.87}$$

From here, we can calculate all Cartesian components (9) of the strain tensor:

$$s_{xx} = s_{yy} = s_{zz} = 0, \quad s_{xy} = s_{yx} = 0, \quad s_{xz} = s_{zx} = -\frac{\kappa}{2} y, \quad s_{yz} = s_{zy} = \frac{\kappa}{2} x. \tag{7.88}$$

The first of these equalities means that volume does not change, i.e. we are dealing with a pure shear deformation. As a result, all nonvanishing components of the stress tensor, calculated from Eqs. (34),[29] are proportional to the shear modulus alone:

$$\sigma_{xx} = \sigma_{yy} = \sigma_{zz} = 0, \quad \sigma_{xy} = \sigma_{yx} = 0, \quad \sigma_{xz} = \sigma_{zx} = -\mu\kappa y, \quad \sigma_{yz} = \sigma_{zy} = \mu\kappa x. \tag{7.89}$$

Now it is straightforward to use this result to calculate the full torque as an integral over the cross-section area A:

$$\tau_z \equiv \int_A (\mathbf{r} \times d\mathbf{F})_z = \int_A (x dF_y - y dF_x) = \int_A (x\sigma_{yz} - y\sigma_{xz}) dx dy. \tag{7.90}$$

Using Eq. (89), we get $\tau_z = \mu\kappa I_z$, i.e.

C for axially symmetric rods

$$C = \mu I_z, \quad \text{where} \quad I_z \equiv \int_A (x^2 + y^2) dx dy. \tag{7.91}$$

Again, just as in the case of thin rod bending, we have got an integral similar to a moment of inertia, this time for rotation about axis z passing through a certain point of the cross-section. For any axially-symmetric cross-section, this evidently should be the central point. Then, for example, for the practically important case of a round pipe with internal radius R_1 and external radius R_2, Eq. (91) yields

$$C = \mu\, 2\pi \int_{R_1}^{R_2} \rho^3 d\rho = \frac{\pi}{2} \mu \left(R_2^4 - R_1^4 \right). \tag{7.92}$$

In particular, for the solid rod of radius R this gives torsional rigidity $C = (\pi/2)\mu R^4$, while for a hollow pipe of small thickness $t << R$, Eq. (92) is reduced to

[29] For this problem, with purely shear deformation, using alternative elastic moduli E and σ would be rather unnatural. If needed, we may always use the second of Eqs. (50): $\mu = E/2(1 + \sigma)$.

$$C = 2\pi\mu R^3 t\ . \tag{7.93}$$

Note that per unit cross-section area A (and hence per unit mass) this rigidity is twice higher that of a solid rod:

$$\frac{C}{A}\Big|_{\text{thin round pipe}} = \mu R^2 > \frac{C}{A}\Big|_{\text{solid round rod}} = \frac{1}{2}\mu R^2\ . \tag{7.94}$$

This fact is the basis of a broad use of thin pipes in construction.

However, for rods with axially-asymmetric cross-sections, Eq. (91) gives *wrong* results. For example, for a narrow rectangle of area $A = wt$ with $t << w$, it yields $C = \mu t w^3/12$ [WRONG!], even functionally different from the correct result – cf. Eq. (106) below. The reason of the failure of the above analysis is that does not describe possible bending q_z of rod's cross-section in the direction along the rod. (For axially-symmetric rods, such bending is evidently forbidden by the symmetry, so that Eq. (91) is valid, and results (92)-(94) are absolutely correct.) Let us describe[30] this, rather counter-intuitive effect by taking

$$q_z = \kappa\psi(x, y), \tag{7.95}$$

(where ψ is some function to be determined), but still keeping Eq. (87) for two other components of the displacement vector. The addition of ψ does not change the equality to zero of the diagonal components of the strain tensor, as well as of $s_{xy} = s_{yx}$, but contributes to other off-diagonal components:

$$s_{xz} = s_{zx} = \frac{\kappa}{2}\left(-y + \frac{\partial\psi}{\partial x}\right), \quad s_{yz} = s_{zy} = \frac{\kappa}{2}\left(x + \frac{\partial\psi}{\partial y}\right), \tag{7.96}$$

and hence to the corresponding elements of the stress tensor:

$$\sigma_{xz} = \sigma_{zx} = \mu\kappa\left(-y + \frac{\partial\psi}{\partial x}\right), \quad \sigma_{yz} = \sigma_{zy} = \mu\kappa\left(x + \frac{\partial\psi}{\partial y}\right). \tag{7.97}$$

Now let us find the requirement imposed on function $\psi(x,y)$ by the fact that the stress force component parallel to rod's axis,

$$dF_z = \sigma_{zx}dA_x + \sigma_{zy}dA_y = \mu\kappa dA\left[\left(-y + \frac{\partial\psi}{\partial x}\right)\frac{dA_x}{dA} + \left(x + \frac{\partial\psi}{\partial y}\right)\frac{dA_y}{dA}\right], \tag{7.98}$$

has to vanish at rod's surface(s), i.e. at each border of its cross-section. Coordinates $\{x, y\}$ of points at a border may be considered functions of the arc l of that line – see Fig. 11. As this figure shows, the elementary area ratios participating in Eq. (98) may be readily expressed via derivatives of functions $x(l)$ and $y(l)$: $dA_x/dA = \sin\alpha = dy/dl$, $dA_y/dA = \cos\alpha = -dx/dl$, so that we may write

$$\left[\left(-y + \frac{\partial\psi}{\partial x}\right)\left(\frac{dy}{dl}\right) + \left(x + \frac{\partial\psi}{\partial y}\right)\left(-\frac{dx}{dl}\right)\right]_{\text{border}} = 0. \tag{7.99}$$

Introducing, instead of ψ, a new function $\chi(x,y)$, defined by its derivatives as

[30] I would not be terribly shocked if the reader skipped the balance of this section at the first reading. Though the following calculation is very elegant and instructive, its results will not be used in other parts of these notes.

$$\frac{\partial\chi}{\partial x} \equiv \frac{1}{2}\left(-x - \frac{\partial\psi}{\partial y}\right), \quad \frac{\partial\chi}{\partial y} \equiv \frac{1}{2}\left(-y + \frac{\partial\psi}{\partial x}\right), \tag{7.100}$$

we may rewrite condition (99) as

$$2\left(\frac{\partial\chi}{\partial y}\frac{dy}{dl} + \frac{\partial\chi}{\partial x}\frac{dx}{dl}\right)_{\text{border}} \equiv 2\frac{d\chi}{dl}\Big|_{\text{border}} = 0, \tag{7.101}$$

so that function χ should be constant at each border of the cross-section.

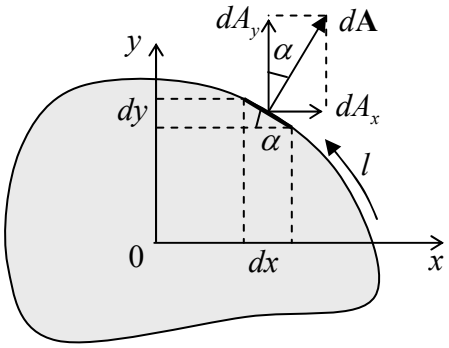

Fig. 7.11. Deriving Eq. (101).

In particular, for a singly-connected cross-section, limited by just one continuous border line, the constant is arbitrary, because according to Eqs. (100), its choice does not affect the longitudinal deformation function $\psi(x,y)$ and hence the deformation as the whole. Now let use the definition (100) of function χ to calculate the 2D Laplace operator of this function:

$$\nabla^2_{x,y}\chi \equiv \frac{\partial^2\chi}{\partial^2 x} + \frac{\partial^2\chi}{\partial^2 y} = \frac{1}{2}\frac{\partial}{\partial x}\left(-x - \frac{\partial\psi}{\partial y}\right) + \frac{1}{2}\frac{\partial}{\partial y}\left(-y + \frac{\partial\psi}{\partial y}\right) = -1. \tag{7.102}$$

This a 2D *Poisson equation* (frequently met, for example, in electrostatics), but with a very simple, constant right-hand part. Plugging Eqs. (100) into Eqs. (97), and those into Eq. (90), we may express torque τ, and hence the torsional rigidity C, via the same function:

C for arbitrary cross-section

$$C \equiv \frac{\tau_z}{\kappa} = -2\mu\int_A \left(x\frac{\partial\chi}{\partial x} + y\frac{\partial\chi}{\partial y}\right)dxdy. \tag{7.103a}$$

Sometimes, it is easier to use this result in one of its two different forms. The first of them may be readily obtained from Eq. (103a) using integration by parts:

$$\begin{aligned} C &= -2\mu\left(\int dy\int x d\chi + \int dx\int y d\chi\right) = -2\mu\left[\int dy\left(x\chi_{\text{border}} - \int \chi dx\right) + \int dx\left(y\chi_{\text{border}} - \int \chi dy\right)\right] \\ &= 4\mu\left[\int_A \chi dxdy - \chi_{\text{border}}\int_A dxdy\right], \end{aligned} \tag{7.103b}$$

while the proof of one more form,

$$C = 4\mu\int_A \left(\nabla_{x,y}\chi\right)^2 dxdy, \tag{7.103c}$$

is left for reader's exercise.

Thus, if we need to know rod's rigidity alone, it is sufficient to calculate function $\chi(x,y)$ from Eq. (102) with boundary condition (101), and plug it into any of Eqs. (103). Only if we are also curious about the longitudinal deformation (95) of the cross-section, we may continue by using Eq. (100) to find function $\psi(x,y)$. Let us see how does this general result work for the two examples discussed above. For the round cross-section of radius R, both the Poisson equation (102) and the boundary condition, χ = const at $x^2 + y^2 = R^2$, are evidently satisfied by the axially-symmetric function

$$\chi = -\frac{1}{4}(x^2 + y^2) + \text{const}. \tag{7.104}$$

For this case, either of Eqs. (103) yields

$$C = 4\mu \int_A \left[\left(-\frac{1}{2}x \right)^2 + \left(-\frac{1}{2}y \right)^2 \right] dxdy = \mu \int_A \left(x^2 + y^2 \right) d^2 r, \tag{7.105}$$

i.e. the same result (91) that we had for $\psi = 0$. Indeed, plugging Eq. (104) into Eqs. (100), we see that in this case $\partial\psi/\partial x = \partial\psi/\partial y = 0$, so that $\psi(x,y)$ = const, i.e. the cross-section is not bent. (As we have discussed in Sec. 1, a uniform translation $dq_z = \kappa\psi$ = const does not give any deformation.)

Now, turning to a rod with a narrow rectangular cross-section wt with $t << w$, we may use this strong inequality to solve the Poisson equation (102) approximately, neglecting the derivative along the wider dimension (say, y). The remaining 1D differential equation $d^2\chi/d^2x = -1$, with boundary conditions $\chi|_{x=+t/2} = \chi|_{x=-t/2}$ has an evident solution $\chi = -x^2/2 + \text{const}$. Plugging this expression into any form of Eq. (103), we get the correct result for the torsional rigidity:

$$C = \frac{1}{6}\mu w t^3. \tag{7.106}$$

Now let us have a look at the cross-section bending law (95) for this particular case. Using Eqs. (100), we get

$$\frac{\partial\psi}{\partial y} = -x - 2\frac{\partial\chi}{\partial x} = x, \quad \frac{\partial\psi}{\partial x} = y + 2\frac{\partial\chi}{\partial y} = y. \tag{7.107}$$

Integrating these differential equations over the cross-section, and taking the integration constant (again, not contributing to the deformation) for zero, we get a beautifully simple result:

$$\psi = xy, \quad \text{i.e.}\, q_z = \kappa xy\,. \tag{7.108}$$

It means that the longitudinal deformation of the rod has a "propeller bending" form: while the regions near the opposite corners (sitting on the same diagonal) of the cross-section bend toward one direction of axis z, corners on the other diagonal bend in the opposite direction. (This qualitative conclusion remains valid for rectangular cross-sections with any aspect ratio t/w.)

For rods with several surfaces, i.e. with cross-sections limited by several boundaries (say, hollow pipes), the boundary conditions for function $\chi(x, y)$ require a bit more care, and Eq. (103b) has to be modified, because the function may be equal to a different constant at each boundary. Let me leave the calculation of the torsional rigidity for this case for reader's exercise.

7.7. 3D acoustic waves

Now moving to elastic dynamics, we may start with Eq. (24) that may be transformed into the vector form exactly as this was done for the static case in the beginning of Sec. 4. Comparing Eqs. (24) and (54), we immediately see that the result may be presented as

Elastic medium dynamics equation

$$\rho\frac{\partial^2\mathbf{q}}{\partial t^2}=\frac{E}{2(1+\sigma)}\nabla^2\mathbf{q}+\frac{E}{2(1+\sigma)(1-2\sigma)}\nabla(\nabla\cdot\mathbf{q})+\mathbf{f}(\mathbf{r},t)\,. \tag{7.109}$$

Let us use this general equation for analysis of probably the most important type of time-dependent deformations: *elastic waves*. First, let us address the simplest case of a virtually infinite, uniform elastic medium, without any external forces **f**. In this case, due to the linearity and homogeneity of the resulting equation of motion, and in clear analogy with the 1D case (see Sec. 5.3), we may look for a particular time-dependent solution in the form of a sinusoidal, *linearly-polarized*, *plane wave*

3D plane, sinusoidal wave

$$\mathbf{q}(\mathbf{r},t)=\mathrm{Re}\left[\mathbf{a}e^{i\left(\mathbf{k}\cdot\mathbf{r}-\omega t\right)}\right], \tag{7.110}$$

where **a** is the constant complex amplitude of a wave (now a vector!), and **k** is the *wave vector* whose magnitude is equal to the wave number *k*. The direction of these two vectors should be clearly distinguished: while **a** determined wave's *polarization*, i.e. the direction of the particle displacements, vector **k** is directed along the spatial gradient of the full phase of the wave

$$\Psi\equiv\mathbf{k}\cdot\mathbf{r}-\omega t+\arg a\,, \tag{7.111}$$

i.e. along the direction of the wave front propagation.

The importance of the angle between these two vectors may be readily seen from the following simple calculation. Let us point axis *z* of an (inertial) reference frame along the direction of vector **k,** and axis *x* in such direction that vector **q**, and hence **a** lie within the {*x, z*} plane. In this case, all variables may change only along that axis, i.e. $\nabla = \mathbf{n}_z(\partial/\partial z)$, while the amplitude vector may be presented as the sum of just two Cartesian components:

$$\mathbf{a}=a_x\mathbf{n}_x+a_z\mathbf{n}_z. \tag{7.112}$$

Let us first consider a *longitudinal* wave,[31] with the particle motion along the wave direction: $a_x = 0$, $a_z = a$. Then vector **q** in Eq. (109), describing that wave, has only one (*z*) component, so that $\nabla\cdot\mathbf{q} = dq_z/dz$ and $\nabla(\nabla\cdot\mathbf{q}) = \mathbf{n}_z(\partial^2\mathbf{q}/\partial z^2)$, and the Laplace operator gives the same expression: $\nabla^2\mathbf{q} = \mathbf{n}_z(\partial^2\mathbf{q}/\partial z^2)$. As a result, Eq. (109), with $\mathbf{f} = 0$, yields

$$\rho\frac{\partial^2 q_z}{\partial t^2}=\left[\frac{E}{2(1+\sigma)}+\frac{E}{2(1+\sigma)(1-2\sigma)}\right]\frac{\partial^2 q_z}{\partial z^2}=\frac{E(1-\sigma)}{(1+\sigma)(1-2\sigma)}\frac{\partial^2 q_z}{\partial z^2}. \tag{7.113}$$

Plugging the plane-wave solution (110) into this equation, we see that it is indeed satisfied if the wave number and wave frequency are related as

[31] In geophysics, the longitudinal waves are known as *P-waves* (with letter *P* standing for "primary"), because due to their higher velocity (see below) they arrive at the detection site (from a distant earthquake or explosion) before waves of other types.

$$\omega = v_l k, \quad v_l^2 = \frac{E(1-\sigma)}{(1+\sigma)(1-2\sigma)\rho} = \frac{K+(4/3)\mu}{\rho}. \tag{7.114}$$

Longitudinal waves: velocity

This expression allows a simple interpretation. Let us consider a static experiment, similar to the tensile test experiment shown in Fig. 6, but with a sample much wider than L in both directions perpendicular to the force. Then the lateral contraction is impossible, and we can calculate the only finite stress component, σ_{zz}, directly from Eq. (34) with Tr (s) = s_{zz}:

$$\sigma_{zz} = 2\mu\left(s_{zz} - \frac{1}{3}s_{zz}\right) + 3K\left(\frac{1}{3}s_{zz}\right) = \left(K + \frac{4}{3}\mu\right)s_{zz}. \tag{7.115}$$

We see that the nominator in Eq. (114) is nothing more than the static elastic modulus for such a uniaxial deformation, and it is recalculated into the velocity exactly as the spring constant in the 1D waves considered in Sec. 5.3 – cf. Eq. (5.32).[32] Thus, the longitudinal acoustic waves are just simple waves of uniaxial extension/compression along the propagation axis. Formula (114) becomes especially simple in fluids, where $\mu = 0$, and the wave velocity is described by well-known expression

$$v_l = \left(\frac{K}{\rho}\right)^{1/2}. \tag{7.116}$$

Longitudinal waves: velocity in fluids

Note, however, that for gases, with their high compressibility and temperature sensitivity, the value of K participating in this formula may differ, at high frequencies, from that given by Eq. (42), because the fast compressions/extensions of gas are nearly adiabatic rather than isothermal. This difference is noticeable in Table 1 which, in particular, lists the values of v_l for some representative materials.

Now let us consider an opposite case of *transverse* waves with $a_x = a$, $a_z = 0$. In such a wave, the displacement vector is perpendicular to z, so that $\nabla\cdot\mathbf{q} = 0$, and the second term in the right-hand part of Eq. (109) vanishes. On the contrary, the Laplace operator acting on such vector still gives the same non-zero contribution, $\nabla^2\mathbf{q} = n_z(\partial^2\mathbf{q}/\partial z^2)$, to Eq. (109), so that the equation yields

$$\rho\frac{\partial^2 q_x}{\partial t^2} = \frac{E}{2(1+\sigma)}\frac{\partial^2 q_x}{\partial z^2}, \tag{7.117}$$

and instead of Eq. (114) we now get

$$\omega = v_t k, \quad v_t^2 = \frac{E}{2(1+\sigma)\rho} = \frac{\mu}{\rho}. \tag{7.118}$$

Transverse waves: velocity

We see that the speed of transverse waves depends exclusively from the shear modulus μ of the medium.[33] This is also very natural: in such waves, the particle displacements $\mathbf{q} = \mathbf{n}_x q$ are perpendicular to the elastic forces $d\mathbf{F} = \mathbf{n}_z dF$, so that the only one component σ_{xz} of the stress tensor is involved. Also,

[32] Actually, we can identify these results even qualitatively, if we consider a medium consisting of n parallel, independent 1D chains per unit area. Extension of each chain fragment, of length d, by $\Delta d << d$ gives force $F = k\Delta d$, so that the total longitudinal stress, $\sigma_{zz} \equiv Fn$, is related to strain $s_{zz} \equiv \Delta d/d$, as $\sigma_{zz}/s_{zz} = kn/d$. Multiplying both parts of Eq. (5.33a) by n/d, and noticing that (mn/d) is nothing more than the average mass density ρ, we make that equation absolutely similar to Eq. (113), just with a different notation for the longitudinal rigidity σ_{zz}/s_{zz}.

[33] Because of that, one can frequently meet term *shear waves*. In geophysics, they are also known as *S-waves*, S standing for "secondary", again in the sense of arrival time.

the strain tensor $s_{jj'}$ has no diagonal components, Tr (s) = 0, so that μ is the only elastic modulus actively participating in the Hooke's law (34).

In particular, fluids cannot carry transverse waves at all (formally, their velocity (118) vanishes), because they do not resist shear deformations. For all other materials, longitudinal waves are faster than the transverse ones. Indeed, for all known materials the Poisson ratio is positive, so that the velocity ratio that follows from Eqs. (114) and (118),

$$\frac{v_l}{v_t} = \left(\frac{2-2\sigma}{1-2\sigma}\right)^{1/2}, \tag{7.119}$$

is above $\sqrt{2} \approx 1.4$. For the most popular construction materials, with $\sigma \approx 0.3$, the ratio is about 2 – see Table 1.

Let me emphasize again that for both longitudinal and transverse waves the relation between the wave number and frequency is linear: $\omega = vk$. As has already been discussed in Sec. 5.3, in this case of *acoustic waves* (or just "sound") there is no dispersion, i.e. a transverse or longitudinal wave of more complex form, consisting of several (or many) Fourier components of the type (110), preserves its form during propagation:[34]

$$\mathbf{q}(z,t) = \mathbf{q}(z - vt, 0). \tag{7.120}$$

As one may infer from the analysis in Sec. 5.3, the dispersion would be back at very high (*hypersound*) frequencies where the wave number k becomes of the order of the reciprocal distance between the particles of the medium (e.g., atoms or molecules), and hence the approximation of the medium as a continuum, used through this chapter, became invalid.

As we already know from Sec. 5.3, besides the velocity, an important parameter characterizing waves of each type is the wave impedance Z of the medium, for acoustic waves frequently called the *acoustic impedance*. Generalizing Eq. (5.44) to the 3D case, we may define the impedance as the ratio of the force *per unit area* (i.e. the corresponding component of the stress tensor) exerted by the wave, to particles' velocity. For example, for the longitudinal waves, propagating in the positive/negative direction along z axis,

$$Z_l \equiv \mp\frac{\sigma_{zz}}{\partial q_z / \partial t} = \mp\frac{\sigma_{zz}}{s_{zz}}\frac{s_{zz}}{\partial q_z / \partial t} = \mp\frac{\sigma_{zz}}{s_{zz}}\frac{\partial q_z / \partial z}{\partial q_z / \partial t}. \tag{7.121}$$

Plugging in Eqs. (110), (114), and (115), we get

Longitudinal waves: impedance

$$\boxed{Z_l = \left[(K + \frac{4}{3}\mu)\rho\right]^{1/2}}, \tag{7.122}$$

in a clear analogy with Eq. (5.45). Similarly, for the transverse wave, the appropriately modified definition, $Z_t \equiv \mp\sigma_{xz}/(\partial q_x/\partial z)$, yields

Transverse waves: impedance

$$\boxed{Z_t = (\mu\rho)^{1/2}}. \tag{7.123}$$

[34] However, if the initial wave is an arbitrary mixture (109) of longitudinal and transverse components, these components, propagating with different velocities, will "run from each other".

Just like in the 1D waves, one role of impedance is to scale the power carried by the wave. For plane 3D waves in infinite media, with their infinite wave front area, it is more appropriate to speak it is more appropriate to speak about *power density*, i.e. power $\mathcal{P} = d\mathcal{P}/dA$ per unit area of the front, and characterize it by not only its magnitude,

$$\mathcal{P} = \frac{d\mathbf{F}}{dA} \cdot \frac{\partial \mathbf{q}}{\partial t}, \tag{7.124}$$

but also the direction of the energy propagation, that (for a plane wave in an isotropic medium) coincides with the direction of the wave vector $\mathbf{k}$: $\mathcal{P} \equiv \mathcal{P}\mathbf{n}_{\mathbf{k}}$. Using definition (18) of the stress tensor, we may present the Cartesian components of this *Umov vector*[35] as

$$\mathcal{P}_j = \sum_{j'} \sigma_{jj'} \frac{\partial q_{j'}}{\partial t}. \tag{7.125}$$

Returning to plane waves propagating along axis z, and acting exactly like in Sec. 5.3, for both the longitudinal and transverse waves we arrive at the following 3D analog Eq. (5.46),

$$\mathcal{P}_z = \frac{\omega^2 Z}{2} aa^*, \tag{7.126}$$

with Z being the corresponding impedance – either Z_l or Z_t.

Just as in 1D case, one more important effect in which the notion of impedance is crucial is *wave reflection* from at an interface between two media. The two boundary conditions, necessary for the analysis of these processes, may be obtained from the continuity of vectors $\mathbf{q}$ and $d\mathbf{F}$. (The former condition is evident, while the latter one may be obtained by applying the 2nd Newton law to the infinitesimal volume $dV = dAdz$, where segment dz straddles the boundary.) Let us start from the simplest case of the *normal incidence* on a plane interface between two uniform media with different elastic moduli and mass densities. Due to the symmetry, it is evident that the incident longitudinal/transverse wave may only excite longitudinal/transverse reflected and transferred waves, but not the counterpart wave type. Thus we can literally repeat all the calculations of Sec. 5.4, again arriving at the fundamental relations (5.53) and (5.54), with the only replacement of Z and Z' with the corresponding values of either Z_l (121) or Z_t (123). Thus, at the normal incidence the wave reflection is determined solely by the acoustic impedances of the media, while the sound velocities are not involved.

The situation, however, becomes more involved at a nonvanishing incidence angle $\theta^{(i)}$ (Fig. 12), where the transmitted wave is generally also *refracted*, i.e. propagates under a different angle, $\theta^{(r)} \neq \theta^{(i)}$, to the interface. Moreover, at $\theta^{(i)} \neq 0$ the directions of particle motion (vector $\mathbf{q}$) and of the stress forces (vector $d\mathbf{F}$) in the incident wave are neither exactly parallel nor exactly perpendicular to the interface, and thus this wave serves as an actuator for reflected and refracted waves of both types – see Fig. 12. (It shows the particular case when the incident wave is transverse.) The corresponding four angles, $\theta_t^{(r)}$, $\theta_t^{(r)}$, θ_l', θ_t', may be readily related to $\theta^{(i)}$ by the "kinematic" condition that the incident wave, as well as

[35] Named after N. Umov who introduced this concept in 1874. Ten years later, a similar concept for electromagnetic waves (see, e.g., EM Sec. 6.4) was suggested by J. Poynting, so that some textbooks use the term "Umov-Poynting vector". In a dissipation-free, elastic medium, the Umov vector obeys the following continuity equation, $\partial\left(\rho v^2/2 + u\right)/\partial t + \nabla \cdot \mathcal{P} = 0$, with u given by Eq. (52), which expresses the conservation of the total (kinetic plus potential) energy of elastic deformation.

the reflected and refracted waves of both types should have the same spatial distribution along the interface plane, i.e. for the material particles participating in all five waves. According to Eq. (110), the necessary boundary condition is the equality of the tangential components (in Fig. 12, k_x), of all five wave vectors:

$$k_t \sin\theta_t^{(r)} = k_l \sin\theta_l^{(r)} = k_l' \sin\theta_l' = k_t' \sin\theta_t' = k_x \equiv k_t \sin\theta_t^{(i)}. \tag{7.127}$$

Since the acoustic wave vectors, at fixed frequency, are inversely proportional to the corresponding wave velocities, we immediately get the following relations:

Reflection and refraction angles

$$\theta_t^{(r)} = \theta_t^{(i)}, \quad \frac{\sin\theta_l^{(r)}}{v_l} = \frac{\sin\theta_l'}{v_l'} = \frac{\sin\theta_t'}{v_t'} = \frac{\sin\theta_t^{(i)}}{v_t}, \tag{7.128}$$

so that generally all 4 angles are different. (In optics, the latter relation, reduced to just one equality for the only possible, transverse waves, is known as the *Snell law*.) These relations show that, just like in optics, the direction of a wave propagating into a medium with lower velocity is closer to the normal (axis z). In particular, this means that if $v' > v$, the acoustic waves, at larger angles of incidence, may exhibit the effect of total internal reflection, so well known from optics[36], when the *refracted* wave vanishes. In addition, Eqs. (128) show that in acoustics, a *reflected* longitudinal wave, with velocity $v_l > v_t$, may vanish at sufficiently large angles of transverse wave incidence.

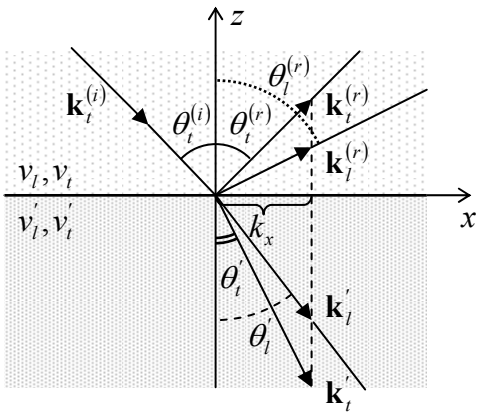

Fig. 7.12. "Kinematic" condition of acoustic wave reflection and refraction.

All these fact automatically follow from general expressions for amplitudes of the reflected and refracted waves via the amplitude of the incident wave. These relations are straightforward to derive (again, from the continuity of vectors **q** and $d\mathbf{F}$), but since they are much more bulky then those in the electromagnetic wave theory (where they are called the *Fresnel formulas*[37]), I would not have time/space for spelling them up. Let me only note that, in contrast to the case of normal incidence, these relations involve 8 media parameters: the values of impedances Z, Z', and velocities v, v' on both sides of the interface, and for both the longitudinal and transverse waves.

There is another factor that makes boundary acoustic effects more complex. Within certain frequency ranges, interfaces (and in particular surfaces) of elastic solids may sustain so-called *surface*

[36] See, e.g., EM Sec. 7.5.
[37] Their discussion may be also found in EM Sec. 7.5.

acoustic waves (SAW), in particular, the *Rayleigh waves* and *Love waves*.[38] The main feature that distinguishes such waves from their bulk (longitudinal and transverse) counterparts is that the particle displacement amplitude is maximal at the interface and decays exponentially into the bulk of both adjacent media. The characteristic depth of this penetration is of the order of, though not exactly equal to the wavelength.

In the Rayleigh waves, the particle displacement vector **q** has two components: one longitudinal (and hence parallel to the interface along which the wave propagates) and another transverse (perpendicular to the interface). In contrast to the bulk waves discussed above, the components are coupled (via their interaction with the interface) and as a result propagate with a single velocity v_R. As a result, the trajectory of each particle in the Rayleigh wave is an ellipse in the plane perpendicular to the interface. A straightforward analysis[39] of the Rayleigh waves on the *surface* of an elastic solid (i.e. its interface with vacuum) yields the following equation for v_R:

$$\left(2-\frac{v_R^2}{v_t^2}\right)^4 = 16\left(1-\frac{v_R^2}{v_t^2}\right)^2\left(1-\frac{v_R^2}{v_l^2}\right)^2. \tag{7.129}$$

According to this formula, and Eqs. (114) and (118), for realistic materials with $0 < \sigma < ½$, the Rayleigh waves are slightly (by 4 to 13%) slower than the bulk transverse waves - and hence substantially slower than the bulk longitudinal waves.

In contrast, the Love waves are purely transverse, with vector **q** oriented parallel to the interface. However, the interaction of these waves with the interface reduces their velocity v_L in comparison with that (v_t) of the bulk transverse waves, keeping it in the narrow interval between v_t and v_R:

$$v_R < v_L < v_t < v_l. \tag{7.130}$$

The practical importance of surface acoustic waves is that their amplitude decays very slowly with distance r from their point-like source: $a \propto 1/r^{1/2}$, while any bulk waves decay much faster, as $a \propto 1/r$. (Indeed, in the latter case power $\mathcal{P} \propto a^2$, emitted by such source, is distributed over a spherical surface area proportional to r^2, while in the former case all the power goes into a thin surface circle whose length scales as r.) At least two areas of applications of the surface acoustic waves have to be mentioned: in geophysics (for earthquake detection and Earth crust seismology), and electronics (for signal processing, with a focus on frequency filtering). Unfortunately, I cannot dwell on these interesting topics and I have to refer the reader to special literature.[40]

7.8. Elastic waves in restricted geometries

From what we have discussed in the end of the last section, it should be pretty clear that generally the propagation of acoustic waves in elastic bodies of finite size may be very complicated. There is, however, one important limit in which several important results may be readily obtained. This is the limit of (relatively) low frequencies, where the wavelength is much larger than at least one

[38] Named, respectively, after Lord Rayleigh (born J. Strutt, 1842-1919) who has theoretically predicted the very existence of surface acoustic waves, and A. Love (1863-1940).

[39] See, e.g., Sec. 24 in L. Landau and E. Lifshitz, *Theory of Elasticity*, 3rd ed., Butterworth-Heinemann, 1986.

[40] See, for example, K. Aki and P. G. Richards, *Quantitative Seismology*, 2nd ed., University Science Books, 2002, and D. Morgan, *Surface Acoustic Waves*, 2nd ed., Academic Press, 2007.

dimension of a system. Let us consider, for example, various waves that may propagate along thin rods, in this case "thin" meaning that the characteristic size a of rod's cross-section is much smaller than not only the length of the rod, but also the wavelength $\lambda = 2\pi/k$. In this case there is a considerable range of distances z along the rod,

$$a << \Delta z << \lambda, \tag{7.131}$$

in which we can neglect the dynamic effects due to medium inertia, and apply results of our earlier static analyses.

For example, for a longitudinal wave of stress, which is essentially a wave of periodic tensile extensions and compressions of the rod, within range (131) we can use the static relation (44):

$$\sigma_{zz} = E s_{zz}. \tag{7.132}$$

For what follows, it is easier to use the general equation of elastic dynamics not in its vector form (109), but rather in the precursor, Cartesian-component form (25), with $f_j = 0$. For plane waves propagating along axis z, only one component (with $j' \to z$) of the sum in the right-hand part of this equation is non-vanishing, and it is reduced to

$$\rho \frac{\partial^2 q_j}{\partial^2 t^2} = \frac{\partial \sigma_{jz}}{\partial z}. \tag{7.133}$$

In our current case of longitudinal waves, all components of the stress tensor but σ_{zz} are equal to zero. With σ_{zz} from Eq. (132), and using the definition $s_{zz} = \partial q_z/\partial z = \partial q_z/\partial z$, Eq. (133) is reduced to a very simple wave equation,

$$\rho \frac{\partial^2 q_z}{\partial^2 t^2} = E \frac{\partial^2 q_z}{\partial z^2}, \tag{7.134}$$

which shows that the velocity of such *tensile waves* is

Tensile waves: velocity

$$v = \left(\frac{E}{\rho} \right)^{1/2}. \tag{7.135}$$

Comparing this result with Eq. (114), we see that the tensile wave velocity, for any medium with $\sigma > 0$, is lower than the velocity v_l of longitudinal waves in the bulk of the same material. The reason for this difference in simple: in thin rods, the cross-section is free to oscillate (e.g., shrink in the longitudinal extension phase of the passing wave),[41] so that the effective force resisting the longitudinal deformation is smaller than in a border-free space. Since (as clearly visible from the wave equation), the scale of the force gives the scale of v^2, this difference translates into slower waves in rods. Of course as wave frequency is increased, at $ka \sim 1$ there is a (rather complex and cross-section-depending) crossover from Eq. (135) to Eq. (114).

Proceeding to transverse waves in rods, let us first have a look at long *bending waves*, with vector $\mathbf{q} = \mathbf{n}_x q_x$ (with axis x along the bending direction – see Fig. 8) being approximately constant in the whole cross-section. In this case, the only component of the stress tensor contributing to the net transverse force F_x is σ_{xz}, so that the integral of Eq. (133) over the cross-section is

[41] Due to this reason, the tensile waves can be called longitudinal only in a limited sense: while the stress wave is purely longitudinal $\sigma_{xx} = \sigma_{yy} = 0$, the strain wave is not: $s_{xx} = s_{yy} = -\sigma s_{zz} \neq 0$, i.e. $\mathbf{q}(\mathbf{r}, t) \neq \mathbf{n}_z q_z$,.

$$\rho A\frac{\partial^2 q_x}{\partial t^2}=\frac{\partial F_x}{\partial z},\quad F_x=\int_A \sigma_{xz}\,dA. \tag{7.136}$$

Now, if Eq. (131) is satisfied, we again may use static local relations (77)-(79), with all derivatives d/dz duly replaced with their partial form $\partial/\partial z$, to express force F_x via the bending deformation q_x. Plugging these relations into each other one by one, we arrive at a very unusual differential equation

$$\rho A\frac{\partial^2 q_x}{\partial t^2}=-EI_y\frac{\partial^4 q_x}{\partial z^4}. \tag{7.137}$$

Looking for its solution in the form of a sinusoidal wave (110), we get a nonlinear dispersion relation:[42]

$$\omega=\left(\frac{EI_y}{\rho A}\right)^{1/2}k^2. \tag{7.138}$$

Such relation means that the bending waves are not acoustic at *any* frequency, and cannot be characterized by a single velocity that would be valid for all wave numbers k, i.e. for all spatial Fourier components of a waveform. According to our discussion in Sec. 5.3, such *strongly dispersive* systems cannot pass non-sinusoidal waveforms too far without changing their waveform very considerably.

This situation changes, however, if the rod has an initial uniform longitudinal stress $\sigma_{zz} = \mathcal{T}/A$ (where force $\mathcal{T}$ is usually called *tension*), on whose background the transverse waves propagate. To analyze its effect, let us redraw Fig. 6, for a minute neglecting the bending stress – see Fig. 13.

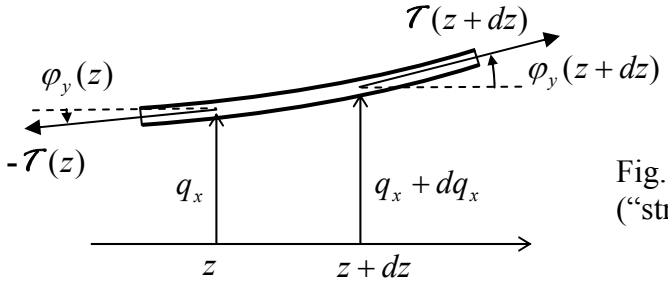

Fig. 7.13. Additional forces in a thin rod ("string"), due to background tension $\mathcal{T}$.

Still sticking to the limit of small angles φ, the additional vertical component $d\mathcal{T}_x$ of the net force acting on a small rod fragment of length dz is $\mathcal{T}_x(z - dz) - \mathcal{T}_x(z) = \mathcal{T}\varphi_y(z + dz) - \mathcal{T}\varphi_y(z) \approx \mathcal{T}(\partial\varphi_y/\partial z)dz$, so that $\partial F_x/\partial z = \mathcal{T}(\partial\varphi_y/\partial z)$. With the geometric relation (79) in its partial-derivative form $\partial q_x/\partial z = \varphi_y$, this additional term becomes $\mathcal{T}(\partial^2 q_x/\partial z^2)$. Adding it to the right-hand part of into Eq. (137), we get the following dispersion relation

$$\omega^2=\frac{1}{\rho A}\left(EI_y k^4+\mathcal{T}k^2\right). \tag{7.139}$$

Bending waves: dispersion relation

[42] Note that since the "moment of inertia" I_y, defined by Eq. (72), may depend on the bending direction (unless the cross-section is sufficiently symmetric), the dispersion relation (138) may give different results for different directions of the bending wave polarization.

At low k (and hence low frequencies), it describes acoustic waves with the "guitar string" velocity that should be well known to the reader from undergraduate courses:

Waves on a string: velocity

$$v^2 = \frac{\mathcal{T}}{\rho A}, \tag{7.140}$$

where the denominator is nothing else than the linear mass density. However, as the frequency grows, Eq. (139) describes a crossover to highly-dispersive bending waves (138).

Now let us consider the so-called *torsional waves* that are essentially the dynamic propagation of the torsional deformation discussed in Sec. 6. The easiest way to describe these waves, again within the limits given by Eq. (131), is to write the equation of rotation of a small segment dz of the rod about axis z, passing through the "center of mass" of its cross-section, under the difference of torques $\boldsymbol{\tau} = \mathbf{n}_z \tau_z$ applied on its ends – see Fig. 10:

$$\rho I_z dz \frac{\partial^2 \varphi_z}{\partial t^2} = d\tau_z, \tag{7.141}$$

where I_z is the "moment of inertia" defined by Eq. (91), which now, after its multiplication by ρdz, i.e. by the mass per unit area, has turned into the real moment of inertia of a dz-thick slice of the rod. Dividing both parts by dz, using the static local relation (86), $\tau_z = C\kappa = C(\partial\varphi_z/\partial z)$, we get the following differential equation

$$\rho I_z \frac{\partial^2 \varphi_z}{\partial t^2} = C \frac{\partial^2 \varphi_z}{\partial z^2}. \tag{7.142}$$

Just as Eqs. (114), (118), (135) and (140), this equation describes an acoustic (dispersion-free) wave that propagates with frequency-independent velocity

Torsional waves: velocity

$$v = \left(\frac{C}{\rho I_z} \right)^{1/2}. \tag{7.143}$$

As we have seen in Sec. 6, for rods with axially-symmetric cross-sections, the torsional rigidity C is described by the simple equation (91), $C = \mu I_z$, so that expression (143) is reduced to Eq. (118) for the transverse waves in infinite media. The reason for this similarity is simple: in a torsional wave, particles oscillate along small arcs (Fig. 14a), so that if the rod's cross-section is round, the stress-free surface does not perturb or modify the motion in any way, and hence does not affect the transverse velocity.

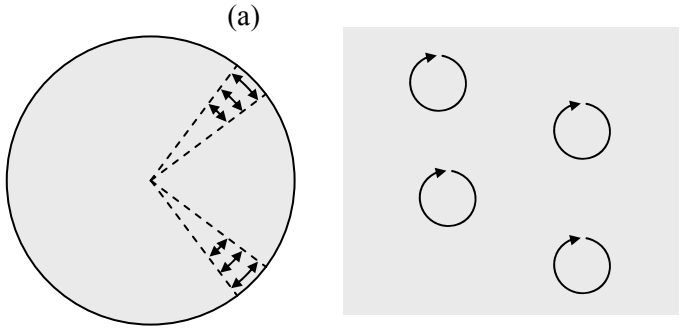

Fig. 7.14. Particle trajectories in two different transverse waves with the same velocity: (a) torsional waves in a thin round rod and (b) circularly-polarized waves in an infinite (or very broad) sample.

This fact raises an interesting issue of the relation between the torsional and *circularly-polarized* waves. Indeed, in Sec. 7, I have not emphasized enough that Eq. (118) is valid for a transverse wave polarized in any direction perpendicular to vector **k** (in our notation, directed along axis *z*). In particular, this means that such waves are *doubly-degenerate*: any isotropic elastic medium can carry simultaneously two non-interacting transverse waves propagating in the same direction with the same velocity (118), with mutually perpendicular linear polarizations (directions of vector **a**), for example, directed along axes *x* and *y*. If both waves are sinusoidal (110), with the same frequency, each point of the medium participates in two simultaneous sinusoidal motions within the [*x,y*] plane:

$$q_x = \mathrm{Re}\left[a_x e^{i(kz-\omega t)}\right] = A_x \cos\Psi, \quad q_y = \mathrm{Re}\left[a_y e^{i(kz-\omega t)}\right] = A_y \cos(\Psi+\varphi), \tag{7.144}$$

where $\Psi \equiv kz - \omega t + \varphi_x$, and $\varphi \equiv \varphi_y - \varphi_x$. Trigonometry tells us that the trajectory of such motion on the [*x, y*] plane is an ellipse (Fig. 15), so that such waves are called *elliptically-polarized*. The most important particular cases of such polarization are:

(i) $\varphi = 0$ or π: a linearly-polarized wave, with vector **a** turned by angle $\theta = \mathrm{Arctan}\,(A_y/A_x)$ from axis *x*; and

(ii) $\varphi = \pm \pi/2$ and $A_x = A_y$: *circularly polarized* waves, with the *right* or *left* polarization, respectively.

The circularly polarized waves play an important role in quantum mechanics, where such waves may be most naturally quantized, with elementary excitations (in the case of mechanical waves we are discussing, called *phonons*) having either positive or negative angular momentum $L_z = \pm\hbar$.

Now comparing the trajectories of particles in the torsional wave in a thin round rod (or pipe) and the circularly-polarized wave in a broad sample (Fig. 14), we see that, despite the same wave propagation velocity, these transverse waves are rather different. In the former case (Fig. 14a) each particle moves back and forth along an arc, with the arc length different for different particles (and vanishing at rod's center). On the other hand, in a circularly-polarized, plane wave all particles move along similar, circular trajectories.

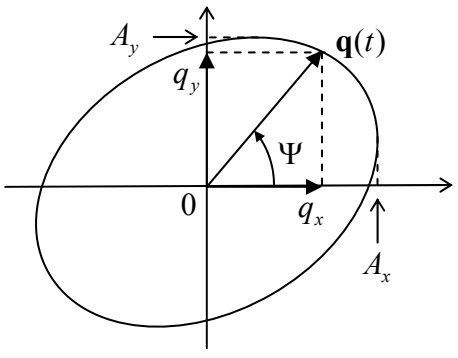

Fig. 7.15. Trajectory of a particle of an infinite medium with elliptically-polarized transverse wave, within the plane perpendicular to the direction of wave propagation.

In conclusion, let me briefly mention the opposite limit, when the size of the body, from whose boundary are completely reflected,[43] is much larger than the wavelength. In this case, the waves

[43] For acoustic waves, such condition is easy to implement. Indeed, from Sec. 7 we already know that the strong inequality of wave impedances *Z* is sufficient for such reflection. The numbers of Table 1 show that, for example,

propagate almost as in an infinite 3D medium (Sec. 7), and the most important new effect is the finite numbers of wave modes in the body. Repeating 1D analysis of Sec. 5.4 for each dimension of a 3D cuboid of volume $V = L_1L_2L_3$ (for example, using the Born-Karman boundary conditions in each dimension), we obtain Eq. (5.59) for the spectrum of components of wave vector **k** along each side. This means that all possible wave vectors are located in nodes of a rectangular 3D mesh with steps $2\pi/L_j$ in each direction, and hence with the k-space ("reciprocal space") volume

Reciprocal volume per wave vector

$$V_k = \frac{2\pi}{L_1}\frac{2\pi}{L_2}\frac{2\pi}{L_3} = \frac{(2\pi)^3}{V}. \tag{7.145}$$

per each vector. It is possible (though not quite as straightforward as it is sometimes assumed) to prove that this relation is valid regardless of the shape of volume V. Hence the number of different wave vectors within the reciprocal space volume $d^3k >> V_k$ is

$$dN = \frac{d^3k}{V_k} = \frac{V}{(2\pi)^3}d^3k >> 1. \tag{7.146a}$$

In quantum mechanics, this relation takes the form of the *density of quantum states* in k-space:

3D density of states

$$g_k \equiv g\frac{dN}{d^3k} = \frac{gV}{(2\pi)^3}, \tag{7.146b}$$

where g is the number of possible different quantum states with the same de Broglie wave vector **k**. In this form, Eq. (146) is ubiquitous in physics.[44] For phonons, formed from quantization of one longitudinal mode, and two transverse modes with different polarizations, $g = 3$.

7.9. Exercise problems

7.1. A uniform thin sheet of an isotropic, elastic material is compressed, along its thickness t, by two plane, parallel, broad (of area $A >> t^2$) rigid surfaces – see Fig. on the right. Assuming no slippage between the sheet and the surfaces, calculate the relative compression $(-\Delta t/t)$ as a function of the compressing force. Compare the result with that for the tensile stress, given by Eq. (47).

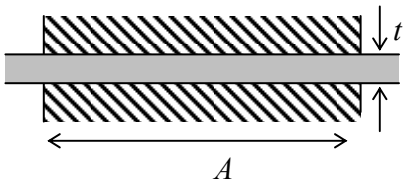

7.2. A thin, wide sheet of an isotropic, elastic material is clamped in two rigid, plane, parallel surfaces that are pulled apart with force F. Find the relative extension $\Delta L/L$ of the sheet in the direction of the force, and its relative compression $\Delta t/t$ in the perpendicular direction, and compare the results with Eqs. (47)-(48) for the tensile stress, and the solution of Problem 1.

the impedance of a longitudinal wave in a typical metal (say, steel) is almost two orders of magnitude higher than that in air, ensuring their virtually full reflection from the surface.

[44] See, e.g., EM Secs. 7.7 and 7.9, and QM Sec. 1.5.

7.3. Calculate the radial extension ΔR of a thin, long, round cylindrical pipe under the effect of its rotation with a constant angular velocity ω about its symmetry axis (see Fig. on the right), in terms of the elastic moduli E and σ, assuming that pressure both inside and outside the pipe is negligible.

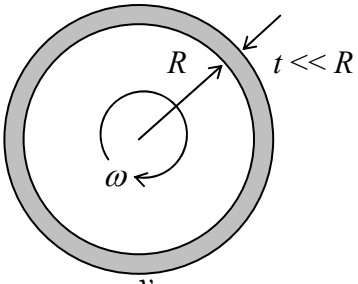

7.4. A long, uniform rail with the cross-section shown in Fig. on the right, is being bent with the same (small) torque twice: first within plane xz and then within plane yz. Assuming that $t << L$, find the ratio of rail deformations in these two cases.

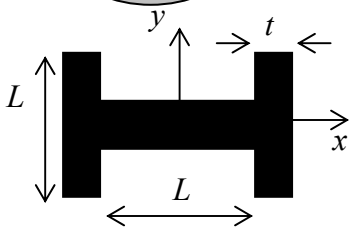

7.5. Two thin rods of the same length and mass have been made of the same elastic, isotropic material. The cross-section of one of them is a circle, while another one is an equilateral triangle - see Fig. on the right. Which of the rods is more stiff for bending along its length? Quantify the relation. Does the result depend on the bending plane orientation?

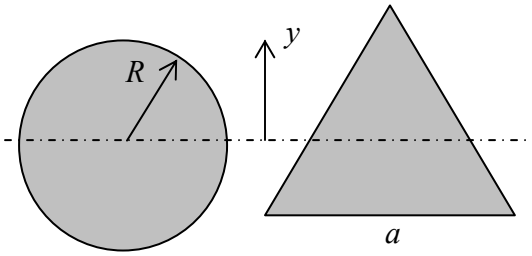

7.6. A thin, elastic, uniform, initially straight beam is placed on two point supports at the same height - see Fig. on the right. What support point placement minimizes the largest deviation of the beam from the horizontal line, under its own weight?

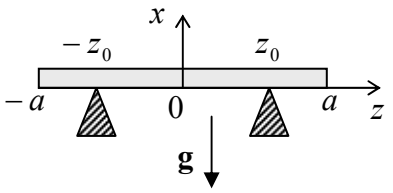

7.7. Calculate the largest compression force $\mathcal{T}$ that may be withstood by a thin, straight, elastic rod without bucking (see Figs. on the right) for two shown cases:

(i) rod's ends are clamped, and
(ii) the rod it free to rotate about the support points.

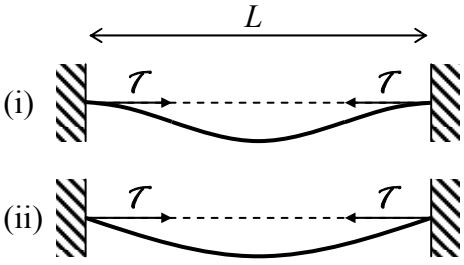

7.8. Calculate the potential energy of a small and slowly changing, but otherwise arbitrary bending deformation of a uniform, elastic, initially straight rod. Can the result be used to derive the dispersion relation (7.138)?

7.9.* Calculate the spring constant dF/dL of a coil spring made of a uniform, elastic wire, with circular cross-section of diameter d, wound as a dense round spiral of $N >> 1$ turns of diameter $D >> d$ - see Fig. on the right. Comment on the type of material's deformation.

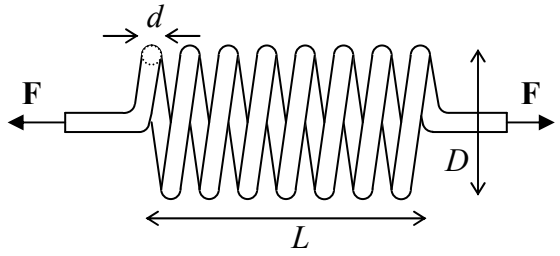

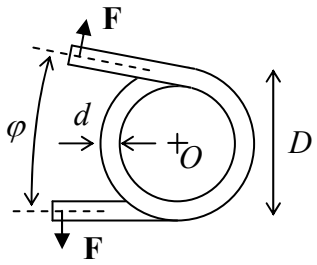

7.10. The coil discussed in Problem 9 is now used as what is sometimes called the *torsion spring* - see Fig. on the right. Find the corresponding spring constant $d\tau/d\varphi$, where τ is the torque of external forces **F** relative the center of the coil (point *O*).

7.11. Use Eqs. (101) and (102) to recast Eq. (103b) for the torsional rigidity *C* into the form given by Eq. (103c).

7.12.* Generalize Eq. (103b) to the case of rods with more than one cross-section boundary. Use the result to calculate the torsional rigidity of a thin round pipe, and compare it with Eq. (93).

7.13. Calculate the potential energy of a small but otherwise arbitrary torsional deformation $\varphi_z(z)$ of a uniform, straight, elastic rod.

7.14. A steel wire with the circular cross-section of a 3-mm diameter is stretched with a constant force of 10 N and excited at frequency 1 kHz by an actuator that excites all modes of longitudinal and transverse waves. Which wave has the highest group velocity? Accept the following parameters for steel (see Table 7.1): $E = 170$ GPa, $\sigma = 0.30$, $\rho = 7.8$ g/cm^3.

7.15. Define and calculate appropriate wave impedances for (i) tensile and (ii) torsional waves in a thin rod. Use the results to calculate what fraction of each wave's power is reflected from the connection of a long rod with round cross-section to a similar rod, but with twice larger diameter – see Fig. on the right.

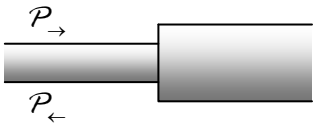

This page is intentionally left blank

Chapter 8. Fluid Mechanics

This chapter describes the basic notions of mechanics of fluids, discusses a few core problems of statics and dynamics of ideal and viscous fluids, and gives a very brief review of such a complex phenomenon as turbulence. Also, the viscous fluid flow is used to give an elementary introduction to numerical methods of partial differential equation solution - whose importance extends well beyond this particular field.

8.1. Hydrostatics

The mechanics of *fluids* (the class of materials that includes both liquids and gases) is both more simple and more complex than that of the elastic solids, with the simplicity falling squarely to the domain of *statics* - often called *hydrostatics*, because water has always been the main fluid for the human race and hence for science and engineering. Indeed, fluids are, by definition, the media that cannot resist static shear deformations. There are two ways to express this fact. First, we can formally take the shear modulus μ, describing this resistance, to be equal zero. Then the Hooke's law (7.34) shows that the stress tensor is diagonal:

$$\sigma_{jj'} = \delta_{jj'}\sigma_{jj}. \tag{8.1}$$

Alternatively, the same conclusion may be reached by looking at the stress tensor definition (7.19) and saying that in the absence of shear stress, the elementary interface $d\mathbf{F}$ has to be perpendicular to the area element dA, i.e. parallel to vector $d\mathbf{A}$.

Moreover, in fluids at equilibrium, all three diagonal components σ_{jj} of the stress tensor have to be equal. To prove that, it is sufficient to single out (mentally rather than physically) from a fluid a small volume in the shape of a right prism, with mutually perpendicular faces normal to the two directions we are interested in (Fig. 1, along axes x and y).

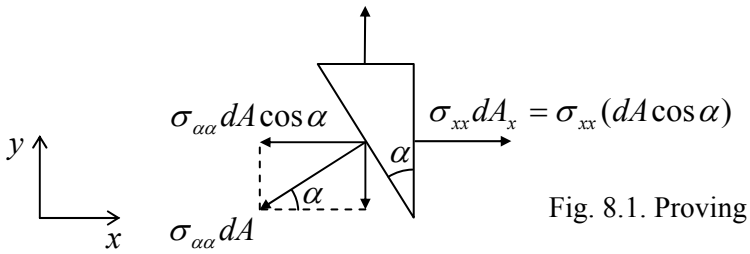

Fig. 8.1. Proving the pressure isotropy.

The prism is in equilibrium if each Cartesian component of the total force acting on all its faces nets to zero. For the x-component this balance is $\sigma_{xx}dA_x - (\sigma_{\alpha\alpha}dA)\cos\alpha = 0$. However, from the geometry (Fig. 1), $dA_x = dA\cos\alpha$, and the above balance condition yields $\sigma_{\alpha\alpha} = \sigma_{xx}$. A similar argument for the vertical forces gives $\sigma_{\alpha\alpha} = \sigma_{yy}$, so that $\sigma_{xx} = \sigma_{yy}$ .Since such equality holds for any pair of diagonal components of the stress tensor, σ_{jj}, all three of them have to be equal. This common component is usually represented as $(-P)$, because in the vast majority of cases, parameter P, called *pressure*, is positive. Thus we arrive at the key relation (which has already been mentioned in Ch. 7):

Pressure

$$\sigma_{jj'} = -P\delta_{jj'}. \tag{8.2}$$

In the absence of bulk forces, pressure should be constant through the volume of fluid, due to symmetry. Let us see how this result is affected by bulk forces. With the simple stress tensor (2), the general condition of equilibrium of a continuous medium, expressed by Eq. (7.25) with zero left-hand part, becomes just

$$-\frac{\partial P}{\partial r_j} + f_j = 0\,, \tag{8.3}$$

and may be re-written in a convenient vector form:

$$-\nabla P + \mathbf{f} = 0. \tag{8.4}$$

In the simplest case of a heavy fluid, with mass density ρ, in a uniform gravity field, $\mathbf{f} = \rho\mathbf{g}$, and the equation of equilibrium becomes,

$$-\nabla P + \rho\mathbf{g} = 0\,, \tag{8.5}$$

with only one nonvanishing component (vertical, near the Earth surface). If, in addition, the fluid may be considered *incompressible,* with its density ρ constant,[1] this equation may be readily integrated to give the so-called *Pascal equation*:[2]

$$\boxed{P + \rho g y = \text{const}\,,} \tag{8.6}$$

Pascal equation

where y is the vertical coordinate, with the direction opposite to that of vector $\mathbf{g}$.

Let me hope that this equation, and its simple applications (including buoyant force calculations using the Archimedes principle), are well familiar to the reader from his or her undergraduate physics courses, so that I may save time by skipping their discussion. I would only like to note, that the integration of Eq. (4) may be more complex in the case if the bulk forces $\mathbf{f}$ depend on position,[3] and/or if the fluid is substantially compressible. In the latter case, Eq. (4) should be solved together with the media-specific *equation of state* $\rho = \rho(P)$ describing the compressibility law – whose example is given by Eq. (7.40) for ideal gases: $\rho \equiv mN/V = mP/k_B T$, where m is the mass of one gas molecule.

8.2. Surface tension effects

Besides the bulk (volume-distributed) forces, one more possible source of pressure is *surface tension*. This effect results from the difference between the potential energy of atomic interactions on the interface between two different fluids and that in their bulks, and thus may be described by an additional potential energy

$$\boxed{U_i = \gamma A\,,} \tag{8.7}$$

Surface tension description

[1] As was discussed in Sec. 7.3 in the context of Table 7.1, this is an excellent approximation, for example, for human-scale experiments with water.

[2] The equation, and the SI unit of pressure 1 Pa = 1N/m^2, are named after B. Pascal (1623-1662) who has not only pioneered hydrostatics, but also invented the first mechanical calculator and made several other important contributions to mathematics - and Christian philosophy!

[3] An example of such a problem is given by fluid equilibrium in coordinate systems rotating with a constant angular velocity. Here the real bulk forces should be complemented by the centrifugal "force" - the only inertial force which does not vanish at constant $\boldsymbol{\omega}$ and $\mathbf{r}$ – see Eq. (6.92).

where A is the interface area, and γ is called the *surface tension constant* (or just the "surface tension"), evidently of the dimensionality of J/m^2, i.e. N/m. For a stable interface of any two fluids, γ is always positive.[4] In the absence of other forces, the surface tension makes a liquid drop spherical to minimize its surface area at fixed volume.

For the analysis of the surface tension effects in the presence of other forces, it is convenient to reduce it to a certain additional effective pressure drop ΔP_{ef} at the interface. In order to calculate ΔP_{ef}, let us consider the condition of equilibrium of a small part dA of a smooth interface between two fluids (Fig. 2), in the absence of bulk forces.

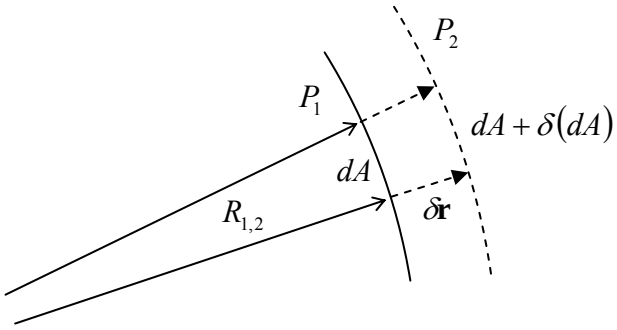

Fig. 8.2. Deriving the Young-Laplace formula (10).

If pressures $P_{1,2}$ on two sides of the interface are different, the work of stress forces on fluid 1 at a small virtual displacement $\delta\mathbf{r} = \mathbf{n}\delta r$ of the interface (where $\mathbf{n} = d\mathbf{A}/dA$ is the unit vector normal to the interface) equals[5]

$$\delta W = dA\,\delta r\left(P_1 - P_2\right). \tag{8.8}$$

For equilibrium, this work has to be compensated by an equal change of the interface energy, $\delta U_i = \gamma\delta(dA)$. Differential geometry tells us that in the linear approximation in δr, the relative change of the elementary surface area, corresponding to a fixed solid angle $d\Omega$, may be expressed as

$$\frac{\delta(dA)}{dA} = \frac{\delta r}{R_1} + \frac{\delta r}{R_2}, \tag{8.9}$$

where $R_{1,2}$ are the so-called *principal radii* of the interface curvature.[6] Combining Eqs. (7)-(9), we get the *Young-Laplace formula*[7]

[4] If γ of the interface of certain two fluids is negative, it self-reconfigures to decrease U_s by the interface area, i.e. fragments the system into a solution.

[5] This equality readily follows from the general Eq. (7.32), with the stress tensor elements expressed by Eq. (2), but in this simple case of the net stress force $d\mathbf{F} = (P_1 - P_2)d\mathbf{A}$ parallel to the interface element vector $d\mathbf{A}$, it may be even more simply obtained just from the definition of work $\delta W = d\mathbf{F}\cdot\delta\mathbf{r}$ at the virtual displacement $\delta\mathbf{r} = \mathbf{n}\delta r$.

[6] This general formula may be verified by elementary means for a sphere of radius r (for which $R_1 = R_2 = r$ and $dA = r^2 d\Omega$, so that $\delta(dA)/dA = \delta(r^2)/r^2 = 2\delta r/r$), and a round cylindrical interface of radius R (for which $R_1 = r$, $R_2 = \infty$, and $dA = rd\varphi dz$, so that $\delta(dA)/dA = \delta r/r$).

[7] This formula (not to be confused with Eq. (12), called the *Young's equation*) was derived in 1806 by P.-S. Laplace (of the Laplace operator/equation fame) on the basis of the first analysis of the surface tension effects by T. Young a year earlier.

$$P_1 - P_2 = \Delta P_{ef} \equiv \gamma\left(\frac{1}{R_1} + \frac{1}{R_2}\right). \qquad (8.10)$$

Young-Laplace formula

In particular, this formula shows that the additional pressure created by surface tension inside a spherical drop of a liquid, of radius R, equals $2\gamma/R$, i.e. decreases with R. In contrast, according to Eqs. (5)-(6), the effects of bulk forces, for example gravity, grow as $\rho g R$. The comparison of these two pressure components shows that if the drop radius (or more generally, the characteristic linear size of a fluid sample) is much larger than the so-called *capillary length*

$$a_c \equiv \left(\frac{2\gamma}{\rho g}\right)^{1/2}, \qquad (8.11)$$

Capillary length

the surface tension may be safely ignored – as will be done in the following sections of this chapter, besides a brief discussion of Eq. (48). For the water surface, or more exactly its interface with air at ambient conditions, $\gamma \approx 0.073$ N/m, while $\rho \approx 1{,}000$ kg/m^3, so that $a_c \approx 4$ mm.

On the other hand, in very narrow tubes, such as blood capillary vessels with radius $a \sim 1$ μm, i.e. $a << a_c$, the surface tension effects are very important. The key notion for the analysis of these effects is the equilibrium *contact angle* θ_c (also called the "wetting angle") at the edge of a liquid wetting a solid - see Fig. 3.

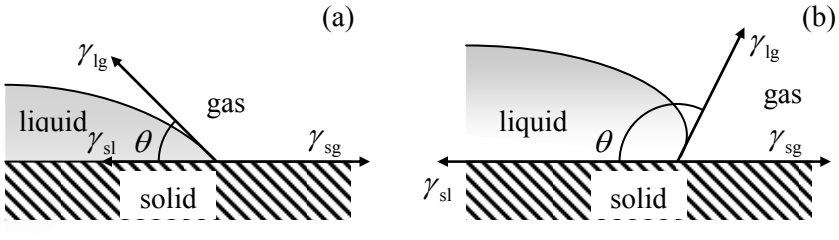

Fig. 8.3. Contact angles for (a) hydrophilic and (b) hydrophobic surfaces.

According to its definition (7), constant γ may be interpreted as a force (per unit length of the interface boundary) directed along the interface and trying to reduce its area. As a result, the balance of horizontal components of the three such forces, shown in Fig. 3, immediately yields

$$\gamma_{sl} + \gamma_{lg}\cos\theta_c = \gamma_{sg}, \qquad (8.12)$$

Young's equation

where the indices at constants γ correspond to three possible interfaces between the liquid, solid and gas. For the so-called *hydrophilic* surfaces that "like to be wet" by this particular liquid (not necessarily water), meaning that $\gamma_{sl} < \gamma_{sg}$, this relation yields $\cos\theta_c > 0$, i.e. $\theta_c < \pi/2$ – the situation shown in Fig. 3a. On the other hand, for *hydrophobic* surfaces with $\gamma_{sl} > \gamma_{sg}$, Young's equation (12) yields larger contact angles, $\theta_c > \pi/2$ – see Fig. 3b.

Let us use this notion to solve the simplest but perhaps the most important problem of this field - find the height h of the fluid column in a narrow vertical tube made of a hydrophilic material, lifted by the surface tension forces, assuming its internal surface to be a round cylinder of radius a – see Fig. 4. Inside an incompressible fluid, pressure drops with height according to the Pascal equation (6), so that just below the surface, $P \approx P_0 - \rho g h$, where P_0 is the background (e.g., atmospheric) pressure. This

means that at $a << h$ the pressure variation along the concave surface (called the *meniscus*) of the liquid is negligible, so that according to the Young-Poisson equation (10) the sum $(1/R_1 + 1/R_2)$ has to be virtually constant along the surface. Due to the axial symmetry of the problem, this means that the surface has to be a part of a sphere.[8] From the contact angle definition, radius R of the sphere is equal to $a/\cos\theta_c$ – see Fig. 4.

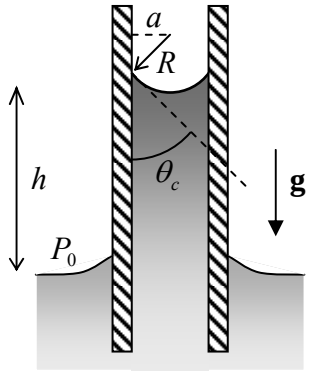

Fig. 8.4. Liquid rise in a vertical capillary tube.

Plugging this relation into Eq. (10) with $P_1 - P_2 = \rho g h$, we get the following equation for h:

$$\rho g h = \frac{2\gamma \cos\theta_c}{a}. \tag{8.13a}$$

In hindsight, this result might be obtained more directly – by requiring the total weight $\rho g V = \rho g(\pi a^2 h)$ of the lifted liquid's column to be equal to the vertical component $F\cos\theta_c$ of the full surface tension force $F = \gamma p$ acting on the perimeter $p = 2\pi a$ of the meniscus. Using the definition (11) of the capillary length a_c, Eq. (13a) may be presented as the so-called *Jurin rule:*

Jurin rule

$$h = \frac{a_c^2}{a}\cos\theta_c \le \frac{a_c^2}{a}; \tag{8.13b}$$

according to our initial assumption $h >> a$, Eq. (13) is only valid for narrow tubes, with radius $a << a_c$. This capillary rise is the basic mechanism of lifting water with nutrients from roots to the branches and leaves of plants, so that the tallest tree height is practically established by the Jurin rule (13), with $\cos\theta_c \approx 1$ and the pore radius a limited from below by a few microns, because of the viscosity effects restricting the fluid discharge – see Sec. 5 below and in particular the Poiseuille formula (60).

8.3. Kinematics

In contrast to the stress tensor, which is useful and simple – see Eq. (2), the strain tensor is *not* a very useful notion in fluid mechanics. Indeed, besides a very few situations,[9] typical problems of this field involve fluid *flow*, i.e. a state when velocity of fluid particles has some nonzero time average. This

[8] Note that this is not true for tubes with different shapes of their cross-section.

[9] One of them is the sound propagation, where particle displacements **q** are typically small, so that results of Sec. 7.7 are applicable. As a reminder, they show that in fluids, with $\mu = 0$, the transverse sound cannot propagate (formally, has zero velocity and impedance), while the longitudinal sound's velocity is finite – see Eq. (7.116).

means that the trajectory of each individual particle is a long line, and the notion of its displacement **q** becomes impracticable. However, particle's velocity $\mathbf{v} \equiv d\mathbf{q}/dt$ is a much more useful notion, especially if it is considered as a function the *observation point* **r** and (generally) time t. In an important class of fluid dynamics problem, the so-called *stationary* (or "steady", or "static") *flow,* the velocity defined in this way does not depend on time, $\mathbf{v} = \mathbf{v}(\mathbf{r})$.

There is, however, a price to pay for the convenience of this notion: namely, due to the difference between vectors **q** and **r**, particle's acceleration $\mathbf{a} = d^2\mathbf{q}/dt^2$ (that participates, in particular, in the 2nd Newton law) cannot be calculated just as a time derivative of velocity $\mathbf{v}(\mathbf{r}, t)$. This fact is evident, for example, for the static flow case, in which the acceleration of individual fluid particles may be very significant even if $\mathbf{v}(\mathbf{r})$ does not depend on time - just think about the acceleration of a drop of water flowing over the Niagara Falls rim, first accelerating fast and then virtually stopping below, while the water velocity **v** at every particular point, as measured from a bank-based reference frame, is nearly constant. Thus the main task of fluid kinematics is to express **a** via $\mathbf{v}(\mathbf{r},t)$; let us do this.

Since each Cartesian component v_j of the velocity has to be considered as a function of four *independent* scalar variables, three Cartesian components $r_{j'}$ of vector **r** and time t, its full time derivative may be presented as

$$\frac{dv_j}{dt} = \frac{\partial v_j}{\partial t} + \sum_{j'=1}^{3} \frac{\partial v_j}{\partial r_{j'}} \frac{dr_{j'}}{dt}. \tag{8.14}$$

Let us apply this *general* relation to a *specific* set of infinitesimal changes $\{dr_1, dr_2, dr_3\}$ that follows a small displacement $d\mathbf{q}$ of a certain particular particle of the fluid, $d\mathbf{r} = d\mathbf{q} = \mathbf{v}dt$, i.e.

$$dr_j = v_j dt. \tag{8.15}$$

In this case dv_j/dt is the j-th component a_j of the particle's acceleration **a**, so that Eq. (14) yields the following key relation of fluid kinematics:

$$a_j = \frac{\partial v_j}{\partial t} + \sum_{j'=1}^{3} v_{j'} \frac{\partial v_j}{\partial r_{j'}}. \tag{8.16a}$$

Fluid particle's acceleration

Using operator ∇, this result may be rewritten in the following compact vector form:[10]

$$\mathbf{a} = \frac{\partial \mathbf{v}}{\partial t} + (\mathbf{v}\cdot\nabla)\mathbf{v}. \tag{8.16b}$$

This relation already signals the main technical problem of the fluid dynamics: many equations involving particle's acceleration are nonlinear in velocity, excluding such a powerful tool the linear superposition principle from the applicable mathematical arsenal.

One more basic relation of the fluid kinematics is the so-called *continuity equation*, which is essentially just the differential version of the mass conservation law. Let us mark, inside a fluid flow, an

[10] The operator relation $d/dt = \partial/\partial t + (\mathbf{v}\cdot\nabla)$, applicable to an arbitrary (scalar or vector) function, is frequently called the *convective derivative*. (Alternative adjectives, such as "Lagrangian", "substantial", or "Stokes", are sometimes used for this derivative as well.) The relation has numerous applications well beyond the fluid dynamics – see, e.g., EM Chapter 9 and QM Chapter 1.

arbitrary volume V limited by stationary (time-independent) surface S. The total mass of the fluid inside the volume may change only due to its flow though the boundary:

$$\frac{dM}{dt} \equiv \frac{d}{dt}\int_V \rho\, d^3r = -\int_S \rho v_n d^2r \equiv -\int_S \rho\, \mathbf{v}\cdot d\mathbf{A}, \tag{8.17a}$$

where the elementary area vector $d\mathbf{A}$ is defined just as in Sec. 7.2 – see Fig. 5.

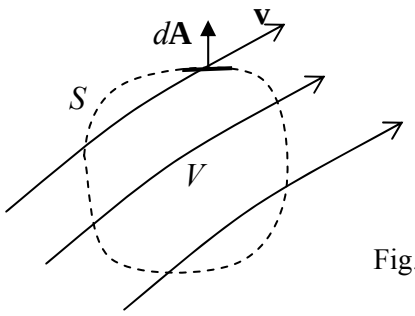

Fig. 8.5. Deriving the continuity equation.

Using the same the same divergence theorem that has been used several times in this course,[11] the surface integral in Eq. (17a) may be transformed into the integral of $\nabla(\rho\mathbf{v})$ over volume V, so that this relation may be rewritten as

$$\int_V \left(\frac{\partial\rho}{\partial t} + \nabla\cdot\mathbf{j}\right) d^3r = 0, \tag{8.17b}$$

where vector $\mathbf{j} \equiv \rho\mathbf{v}$ defined is called either the *mass flux density* or the *mass current*. Since Eq. (17b) is valid for an arbitrary volume, the function under the integral has to vanish at any point:

Continuity equation

$$\boxed{\frac{\partial\rho}{\partial t} + \nabla\cdot\mathbf{j} = 0.} \tag{8.18}$$

Note that such continuity equation is valid not only for mass, but for other conserved physics quantities (e.g., the electric charge, quantum-mechanical probability, etc.), with the proper re-definition of ρ and $\mathbf{j}$.[12]

8.4. Dynamics: Ideal fluids

Let us start our discussion of fluid dynamics from the simplest case when the stress tensor obeys the simple expression (2) even at the fluid motion. Physically, this means that fluid viscosity effects, including mechanical energy loss, are negligible. (We will discuss the conditions of this assumption in the next section.) Then the equation of motion of such an *ideal fluid* (essentially the 2nd Newton law for its unit volume) may be obtained from Eq. (7.25) using the simplifications of its right-hand part, discussed in Sec. 1:

$$\rho\mathbf{a} = -\nabla P + \mathbf{f}. \tag{8.19}$$

[11] If the reader still needs a reminder, see MA Eq. (12.1).
[12] See, e.g., EM Sec. 4.1 and QM Sec. 1.4.

Now using the basic kinematic relation (16), we arrive at the following *Euler equation*:[13]

$$\rho\frac{\partial \mathbf{v}}{\partial t}+\rho(\mathbf{v}\cdot\nabla)\mathbf{v}=-\nabla P+\mathbf{f}\ . \tag{8.20}$$

Euler equation

Generally this equation has to be solved together with the continuity equation (11) and equation of state of the particular fluid, $\rho = \rho(P)$. However, as we have already discussed, in many situations the compressibility of water and other important fluids is very low and may be ignored, so that ρ may be treated as a given constant. Moreover, in many cases the bulk forces $\mathbf{f}$ are conservative and may be presented as a gradient of a certain potential function $u(\mathbf{r})$ – the potential energy per unit volume:

$$\mathbf{f}=-\nabla u\ ; \tag{8.21}$$

for example, for a uniform gravity field, $u = \rho gh$. In this case the right-hand part of Eq. (20) becomes $-\nabla(P + u)$. For these cases, it is beneficial to recast the left-hand of that equation as well, using the following well-know identity of vector algebra[14]

$$(\mathbf{v}\cdot\nabla)\mathbf{v}=\nabla\left(\frac{v^2}{2}\right)-\mathbf{v}\times(\nabla\times\mathbf{v}). \tag{8.22}$$

As a result, the Euler equation takes the form

$$\rho\frac{\partial \mathbf{v}}{\partial t}-\rho\mathbf{v}\times(\nabla\times\mathbf{v})+\nabla\left(P+u+\rho\frac{v^2}{2}\right)=0. \tag{8.23}$$

In a stationary flow, the first term of this equation vanishes. If the second term, describing fluid's *vorticity*, is zero as well, then Eq. (23) has the first integral of motion,

$$P+u+\frac{\rho}{2}v^2=\text{const}\ , \tag{8.24}$$

Bernoulli equation

called the *Bernoulli equation*. Numerous examples of application of Eq. (17) to simple problems of stationary flow in pipes, in the Earth gravity field (giving $u = \rho gh$), should be well known to the reader, so I hope I can skip their discussion without much harm.

In the general case an ideal fluid may have vorticity, so that Eq. (24) is not always valid. Moreover, due to absence of viscosity in an ideal fluid, the vorticity, once created, does not decrease along the *streamline* - the fluid particle's trajectory, to which the velocity is tangential in every point.[15] Mathematically, this fact[16] is expressed by the following *Kelvin theorem*: $(\nabla\times\mathbf{v})\cdot d\mathbf{A}$ = const along any small contiguous group of streamlines crossing an elementary area dA.[17]

---

[13] It was derived in 1755 by the same L. Euler whose name has already been (reverently) mentioned several times in this course.

[14] It readily follows, for example, from MA Eq. (11.6) with $\mathbf{g} = \mathbf{f} = \mathbf{v}$.

[15] Perhaps the most spectacular manifestation of the vorticity conservation are the famous toroidal vortex rings (see, e.g., nice photo and movie at https://en.wikipedia.org/wiki/Vortex_ring), predicted in 1858 by H. von Helmholtz, and then demonstrated by P. Tait in a series of spectacular experiments with smoke in air. The persistence of such a ring, once created, is only limited by fluid's viscosity – see the next section.

[16] First formulated verbally by H. von Helmholtz.

[17] Its proof may be found, e.g., in Sec. 8 of L. Landau and E. Lifshitz, *Fluid Mechanics*, 2nd ed., Butterworth-Heinemann, 1987.

In many important cases the vorticity of fluid is negligible. For example, if a solid body of arbitrary shape is embedded into an ideal fluid that is uniform (meaning, by definition, that $\mathbf{v}(\mathbf{r},t) = \mathbf{v}_0 =$ const) at large distances, its vorticity is zero everywhere. (Indeed, since $\nabla\times\mathbf{v}$ at the uniform flow, the vorticity is zero at distant points of any streamline, and according to the Kelvin theorem, should equal zero everywhere.) In this case the velocity, as any curl-free vector field, may be presented as a gradient of some effective potential function,

$$\mathbf{v} = -\nabla\phi. \tag{8.25}$$

Such *potential flow* may be described by a simple differential equation. Indeed, the continuity equation (18) for a steady flow of an incompressible fluid is reduced to $\nabla\cdot\mathbf{v} = 0$. Plugging Eq. (25) into this relation, we get the scalar Laplace equation,

$$\nabla^2\phi = 0, \tag{8.26}$$

which should be solved with appropriate boundary conditions. For example, the fluid flow may be limited by solid bodies inside which that the fluid cannot penetrate. Then the fluid velocity at these boundaries should not have a normal component:

$$\frac{\partial\phi}{\partial n} = 0. \tag{8.27}$$

On the other hand, at large distances from the body in question the fluid flow is known, e.g., uniform:

$$\nabla\phi = -\mathbf{v}_0, \quad \text{at } r \to \infty. \tag{8.28}$$

As the reader may already know (for example, from a course of electrodynamics[18]), the Laplace equation (26) is readily solvable analytically in several simple (symmetric) but important situations. Let us consider, for example, the case of a round cylinder, with radius R, immersed into a flow with the initial velocity $\mathbf{v}_0$ perpendicular to the cylinder axis (Fig. 6).[19]

For this problem, it is natural to use cylindrical coordinates with axis z parallel to cylinder's axis. In this case the velocity distribution is evidently independent of z, so that we may simplify the general expression of the Laplace operator in cylindrical coordinates[20] by taking $\partial/\partial z = 0$. As a result, Eq. (26) is reduced to[21]

$$\frac{1}{\rho}\frac{\partial}{\partial\rho}\left(\rho\frac{\partial\phi}{\partial r}\right) + \frac{1}{\rho^2}\frac{\partial^2\phi}{\partial\theta^2} = 0, \quad \text{at } \rho \geq R. \tag{8.29}$$

The general solution of this equation may be obtained using the variable separation method:[22]

[18] See, e.g., EM Secs. 2.3 and 2.4.

[19] Evidently, motion of the cylinder, with constant velocity $(-\mathbf{v}_0)$, in the otherwise stationary fluid leads to exactly the same problem - in the reference frame bound to the moving body.

[20] See, e.g., MA Eq. (10.3).

[21] Let me hope that letter ρ, used here for the magnitude 2D radius-vector $\boldsymbol{\rho} = \{x, y\}$, will not be confused with fluid's density – which does not participate in this boundary problem.

[22] See, e.g., EM Eq. (2.112). Note that the most general solution of Eq. (29) also includes a term proportional to φ, but this term should be zero for such a single-valued function as the velocity potential.

$$\phi = a_0 + b_0 \ln \rho + \sum_{n=1}^{\infty} \left(c_n \cos n\varphi + s_n \sin n\varphi\right)\left(a_n \rho^n + b_n \rho^{-n}\right), \tag{8.30}$$

where coefficients a_n and b_n have to be found from the boundary conditions (27) and (28). Choosing axis $x = r\cos\varphi$ to be parallel to vector $\mathbf{v}_0$ (Fig. 6a) we may rewrite these the conditions in the form

$$\frac{\partial \phi}{\partial \rho} = 0, \quad \text{at } \rho = R, \tag{8.31}$$

$$\phi \to -v_0 \rho \cos\varphi + \phi_0, \quad \text{at } \rho >> R, \tag{8.32}$$

where ϕ_0 is an arbitrary constant, which does not affect the velocity distribution, and may be taken for zero. The latter condition is incompatible with all terms of Eq. (30) except the term with $n = 1$ (with $s_1 = 0$ and $c_1 a_1 = - v_0$) , so it is reduced to

$$\phi = \left(-v_0 \rho + \frac{c_1 b_1}{\rho}\right)\cos\varphi. \tag{8.33}$$

Now, plugging this solution into Eq. (31), we get $c_1 b_1 = -v_0 R^2$, so that, finally,

$$\phi = -v_0\left(\rho + \frac{R^2}{\rho}\right)\cos\varphi. \tag{8.34}$$

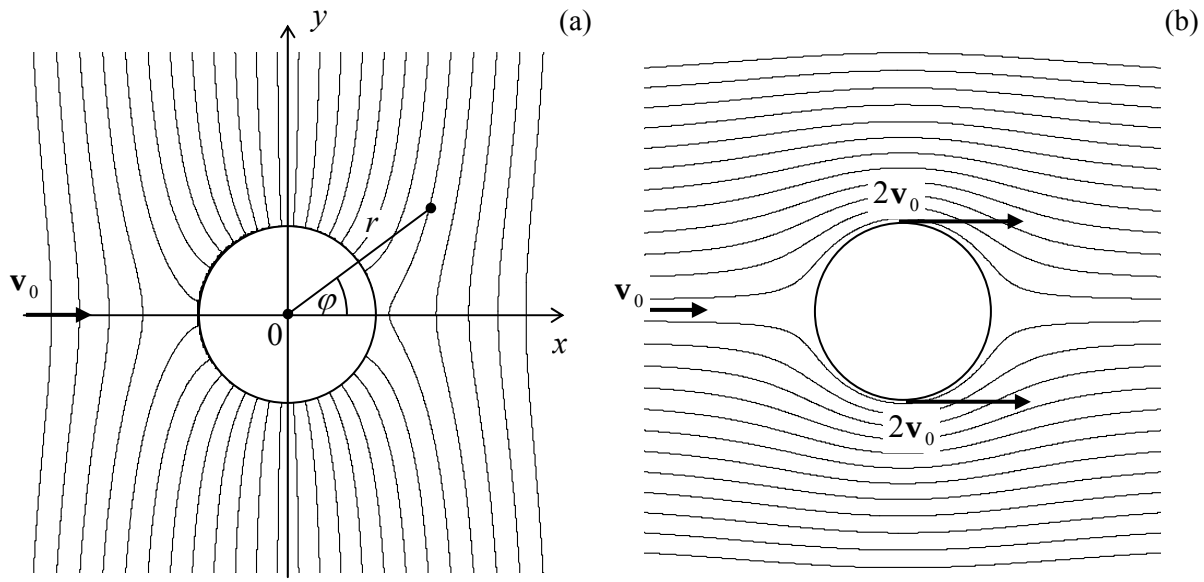

Fig. 8.6. Flow of ideal, incompressible fluid around a round cylinder: (a) equipotential surfaces and (b) streamlines.

Figure 6a shows the surfaces of constant velocity potential ϕ. In order to find the fluid velocity, it is easier to rewrite result (34) in the Cartesian coordinates $x = \rho\cos\varphi$, $y = \rho\sin\varphi$:

$$\phi = -v_0 x\left(1+\frac{R^2}{\rho^2}\right) = -v_0 x\left(1+\frac{R^2}{x^2+y^2}\right). \tag{8.35}$$

From this equation, we may readily calculate the Cartesian components $v_x = -\partial\phi/\partial x$ and $v_y = -\partial\phi/\partial y$ of the fluid velocity. Figure 6b shows particle streamlines.[23] One can see that the largest potential gradient, and hence the maximum speed, is achieved at points near the vertical diameter ($\rho = R$, $\varphi = \pm\pi/2$), where

$$v = v_x = -\left.\frac{\partial\phi}{\partial x}\right|_{\substack{R=r,\\ x=0}} = 2v_0. \tag{8.36}$$

Now the pressure distribution may now be found from the Bernoulli equation (24). For $u(\mathbf{r}) = 0$, it shows that the pressure reaches maximum at the ends of the longitudinal diameter $y = 0$, while at the ends of the transverse diameter $x = 0$, where the velocity is largest, it is less by $2\rho v_0^2$ (where ρ is the fluid density again - sorry for the notation jitters!) Note that the distributions of both velocity and pressure are symmetric about the transverse axis $x = 0$, so that the fluid flow does not create any net *drag force* in its direction. This result, which stems from the conservation of the mechanical energy of an ideal fluid, remains valid for a solid body of arbitrary shape moving inside an infinite volume of such ideal fluid – the so-called *D'Alambert paradox*. However, if a body moves near ideal fluid's surface, its energy may be transformed into that of surface waves, and the drag becomes possible.

Speaking about the *surface waves* in a gravity field[24], their description is one more classical problem of the ideal fluid dynamics. Let us consider an open surface of an ideal fluid of density ρ in a uniform gravity field $\mathbf{f} = \rho\mathbf{g} = -\rho g\mathbf{n}_y$ – see Fig. 7. If the wave amplitude A is sufficiently small, we can neglect the nonlinear term $(\mathbf{v}\cdot\nabla)\mathbf{v} \propto A^2$ in the Euler equation (13) in comparison with the first term, $\partial\mathbf{v}/\partial t$, that is linear in A. For a wave with frequency ω and wavenumber k, particle's velocity $\mathbf{v} = d\mathbf{q}/dt$ is of the order of ωA, so that this approximation is legitimate if $\omega^2 A >> k(\omega A)^2$, i.e. when

$$kA << 1, \tag{8.37}$$

i.e. when the wave amplitude is much smaller than its wavelength $\lambda = 2\pi/k$. By this assumption, we may neglect the fluid vorticity effects, and again use Eq. (25) and (for an incompressible fluid) Eq. (26).

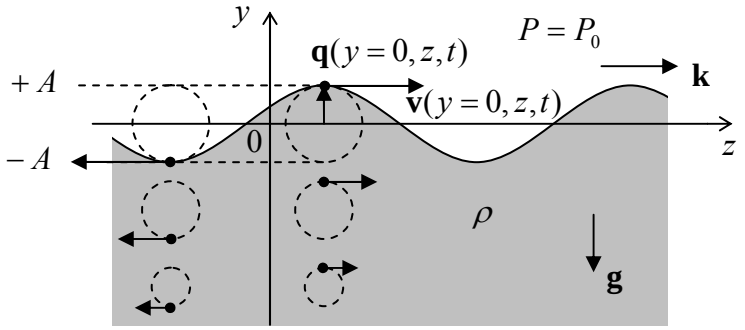

Fig. 8.7. Small "plane" surface wave on a deep fluid. Dashed lines show fluid particle trajectories. (For clarity, the displacement amplitude $A \equiv (k/\omega)\Phi_0$ is strongly exaggerated.)

[23] They may be found by integration of the evident equation $dy/dx = v_y(x,y)/v_x(x,y)$. For our simple problem this integration may be done analytically, giving the relation $y[1 - R^2/(x^2 + y^2)] = \text{const}$, where the constant is specific for each streamline.

[24] The alternative, historic term "gravity waves" for this phenomenon may nowadays lead to a confusion with the relativistic effect of gravity waves (which may propagate in vacuum), whose direct detection is a focus of so much current experimental effort.

Looking for the solution of the Laplace equation (26) in the natural form of a 1D sinusoidal wave,[25]

$$\phi = \mathrm{Re}\left[\Phi(y) e^{i(kz - \omega t)} \right], \tag{8.38}$$

we get a simple equation

$$\frac{d^2\Phi}{dy^2} - k^2\Phi = 0, \tag{8.39}$$

with an exponential solution (decaying, as it has to, at $y \to -\infty$) $\Phi = \Phi_0 \exp\{ky\}$, so that Eq. (38) becomes

$$\phi = \mathrm{Re}\left[\Phi_0 e^{ky} e^{i(kz - \omega t)} \right] = \Phi_0 e^{ky} \cos(kz - \omega t), \tag{8.40}$$

where the last form is valid if Φ_0 is real - which may be always arranged by a proper selection of origins of z and/or t. Note that the rate of wave decay with depth is exactly equal to the wavenumber of its propagation along the surface. Because of that, the trajectories of fluid particles are exactly circular. Indeed, using Eqs. (25) and (40) (with amplitude) to calculate velocity components,

$$v_x = 0, \qquad v_y = -\frac{\partial \phi}{\partial y} = -k\Phi_0 e^{ky} \cos(kz - \omega t), \qquad v_z = -\frac{\partial \phi}{\partial z} = k\Phi_0 e^{ky} \sin(kz - \omega t), \tag{8.41}$$

we see that they have equal real amplitudes, and are phase-shifted by $\pi/2$. This result becomes even more clear if we use the velocity definition $\mathbf{v} = d\mathbf{q}/dt$ to integrate Eqs. (41) over time to recover the particle displacement law $\mathbf{q}(t)$. Due to the strong inequality (37), the integration may be done at fixed y and z:

$$q_y = \frac{k}{\omega} \Phi_0 e^{ky} \sin(kz - \omega t), \qquad q_z = \frac{k}{\omega} \Phi_0 e^{ky} \cos(kz - \omega t). \tag{8.42}$$

Note that the phase of oscillations of v_z coincides with that of q_y. It means, in particular, that at wave's top ("crest"), fluid particles are moving in the direction of wave's propagation – see arrows in Fig. 7.

It is remarkable that all this picture follows from the Laplace equation alone! The "only" remaining feature to calculate is the dispersion law $\omega(k)$, and for that we need to combine Eq. (40) with what remains, in our linear approximation, of the Euler equation (23). In this approximation, and with the bulk force potential $u = \rho g y$, this equation is reduced to

$$\nabla\left(-\rho \frac{\partial \phi}{\partial t} + P + \rho g y \right) = 0. \tag{8.43}$$

This equation means that the function in the parentheses is constant in space; at the surface, it should equal to pressure P_0 above the surface (say, the atmospheric pressure), that we assume to be constant. This means that on the surface, the contributions to P that come from the first and the third term in Eq. (43), should compensate each other. Let us take the average surface position for $y = 0$; then the surface with waves is described by relation $y = q_y$ – see Fig. 7. Due to the strong relation (37), which means $k|q_y| \ll 1$, we can use Eqs. (40) and (42) with $y = 0$, so that the above compensation condition yields

[25] Such a wave is "plane" only in direction x (perpendicular to the propagation direction z, see Fig. 4).

$$-\rho\omega\Phi_0 \sin(kz-\omega t)+\rho g\frac{k}{\omega}\Phi_0 \sin(kz-\omega t)=0\,. \tag{8.44}$$

Surface waves' dispersion

This condition is identically satisfied on the whole surface (and for any Φ_0) as soon as

$$\boxed{\omega^2 = gk\,,} \tag{8.45}$$

this equality giving the dispersion relation we were looking for.

Looking at this surprisingly simple result (which includes just one constant, g), note, first of all, that it does not involved fluid's density. This is not too much surprising, because due to the weak equivalence principle, particle masses always drop out of the results of problems involving gravitational forces alone. Second, the dispersion law (45) is strongly nonlinear, and in particular does not have the acoustic wave limit. This means that the surface wave propagation is strongly dispersive, with the phase velocity $\omega/k \propto 1/\omega$ diverging at $\omega \to 0$. This divergence is an artifact of our assumption of the infinite fluid thickness. A rather straightforward generalization of the above calculations to a layer of finite thickness h, using the additional boundary condition $v_y|_{y=-h} = 0$, yields the following modified dispersion relation,

$$\omega^2 = gk\tanh kh\,. \tag{8.46}$$

It shows that relatively long waves, with $\lambda >> h$, i.e. with $kh << 1$, propagate without dispersion (i.e. have $\omega/k = \text{const} \equiv v$), with velocity

$$v = (gh)^{1/2}\,. \tag{8.47}$$

For the Earth oceans, this velocity is rather high, approaching 300 m/s (!) for h = 10 km. This result explains, in particular, the very fast propagation of tsunami waves.

In the opposite limit of very short waves (large k), Eq. (45) also does not give a good description of experimental data, due to the effects of surface tension (see Sec. 2 above). Using Eq. (8.10), it is easy (and hence left for the reader :-) to show that their account leads (at $kh >> 1$) to the following modification of Eq. (45):

$$\omega^2 = gk + \frac{\gamma k^3}{\rho}\,. \tag{8.48}$$

According to this formula, the surface tension is important at wavelengths smaller than the capillary constant a_s given by Eq. (11). Much shorter waves, for whom Eq. (48) yields $\omega \propto k^{3/2}$, are called the *capillary waves* - or just "ripples".

All these generalizations are still limited to potential forces, and do not allow one to describe energy loss, in particular the attenuation of either bulk or surface waves in fluids. For that, as well as for the drag force description, we need to proceed to the effects of viscosity.

8.5. Dynamics: Viscous fluids

Fluid viscosity of many fluids, at not too high velocities, may be described surprisingly well by adding, to the static stress tensor (2), additional components proportional to velocity $\mathbf{v} \equiv d\mathbf{q}/dt$:

$$\sigma_{jj'} = -P\delta_{jj'} + \tilde{\sigma}_{jj'}(\mathbf{v})\,. \tag{8.49}$$

Since the Hooke law (7.34) has taught us about the natural structure of such a tensor in the case of stress proportional to displacement **q**, we may expect a similar expression with replacement $\mathbf{q} \to \mathbf{v} = d\mathbf{q}/dt$:

$$\tilde{\sigma}_{jj'} = 2\eta\left(e_{jj'} - \frac{1}{3}\delta_{jj'}\mathrm{Tr}(\mathrm{e})\right) + 3\zeta\left(\frac{1}{3}\delta_{jj'}\mathrm{Tr}(\mathrm{e})\right), . \tag{8.50a}$$

where $e_{jj'}$ are the elements of the symmetrized strain derivative tensor:

$$e_{jj'} \equiv \frac{ds_{jj'}}{dt} = \frac{1}{2}\left(\frac{\partial v_j}{\partial r_{j'}} + \frac{\partial v_{j'}}{\partial r_j}\right). \tag{8.50b}$$

Experiment confirms that Eq. (50) gives a good description of the viscosity effects in a broad range of isotropic fluids. Coefficient η is called either the *shear viscosity,* or the *dynamic viscosity,* or just *viscosity*, while ζ is called the *second* (or *bulk*) viscosity.

In the most frequent case of a virtually incompressible fluid, $\mathrm{Tr}(\mathrm{u}) = d[\mathrm{Tr}(\mathrm{s})]/dt = (dV/dt)/V = 0$, so that the term proportional to ζ vanishes, and η is the only important viscosity parameter.[26] Table 1 shows the approximate values of the viscosity, together with the mass density ρ, for several common fluids. One can see that η may vary in extremely broad limits; the extreme cases are glasses (somewhat counter-intuitively, these amorphous materials are not stable solids even at room temperature, but rather may "flow", though extremely slowly, until they eventually crystallize) and liquid helium.[27]

Table 8.1. Important parameters of several representative fluids (approximate values)

Fluid (all at 300 K, besides the helium)	η (mPa·s)	ρ (kg/m^3)
Glasses	10^{21}-10^{24}	2,200-2,500
Machine oils (SAE 10W – 40 W)	65-320	900
Water	0.89	1,000
Mercury	1.53	13,530
Liquid helium 4 (at 4.2K, 10^5 Pa)	0.019	130
Air (at 10^5 Pa)	0.018	1.3

Incorporating the additional components of $\sigma_{jj'}$ to the equation (20) of fluid motion, absolutely similarly to how it was done at the derivation of Eq. (7.109) of the elasticity theory, with the account of Eq. (16) we arrive at the famous *Navier-Stokes* equation:[28]

$$\rho\frac{\partial \mathbf{v}}{\partial t} + \rho(\mathbf{v}\cdot\nabla)\mathbf{v} = -\nabla P + \mathbf{f} + \eta\nabla^2\mathbf{v} + \left(\varsigma + \frac{\eta}{3}\right)\nabla(\nabla\cdot\mathbf{v}). \tag{8.51}$$

Navier-Stokes equation

[26] Probably the most important effect we miss by neglecting ζ is the attenuation of (longitudinal) acoustic waves, into which the second viscosity makes a major (and in some cases, the main) contribution.

[27] Actually, at even lower temperatures (for He 4, $T < T_\lambda \approx 2.17$ K), helium becomes a *superfluid*, i.e. looses viscosity completely, as result of the Bose-Einstein condensation - see, e.g., SM Sec. 3.4.

[28] Named after C.-L. Navier (1785-1836) who had suggested the equation, and G. Stokes (1819-1903) who has demonstrated its relevance by solving it for several key situations.

The apparent simplicity of this equation should not mask an enormous range of phenomena, notably including turbulence (see the next section), that are described by it, and the complexity of its solutions even for some simple geometries. In most problems interesting for practice the only option is to use numerical methods, but due to the large number of parameters (ρ, η, ζ, plus geometrical parameters of the involved bodies, plus the distribution of bulk forces **f,** plus boundary conditions), this way is strongly plagued by the "curse of dimensionality" that was discussed in Sec. 4.8.

Let us see how does the Navier-Stokes equation work, on several simple examples. As the simplest case, let us consider the so-called *Couette flow* caused in an incompressible fluid layer between two wide, horizontal plates (Fig. 8) by mutual sliding of the plates with a constant relative velocity $\mathbf{v}_0$.

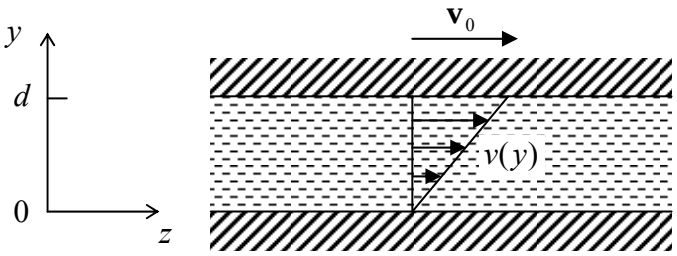

Fig. 8.8. The simplest problem of the viscous fluid flow.

Let us assume a *laminar* (vorticity-free) fluid flow. (As will be discussed in the next section, this assumption is only valid within certain limits.) Then we may use the evident symmetry of the problem, to take, in the reference frame shown in Fig. 8, $\mathbf{v} = \mathbf{n}_z v(y)$. Let the bulk forces be vertical, $\mathbf{f} = \mathbf{n}_y f$, so they do not give an additional drive to fluid flow. Then for the stationary flow ($\partial\mathbf{v}/\partial t = 0$), the vertical, y-component of the Navier-Stokes equation is reduced to the static Pascal equation (3), showing that the pressure distribution is not affected by the plate (and fluid) motion. In the horizontal, z-component of the equation only one term, $\nabla^2 v$, survives, so that for the only Cartesian component of velocity we get the 1D Laplace equation

$$\frac{d^2 v}{dy^2} = 0. \tag{8.52}$$

In contract to the ideal fluid (see, e.g., Fig. 6b), the relative velocity of a viscous fluid and a solid wall it flows by should approach zero at the wall,[29] so that Eq. (52) should be solved with boundary conditions

$$v = \begin{cases} 0, & \text{at } y = 0, \\ v_0, & \text{at } y = d. \end{cases} \tag{8.53}$$

Using the evident solution of this boundary problem, $v(y) = (y/d)v_0$, illustrated by arrows in Fig. 8, we can now calculate the horizontal drag force acting on a unit area of each plate. For the bottom plate,

$$\frac{F_z}{A_y} = \sigma_{zy}\Big|_{y=0} = \eta \frac{\partial v}{\partial y}\Big|_{y=0} = \eta \frac{v_0}{d}. \tag{8.54}$$

[29] This is essentially an additional experimental fact, but may be readily understood as follows. A solid may be considered as an ultimate case of a fluid (with infinite viscosity), and the tangential component of velocity should be a continuous an interface between two fluids, in order to avoid infinite stress – see Eq. (50).

(For the top plate, the derivative $\partial v/\partial y$ has the same value, but the sign of dA_y has to be changed to reflect the direction of the outer normal to the solid surface, so that we get a similar force but with the negative sign.) The well-known result (54) is often used, in undergraduate courses, for a definition of the dynamic viscosity η, and indeed shows its physical meaning very well.

As the next, slightly less trivial example let us consider the so-called *Poiseuille problem*[30] of the relation between the constant external pressure gradient $\chi \equiv -\partial P/\partial z$ applied along a round pipe with internal radius R (Fig. 9) and the so-called *discharge* Q - defined as the mass of fluid flowing through pipe's cross-section per unit time.

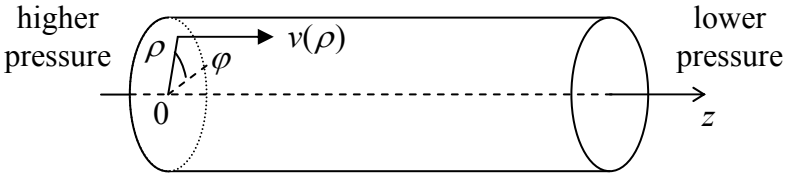

Fig. 8.9. The Poiseuille problem.

Again assuming a laminar flow, we can involve the problem uniformity along the z axis and its axial symmetry to infer that $\mathbf{v} = \mathbf{n}_z v(\rho)$, and $P = -\chi z + f(\rho, \varphi) + \text{const}$ (where $\boldsymbol{\rho} = \{\rho, \varphi\}$ is the 2D radius-vector rather than fluid density), so that the Navier-Stokes equation (44) for an incompressible fluid (with $\nabla \cdot \mathbf{v} = 0$) is reduced to a 2D Poisson equation

$$\eta \nabla_2^2 v = -\chi . \tag{8.55}$$

After spelling out the 2D Laplace operator in polar coordinates for our axially-symmetric case $\partial/\partial\varphi = 0$, Eq. (55) becomes a simple ordinary differential equation,

$$\eta \frac{1}{\rho}\frac{d}{d\rho}\left(\rho \frac{dv}{d\rho}\right) = -\chi , \tag{8.56}$$

that has to be solved at the segment $0 \le \rho \le R$, with the following boundary conditions:

$$\begin{aligned} &v = 0, \quad \text{at } \rho = R, \\ &\frac{dv}{d\rho} = 0, \quad \text{at } \rho = 0. \end{aligned} \tag{8.57}$$

(The latter condition is required by the axial symmetry.) A straightforward double integration yields:

$$v = \frac{\chi}{4\eta}(R^2 - \rho^2), \tag{8.58}$$

so that the integration of the mass flow density over the cross-section of the pipe,

$$Q \equiv \int_A \rho v d^2 r = 2\pi\rho \frac{\chi}{4\eta}\int_0^R (R^2 - \rho'^2)\rho' d\rho', \tag{8.59}$$

immediately gives us the so-called *Poiseuille* (or "Hagen-Poiseuille") *law* for the fluid discharge:

[30] It was solved theoretically by G. Stokes in 1845 in order to explain Eq. (60) that had been formulated by J. Poiseuille in 1840 on the basis of his experimental results.

Poiseuille law

$$Q = \frac{\pi}{8}\rho\frac{\chi}{\eta}R^4, \tag{8.60}$$

where (sorry!) ρ is the mass density again.

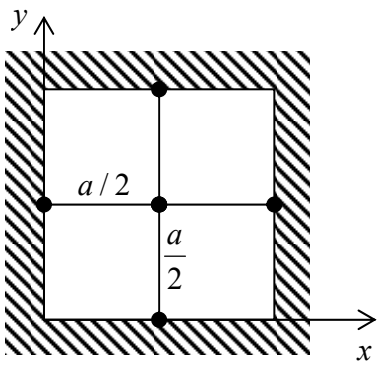

Fig. 8.10. Application of the finite-difference method with a very coarse mesh (with step $h = a/2$) to the problem of viscous fluid flow in a pipe with a square cross-section.

Of course, not for each cross-section shape the 2D Poisson equation (55) is so readily solvable. For example, consider a very simple, square-shape cross-section with side a (Fig. 10). For it, it is natural to use the Cartesian coordinates, so that Eq. (55) becomes

$$\frac{\partial^2 v}{\partial x^2} + \frac{\partial^2 v}{\partial y^2} = -\frac{\chi}{\eta} = \text{const}, \quad \text{for } 0 \le x, y \le a, \tag{8.61}$$

and has to be solved with boundary conditions

$$v = 0, \quad \text{at } x, y = 0, L. \tag{8.62}$$

For this boundary problem, analytical methods[31] give answers in the form of an infinite series that ultimately require computers for their plotting and comprehension. Let me use this pretext to discuss how explicitly numerical methods may be used for such problems - or any partial differential equations involving the Laplace operator. The simplest of them is the *finite-difference* method[32] in which the function to be calculated, $f(r_1,r_2,\ldots)$, is represented by its values in discrete points of a rectangular grid (frequently called *mesh*) of the corresponding dimensionality (Fig. 11).

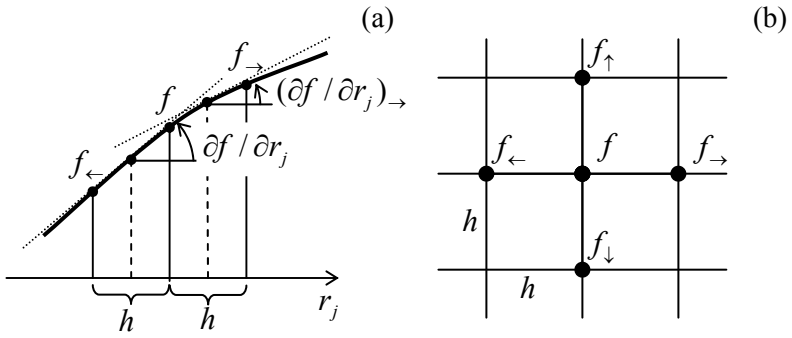

Fig. 8.11. Idea of the finite-difference method in (a) one and (b) two dimensions.

[31] For example, the Green's function method (see, e.g., EM Sec. 2.7).

[32] For more details see, e.g., R. J. Leveque, *Finite Difference Methods for Ordinary and Partial Differential Equations*, SIAM, 2007.

In Sec. 4.7, we have already discussed how to use such a grid to approximate the first derivative – see Eq. (4.98). Its extension to the second derivative is straightforward – see Fig. 11a:

$$\frac{\partial^2 f}{\partial r_j^2} = \frac{\partial}{\partial r_j}\left(\frac{\partial f}{\partial r_j}\right) \approx \frac{1}{h}\left(\frac{\partial f}{\partial r_j}_{\rightarrow} - \frac{\partial f}{\partial r_j}_{\leftarrow}\right) \approx \frac{1}{h}\left[\frac{f_{\rightarrow} - f}{h} - \frac{f - f_{\leftarrow}}{h}\right] = \frac{f_{\rightarrow} + f_{\leftarrow} - 2f}{h^2}. \tag{8.63}$$

The relative error of this approximation is of the order of $h^2\partial^4/\partial r_j^4$, quite acceptable in many cases. As a result, the left-hand part of Eq. (61), treated on a square mesh with step h (Fig. 11b), may be presented as the so-called *5-point scheme*:

$$\frac{\partial^2 v}{\partial x^2} + \frac{\partial^2 v}{\partial y^2} \approx \frac{v_{\rightarrow} + v_{\leftarrow} - 2v}{h^2} + \frac{v_{\uparrow} + v_{\downarrow} - 2v}{h^2} = \frac{v_{\rightarrow} + v_{\leftarrow} + v_{\uparrow} + v_{\downarrow} - 4v}{h^2}. \tag{8.64}$$

(The generalization to the *7-point scheme*, appropriate for 3D problems, is straightforward.)

Let us apply this scheme to the pipe with the square cross-section, using an extremely coarse mesh with step $h = a/2$ (Fig. 10). In this case the fluid velocity v should equal zero on the walls, i.e. in all points of the five-point scheme (Fig. 11b) except for the central point (in which velocity is evidently the largest), so that Eqs. (61) and (64) yield[33]

$$\frac{0 + 0 + 0 + 0 - 4v_{\max}}{(a/2)^2} \approx -\frac{\chi}{\eta}, \qquad \text{i.e. } v_{\max} \approx \frac{1}{16}\frac{\chi a^2}{\eta} \tag{8.65}$$

The resulting expression for the maximal velocity is only ~20% different from the exact value. Using a slightly finer mesh with $h = a/4$, which gives a readily solvable system of 3 linear equations for 3 different velocity values (the exercise highly recommended to the reader), brings us within a couple percent from the exact result. This shows that such "numerical" methods may be more efficient practically than the "analytical" ones, even if the only available tool is a calculator app on your smartphone rather than an advanced computer.

Of course, many practical problems of fluid dynamics do require high-performance computing, especially in conditions of turbulence (see the next section) with its complex, irregular spatial-temporal structure. In these conditions, the finite-difference approach may become unsatisfactory, because is implies the same accuracy of derivative approximation through the whole volume. A more powerful (but also much more complex for implementation) approach is the *finite-element method* in which the discrete point mesh is based on triangles with uneven sides, and is (in most cases, automatically) generated in accordance with the system geometry - see Fig. 12. Unfortunately I do not have time for going into the details of that method, so the reader is referred to the special literature on this subject.[34]

Before proceeding to our next topic, let me note one more important problem that is analytically solvable using the Navier-Stokes equation (51): a slow motion of a solid sphere of radius R, with a constant velocity $\mathbf{v}_0$, through an incompressible viscous fluid – or equivalently, a slow flow of the fluid

[33] Note that value (65) is exactly the same as given for $v_{\max} = v|_{\rho=0}$ by the analytical formula (58) for the round cross-section with radius $R = a/2$. This is not an occasional coincidence. The velocity distribution given by (58) is a quadratic function of both x and y. For such functions, with all derivatives higher than $\partial^2/\partial r_j^2$ being equal to zero, equation (64) is exact rather than approximate.

[34] See, e.g., C. Johnson, *Numerical Solution of Partial Differential Equations by the Finite Element Method*, Dover, 2009, or T. J. R. Hughes, *The Finite Element Method*, Dover, 2000.

(uniform at large distances) around an immobile sphere. Indeed, in the limit $v \to 0$, the second term in the left-hand part of this equation is negligible (just as at the surface wave analysis in Sec. 3), and the equation takes the form

$$-\nabla P + \eta \nabla^2 \mathbf{v} = 0, \tag{8.66}$$

which should be complemented with the incompressibility condition $\nabla \cdot \mathbf{v} = 0$ and boundary conditions

$$\begin{aligned} &\mathbf{v} = 0, \quad \text{at } r = R, \\ &\mathbf{v} \to \mathbf{v}_0, \text{ at } r \to \infty. \end{aligned} \tag{8.67}$$

In spherical coordinates, with the polar axis directed along vector $\mathbf{v}_0$, this boundary problem has the axial symmetry (so that $\partial \mathbf{v}/\partial \varphi = 0$ and $v_\varphi = 0$), and allows the following analytical solution:

$$v_r = v_0 \cos\theta \left(1 - \frac{3R}{2r} + \frac{R^3}{2r^2}\right), \quad v_\theta = -v_0 \sin\theta \left(1 - \frac{3R}{4r} - \frac{R^3}{4r^2}\right). \tag{8.68}$$

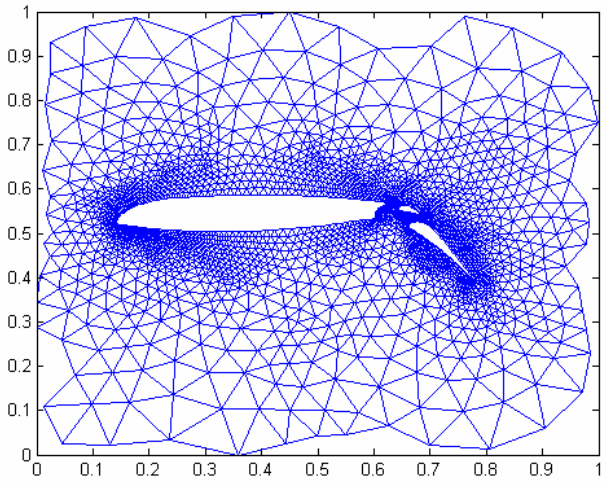

Fig. 8.12. Typical finite-element mesh generated automatically for an object of complex geometry – in this case, a plane wing's cross-section. (Figure adapted from www.mathworks.com.)

Calculating pressure from Eq. (66), and integrating it over the surface of the sphere it is now straightforward to obtain the famous *Stokes formula* for the drag force acting on the sphere:

Stokes formula

$$F = 6\pi\eta R v_0. \tag{8.69}$$

Historically, this formula has played an important role in the first precise (with accuracy better than 1%) calculation of the fundamental electric charge e by R. Millikan and H. Fletcher from their famous oil drop experiments in 1909-1913.

8.6. Turbulence

The Stokes formula (69), whose derivation is limited to low velocities at that the nonlinear term $(\mathbf{v}\cdot\nabla)\mathbf{v}$ could be neglected, become invalid if the fluid velocity is increased. For example, Fig. 13 shows the *drag coefficient* defined as

$$C_D \equiv \frac{F}{\rho v_0^2 A/2} \tag{8.70}$$

where A is the cross-section of the body as seen from the fluid flow direction, for a sphere of radius R (so that $A = \pi R^2$), as a function of the so-called *Reynolds number*,[35] for this particular geometry defined as

$$Re \equiv \frac{\rho v_0 (2R)}{\eta} = \frac{\rho v_0 D}{\eta}. \tag{8.71}$$

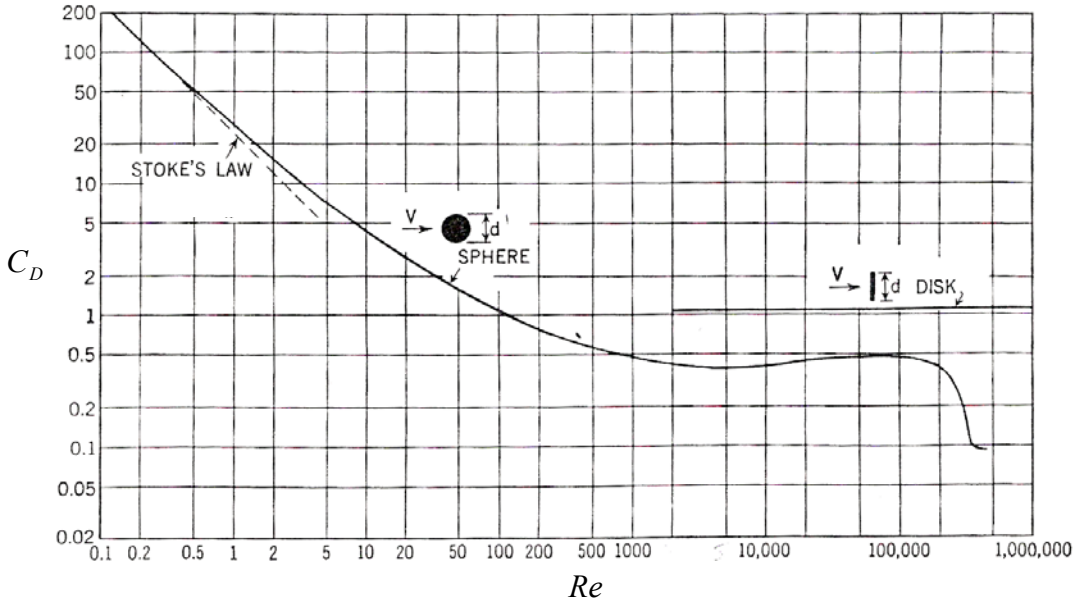

Fig. 8.13. The drag coefficient for a sphere and a round thin disk as functions of the Reynolds number. Adapted from F. Eisner, *Das Widerstandsproblem*, Proc. 3rd Int. Cong. On Appl. Mech., Stockholm, 1931.

In this notation, the Stokes formula (69) reads $C_D = 24/Re$. One can see this formula is only valid at $Re << 1$, while at larger velocities the drag force becomes substantially higher than that prediction, and its dependence on velocity very complicated, so that only its general, semi-quantitative features may be readily understood from simple arguments.[36]

The reason for this complexity is a gradual development of very intricate, time-dependent fluid patterns, called *turbulence*, rich with vortices – for an example, see Fig. 14. These vortices are especially pronounced in the region behind the moving body (so-called *wake*), while the region before

[35] This notion was introduced in 1851 by the same G. Stokes, but eventually named after O. Reynolds who popularized it three decades later.

[36] For example, Fig. 13 shows that, within a very broad range of Reynolds numbers, from ~10^2 to ~3×10^5, C_D for sphere is of the order of (and for a flat disk, remarkably close to) unity. This level, i.e., the approximate equality $F \approx \rho v_0^2 A/2$, may be understood (in the picture where the object is moved by an external force F with velocity v_0 through a fluid which is initially at rest) as the equality of force's power Fv_0 and fluid's kinetic energy $(\rho v_0^2/2)V$ created in volume $V = v_0 A$ in unit time. This relation would be exact if the object gave velocity v_0 to each and every fluid particle its cross-section runs into, for example by dragging all such particles behind itself. In reality, much of this kinetic energy goes into vortices – see Fig. 14 and its discussion below.

the body is virtually unperturbed. Figure 14 indicates that turbulence exhibits rather different behaviors in an extremely broad range of velocities (i.e. values of *Re*), and sometimes changes rather abruptly – see, for example, the significant drag drop at $Re \approx 5\times10^5$.

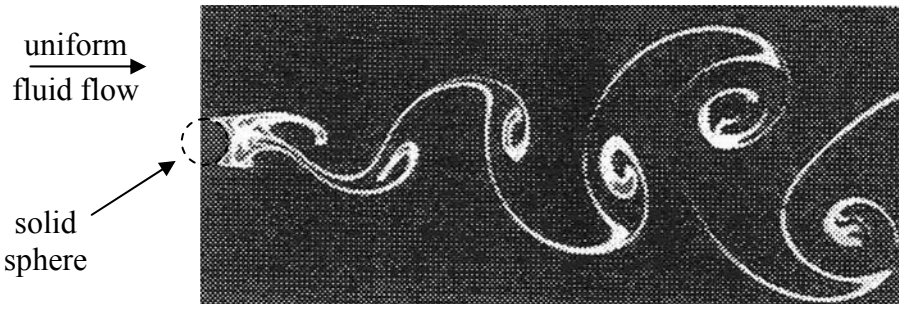

Fig. 8.14. Snapshot of the turbulent tail (*wake*) behind a sphere moving in a fluid with a high Reynolds number, showing the so-called *von Kármán vortex street*. A nice animation of such a pattern may be found at http://en.wikipedia.org/wiki/Reynolds_number.

In order to understand the conditions of this phenomenon, let us estimate the scale of various terms in the Navier-Stokes equation (51) for the generic case of a body with characteristic size l moving in an otherwise static, incompressible fluid, with velocity v. In this case the characteristic time scale of possible non-stationary phenomena is given by the ratio l/v,[37] so that we arrive at the following estimates:

$$\begin{array}{lcccc} \text{Equation term:} & \rho\dfrac{\partial \mathbf{v}}{\partial t} & \rho(\mathbf{v}\cdot\nabla)\mathbf{v} & \mathbf{f} & \eta\nabla^2\mathbf{v} \\ \text{Order of magnitude:} & \rho\dfrac{v^2}{l} & \rho\dfrac{v^2}{l} & \rho g & \eta\dfrac{v}{l^2} \end{array} \qquad (8.72)$$

(I have skipped term ∇P, because as we saw in the previous section, in typical fluid flow problems it balances the viscosity term, and hence is of the same order of magnitude.) This table shows that relative importance of the terms may be characterized by two dimensionless ratios.[38]

The first of them is the so-called *Froude number*

[37] The time scale of some problems may be different from l/v; for example, for forced oscillations of a fluid flow it is given by the reciprocal oscillation frequency f. For such problems, ratio $S \equiv f(l/v)$ serves as another, independent dimensionless constant, commonly called either the *Strouhal number* or the *reduced frequency*.

[38] For substantially compressible fluids (e.g., gases), the most important additional dimensionless parameter is the *Mach number* $M \equiv v/v_l$, where $v_l = (K/\rho)^{1/2}$ is the velocity of the longitudinal sound - which is, as we already know, the only wave mode possible in an infinite fluid. Especially significant for practice are *supersonic effects* (including the shock wave in the form of the famous *Mach cone* with half-angle $\theta_M = \arcsin M^{-1}$) which arise at $M > 1$. For a more thorough discussion of these issues, I have to refer the reader to more specialized texts – e.g., Chapter IX of the Landau and Lifshitz volume cited above, or Chapter 15 in I. M. Cohen and P. K. Kundu, *Fluid Mechanics*, 4th ed., Academic Press, 2007 - which is generally a good book on the subject. Another popular, rather simple textbook is R. A. Granger, *Fluid Mechanics*, Dover, 1995.

$$F \equiv \frac{\rho v^2 / l}{\rho g} = \frac{v^2}{lg}, \tag{8.73}$$

which characterizes the relative importance of bulk gravity - or, upon an appropriate modification, other bulk forces. In most practical problems (with the important exception of surface waves, see Sec. 4 above) $F >> 1$, so that the gravity effects may be neglected.

Much more important is another ratio, the Reynolds number (71), in the general case defined as

$$Re \equiv \frac{\rho v^2 / l}{\eta v / l^2} = \frac{\rho v l}{\eta}, \tag{8.74}$$

Reynolds number

which is a measure of the relative importance of the fluid particle's inertia in comparison with the viscosity effects.[39] Thus, it is not quite surprising that for a sphere, the role of the vorticity-creating term $(\mathbf{v}\cdot\nabla)\mathbf{v}$ becomes noticeable already at $Re \sim 1$ – see Fig. 13. Much more surprising is the onset of turbulence in systems where the laminar (turbulence-free) flow is formally an exact solution to the Navier-Stokes equation for any Re. For example, at $Re > Re_t \approx 2{,}100$ (with $l = 2R$ and $v = v_{max}$) the laminar flow in a round pipe, described by Eq. (58), becomes unstable, and the resulting turbulence decreases the fluid discharge Q in comparison with the Poiseuille law (60). Even more strikingly, the critical value of Re is rather insensitive to the pipe wall roughness.

Since $Re >> 1$ in many real-life situations,[40] turbulence is very important for practice. However, despite nearly a century of intensive research, there is no general, quantitative analytical theory of this phenomenon,[41] and most results are still obtained either by rather approximate analytical treatments, or by the numerical solution of the Navier-Stokes equations using the approaches discussed in the previous section, or in experiments (e.g., on scaled models[42] in *wind tunnels*).

Unfortunately, due to the time/space restrictions, for a more detailed discussion of these results I have to refer the reader to more specialized literature,[43] and will conclude the chapter with a brief discussion of just one issue: can the turbulence be "explained by a singe mechanism"? (In other words, can it be reduced, at least on a semi-quantitative level, to a set of simpler phenomena that are commonly considered "well understood"?) Apparently the answer in *no*,[44] though nonlinear dynamics of simpler systems may provide some useful insights.

---

[39] Note that the "dynamic" viscosity η participates in this number (and many other problems of fluid dynamics) only in the combination η/ρ that thereby has deserved a special name of *kinematic viscosity*.

[40] For example, the values of η and ρ for water listed in Table 1 imply that for a few-meter object, $Re > 1{,}000$ at any speed above just ~1 mm/s.

[41] A rare exception is the relatively recent theoretical result by S. Orszag (1971) for the turbulence threshold in a flow of an incompressible fluid through a gap of thickness t between two parallel plane walls: $Re_t \approx 5{,}772$ (for $l = t/2$, $v = v_{max}$). However, this result does not predict the turbulence patterns at $Re > Re_t$.

[42] The crucial condition of correct modeling is the equality of the Reynolds numbers (74) (and if relevant, also of the Froude numbers and/or the Mach numbers) of the object of interest and its model.

[43] See, e.g., P. A. Davidson, *Turbulence*, Oxford U. Press, 2004.

[44] The following famous quote is attributed to W. Heisenberg on his deathbed: "When I meet God, I will ask him two questions: Why relativity? And why turbulence? I think he will have an answer for the first question." Though probably inaccurate, this story reflects rather well the understandable frustration of the fundamental physics community, known for their reductionist mentality, with the enormous complexity of phenomena which obey simple (e.g., Navier-Stokes) equations.

At the middle of the past century, the most popular qualitative explanation of turbulence had been the formation of an "energy cascade" that would transfer energy from larger to smaller vortices. With our background, it is easier to retell that story in the time-domain language (with velocity v serving as the conversion factor), using the fact that in a rotating vortex each component of the particle radius-vector oscillates in time, so that to some extent the vortex plays the role of an oscillatory motion mode. Let us consider the passage of a solid body between the two, initially close, small parts of fluid. The body pushes them apart, but after its passage these partial volumes are free to return to their initial positions. However, the domination of inertia effects at motion with $Re >> 1$ means that the volumes continue to "oscillate" for a while about those equilibrium positions. (Since elementary volumes of an incompressible fluid cannot merge, these oscillations take the form of rotating vortices.)

Now, from Sec. 4.8 we know that intensive oscillations in a system with quadratic nonlinearity, in this case provided by the convective term $(\mathbf{v}\cdot\nabla)\mathbf{v}$, are equivalent, for small perturbations, to the oscillation of the system parameters at the corresponding frequency. On the other hand, the discussion in Sec. 5.5 shows that in a system with two oscillatory degrees of freedom, a periodic parameter change with frequency ω_p may lead to non-degenerate parametric excitation of oscillations with frequencies $\omega_{1,2}$ satisfying relation $\omega_1 + \omega_2 = \omega_p$. Moreover, the spectrum of oscillations in such system also has higher combinational frequencies such as $(\omega_p + \omega_1)$, thus pushing the oscillation energy up the frequency scale. In the presence of other oscillatory modes, these oscillations may in turn produce, via the same nonlinearity, even higher frequencies, etc. In a fluid, the spectrum of these "oscillatory modes" (actually, vortex structures) is essentially continuous, so that the above arguments make very plausible a sequential transfer of energy to a broad spectrum of modes - whose frequency spectrum is limited from above by the energy dissipation due to viscosity. When excited, these modes interact (in particular, phase-lock) through system's nonlinearity, creating the complex motion we call turbulence.

Though not having much quantitative predictive power, such handwaving explanations, which are essentially based on the excitation of a *large* number of effective degrees of freedom, had been dominating the fluid dynamics reviews until the mid-1960s. At that point, the discovery (or rather re-discovery) of quasi-random motion in classical dynamic systems with just *a few* degrees of freedom altered the discussion substantially. Since this phenomenon, called the *deterministic chaos*, extends well beyond the fluid dynamics, and I will devote to it a separate (albeit short) next chapter, and in its end briefly return to the discussion of turbulence.

8.7. Exercise problems

8.1. A solid round cylinder of radius r is let to float in a water inside the glass, also of a round cylindrical form with radius R - see Fig. on the right, which shows the water levels before and after the submersion, and some vertical dimensions of the system. Calculate the buoyant force F exerted by water on the floating body.

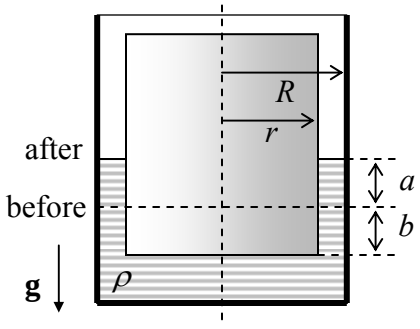

Hint: This is just a fast check whether the reader understands the Archimedes principle correctly.

8.2. Pressure P under a free water surface crudely obeys the Pascal law, Eq. (6). Find the first-order corrections to this result, due to small compressibility of water.

8.3. Find the stationary shape of the open surface of an incompressible, heavy fluid rotated about a vertical axis with a constant angular velocity ω – see Fig. on the right.

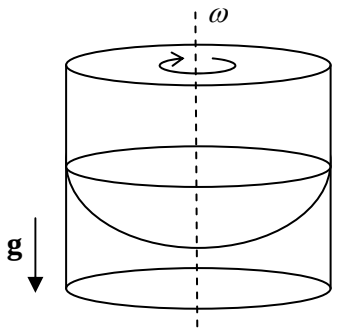

8.4.* Calculate the shape of the surface of an incompressible fluid of density ρ near a vertical plane wall, in a uniform gravity field – see Fig. on the right. In particular, find the height h of liquid's rise at the wall surface as a function of the contact angle θ_c.

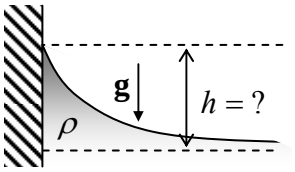

8.5.* A soap film with surface tension γ is stretched between two similar, coaxial, thin, round rings of radius R, separated by distance d – see Fig. on the right. Neglecting gravity, calculate the equilibrium shape of the film, and the force needed for keeping it stretched.

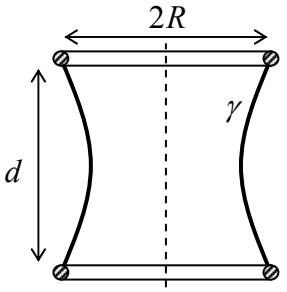

8.6. A solid sphere of radius R is kept in a steady, vorticity-free flow of an ideal incompressible fluid, with velocity v_0. Find the spatial distribution of velocity and pressure, and in particular their extremal values. Compare the results with those obtained in Sec. 4 for a round cylinder.

8.7.* A small source, located at distance d from a plane wall of a container filled with an ideal, incompressible fluid of density ρ, injects additional fluid isotropically, at a constant mass current ("discharge") $Q \equiv dM/dt$ – see Fig. on the right. Calculate fluid's velocity distribution, and its pressure on the wall, created by the flow.

Hint: Recall the charge image method in electrostatics,[45] and contemplate its possible analog.

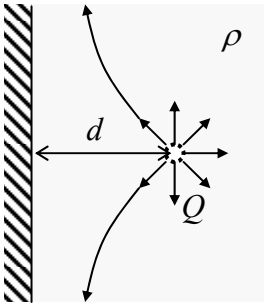

8.8. Derive Eq. (46) for surface waves on a finite-thickness layer of a heavy liquid.

8.9. Derive Eq. (48) for the capillary waves ("ripples").

[45] See, e.g., EM Secs. 2.6, 3.3, and 4.3.

8.10.* Derive a 2D differential equation describing propagation of waves on the surface of a broad layer, of constant thickness h, of an ideal, incompressible fluid, and use it to calculate the longest standing wave modes and frequencies in a layer covering a spherical planet of radius $R >> h$.

Hint: The second assignment requires some familiarity with the basic properties of spherical harmonics.[46]

8.11. Calculate the velocity distribution and dispersion relation of waves propagating along the horizontal interface of two ideal, incompressible fluids of different densities.

8.12. Calculate the energy of a monochromatic, plane surface wave on an, ideal, incompressible, deep fluid, and the power it carries (per unit width of wave's front).

8.13. Use the finite-difference approximation for the Laplace operator, with mesh $h = a/4$, to find the maximum velocity and total mass flow Q of a viscous, incompressible fluid through a long pipe with a square-shaped cross-section of side a. Compare the results with those described in Sec. 4 for:

(i) the same problem with mesh $h = a/2$, and
(ii) a pipe with circular cross-section of the same area.

8.14. A layer, of thickness h, of a heavy, viscous, incompressible fluid flows down a long and wide incline plane, under its own weight – see Fig. on the right. Find the stationary velocity distribution profile, and the total fluid discharge (per unit width.)

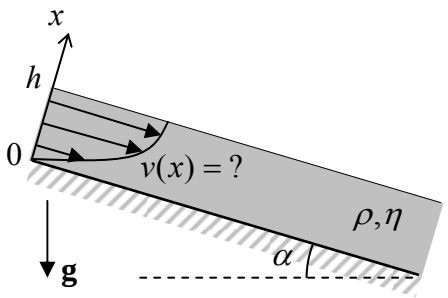

8.15. Calculate the torque exerted on a unit length of a solid round cylinder of radius R that rotates about its axis, with angular velocity ω, inside an incompressible fluid with viscosity η.

8.16. Calculate the tangential force (per unit area) exerted by incompressible fluid, with density ρ and viscosity η, on a broad solid plane placed over its surface and forced to oscillate, along the surface, with amplitude a and frequency ω.

8.17. A massive barge, with a flat bottom of area A, floats in shallow water, with clearance $h << A^{1/2}$ (see Fig. on the right). Calculate the time dependence of barge's velocity $V(t)$, and the water velocity profile, after the barge's engine has been turned off. Discuss the limits of large and small values of the dimensionless parameter $M/\rho A h$.

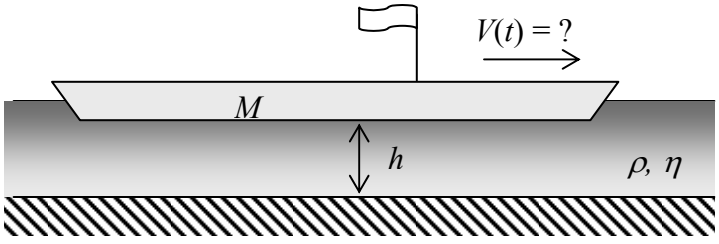

[46] See, e.g., EM Sec. 2.5(iv) and/or QM Sec. 3.6.

8.18.* Derive a general expression for mechanical energy loss rate in a viscous incompressible fluid that obeys the Navier-Stokes equation, and use this expression to calculate the attenuation coefficient of surface waves, assuming that the viscosity is small (quantify this condition).

8.19. Use the Navier-Stokes equation to calculate the attenuation coefficient for a plane, sinusoidal acoustic wave.

Chapter 9. Deterministic Chaos

This chapter gives a very brief review of chaotic phenomena in deterministic maps and dynamic systems with and without dissipation, and an even shorter discussion of the possible role of chaos in fluid turbulence.

9.1. Chaos in maps

Chaotic behavior of dynamic systems[1] (sometimes called the *deterministic chaos*) has become broadly recognized[2] after the publication of a 1963 paper by E. Lorenz who was examining numerical solutions of the following system of three nonlinear, ordinary differential equations,

Lorenz system

$$\begin{aligned} \dot{q}_1 &= a_1(q_2 - q_1), \\ \dot{q}_2 &= a_2 q_1 - q_2 - q_1 q_3, \\ \dot{q}_3 &= q_1 q_2 - a_3 q_3, \end{aligned} \tag{9.1}$$

as a rudimentary model for heat transfer through a horizontal liquid layer between two solid plates. (Experiment shows that if the bottom plate is kept hotter than the top one, the liquid may exhibit turbulent convection.) He has found that within a certain range of constants $a_{1,2,3}$, the solutions of Eq. (1) follow complex, unpredictable, non-repeating trajectories in the 3D q-space. Moreover, the resulting functions $q_j(t)$ (where $j = 1, 2, 3$) are so sensitive to initial conditions $q_j(0)$ that at sufficiently large times t, solutions corresponding to slightly different initial conditions are completely different.

Very soon it was realized that such behavior is typical for even simpler mathematical objects called *maps*, so that I will start my discussion of chaos from these objects. A 1D map is essentially a rule for finding the next number q_{n+1} of a series, in the simplest case using only its last known value q_n, in a discrete series numbered by integer index n. The most famous example is the so-called *logistic map*:[3]

Logistic map

$$q_{n+1} = f(q_n) \equiv r q_n (1 - q_n). \tag{9.2}$$

The basic properties of this map may be understood using the (hopefully, self-explanatory) graphical presentation shown in Fig. 1.[4] One can readily see that at $r < 1$ (Fig. 1a) the map rapidly converges to the trivial fixed point $q^{(0)} = 0$, because each next value of q is less than the previous one. However, if r is increased above 1 (as in the example shown in Fig. 1b), fixed point $q^{(0)}$ becomes unstable. Indeed, at $q_n << 1$, map (2) yields $q_{n+1} = r q_n$, so that at $r > 1$, values q_n grow with each iteration. Instead of the unstable point $q^{(0)} = 0$, in the range $1 < r < r_1$, where $r_1 \equiv 3$, the map has a stable fixed point, $q^{(1)}$, that may be found by plugging this value into both parts of Eq. (2):

---

[1] In this context, this term is understood as "systems described by deterministic differential equations".

[2] Actually, the notion of quasi-random dynamics due to the exponential divergence of trajectories may be traced back at least to (apparently independent) works by J. Poincaré in 1892 and by J. Hadamard in 1898. Citing Poincaré, "*...it may happen that small differences in the initial conditions produce very great ones in the final phenomena*. […] *Prediction becomes impossible*."

[3] Its chaotic properties were first discussed in 1976 by R. May, though the map itself is one of simple ecological models repeatedly discussed earlier, and may be traced back at least to the 1838 work by P. Verhulst.

[4] Since the maximum value of function $f(q)$, achieved at $q = ½$, equals $r/4$, the mapping may be limited by segment $x = [0, 1]$, if parameter r is between 0 and 4. Since all interesting properties of the map, including chaos, may be found within these limits, I will focus on this range.

$$q^{(1)} = rq^{(1)}(1-q^{(1)}), \tag{9.3}$$

giving $q^{(1)} = (1 - 1/r)$ – see the left branch of the plot shown in Fig. 2.

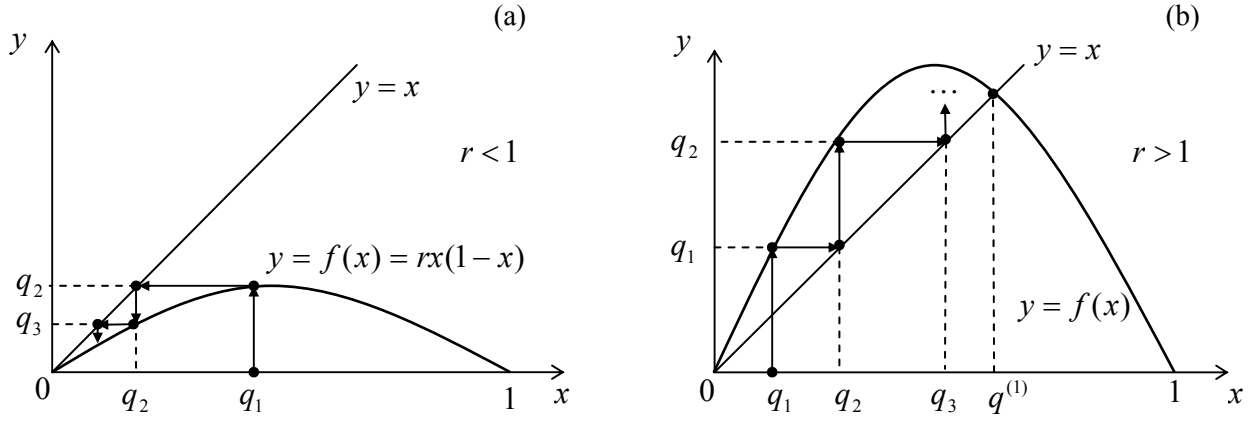

Fig. 9.1. Graphical analysis of the logistic map for: (a) $r < 1$ and (b) $r > 1$.

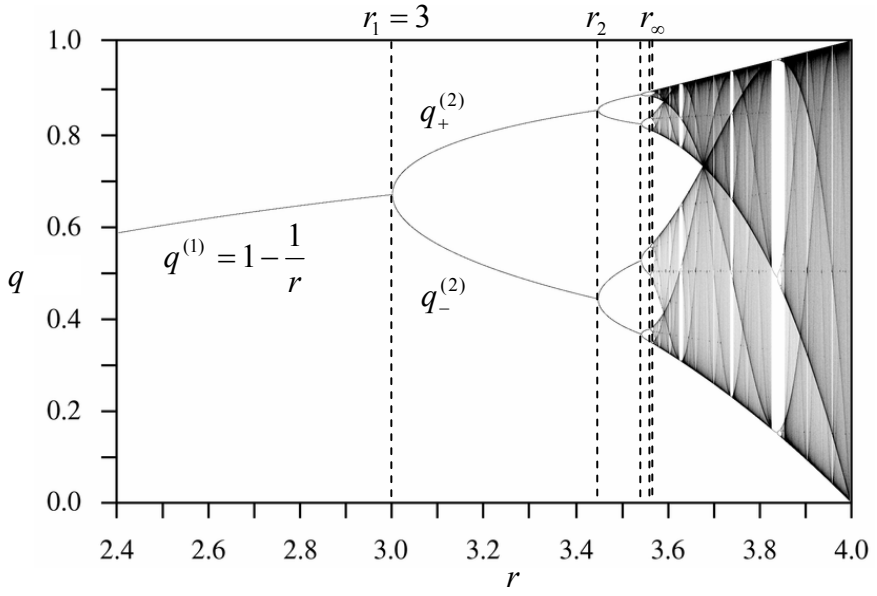

Fig. 9.2. Fixed points and chaotic regions of the logistic map. The plot is adapted from http://en.wikipedia.org/wiki/Logistic_map; a very nice live simulation of the map is also available on this Web site.

At $r > r_1 = 3$, the plot gets thicker: here the fixed point $q^{(1)}$ also becomes unstable. To prove that, let us take $q_n = q^{(1)} + \tilde{q}_n$, assume that deviation $\tilde{q}_n$ from the fixed point $q^{(1)}$ is small, and linearize map (3) in $\tilde{q}_n$, just as we repeatedly did for differential equations earlier in this course. The result is

$$\tilde{q}_{n+1} = \left.\frac{df}{dq}\right|_{q=q^{(1)}} \tilde{q}_n = r(1-2q^{(1)})\tilde{q}_n = (2-r)\tilde{q}_n. \tag{9.4}$$

It shows that $0 < 2 - r < 1$, i.e. $1 < r < 2$, deviations $\tilde{q}_n$ decrease monotonically. At $-1 < 2 - r < 0$, i.e. in the range $2 < r < 3$, the deviation signs alternate but the magnitude still decreases (as in a stable focus – see Sec. 4.6). However, at $-1 < 2 - r$, i.e. $r > r_1 = 3$, the deviations are growing by magnitude, while still changing sign, at each step. Since Eq. (2) has no other fixed points, this means that at $n \to \infty$, values

q_n do not converge to one point; rather, within the range $r_1 < r < r_2$, they approach a *limit cycle* of alternation of two points, $q_+^{(2)}$ and $q_-^{(2)}$ that satisfy the following system of algebraic equations

$$q_+^{(2)} = f(q_-^{(2)}),\ q_-^{(2)} = f(q_+^{(2)}). \tag{9.5}$$

(These points are also plotted in Fig. 2, as functions of parameter r.) What has happened at point r_1 is called the *period-doubling bifurcation*. The story repeats at $r = r_2 = 1 + \sqrt{6} \approx 3.45$ where the system goes from the 2-point limit cycle to a 4-point cycle, then at point $r = r_3 \approx 3.54$ at that the limit cycle becomes consisting of 8 alternating points, etc. Most remarkably, the period-doubling bifurcation points r_n, at that the number of points in the limit cycle doubles from 2^{n-1} points to 2^n points, become closer and closer. Numerical calculations have shown that these points obey the following asymptotic behavior:

Feigenbaum bifurcation sequence

$$r_n \to r_\infty - \frac{C}{\delta^n}, \quad \text{where } r_\infty = 3.5699..., \quad \delta = 4.6692... \tag{9.6}$$

Parameter δ is called the *Feigenbaum constant*; for other maps, and some dynamic systems (see the next section), period-doubling sequences follow a similar law, but with different parameter δ.

More important for us, however, is what happens at $r > r_\infty$. Numerous numerical experiments, repeated with increasing precision,[5] have confirmed that here the system is fully disordered, with no reproducible limit cycle, though (as Fig. 2 shows) at $r \approx r_\infty$, all sequential values q_n are still confined to a few narrow regions.[6] However, as parameter r is increased well beyond r_∞, these regions broaden and merge. This the so-called *full*, or *well-developed* chaos, with no apparent order at all.[7]

The most important feature of chaos (in this and any other system) is the *exponential divergence of trajectories*. For a 1D map, this means that even if the initial conditions q_1 in two map implementations differ by a very small amount Δq_1, the difference Δq_n between the corresponding sequences q_n is growing (on the average) exponentially with n. Such exponents may be used to characterize chaos. Indeed, let us assume that Δq_1 is so small that N first values q_n are relatively close to each other. Then an evident generalization of the first of Eqs. (4) to an arbitrary point q_n is

$$\Delta q_{n+1} = e_n \Delta q_n, \qquad e_n \equiv \left.\frac{df}{dq}\right|_{q=q_n}. \tag{9.7}$$

Using this result iteratively for N steps, we get

$$\Delta q_N = \Delta q_1 \prod_{n=1}^{N} e_n, \qquad \text{so that } \ln\left|\frac{\Delta q_N}{\Delta q_1}\right| = \sum_{n=1}^{N} \ln|e_n|. \tag{9.8}$$

[5] The reader should remember that just as the usual ("nature") experiments, numerical experiments also have limited accuracy, due to unavoidable rounding errors.

[6] The geometry of these regions are essentially *fractal*, i.e. has a dimensionality intermediate between 0 (which any final set of geometric points would have) and 1 (pertinent to a 1D continuum). An extensive discussion of fractal geometries, and their relation to the deterministic chaos may be found, e.g., in the book by B. B. Mandelbrot, *The Fractal Geometry of Nature*, W. H. Freeman, 1983.

[7] This does not mean that the chaos development is a monotonic function of r. As Fig. 2 shows, within certain intervals of this parameter chaos suddenly disappears, being replaced, typically, with a few-point limit cycle, just to resume on the other side of the interval. Sometimes (but not always!) the "route to chaos" on the borders of these intervals follows the same Feigenbaum sequence of period-doubling bifurcations.

Numerical experiments show that in most chaotic regimes, at $N \to \infty$ such a sum fluctuates about an average, which grows as λN, with parameter

$$\lambda = \lim_{\Delta q_1 \to 0} \lim_{N \to \infty} \frac{1}{N} \sum_{n=1}^{N} \ln |e_n| , \tag{9.9}$$

Lyapunov exponent

called the *Lyapunov exponent*,[8] being independent on the initial conditions. The bottom panel in Fig. 3 shows it as a function of the parameter r for the logistic map (2).

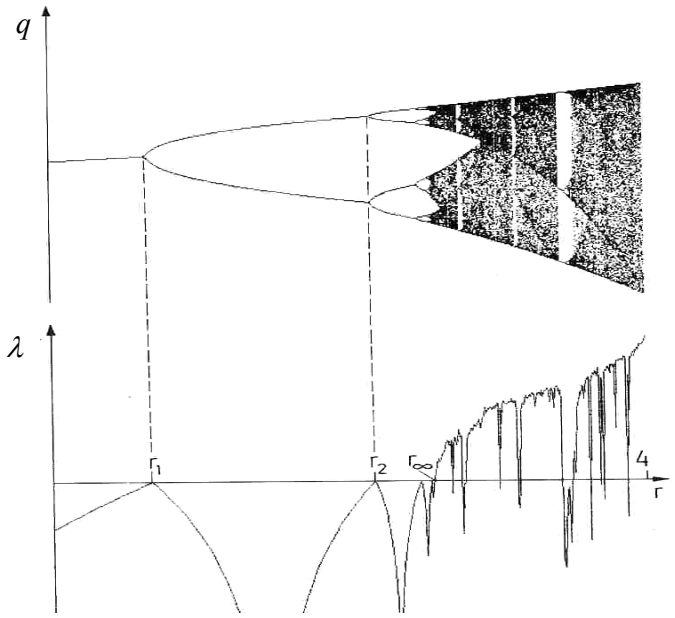

Fig. 9.3. The Lyapunov exponent for the logistic map. Adapted from the monograph by Schuster and Just (cited below). © WileyVCH Verlag GmbH & Co. KGaA.

Note that at $r < r_\infty$, λ is negative, indicating trajectory's stability, besides points r_1, r_2, … where λ would become positive if the limit cycle change had not brought it back to the negative territory. However, at $r > r_\infty$, λ becomes positive, returning the negative values only in limited intervals of stable limit cycles. It is evident that in numerical experiments (which dominate the studies of the deterministic chaos) the Lyapunov exponent may be used as a good measure of chaos' "depth".[9]

Despite all the abundance of results published for particular maps,[10] and several interesting general observations (like the existence of the Feigenbaum bifurcation sequences), to the best of my knowledge nobody can yet predict the patterns like those shown in Fig. 2 and 3, from just looking at the map rule itself, i.e. without carrying out actual numerical experiments with in. Unfortunately the situation with chaos in other systems is not much better.

[8] After A. Lyapunov (1857-1918), famous for his studies of stability of dynamic systems.

[9] N-dimensions maps, which relate N-dimensional vectors rather than scalars, may be characterized by N Lyapunov exponents rather than one. In order to have chaotic behavior, it is sufficient for just one of them to become positive. For such systems, another measure of chaos, the *Kolmogorov entropy,* may be more relevant. This measure, and its relation with the Lyapunov exponents, are discussed, e.g., in SM Sec. 2.2.

[10] See, e.g., Chapters 2-4 in H. G. Schuster and W. Just, *Deterministic Chaos*, 4th ed., Wiley-VCH, 2005, or Chapters 8-9 in J. M. T. Thompson and H. B. Stewart, *Nonlinear Dynamics and Chaos*, 2nd ed., Wiley, 2002.

9.2. Chaos in dynamic systems

Proceeding to the discussion of chaos in dynamic systems, it is more natural, with our background, to illustrate this discussion not with the Lorenz' system Eqs. (1), but with the system of equations describing a dissipative pendulum driven by a sinusoidal external force, which was repeatedly discussed in Chapter 4. Introducing two new variables, the normalized momentum $p \equiv \dot{q}/\omega_0$ and the external force's full phase $\psi \equiv \omega t$, we may rewrite Eq. (4.42) describing the pendulum,

$$\ddot{q} + 2\delta\dot{q} + \omega_0^2 \sin q = f_0 \cos\omega t\,, \tag{9.10a}$$

in a form similar to Eq. (1), i.e. as a system of three first-order ordinary differential equations:

$$\begin{aligned} \dot{q} &= \omega_0 p, \\ \dot{p} &= -\omega_0 \sin q - 2\delta p + (f_0/\omega_0)\cos\psi, \\ \dot{\psi} &= \omega. \end{aligned} \tag{9.10b}$$

Figure 4 several results of numerical solution of Eq. (10).[11] In all cases, the internal parameters δ and ω_0 of the system, and the external force amplitude f_0 are fixed, while the external frequency ω is gradually changed. For the case shown on the top panel, the system still tends to a stable periodic solution, with low contents of higher harmonics. If the external force frequency is reduced by a just few percent, the 3rd subharmonic may be excited. (This effect has already been discussed in Sec. 4.8 – see, e.g., Fig. 4.15.) The next panel shows that just a very small further reduction of frequency leads to a new tripling of the period, i.e. the generation of a complex waveform with the 9th subharmonic. Finally, even a minor further change of parameters leads to oscillations without any visible period, e.g., chaos.

In order to trace this transition, direct observation of the oscillation waveforms $q(t)$ is not very convenient, and trajectories on the phase plane $[q, p]$ also become messy if plotted for many periods of the external frequency. In situations like this, the Poincaré (or "stroboscopic") plane, already discussed in Sec. 4.6, is much more useful. As a reminder, this is essentially just the phase plane $[q, p]$, but with the points highlighted only once a period, e.g., at $\psi = 2\pi n$, with $n = 1, 2, \ldots$ On this plane, periodic oscillations of frequency ω are presented just as one fixed point – see, e.g. the top panel in the right column of Fig. 4. The beginning of the 3rd subharmonic generation, shown on the next panel, means tripling of the oscillation period, and is reflected on the Poincaré plane by splitting the fixed point into three. It is evident that this transition is similar to the period-doubling bifurcation in the logistic map, besides the fact (already discussed in Sec. 4.8) that in systems with an asymmetric nonlinearity, such as the pendulum (10), the 3rd subharmonic is easier to excite. From this point, the 9th harmonic generation (shown on the 3rd panel of Fig. 4), i.e. one more splitting of the points on the Poincaré plane, may be understood as one more step on the Feigenbaum-like route to chaos – see the bottom panel of that figure.

So, the transition to chaos in dynamic systems may be at least qualitatively similar to than in 1D maps, with the similar law (6) for the critical values of some parameter r of the system (in Fig. 4, frequency ω), though generally with a different value of exponent δ. Moreover, it is evident that we can always consider the first two differential equations of system (10b) as a 2D map that relates the vector $\{q_{n+1}, p_{n+1}\}$ of the coordinate and velocity, measured at $\psi = 2\pi(n + 1)$, with the previous value $\{q_n, p_n\}$

[11] In the actual simulation, a small term εq, with $\varepsilon << 1$, has been added to the left-hand part of this equation. This term slightly somewhat tames the trend of the solution to spread along q axis, and makes the presentation of results easier, without affecting the system dynamics too much.

of that vector (reached at $\psi = 2\pi m$). Unfortunately this similarity also implies that chaos in dynamical systems is at least as complex, and it as little understood, as in maps.

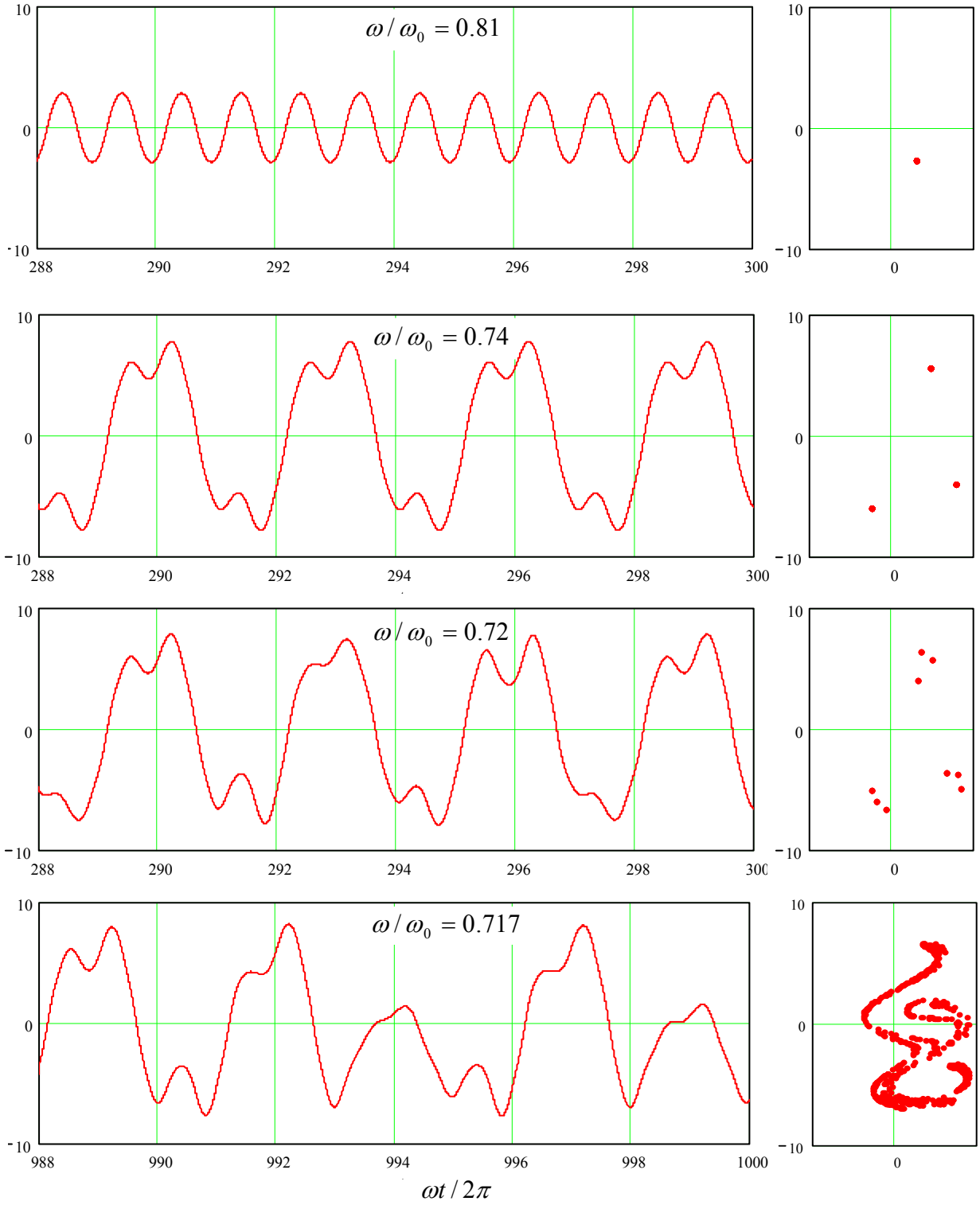

Fig. 9.4. Oscillations in a pendulum with weak damping, $\delta/\omega_0 = 0.1$, driven by a sinusoidal external force with a fixed effective amplitude $f_0/\omega_0^2 = 1$, and several close values of the frequency (listed on the panels). Left column: oscillation waveforms $q(t)$ recorded after certain initial transient intervals. Right column: representations of the same processes on the Poincaré plane of variables $[p, q]$.

For example, Fig. 5 shows (a part of) the state diagram of the externally-driven pendulum, with the red bar marking the route to chaos traced in Fig. 4, and shading/hatching styles marking different regimes. One can that the pattern is at least as complex as that shown in Figs. 2 and 3, and besides a few features,[12] is equally unpredictable from the form of the equation.

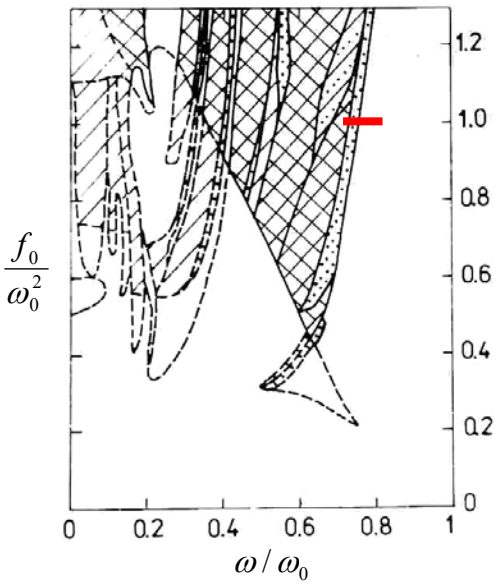

Fig. 9.5. Phase diagram of an externally-driven pendulum with $\delta/\omega_0 = 0.1$. Regions of oscillations with the basic period are not shaded. The notation for other regions is as follows. Doted: subharmonic generation; cross-hatched: chaos; hatched: chaos or basic period (depending on the initial conditions); hatch-dotted: basic period or subharmonics. Solid lines show boundaries of single-regime regions, while dashed lines are boundaries of regions in which several types of motion are possible, depending on history. (Figure courtesy V. Kornev.)

Are there any valuable general results concerning chaos in dynamic systems? The most important (though an almost evident) result is that this phenomenon is impossible in any system described by one or two first-order differential equations with right-hand parts independent of time. Indeed, let us start with a single equation

$$\dot{q} = f(q), \tag{9.11}$$

where $f(q)$ is any single-valued function. This equation may be directly integrated to give

$$t = \int^{q} \frac{dq'}{f(q')} + \text{const}, \tag{9.12}$$

showing that the relation between q and t is unique and hence does not leave place for chaos.

Now, let us explore the system of two such equations:

$$\begin{aligned} \dot{q}_1 &= f_1(q_1, q_2), \\ \dot{q}_2 &= f_2(q_1, q_2). \end{aligned} \tag{9.13}$$

Consider its phase plane shown schematically in Fig. 6. In a "usual" system, the trajectories approach either some fixed point (Fig. 6a) describing static equilibrium, or a limit cycle (Fig. 6b) describing periodic oscillations. (Both notions are united by the term *attractor*, because they "attract" trajectories launched from various initial conditions.) However, phase plane trajectories of a chaotic system of

[12] In some cases, it is possible to predict a parameter region where chaos *cannot* happen, due to lack of any instability-amplification mechanism. Unfortunately, typically the analytically predicted boundaries of such region form a rather loose envelope of the actual (numerically simulated) chaotic regions.

equations that describe real physical variables (which cannot tend to infinity), should be confined to a limited phase plane area, and simultaneously cannot start repeating each other. (This topology is frequently called the *strange attractor*.) For that, 2D trajectories need to cross – see, e.g., point *A* in Fig. 6c.

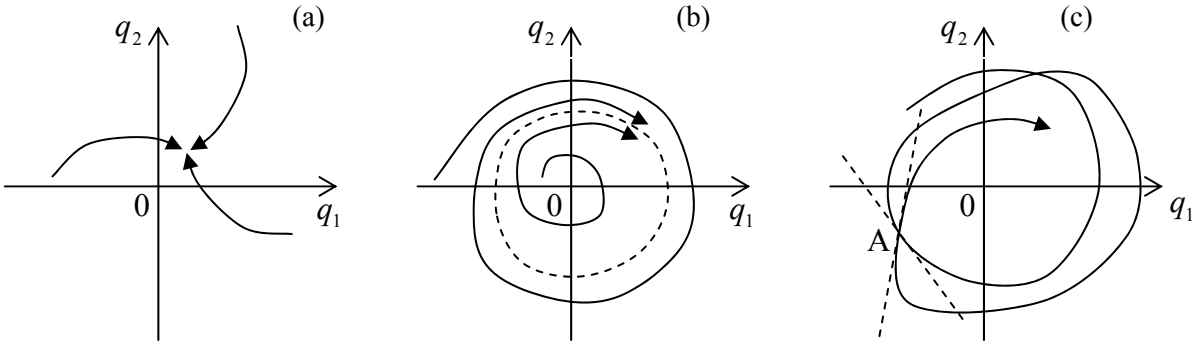

Fig. 9.6. Attractors in dynamical systems: (a) a fixed point, (b) a limit cycle, and (c) a strange attractor.

However, in the case described by Eqs. (13), this is clearly impossible, because according to these equations, the tangent slope on the phase plane is a unique function of point coordinates $\{q_1, q_2\}$:

$$\frac{dq_1}{dq_2} = \frac{f_1(q_1, q_2)}{f_2(q_1, q_2)}. \tag{9.14}$$

Thus, in this case the deterministic chaos is impossible.[13] It becomes, however, readily possible if the right-hand parts of a system similar to Eq. (13) depend either on other variables of the system or time. For example, if we consider the first two differential equations of system (10b), in the case $f_0 = 0$ they have the structure of the system (13) and hence chaos is impossible, even at $\delta < 0$ when (as we know from Sec. 4.4) the system allows self-excitation of oscillations – leading to a limit-cycle attractor. However, if $f_0 \neq 0$, this argument does not work any longer and (as we have already seen) the system may have a strange attractor – which is, for dynamic systems, a synonym for the deterministic chaos. Thus, chaos is possible in dynamic systems that may be described by three or more differential equations of the first order.[14]

9.3. Chaos in Hamiltonian systems

The last analysis is of course valid for Hamiltonian systems, which are just a particular type of dynamic systems. However, one may wonder whether these systems, that feature at least one first integral of motion, H = const, and hence are more "ordered" than the systems discussed above, can exhibit chaos at all. The question is yes, because such systems still can have mechanisms for an exponential growth of a small initial perturbation.

[13] A mathematically-strict formulation of this statement is called the Poincaré-Bendixon theorem, which was proved by I. Bendixon as early as in 1901.

[14] Since a typical dynamic system with one degree of freedom is described by two such equations, the number of the first-order equations describing a dynamic system is sometimes called the number of *half-degrees of freedom*. This notion is very useful and popular in statistical mechanics – see, e.g., SM Sec. 2.2 and on.

As the simplest way to show it, let us consider a so-called *mathematical billiard*, i.e. a ballistic particle (a "ball") moving freely by inertia on a horizontal plane surface ("table") limited by rigid impenetrable walls. In this idealized model of the usual game of billiards, ball's velocity $\mathbf{v}$ is conserved when it moves on the table, and when it runs into a wall, the ball is elastically reflected from it as from a mirror,[15] with the reversal of the sign of the normal velocity v_n, and conservation of the tangential velocity v_τ, and hence without any loss of its kinetic (and hence the full) energy

$$E = H = T = \frac{m}{2}v^2 = \frac{m}{2}\left(v_n^2 + v_\tau^2\right). \tag{9.15}$$

This model, while being a legitimate 2D dynamic system,[16] allows geometric analyses for several simple table shapes. The simplest case is a rectangular billiard of area $a \times b$ (Fig. 7), whose analysis may be readily carried out by the replacement of each *ball* reflection event with the mirror reflection of the *table* in that wall – see dashes lines in panel (a).

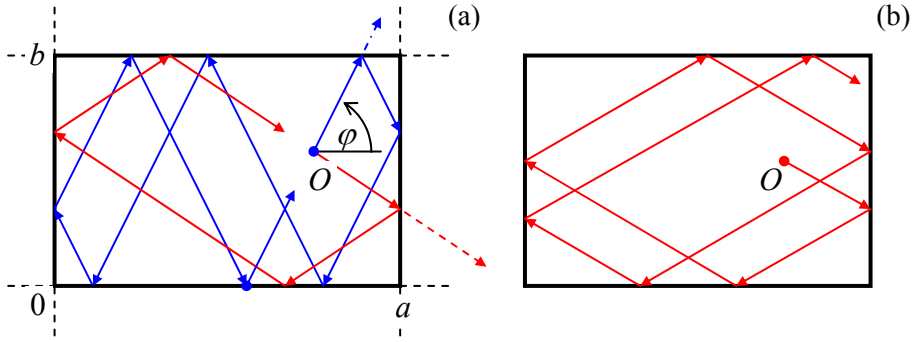

Fig. 9.7. Ball motion on a rectangular billiard at (a) a commensurate, and (b) an incommensurate launch angle.

Such analysis (left for reader' pleasure :-) shows that if the tangent of the ball launching angle φ is commensurate with the side length ratio,

$$\tan\varphi = \pm\frac{m}{n}\frac{b}{a}, \tag{9.16}$$

where n and m are non-negative integers without common integer multipliers, the ball returns exactly to the launch point O, after bouncing m times from each wall of length a, and n times from each wall of length b. (Red lines in Fig. 7a show an example of such trajectory for $n = m = 1$, while blue lines, for $m = 3$, $n = 1$.) Thus the larger is the sum $(m + n)$, the more complex is such closed trajectory - "orbit".

Finally, if $(n + m) \to \infty$, i.e. $\tan\varphi$ and b/a are incommensurate (meaning that their ratio is an irrational number), the trajectory covers all the table area, and the ball never returns exactly into the launch point. Still, this is not the real chaos. Indeed, a small shift of the launch point shifts all the trajectory fragments by the same displacement. Moreover, at any time t, each of Cartesian components $v_j(t)$ of the ball's velocity (with coordinate axes parallel to the table sides) may take only two values, $\pm v_j(0)$, and hence may vary only as much as the initial velocity is being changed.

[15] A more scientific-sounding name for such a reflection is *specular* (from Latin "speculum" meaning a metallic mirror).

[16] Indeed, it is fully described by Lagrangian function $L = mv^2/2 - U(\boldsymbol{\rho})$, with $U(\boldsymbol{\rho}) = 0$ for 2D radius-vectors $\boldsymbol{\rho}$ belonging to the table area, and $U(\boldsymbol{\rho}) = +\infty$ outside of the area.

In 1963, Ya. Sinai showed that the situation changes completely if an additional wall, in the shape of a circle, is inserted into the rectangular billiard (Fig. 8). For most initial conditions, ball's trajectory eventually runs into the circle (see the red line on panel (a) as an example), and the further trajectory becomes essentially chaotic. Indeed, let us consider ball's reflection from the circle-shaped wall – Fig. 8b. Due to the conservation of the tangential velocity, and the sign change of the normal velocity component, the reflection obeys the mechanical analog of the Snell law (cf. Fig. 7.12 and its discussion): $\theta_r = \theta_i$. Figure 8b shows that as the result, a small difference $\delta\varphi$ between the angles of two close trajectories (as measured in the lab system), doubles by magnitude at each reflection from the curved wall. This means that the small deviation grows along the ball trajectory as

$$\left|\delta\varphi(N)\right| \sim \left|\delta\varphi(0)\right| \times 2^N = \left|\delta\varphi(0)\right| e^{N \ln 2}, \tag{9.17}$$

where N is the number of reflections from the convex wall.[17] As we already know, such exponential divergence of trajectories, with a positive Lyapunov exponent, is the sign of deterministic chaos.[18]

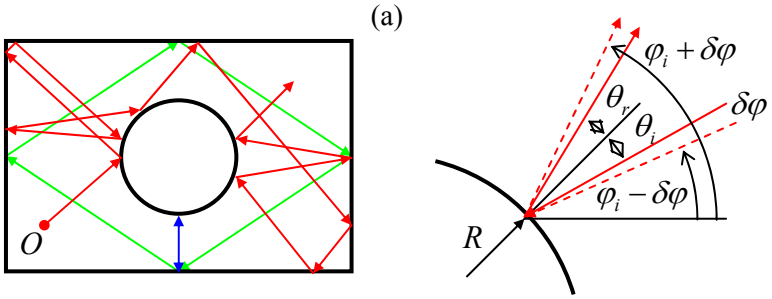

Fig. 9.8. (a) Motion on a Sinai billiard table, and (b) the mechanism of the exponential divergence of close trajectories.

The most important new feature of the dynamic chaos in Hamiltonian systems is its dependence on initial conditions. (In the systems discussed in the previous two previous sections, that lack the integrals of motion, the initial conditions are rapidly "forgotten", and the chaos is usually characterized after cutting out the initial transient period – see, e.g., Fig. 4.) Indeed, even a Sinai billiard allows periodic motion, along closed orbits, at certain initial conditions – see the blue and green lines in Fig. 8a as examples. Thus the chaos "depth" in such systems may be characterized by the "fraction"[19] of the phase space of initial parameters (for a 2D billiard, the 3D space of initial values of x, y, and φ) resulting in chaotic trajectories.

This conclusion is also valid for Hamiltonian systems that are met in experiments more frequently than the billiards, for example, coupled nonlinear oscillators without damping. Perhaps, the

[17] Superficially, Eq. (17) is also valid for a plane wall, but as was discussed above, a billiard with such walls features a full correlation between sequential reflections, so that angle φ always returns to its initial value. In a Sinai billiard, such correlation disappears. Because of that, concave walls may also make a billiard chaotic. A famous example is the *stadium billiard*, suggested by L. Bunimovich, with two straight, parallel walls connecting two semi-circular, concave walls. Another example, which allows a straightforward analysis, is the *Hadamard billiard*: an infinite (or rectangular) table with non-horizontal surface of negative curvature.

[18] Billiards are also a convenient platform for a discussion of a conceptually important issue of quantum properties of classically chaotic systems (sometimes improperly named "quantum chaos").

[19] Actually, quantitative characterization of the fraction is not trivial, because it may have fractal dimensionality. Unfortunately, due to lack of time I have to refer the reader interested in this issue to special literature, e.g., the monograph by B. Mandelbrot (cited above) and references therein.

earliest and the most popular example is the so-called *Hénon-Heiles* system,[20] which may be descrbed by the following Lagrangian function:

$$L = \frac{m_1}{2}\left(\dot{q}_1^2 - \omega_1^2 q_1^2\right) + \frac{m_2}{2}\left(\dot{q}_2^2 - \omega_2^2 q_2^2\right) - \varepsilon\left(q_1^2 - \frac{1}{3}q_2^2\right)q_2 . \tag{9.18}$$

Hénon-Heiles system

It is straightworward to use Eq. (18) to derive the Lagrangian equations of motion,

$$\begin{aligned} m_1\left(\ddot{q}_1 + \omega_1^2 q_1\right) &= -2\varepsilon q_1 q_2 , \\ m_2\left(\ddot{q}_2 + \omega_2^2 q_2\right) &= -\varepsilon\left(q_1^2 - q_2^2\right), \end{aligned} \tag{9.19}$$

and find its first integral of motion (physically, the energy conservation law):

$$H = E = \frac{m_1}{2}\left(\dot{q}_1^2 + \omega_1^2 q_1^2\right) + \frac{m_2}{2}\left(\dot{q}_2^2 + \omega_2^2 q_2^2\right) + \varepsilon\left(q_1^2 - \frac{1}{3}q_2^2\right)q_2 = \text{const} . \tag{9.20}$$

In the conext of our discussions in Chapter 4 and 5, Eqs. (19) may be readily interpreted as those describing two oscillators, with small-oscillation eigenfrequencies ω_1 and ω_2, nonlinearly coupled only as described by the terms in the right-hand parts of the equations. This means that as the oscillation amplitudes $A_{1,2}$, and hence the total energy E of the system, tend to zero, the oscillator subsystems are virtually independent, each performing sinusoidal oscillations at its own frequency. This observation suggestes a convenient way to depict the system motion.[21] Let us consider a Poincaré plane for one of the oscillators (say, with coordinate q_2), similar to that discussed in Sec. 2 above, with the only difference is that (because of the absence of an explicit function of time in system's equations), the trajectory on the $[q_2, \dot{q}_2]$ plane is highlighted at the moments when $q_1 = 0$.

Let us start from the limit $A_{1,2} \to 0$, when oscillations of q_2 are virtually sinusoidal. As we already know (see Fig. 4.9 and its discussion), if the representation point highlighting was perfectly synchronous with frequency ω_2 of the oscillations, there would be only one point on the Poincaré plane – see, e.g. the right top plane in Fig. 4. However, at the q_1 – initiated highlighting, there is not such synchronism, so that each period, a different point of the elliptical (at the proper scaling of the velocity, circular) trajectory is highlighted, so that the resulting points, for certain initial conditions, reside on a circle of radius A_2. If we now vary the initial conditions, i.e. redistribute the initial energy between the oscillators, but keep the total energy E constant, on the Poincaré plane we get a series of ellipses.

Now, if the initial energy is increased, nonlinear interaction of the oscillations start to deform these ellipses, causing also their crossings – see, e.g., the top left panel of Fig. 9. Still, below a certain threshold value of E, all Poincaré points belonging to a certain initial condition sit on a single closed

[20] It was first studied in 1964 by M. Hénon and C. Heiles as a simple model of star rotation about a gallactic center. Most studies of this equation have been carried out for the following particular case: $m_2 = 2m_1$, $m_1\omega_1^2 = m_2\omega_2^2$. In this case, introducing new variables $x \equiv \varepsilon q_1$, $y \equiv \varepsilon q_2$, and $\tau \equiv \omega_1 t$, it is possible to rewrite Eqs. (18)-(20) in parameter-free forms. All the results shown in Fig. 9 below are for this case.

[21] Generally, it has a trajectory in 4D space, e.g., that of coordinates $q_{1,2}$ and their time derivatives, although the first integral of motion (20) means that for each fixed energy E, the motion is limited to a 3D sub-space. Still, this is too much for convenient representation of the motion.

contour. Moreover, these contours may be calculated approximately, but with a pretty good accuracy, using a straighforward generalization of the small parameter method discussed in Sec. 4.2.[22]

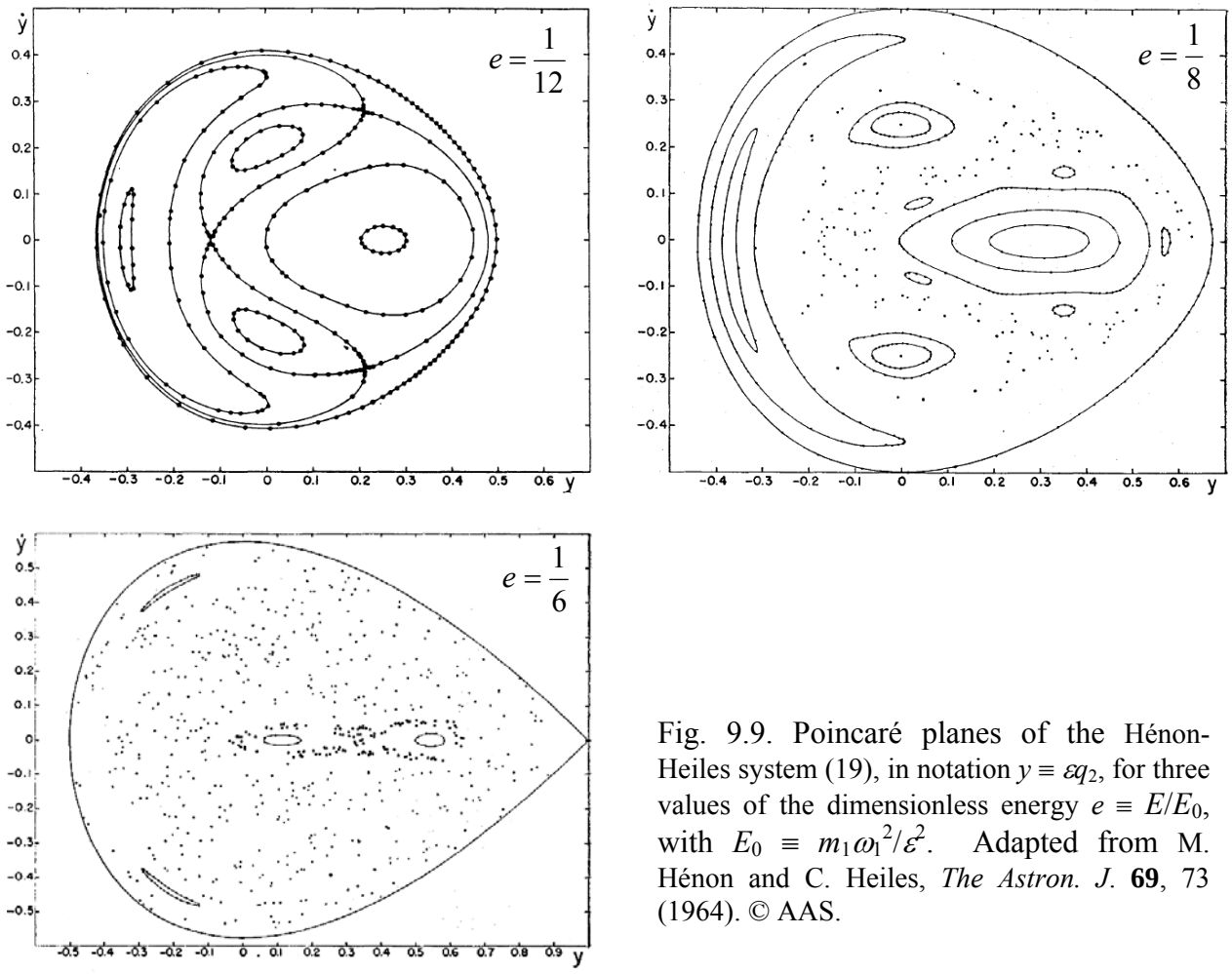

Fig. 9.9. Poincaré planes of the Hénon-Heiles system (19), in notation $y \equiv \varepsilon q_2$, for three values of the dimensionless energy $e \equiv E/E_0$, with $E_0 \equiv m_1\omega_1^2/\varepsilon^2$. Adapted from M. Hénon and C. Heiles, *The Astron. J.* **69**, 73 (1964). © AAS.

However, starting from some value of energy, certain initial conditions lead to series of points scattered over final-area parts of the Poincaré plane – see the top right panel of Fig. 9. This means that the corresponding oscillations $q_2(t)$ do not repeat from one (quasi-) period to the next one – cf. Fig. 4 for the dissipative, forced pendulum. This is chaos.[23] However, some other initial conditions still lead to closed contours. This feature is similar to Sinai billiards, and is typical for Hamiltonian systems. As the energy is increased, the larger and larger part of the Poincaré plane belongs to the chaotic motion, signifying deeper and deeper chaos.

[22] See, e.g., M. V. Berry, in: S. Jorna (ed.), *Topics in Nonlinear Dynamics*, AIP Conf. Proc. No. 46, AIP, 1978, pp. 16-120.

[23] This fact complies with the necessary condition of chaos, discussed in the end of Sec. 2, because Eqs. (19) may be rewritten as a system of four differential equations of the first order.

9.4. Chaos and turbulence

This extremely short section consists of essentially just one statement, extending the discussion in Sec. 8.5. The (re-) discovery of the deterministic chaos in systems with just a few degrees of freedom in the 1960s changed the tone of debates concerning origins of turbulence very considerably. At first, an extreme point of view that equated the notions of chaos and turbulence, became the debate's favorite.[24] However, after an initial excitement, a significant evidence of the Landau-style mechanisms, involving many degrees of freedom, has been rediscovered and could not be ignored any longer. To the best knowledge of this author, who is a very distant albeit interested observer of that field, most experimental and numerical-simulation data carry features of both mechanisms, so that the debate continues.[25] Due to the age difference, most readers of these notes have much better chances than the author to see where will this discussion end (if it does :-).[26]

9.5. Exercise problems

9.1. Generalize the reasoning of Sec. 1 to an arbitrary 1D map $q_{n+1} = f(q_n)$, with function $f(q)$ differentiable at all points of interest. In particular, derive the condition of stability of an N-point limit cycle $q^{(1)} \to q^{(2)} \to \ldots \to q^{(N)} \to q^{(1)}$.

9.2. Use the stability condition, derived in Problem 9.1, to analyze chaos excitation in the so-called *tent map*:

$$f(q) = \begin{cases} rq, & \text{for } 0 \le q \le 1/2, \\ r(1-q), & \text{for } 1/2 \le q \le 1, \end{cases} \quad \text{with } 0 \le r \le 2.$$

9.3. A dynamic system is described by the following system of ordinary differential equations:

$$\dot{q}_1 = -q_1 + a_1 q_2^3,$$
$$\dot{q}_2 = a_2 q_2 - a_3 q_2^3 + a_4 q_2 (1 - q_1^2).$$

Can it exhibit chaos at some set of constant parameters a_1-a_4?

9.4. A periodic function of time has been added to the right-hand part of the first equation of the system considered in the previous problem. Is chaos possible now?

[24] An important milestone on that way was the work by S. Newhouse *et al.*, *Comm. Math. Phys*. **64**, 35 (1978), who proved the existence of a strange attractor in a rather abstract model of fluid flow.

[25] See, e.g., U. Frisch, Turbulence: *The Legacy of A. N. Kolmogorov*, Cambridge U. Press, 1996.

[26] The reader interested in the deterministic chaos as such, may also like to have a look at a very popular book by S. Strogatz, *Nonlinear Dynamics and Chaos*, Westview, 2001.

This page is intentionally left blank

Chapter 10. A Bit More of Analytical Mechanics

This concluding chapter reviews two alternative approaches to analytical mechanics, whose main advantage is a closer parallel to quantum mechanics in general and to its quasiclassical (WKB) approximation in particular. One of them, the Hamiltonian formalism, is also used to derive an important asymptotic result, the adiabatic invariance, for classical systems with slowly changing parameters.

10.1. Hamilton equations

Throughout this course we have seen how useful the analytical mechanics, in its Lagrangian form, may be invaluable for solving various particular problems of classical mechanics. Now let us discuss several alternative formulations[1] that may not be much more useful for this purpose, but shed light on possible extensions of classical mechanics, most importantly to quantum mechanics.

As was already discussed in Sec. 2.3, the partial derivative $p_j \equiv \partial L / \partial \dot{q}_j$ participating in the Lagrange equations (2.19)

$$\frac{d}{dt}\frac{\partial L}{\partial \dot{q}_j} - \frac{\partial L}{\partial q_j} = 0, \tag{10.1}$$

may be considered as the generalized momentum corresponding to generalized coordinate q_j, and the full set of this momenta may be used to define the Hamiltonian function (2.32):

Hamiltonian function

$$H \equiv \sum_j p_j \dot{q}_j - L\,. \tag{10.2}$$

Now let us rewrite the full differential of this function[2] in the following form:

$$\begin{aligned} dH = d\left(\sum_j p_j \dot{q}_j - L\right) &= \sum_j \left[d(p_j)\dot{q}_j + p_j d(\dot{q}_j)\right] - dL \\ &= \sum_j \left[d(p_j)\dot{q}_j + p_j d(\dot{q}_j)\right] - \left[\frac{\partial L}{\partial t}dt + \sum_j \left(\frac{\partial L}{\partial q_j}d(q_j) + \frac{\partial L}{\partial \dot{q}_j}d(\dot{q}_j)\right)\right]. \end{aligned} \tag{10.3}$$

According to the definition of the generalized momentum, the second terms of each sum over j cancel, while according to the Lagrange equation (1), the derivative $\partial L / \partial q_j$ is just $\dot{p}_j$, so that

$$dH = -\frac{\partial L}{\partial t}dt + \sum_j \left(\dot{q}_j dp_j - \dot{p}_j dq_j\right). \tag{10.4}$$

So far, this is just a universal identity. Now comes the main trick of Hamilton's approach: let us consider H a function of the following independent arguments: time t, the generalized coordinates q_j,

[1] Due mostly to W. Hamilton (1805-1865) and C. Jacobi (1804-1851).
[2] Actually, this differential has already been used in Sec. 2.3 to derive Eq. (2.35).

and the generalized momenta p_j (rather than generalized velocities). With this commitment, the general rule of differentiation of a function of several arguments gives

$$dH = \frac{\partial H}{\partial t}dt + \sum_j \left(\frac{\partial H}{\partial q_j}dq_j + \frac{\partial H}{\partial p_j}dp_j \right), \tag{10.5}$$

where dt, dq_j, and dp_j are independent differentials. Since Eq. (5) should be valid for any choice of these argument differentials, it should hold in particular if the differentials correspond to the real law of motion, for which Eq. (4) is valid as well. The comparison of Eqs. (4) and (5) gives us three relations:

$$\frac{\partial H}{\partial t} = -\frac{\partial L}{\partial t}. \tag{10.6}$$

$$\boxed{\begin{aligned} \dot{q}_j &= \frac{\partial H}{\partial p_j}, \\ \dot{p}_j &= -\frac{\partial H}{\partial q_j}. \end{aligned}} \tag{10.7}$$

Hamilton equations

Comparing the first of them with Eq. (2.35), we see that

$$\frac{dH}{dt} = \frac{\partial H}{\partial t}, \tag{10.8}$$

meaning that function $H(t, q_j, p_j)$ can change in time only via its explicit dependence on t. Eqs. (7) are even more substantial: provided that such function $H(t, q_j, p_j)$ has been calculated, they give us two first-order differential equations (called the *Hamilton equations*) for the time evolution of the generalized coordinate and generalized momentum of each degree of freedom of the system.[3]

Let us have a look at these equations for the simplest case of a system with one degree of freedom, with the simple Lagrangian function (3.3):

$$L = \frac{m_{\text{ef}}}{2}\dot{q}^2 - U_{\text{ef}}(q,t). \tag{10.9}$$

In this case, $p \equiv \partial L/\partial \dot{q} = m_{\text{ef}}\dot{q}$, and $H \equiv p\dot{q} - L = m_{\text{ef}}\dot{q}^2/2 + U_{\text{ef}}(q,t)$. In order to honor our new commitment, we need to express the Hamiltonian function explicitly via t, q and p (rather than $\dot{q}$):

$$H = \frac{p^2}{2m_{\text{ef}}} + U_{\text{ef}}(q,t). \tag{10.10}$$

Now we can spell out Eqs. (7) for this particular case:

$$\dot{q} = \frac{\partial H}{\partial p} = \frac{p}{m_{\text{ef}}}, \tag{10.11}$$

[3] Of course, the right-hand part of each equation (7) generally can include coordinates and momenta of other degrees of freedom as well, so that the equations of motion for different j are generally coupled.

$$\dot{p} = -\frac{\partial H}{\partial q} = -\frac{\partial U_{\text{ef}}}{\partial q}. \tag{10.12}$$

While the first of these equations just repeats the definition of the generalized momentum corresponding to coordinate q, the second one gives the equation of momentum change. Differentiating Eq. (11) over time, and plugging Eq. (12) into the result, we get:

$$\ddot{q} = \frac{\dot{p}}{m_{\text{ef}}} = -\frac{1}{m_{\text{ef}}}\frac{\partial U_{\text{ef}}}{\partial q}. \tag{10.13}$$

So, we have returned to the same equation (3.4) that had been derived from the Lagrangian approach.

Thus, the Hamiltonian formalism does not give much new for the solution of most problems of classical mechanics. (This is why I have postponed its discussion until the very end of this course.) Moreover, since the Hamiltonian function $H(t, q_j, p_j)$ does nor include generalized velocities explicitly, the phenomenological introduction of dissipation in this approach is less straightforward than that in the Lagrangian equations whose precursor form (2.17) is valid for dissipative forces as well. However, the Hamilton equations (7), which treat the generalized coordinates and momenta in a manifestly symmetric way, are aesthetically appealing and heuristically fruitful. This is especially true in the cases where these arguments participate in H in a similar way. For example, for the very important case of a dissipation-free harmonic oscillator, for which $U_{\text{ef}} = \kappa_{\text{ef}}q^2/2$, Eq. (10) gives the famous symmetric form

$$H = \frac{p^2}{2m_{\text{ef}}} + \frac{\kappa_{\text{ef}}x^2}{2} = \frac{p^2}{2m_{\text{ef}}} + \frac{m_{\text{ef}}\omega_0^2 x^2}{2}, \quad \text{where } \omega_0^2 \equiv \frac{\kappa_{\text{ef}}}{m_{\text{ef}}}. \tag{10.14}$$

The Hamilton equations (7) for this system preserve the symmetry, especially evident if we introduce the normalized momentum $\not{p} \equiv p/m_{\text{ef}}\omega_0$ (already used in Secs. 4.3 and 9.2):

$$\frac{dq}{dt} = \omega_0 \not{p}, \quad \frac{d\not{p}}{dt} = -\omega_0 q. \tag{10.15}$$

More practically, the Hamilton approach gives additional tools for the search for the integrals of motion. In order to see that, let us consider the full time derivative of an arbitrary function $f(t, q_j, p_j)$:

$$\frac{df}{dt} = \frac{\partial f}{\partial t} + \sum_j \left(\frac{\partial f}{\partial q_j}\dot{q}_j + \frac{\partial f}{\partial p_j}\dot{p}_j \right). \tag{10.16}$$

Plugging in $\dot{q}_j$ and $\dot{p}_j$ from the Hamilton equations (7), we get

Dynamics of arbitrary variable

$$\boxed{\frac{df}{dt} = \frac{\partial f}{\partial t} + \sum_j \left(\frac{\partial H}{\partial p_j}\frac{\partial f}{\partial q_j} - \frac{\partial H}{\partial q_j}\frac{\partial f}{\partial p_j} \right) = \frac{\partial f}{\partial t} + \{H, f\},} \tag{10.17}$$

where the last term in the right-hand part is the so-called *Poisson bracket*[4] that is defined, for two arbitrary functions $f(t, q_j, p_j)$ and $g(t, q_j, p_j)$, as

Poisson bracket

$$\boxed{\{g, f\} \equiv \sum_j \left(\frac{\partial g}{\partial p_j}\frac{\partial f}{\partial q_j} - \frac{\partial f}{\partial p_j}\frac{\partial g}{\partial q_j} \right).} \tag{10.18}$$

[4] Named after S. Poisson - of the Poisson equation and the Poisson statistical distribution fame.

From this definition, one can readily verify that besides evident relations $\{f, f\} = 0$ and $\{f, g\} = -\{g, f\}$, the Poisson brackets obey the following important *Jacobi identity*:

$$\{f,\{g,h\}\}+\{g,\{h,f\}\}+\{h,\{f,g\}\}=0. \tag{10.19}$$

Now let us use these relations for a search for integrals of motion. First, equation (17) shows that if a function f does not depend on time explicitly, and

$$\{H, f\}=0, \tag{10.20}$$

then $df/dt = 0$, i.e. function f is an integral of motion.

Moreover, if we already know two integrals of motion, say f and g, then function

$$F \equiv \{f, g\} \tag{10.21}$$

is also an integral of motion – the so-called *Poisson theorem*. In order to prove it, we may use the Jacobi identity (19) with $h = H$. Now using Eq. (17) to express the Poisson brackets $\{g, H\}$, $\{H, g\}$, and $\{H,\{f, g\}\} = \{H, F\}$ via the full and partial time derivatives of functions f, g, and F, we get

$$\left\{f,\frac{\partial g}{\partial t}-\frac{dg}{dt}\right\}+\left\{g,\frac{df}{dt}-\frac{\partial f}{\partial t}\right\}+\frac{dF}{dt}-\frac{\partial F}{\partial t}=0, \tag{10.22}$$

so that if f and g are indeed integrals of motion, i.e., $df/dt = dg/dt = 0$, then

$$\frac{dF}{dt}=\frac{\partial F}{\partial t}+\left\{g,\frac{\partial f}{\partial t}\right\}-\left\{f,\frac{\partial g}{\partial t}\right\}=\frac{\partial F}{\partial t}-\left[\left\{\frac{\partial f}{\partial t},g\right\}+\left\{f,\frac{\partial g}{\partial t}\right\}\right]. \tag{10.23}$$

Plugging Eq. (21) into the first term of the right-hand part of this equation, and differentiating it by parts, we get $dF/dt = 0$, i.e. F is indeed an integral of motion as well.

Finally, one more important role of the Hamilton formalism is that it allows one to trace the close connection between the classical and quantum mechanics. Indeed, using Eq. (18) to calculate the Poisson brackets of the generalized coordinates and momenta, we readily get

$$\{q_j, q_{j'}\}=0, \quad \{p_j, p_{j'}\}=0, \quad \{q_j, p_{j'}\}=-\delta_{jj'}. \tag{10.24}$$

In quantum mechanics,[5] operators of these quantities ("observables") obey commutation relations

$$[\hat{q}_j,\hat{q}_{j'}]=0, \quad [\hat{p}_j,\hat{p}_{j'}]=0, \quad [\hat{q}_j,\hat{p}_{j'}]=i\hbar\delta_{jj'}, \tag{10.25}$$

where the definition of the commutator, $[\hat{g}, \hat{f}] \equiv \hat{g}\,\hat{f} - \hat{f}\,\hat{g}$, is *to a certain extent* [6] similar to that (18) of the Poisson bracket. We see that the classical relations (24) are similar to quantum-mechanical relations (25) if we following parallel has been made:

$$\{g, f\} \leftrightarrow \frac{i}{\hbar}[\hat{g}, \hat{f}]. \tag{10.26}$$

CM ↔ QM relation

[5] See, e.g., QM Sec. 2.1.

[6] There is of course a conceptual difference between the "usual" products of function derivatives participating in the Poisson brackets, and the operator "products" (meaning their sequential action on a state vector – see, e.g., QM Sec. 4.1) forming the commutator.

This analogy extends well beyond Eqs. (24)-(25). For example, making replacement (26) in Eq. (17), we get

$$\frac{d\hat{f}}{dt} = \frac{\partial \hat{f}}{\partial t} + \frac{i}{\hbar}\left[\hat{H}, \hat{f}\right], \qquad \text{i.e. } i\hbar\frac{d\hat{f}}{dt} = i\hbar\frac{\partial \hat{f}}{\partial t} + \left[\hat{f}, \hat{H}\right], \tag{10.27}$$

which is the correct equation of operator evolution in the Heisenberg picture of quantum mechanics.[7]

This analogy implies, in particular, that the quantum-mechanical operators (and the matrices used for their representation in a particular basis) should satisfy the same identities including Eq. (17).

10.2. Adiabatic invariance

One more application of the Hamiltonian formalism in classical mechanics is the solution of the following problem.[8] Earlier in the course, we already studied some effects of time variation of parameters of a single oscillator (Sec. 4.5) and coupled oscillators (Sec. 5.5). However, those discussions were focused on the case when the parameter variation frequency is comparable with the initial oscillation frequency (or frequencies) of the system. Another practically important case is when some system's parameter (let us call it λ) is changed much more slowly (*adiabatically*[9]),

$$\left|\frac{\dot{\lambda}}{\lambda}\right| << \frac{1}{\mathcal{T}}, \tag{10.28}$$

where $\mathcal{T}$ is a typical time period of oscillations in the system. Let us consider a 1D system whose Hamiltonian $H(q, p, \lambda)$ depends on time only via the slow (28) evolution of parameter $\lambda = \lambda(t)$, and whose initial energy restricts system's motion to a finite coordinate interval – see Fig. 3.2c.

Then, as we know from Sec. 3.3, if parameter λ is constant, the system performs a periodic (though not necessarily sinusoidal) motion back and forth axis q, or, in a different language, along a closed trajectory on the phase plane $[q, p]$ – see Fig. 1.[10] According to Eq. (8), in this case H is constant on the trajectory. (In order to distinguish this particular *value* from the Hamiltonian *function* as such, I will assume that this constant coincides with the full mechanical energy E, like is does for Hamiltonian (10), though this assumption is not necessary for the calculation made below.)

The oscillation period $\mathcal{T}$ may be calculated as a contour integral along this closed trajectory:

$$\mathcal{T} \equiv \int_0^{\mathcal{T}} dt = \oint \frac{dt}{dq} dq = \oint \frac{1}{\dot{q}} dq\,. \tag{10.29}$$

Using the first of the Hamilton equations (7), we may now present this integral as

[7] See, e.g., QM Sec. 4.6.

[8] Various aspects of this problem and its quantum-mechanical extension were first discussed by L. Le Cornu (1895), Lord Rayleigh (1902), H. Lorentz (1911), P. Ehrenfest (1916), and M. Born and V. Fock (1928).

[9] This term has come from thermodynamics and statistical mechanics, where it implies not only a slow parameter variation, but also the thermal insulation of the system - see, e.g., SM Sec. 1.3. Evidently, the latter condition is irrelevant in our current context.

[10] In Sec. 4.6, we discussed this plane for the particular case of sinusoidal oscillations – see Fig. 9

$$\mathcal{T} = \oint \frac{1}{\partial H / \partial p} dq \,. \tag{10.30}$$

At each given point q, $H = E$ is a function of p alone, so that we may flip the partial derivative in the denominator just as a full derivative, and rewrite Eq. (30) as

$$\mathcal{T} = \oint \frac{\partial p}{\partial E} dq \,. \tag{10.31}$$

For the particular Hamiltonian (10), this relation is immediately reduced to Eq. (3.27) in the form of a contour integral:

$$\mathcal{T} = \left(\frac{m_{\text{ef}}}{2} \right)^{1/2} \oint \frac{1}{[E - U_{\text{ef}}(q)]^{1/2}} dq \,. \tag{10.32}$$

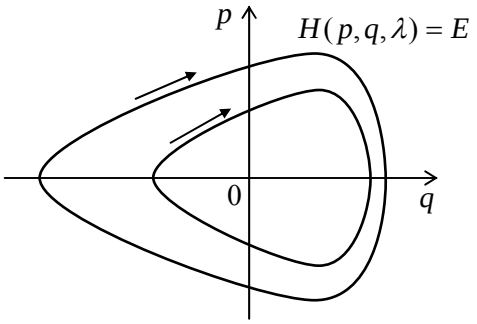

Fig. 10.1. Phase-plane representation of periodic oscillations of a 1D Hamiltonian system, for two values of energy (schematically).

Superficially, it looks that these formulas may be also used to find the motion period change when parameter λ is being changed adiabatically, for example, by plugging known functions $m_{\text{ef}}(\lambda)$ and $U_{\text{ef}}(q, \lambda)$ into Eq. (32). However, there is no guarantee that energy E in that integral would stay constant as the parameter change, and indeed we will see below that this is not necessarily the case. Even more interestingly, in the most important case of the harmonic oscillator ($U_{\text{ef}} = \kappa_{\text{ef}} q^2/2$), whose oscillation period $\mathcal{T}$ does not depend on E (see Eq. (3.29) and its discussion), its variation in the adiabatic limit (28) may be readily predicted: $\mathcal{T}(\lambda) = 2\pi/\omega_0(\lambda) = 2\pi[m_{\text{ef}}(\lambda)/\kappa_{\text{ef}}(\lambda)]^{1/2}$, but the dependence of the oscillation energy E (and hence the oscillation amplitude) on λ is not immediately obvious.

In order to address this issue, let us use Eq. (8) (with $E = H$) to present the energy change with $\lambda(t)$, i.e. in time, as

$$\frac{dE}{dt} = \frac{\partial H}{\partial t} = \frac{\partial H}{\partial \lambda} \frac{d\lambda}{dt} \,. \tag{10.33}$$

Since we are interested in a very slow (adiabatic) time evolution of energy, we can average Eq. (33) over fast oscillations in the system, for example over one oscillation period $\mathcal{T}$, treating $d\lambda/dt$ as a constant during this averaging.[11] The averaging yields

[11] This is the most critical point of this proof, because at any finite rate of parameter change the oscillations are, strictly speaking, non-periodic. Because of the approximate nature of this conjecture (which is very close to the assumptions made at the derivation of the RWA equations in Sec. 4.3), new, more strict (but also much more

$$\overline{\frac{dE}{dt}} \approx \frac{d\lambda}{dt}\overline{\frac{\partial H}{\partial \lambda}} = \frac{d\lambda}{dt}\frac{1}{\mathcal{T}}\int_0^{\mathcal{T}} \frac{\partial H}{\partial \lambda}\,dt\,. \tag{10.34}$$

Transforming the time integral to the contour one, just as we did at the transition from Eq. (29) to Eq. (30), and using Eq. (31) for $\mathcal{T}$, we get

$$\overline{\frac{dE}{dt}} = \frac{d\lambda}{dt}\frac{\oint \frac{\partial H/\partial \lambda}{\partial H/\partial p}\,dq}{\oint \frac{\partial p}{\partial E}\,dq}\,. \tag{10.35}$$

At each point q of the contour, H is a function of not only λ, but also of p, which may be also λ-dependent, so that if E is fixed, the partial differentiation of relation $E = H$ over λ yields

$$\frac{\partial H}{\partial \lambda} + \frac{\partial H}{\partial p}\frac{\partial p}{\partial \lambda} = 0, \quad \text{i.e.} \quad \frac{\partial H/\partial \lambda}{\partial H/\partial p} = -\frac{\partial p}{\partial \lambda}\,. \tag{10.36}$$

Plugging the last relation into Eq.(35), we get

$$\overline{\frac{dE}{dt}} = -\frac{d\lambda}{dt}\frac{\oint \frac{\partial p}{\partial \lambda}\,dq}{\oint \frac{\partial p}{\partial E}\,dq}\,. \tag{10.37}$$

Since the left-hand part of Eq. (37), and the derivative $d\lambda/dt$ do not depend on q, we may move them into the integrals over q as constants, and rewrite that relation as

$$\oint\left(\frac{\partial p}{\partial E}\overline{\frac{dE}{dt}} + \frac{\partial p}{\partial \lambda}\frac{d\lambda}{dt}\right)dq = 0. \tag{10.38}$$

Now let us consider the following integral over the same phase-plane contour,

Action variable

$$J \equiv \frac{1}{2\pi}\oint p\,dq\,, \tag{10.39}$$

called the *action variable*. Just to understand its physical sense, let us calculate J for a harmonic oscillator (14). As we know very well from Chapter 4, for such oscillator, $q = A\cos\Psi$, $p = -m_{\text{ef}}\omega_0 A\sin\Psi$ (with $\Psi = \omega_0 t$ + const), so that J may be easily expressed either via oscillations' amplitude A, or their energy $E = H = m_{\text{ef}}\omega_0^2 A^2/2$:

$$J = \frac{1}{2\pi}\oint p\,dq = \frac{1}{2\pi}\int_{\Psi=0}^{\Psi=2\pi}\left(-m_{\text{ef}}\omega_0 A\sin\Psi\right)d\left(A\cos\Psi\right) = \frac{1}{2\pi}\frac{m_{\text{ef}}\omega_0}{2}A^2 = \frac{E}{\omega_0}. \tag{10.40}$$

Returning to the general oscillator with adiabatically changed parameter λ, let us use the definition of J, Eq. (39), to calculate its time derivative, again taking into account that at each point q of the trajectory, p is a function of E and λ:

---

cumbersome) proofs of Eq. (42) are still being offered in literature – see, e.g., C. Wells and S. Siklos, *Eur. J. Phys.* **28**, 105 (2007) and/or A. Lobo *et al.*, *Eur. J. Phys.* **33**, 1063 (2012).

$$\frac{dJ}{dt} = \frac{1}{2\pi}\oint \frac{dp}{dt}dq = \frac{1}{2\pi}\oint\left(\frac{\partial p}{\partial E}\frac{dE}{dt} + \frac{\partial p}{\partial \lambda}\frac{d\lambda}{dt}\right)dq\,. \tag{10.41}$$

Within the accuracy of our approximation, in which the contour integrals (38) and (41) are calculated along a closed trajectory, factor dE/dt is indistinguishable from its time average, and these integrals coincide, so that result (38) is applicable to Eq. (41) as well. Hence, we have finally arrived at a very important result: at a slow parameter variation, $dJ/dt = 0$, i.e. the action variable remains constant:

$$\boxed{J = \text{const}}\,. \tag{10.42}$$

Adiabatic invariance

This is the famous *adiabatic invariance*.[12] In particular, according to Eq. (40), in a harmonic oscillator, energy of oscillation changes proportionately to the (slowly changed) eigenfrequency.

Before moving on, let me briefly note that the adiabatic invariance is not the only application of the action variable J. Since the initial choice of generalized coordinates and velocities (and hence the generalized momenta) in analytical mechanics is arbitrary (see Sec. 2.1), it is almost evident that J may be taken for a new generalized momentum corresponding to a certain new generalized coordinate Θ,[13] and that pair $\{J, \Theta\}$ should satisfy the Hamilton equations (7), in particular,

$$\frac{d\Theta}{dt} = \frac{\partial H}{\partial J}. \tag{10.43}$$

Following the commitment of Sec. 1 (made there for the "old" arguments q_j, p_j), before the differentiation in the right-hand part in Eq. (43), H should be expressed as a function of t, J, and Θ. For time-independent Hamiltonian systems, H is uniquely defined by J – see, e.g., Eq. (40). Hence the right-hand part of Eq. (43) does not depend on either t or Θ, so that according to that equation, Θ (called the *angle variable*) is a linear function of time:

$$\Theta = \frac{\partial H}{\partial J}t + \text{const}\,. \tag{10.44}$$

For a harmonic oscillator, according to Eq. (40), derivative $\partial H/\partial J = \partial E/\partial J = \omega_0 = 2\pi/\mathcal{T}$, so that $\Theta = \omega_0 t + \text{const}$. It may be shown that a more general form of this relation,

$$\frac{\partial H}{\partial J} = \frac{2\pi}{\mathcal{T}}, \tag{10.45}$$

is valid for an arbitrary oscillator described by Eq. (10). Thus, Eq. (44) becomes

$$\Theta = 2\pi\frac{t}{\mathcal{T}} + \text{const}\,. \tag{10.46}$$

[12] For certain particular oscillators, e.g., a mathematical pendulum, Eq. (42) may be also proved directly – an exercise highly recommended to the reader.

[13] This, again, is a plausible argument but not a strict proof. Indeed, though, according to its definition (39), J is nothing more than a sum of several (formally, infinite number of) values of momentum p, they are not independent, but have to be selected on the same closed trajectory on the phase plane. For more mathematical vigor, the reader is referred to Sec. 45 of *Mechanics* by Landau and Lifshitz (which was repeatedly cited above), which discusses the general rules of the so-called *canonical transformations* from one set of Hamiltonian arguments to another one - say from $\{p, q\}$ to $\{J, \Theta\}$.

To summarize, for a harmonic oscillator, the angle variable Θ is just the full phase Ψ that we used so much in Ch. 4, while for an arbitrary (nonlinear) 1D oscillator, this is a convenient generalization of that notion. Due to this reason, variables J and Θ present a convenient tool for discussion of certain fine points of dynamics strongly nonlinear oscillators – for whose discussion I, unfortunately, do not have time.[14]

10.3. The Hamilton principle

Now let me show that the Lagrangian equations of motion, that have been derived in Sec. 2.1 from the Newton laws, may be also obtained from the so-called *Hamilton principle*, namely the condition of a minimum (or rather an extremum) of the integral called *action*:

Action

$$S \equiv \int_{t_{ini}}^{t_{fin}} L dt , \tag{10.47}$$

where t_{ini} and t_{fin} are, respectively, the initial and final moments of time, at which moments all generalized coordinates and velocities are considered fixed (not varied) – see Fig. 2.

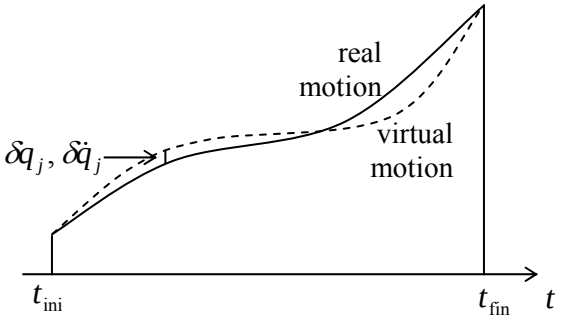

Fig. 10.2. Deriving the Hamilton principle.

The proof of that statement is rather simple. Considering, similarly to Sec. 2.1, a possible virtual variation of the motion, described by infinitesimal deviations $\{\delta q_j(t), \delta \dot{q}_j(t)\}$ from the real motion, the necessary condition for S to be minimal is

Hamilton principle

$$\delta S \equiv \int_{t_{ini}}^{t_{fin}} \delta L \, dt = 0 , \tag{10.48}$$

where δS and δL are the variations of the action and the Lagrange function, corresponding to the set $\{\delta q_j(t), \delta \dot{q}_j(t)\}$. As has been already discussed in Sec. 2.1, we can use the operation of variation just as the usual differentiation (but at fixed time, see Fig. 2.1), swapping these two operations if needed – see Fig. 2.3 and its discussion. Thus, we may write

$$\delta L = \sum_j \left(\frac{\partial L}{\partial q_j} \delta q_j + \frac{\partial L}{\partial \dot{q}_j} \delta \dot{q}_j \right) = \sum_j \frac{\partial L}{\partial q_j} \delta q_j + \sum_j \frac{\partial L}{\partial \dot{q}_j} \frac{d}{dt} \delta q_j . \tag{10.49}$$

[14] See, e.g., Chapter 6 in J. Jose and E. Saletan, *Classical Dynamics*, Cambridge U. Press, 1998.

After plugging the last expression into Eq. (48), we can integrate the second term by parts:

$$\delta S = \int_{t_{\rm ini}}^{t_{\rm fin}} \sum_j \frac{\partial L}{\partial q_j}\delta q_j dt + \sum_j \int_{t_{\rm ini}}^{t_{\rm fin}} \frac{\partial L}{\partial \dot{q}_j}\frac{d}{dt}\delta q_j dt$$

$$= \int_{t_{\rm ini}}^{t_{\rm fin}} \sum_j \frac{\partial L}{\partial q_j}\delta q_j dt + \sum_j \left[\frac{\partial L}{\partial \dot{q}_j}\delta q_j\right]_{t_{\rm ini}}^{t_{\rm fin}} - \sum_j \int_{t_{\rm ini}}^{t_{\rm fin}} \delta q_j d\left(\frac{\partial L}{\partial \dot{q}_j}\right) = 0. \qquad (10.50)$$

Since the generalized coordinates in the initial and final points are considered fixed (not affected by the variation), all $\delta q_j(t_{\rm ini}) = \delta q_j(t_{\rm fin}) = 0$, the second term in the right-hand part of Eq. (50) vanishes. Multiplying and dividing the last term of that part by dt, we finally get

$$\delta S = \int_{t_{\rm ini}}^{t_{\rm fin}} \sum_j \frac{\partial L}{\partial q_j}\delta q_j dt - \sum_j \int_{t_{\rm ini}}^{t_{\rm fin}} \delta q_j \frac{d}{dt}\left(\frac{\partial L}{\partial \dot{q}_j}\right)dt = -\int_{t_{\rm ini}}^{t_{\rm fin}} \sum_j \left[\frac{d}{dt}\left(\frac{\partial L}{\partial \dot{q}_j}\right) - \frac{\partial L}{\partial q_j}\right]\delta q_j dt = 0. \qquad (10.51)$$

This relation should hold for an arbitrary set of functions $\delta q_j(t)$, and for any time interval, so that it is only possible if the expressions in square brackets equal zero for all j, giving us the set of Lagrange equations (2.19). So, the Hamilton principle indeed gives the Lagrange equations of motion.

It is very useful to make the notion of action S, defined by Eq. (47), more transparent by calculating it for the simple case of a single particle moving in a potential field that conserves its energy $E = T + U$. In this case the Lagrangian function $L = T - U$ may be presented as

$$L = T - U = 2T - (T + U) = 2T - E = mv^2 - E, \qquad (10.52)$$

with $E = \text{const}$, so that

$$S = \int L dt = \int mv^2 dt - Et + \text{const}. \qquad (10.53)$$

Presenting the expression under the remaining integral as $m\mathbf{v}\cdot\mathbf{v}dt = \mathbf{p}\cdot(d\mathbf{r}/dt)dt = \mathbf{p}\cdot d\mathbf{r}$, we finally get

$$S = \int \mathbf{p}\cdot d\mathbf{r} - Et + \text{const} = S_0 - Et + \text{const}, \qquad (10.54)$$

where the time-independent integral

$$S_0 \equiv \int \mathbf{p}\cdot d\mathbf{r} \qquad (10.55)$$

is frequently called the *abbreviated action*.[15]

This expression may be used to establish one more connection between the classical and quantum mechanics, now in its Schrödinger picture. Indeed, in the quasiclassical (WKB) approximation of that picture[16] a particle of fixed energy is described by a De Broglie wave

$$\Psi(\mathbf{r},t) \propto \exp\left\{i\left(\int \mathbf{k}\cdot d\mathbf{r} - \omega t + \text{const}\right)\right\}, \qquad (10.56)$$

[15] Please note that despite a close relation between the abbreviated action S_0 and the action variable J defined by Eq. (39), these notions are not identical. Most importantly, J is an integral over a *closed* trajectory, while S_0 in defined for an arbitrary point of a trajectory.

[16] See, e.g., QM Sec. 2.3.

where wavevector **k** is proportional to the particle's momentum, while frequency ω, to its energy:

$$\mathbf{k} = \frac{\mathbf{p}}{\hbar}, \quad \omega = \frac{E}{\hbar}. \tag{10.57}$$

Plugging these expressions into Eq. (56) and comparing the result with Eq. (54), we see that the WKB wavefunction may be presented as

$$\Psi \propto \exp\{iS/\hbar\}. \tag{10.58}$$

Hence the Hamilton's principle (48) means that the total phase of the quasiclassical wavefunction should be minimal along particle's real trajectory. But this is exactly the so-called *eikonal minimum principle* well known from the optics (though valid for any other waves as well), where it serves to define the ray paths in the geometric optics limit – similar to the WKB approximation condition. Thus, the ratio $S/\hbar$ may be considered just as the eikonal, i.e. the total phase accumulation, of the de Broigle waves.[17]

Now, comparing Eq. (55) with Eq. (33), we see that the action variable J is just the change of the abbreviated action S_0 along a single phase-plane contour (divided by 2π). This means that in the WKB approximation, J is the number of de Broglie waves along the classical trajectory of a particle, i.e. an integer value of the corresponding quantum number. If system's parameters are changed slowly, the quantum number has to stay integer, and hence J cannot change, giving a quantum-mechanical interpretation of the adiabatic invariance. It is really fascinating that a fact of classical mechanics may be "derived" (or at least understood) more easily from the quantum mechanics' standpoint.[18]

10.4. The Hamilton-Jacobi equation

Action S, defined by Eq. (47), may be used for one more formulation of classical mechanics. For that, we need one more, different commitment: S to be considered a function of the following independent arguments: the final time point t_{fin} (which I will, for brevity, denote as t in this section), and the set of generalized coordinates (but not of the generalized velocities!) at that point:

Hamilton-Jacobi action

$$S \equiv \int_{t_{\text{ini}}}^{t} L\,dt = S\left[t, q_j(t)\right]. \tag{10.59}$$

Let us calculate a variation of this (essentially, new!) function, resulting from an arbitrary combination of variations of final values $q_j(t)$ of the coordinates, while keeping t fixed. Formally this may be done by repeating the variation calculations described by Eqs. (49)-(52), besides that now variations δq_j at the finite point (t) do not necessarily equal zero. As a result, we get

$$\delta S = \sum_j \frac{\partial L}{\partial \dot{q}_j}\delta q_j\Big|_t - \int_{t_{\text{ini}}}^{t} dt \sum_j \left[\frac{d}{dt}\left(\frac{\partial L}{\partial \dot{q}_j}\right) - \frac{\partial L}{\partial q_j}\right]\delta q_j\,. \tag{10.60}$$

[17] Eq. (58) was the starting point for R. Feynman's development of his path-integral formulation of quantum mechanics – see, e.g., QM Sec. 5.3.

[18] As a reminder, we have run into a similar situation at our discussion of the non-degenerate parametric excitation in Sec. 5.5.

For the motion along the real trajectory, i.e. satisfying the Lagrange equations of motion, the second term of this expression equals zero. Hence Eq. (60) shows that, for (any) fixed time t,

$$\frac{\partial S}{\partial q_j} = \frac{\partial L}{\partial \dot{q}_j}. \tag{10.61}$$

But the last derivative is nothing else than the generalized momentum p_j – see Eq. (2.31), so that

$$\frac{\partial S}{\partial q_j} = p_j. \tag{10.62}$$

(As a reminder, both parts of this relation refer to the final moment t of the trajectory.) As a result, the full derivative of action $S[t, q_j(t)]$ over time takes the form

$$\frac{dS}{dt} = \frac{\partial S}{\partial t} + \sum_j \frac{\partial S}{\partial q_j}\dot{q}_j = \frac{\partial S}{\partial t} + \sum_j p_j \dot{q}_j. \tag{10.63}$$

Now, by the very definition (59), the full derivative dS/dt is nothing more that the Lagrange function L, so that Eq. (63) yields

$$\frac{\partial S}{\partial t} = L - \sum_j p_j \dot{q}_j. \tag{10.64}$$

However, according to the definition (2) of the Hamiltonian function H, the right-hand part of Eq. (63) is just $(-H)$, so that we get an extremely simply-looking *Hamilton-Jacobi equation*

$$\boxed{\frac{\partial S}{\partial t} = -H.} \tag{10.65}$$

Hamilton-Jacobi equation

This simplicity is, however, rather deceiving, because in order to use this equation for the calculation of function $S(t, q_j)$ for any particular problem, the Hamiltonian function has to be first expressed as a function of time t, generalized coordinates q_j, and the generalized momenta p_j (which may be, according to Eq. (62), presented just as derivatives $\partial S/\partial q_j$). Let us see how does this procedure work for the simplest case of a 1D system with the Hamiltonian function given by Eq. (10). In this case, the only generalized momentum is $p = \partial S/\partial q$, so that

$$H = \frac{p^2}{2m_{\text{ef}}} + U_{\text{ef}}(q,t) = \frac{1}{2m_{\text{ef}}}\left(\frac{\partial S}{\partial q}\right)^2 + U_{\text{ef}}(q,t), \tag{10.66}$$

and the Hamilton-Jacobi equation (65) is reduced to a partial differential equation,

$$\frac{\partial S}{\partial t} + \frac{1}{2m_{\text{ef}}}\left(\frac{\partial S}{\partial q}\right)^2 + U_{\text{ef}}(q,t) = 0. \tag{10.67}$$

Its solution may be readily found in the particular case of time-independent potential energy $U_{\text{ef}} = U_{\text{ef}}(q)$. In this case, Eq. (67) is evidently satisfied by a variable-separated solution

$$S(t,q) = S_0(q) + \text{const} \times t. \tag{10.68}$$

Plugging this solution into Eq. (67), we see that since the sum of two last terms in the left-hand part of that equation presents the full mechanical energy E, the constant in Eq. (68) is nothing but ($-E$). Thus for function S_0 we get an ordinary differential equation

$$-E+\frac{1}{2m_{\text{ef}}}\left(\frac{dS_0}{dq}\right)^2+U_{\text{ef}}(q)=0. \tag{10.69}$$

Integrating it, we get

$$S_0=\int\left\{2m_{\text{ef}}\left[E-U_{\text{ef}}(q)\right]\right\}^{1/2}dq+\text{const}, \tag{10.70}$$

so that, finally, the action is equal to

$$S=\int\left\{2m_{\text{ef}}\left[E-U_{\text{ef}}(q)\right]\right\}^{1/2}dq-Et+\text{const}. \tag{10.71}$$

For the case of 1D motion of a single 1D particle, i.e. for $q = x$, $m_{\text{ef}} = m$, $U_{\text{ef}}(q) = U(x)$, this solution is just the 1D case of the more general Eqs. (54)-(55), which were obtained by a much more simple way. (In particular, S_0 is just the abbreviated action.)

This particular case illustrates that the Hamilton-Jacobi equation is not the most efficient way for solution of most practical problems. However, it may be rather useful for studies of certain mathematical aspects of dynamics.[19] Moreover, in the 1940s this approach was extended to a completely different field – the optimal control theory, in which the role of action S is played by the so-called *cost function* – a certain functional of a dynamic system, that should be minimized by an optical choice of a *control signal* – a function of time that affects system's dynamics. From the point of view of this mathematical theory, Eq. (65) is a particular case of a more general *Hamilton-Jacobi-Bellman* equation.[20]

10.5. Exercise problems

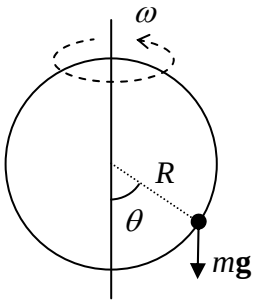

10.1. Derive the Hamilton equations of motion for our testbed problem (a bead on a ring rotating about its vertical diameter – see Fig. 2.1, partly reproduced on the right). Check that the equations are equivalent to those derived from the Lagrangian formalism.

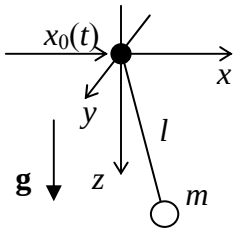

10.2. Perform the same tasks as in Problem 10.1 for the system already considered in Problem 2.3, a fixed-length pendulum hanging from a horizontal support whose motion law $x_0(t)$ is fixed – see Fig. on the right. (No vertical plane constraint.)

[19] See, e.g., Chapters 6-9 in I. C. Percival and D. Richards, *Introduction to Dynamics*, Cambridge U. Press, 1983.

[20] See, e.g., T. P. Bertsekas, *Dynamic Programming and Optimal Control*, vols. 1 and 2, Aetna Scientific, 2005 and 2007. The reader should not be deceived by the unnatural term "dynamic programming" that was invented by the founding father of this field, R. Bellman, to lure government bureaucrats into funding his research, which had been deemed too theoretical at that time, but now has a broad range of important applications.

10.3. Perform the same tasks as in Problems 1 and 2, for the system already considered in Problem 2.5 - a block of mass m that can slide, without friction, along the inclined surface of a heavy wedge (mass m'). The wedge is free to move, also without friction, along a horizontal surface - see Fig. on the right. (Both motions are within the vertical plane containing the steepest slope line.)

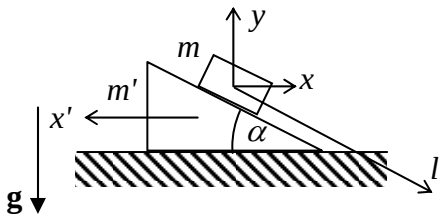

10.4. Find and solve equations of motion of a particle with the following Hamiltonian function:

$$H = \frac{1}{2m}(\mathbf{p} + a\mathbf{r})^2,$$

where a is a constant scalar.

10.5. Let L be the Lagrange function, and H the Hamilton function, of the same system. What three of the following four statements,

$$\text{(i)}\ \frac{dL}{dt} = 0, \qquad \text{(ii)}\ \frac{\partial L}{\partial t} = 0, \qquad \text{(iii)}\ \frac{dH}{dt} = 0, \qquad \text{(iv)}\ \frac{\partial H}{\partial t} = 0,$$

are equivalent? Give an example when those three equalities hold, but the forth one does not.

10.6. Calculate the Poisson brackets of the Cartesian components of the angular momentum $\mathbf{L}$ of a particle moving in a central force field and its Hamiltonian function H, and discuss the most important implication of the result.

10.7. After small oscillations had been initiated in a simple pendulum (Fig. on the right), the thread is being pulled up slowly, so that the pendulum length l is being reduced. Neglecting dissipation,

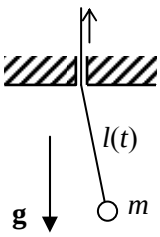

(i) prove by a direct calculation that the oscillation energy is indeed changing proportionately to the oscillation frequency, as it follows from the constancy of the corresponding adiabatic invariant (40), and

(ii) find the l-dependence of amplitudes of the angular and linear deviations from the equilibrium.

10.8. The mass m of a small body that performs 1D oscillations in potential $U(x) = ax^{2n}$, with $n > 0$, is being changed slowly. Calculate the oscillation energy E as a function of m.

10.9. A stiff ball is bouncing vertically from the floor of an elevator whose upward acceleration changes very slowly. Neglecting energy dissipation, calculate how much does the bounce height h change during acceleration's increase from 0 to g.